Department of Biosciences and Bioengineering
Indian Institute of Technology Guwahati
Guwahati-781039
Assam, India

Studies on engineering Entomopathogenic fungi, *Metarhizium anisopliae* and *Beauveria bassiana* to express heterologous insect-specific toxins

THESIS

Submitted for the partial fulfilment of requirement for the award of

DOCTOR OF PHILOSOPHY

Under the guidance of

Prof. Gurvinder Kaur Saini

by

DHANASINGH M

Dedicated to

My Parents, Family, Loved ones and the Almighty

INDIAN INSTITUTE OF TECHNOLOGY GUWAHATI

Department of Biosciences and Bioengineering

DECLARATION

I do hereby declare that the content embodied in this thesis is the result of investigations carried out by me in the **Department of Biosciences and Bioengineering, Indian Institute of Technology Guwahati, Guwahati, India**, under the supervision of **Prof. Gurvinder Kaur Saini.**

In keeping with the general practice of reporting scientific observations, due acknowledgements have been made wherever the work of other investigators are referred.

Date: **Dhanasingh M**

Place: **Roll No:136106005**

INDIAN INSTITUTE OF TECHNOLOGY GUWAHATI

Department of Biosciences and Bioengineering

CERTIFICATE

It is certified that the work described in this thesis entitled **"Studies on engineering entomopathogenic fungi, *Metarhizium anisopliae* and *Beauveria bassiana* to express heterologous insect-specific toxins"** by **Mr. Dhanasingh M** for the award of degree of Doctor of Philosophy is an authentic record of the results obtained from the research work carried out under my supervision at the Department of Biosciences and Bioengineering, Indian Institute of Technology Guwahati, Guwahati, India and this work has not been submitted elsewhere for a degree.

Date:

Place:

Dr. Gurvinder Kaur Saini
Professor
(Thesis supervisor)

ACKNOWLEDGEMENT

The results embodied in thesis are the outcome of cooperation of many helping hands and it could not have seen the light of the day without their voluntary involvement. Here I take the pleasant opportunity to express my gratitude to all of them.

First and foremost, with a deepest sense of respect, I would like to express my sincere gratitude to my supervisor, Dr. Gurvinder Kaur Saini, for her valuable suggestions, encouragement and inspiration. I am indebted to her for introducing me into the realm of this interesting work, training me with the techniques, giving me the freedom in designing and conducting the experiments. I earnestly thank her for imbibing scientific temperament and appreciable work ethics in me which enhanced my grasp of knowledge and made my learning pursuit exciting.

I would like to acknowledge my sincere gratitude to all my doctoral committee members, Dr. K. Pakshirajan, Dr. V.V.Dasu, Dr. Siddhartha S. Ghosh, and Dr. C.V.Sastri for their valuable suggestions and precious time.

I remain thankful to my seniors Dr. Digar singh for the guidance and training. I am immensely thankful to my research group members Balwant, Neha, Ashish, Tusarika, Kawkab, Jena, Arman, and Arupam for their adept hands in fruition of some of my crucial experiments.

Special thanks goes to my friends Muthuvel, Krishnakumar, Anil Kumar, Neha Arora, Himanshu and Yoganand for their academic support and encouragement during my entire journey of PhD Life.

I am thankful to Dr. Nurul, Mrs. Prarthana, Mr.Yadav, Mr. Dipankar and Mr. Niranjan for their technical help and assistance.

I am thankful to the Indian Institute of Technology Guwahati (IITG) for providing me with the state of the art infrastructure for advance level of research. I also thank Central Instrumentation Facility (CIF) at IITG for providing the instrument facilities, National Bureau of Agricultural Insect Resources (NBAIR, Bangalore) for providing the insect cultures, and National center for Cell Sciences

(NCCS), Pune, for providing the cell lines for my research work. I wholeheartedly thank Dr. Daniel R. Zeigler, Bacillus Genetic Stock Center (BGSC), USA, for gifting me the *Bacillus* culture. I am thankful to the Ministry of Human Resource Development (MHRD), New Delhi for the financial support.

Finally, my PhD, endeavor could not have been successful without the unfathomable love, support and blessings of My Parents. I owe my achievements to my sisters and brother. I convey my special thanks to my dearest friend Vartika, without whom, I would have not have been able to cope up the stress of my PhD life.

Dhanasingh M

August, 2019

CONTENT

List of Tables xvii

List of Figures xix

List of Abbreviations xxv

Synopsis xxix

Chapter 1: Introduction, Review of Literature and objectives

1.1 General introduction 3

1.2 Food security challenges associated with agricultural pest and diseases 5

1.3 Global and Indian scenario of insect pest control 6

1.4 Development of pesticide resistance in insect pests 6

1.4.1 Pre-adaptation hypothesis 7

1.4.2 Enhanced detoxification mechanism 7

1.5 Environmental and human health risks associated with insecticides 8

1.5.1 Negative impact on pollinators 9

1.6 Biological pesticides 9

1.6.1 Bacteria as insect biological control agent 10

1.6.1.1 *Bacillus thuringiensis* 10

1.6.2 Baculovirus as biocontrol agents 11

1.6.3 Fungi as biological control agents 12

1.7 Entomopathogenic fungi Metarhizium anisopliae and Beauveria bassiana 12

1.7.1 *Metarhizium anisopliae* 12

1.7.2 *Beauveria bassiana* 14

1.7.3 Entomopathogenic fungi life cycle 15

1.8 Major drawbacks associated with entomopathogenic fungi 16

1.9 Strategies used to improve the virulence of entomopathogenic fungi 17

1.9.1 Endogenous genes overexpression 17

1.9.2 Heterologous genes overexpression 18

1.9.2.1 Scorpion toxins overexpression 18

1.9.2.2 Overexpression of other heterologous proteins 18

1.10 Scorpion and spider toxins 19

1.10.1 Voltage-gated channels 19

1.10.2 β-BUTX Lqq1a toxin 20

1.11 Bacillus thuringiensis Cry and Cyt toxins 20

1.11.1 General aspects of Cry1Ac toxin and insect resistance development 22

1.12 Cytolytic toxin structure overview 23

1.13 General aspects of Lectins 24

1.13.1 GNA Lectin 25

1.14 Lacunae and scope of work 27

1.15 Objectives 28

Chapter 1: Tables and Figures 29-35

Chapter 2: Expression and purification of β-BUTX Lqq1a toxin and its biological activity against insect cells and agricultural insect pests

2.1 Introduction 39-41

2.2 Materials and Methods 42-50

2.2.1 Bacterial strains and reagents 42

2.2.2 β-BUTX Lqq1a gene synthesis 42

2.2.3 Expression cassette construction 42

2.2.4 *E. coli* chemical competent cell preparation 43

2.2.4.1 *E. coli* DH5-α transfection 43

2.2.5 Protein β-BUTX Lqq1a expression and purification 44

2.2.5.1 Shuffle T7 express LysY chemical competent cells preparation 44

2.2.5.2 The $(His)_6$ β-BUTX Lqq1a toxin expression 44

2.2.5.3 The $(His)_6$ β-BUTX Lqq1a toxin affinity purification 45

2.2.5.4 The $(His)_6$ tag removal and size exclusion chromatography purification 45
2.2.6 MALDI-TOF molecular mass determination 46
2.2.7 Western blotting analysis 46
2.2.8 Cytotoxicity assay of purified β-BUTX Lqq1a with Sf-21 insect cell lines 47
2.2.8.1 MTT assay 47
2.2.8.2 Light microscopy analysis 48
2.2.8.3 Fluorescence microscopy analysis 48
2.2.8.4 Ultra-structural analysis using FE-SEM 49
2.2.8.5 Flow cytometry analysis 49
2.2.9 Bioassay of β-BUTX Lqq1a with *H. armigera* and *S. litura* 50
2.2.9.1 Maintenance of insect cultures 50
2.2.9.2 Intrahemocoeilic injection bioassay 50
2.2.10 Statistical data analysis 50
2.3 Results 52-58
2.3.1 Cloning in pET28a expression vector 52
2.3.2 Expression and purification using Ni-NTA affinity chromatography 52
2.3.3 N-Terminal $(His)_6$ tag removal using Thrombin Protease 53
2.3.4 Size exclusion chromatography 53
2.3.5 Mass spectrometry and Western blotting analysis 54
2.3.6 Cytotoxicity analysis of treated *Sf*-21 insect cell line using MTT assay 55
2.3.7 Morphological assessment using Light microscopy 55
2.3.8 Fluorescence microscopy analysis 56
2.3.9 Ultra structural analysis using FE-SEM 56
2.3.10 Flow Cytometry analysis 56
2.3.11 Insect bioassay 57
2.3.11.1 *Helicoverpa armigera* 57
2.3.11.2 *Spodoptera litura* 57

2.4 Discussion 59-62

2.5 Conclusion 63

Chapter 2: Tables and Figures 64-75

Chapter 3: Cloning and expression of β-BUTX Lqq1a in *Beauveria bassiana* and *Metarhizium anisopliae* and insect bioassay

3.1 Introduction 79-81

3.2 Materials and Methods 82-94

3.2.1 Strains and culture conditions 82

3.2.1.1 Fungal spore collection 82

3.2.2 Gene synthesis 82

3.2.3 Vector construction 83

3.2.3.1 Vector construction for *B. bassiana* 83

3.2.3.1.1 Overlap extension PCR 83

3.2.3.1.2 *E. coli* chemical competent cell preparation and transfection 84

3.2.3.1.3 Colony PCR 84

3.2.3.1.4 Plasmid DNA isolation 85

3.2.3.1.5 Clone confirmation by double digestion 85

3.2.3.2 Vector construction for *M. anisopliae* 86

3.2.3.2.1 Cloning Mcl1 gene downstream of β-BUTX Lqq1a gene 86

3.2.3.2.2 pCAMBIA cloning 87

3.2.3.2.3 *E. coli* chemical competent cell preparation and transfection 87

3.2.3.2.4 Colony PCR 87

3.2.3.2.5 Plasmid isolation 88

3.2.3.2.6 Double digestion 88

3.2.4 Protoplast based transformation of *B. bassiana* 88

3.2.4.1 *B. bassiana* protoplast preparation 88

3.2.4.2 *B. bassiana* protoplast electroporation 89

3.2.5 *Agrobacterium*-mediated transformation of *M. anisopliae* 89

3.2.5.1 Electro-competent cell preparation 89

3.2.5.2 Electroporation 90

3.2.5.3 *Agrobacterium* and *Metarhizium* co-cultivation 90

3.2.6 Clone confirmation by isolating genomic DNA 91

3.2.7 Haemolymph induction and Reverse transcription-PCR analysis 92

3.2.8 Western blotting analysis 92

3.2.9 Insect bioassay 93

3.2.10 Statistical data analysis 94

3.3 Results 95-99

3.3.1 pMcl1-BUTX Lqq1a vector construction for *B. bassiana* 95

3.3.2 pMcl1-BUTX Lqq1a transformation into *B. bassiana* 96

3.3.3 pMcl1-BUTX Lqq1a binary vector construction for *M. anisopliae* 96

3.3.4 Genomic integration of BUTX Lqq1a analysis in *B. bassiana* 97

3.3.5 Genomic integration of BUTX Lqq1a analysis in *M. anisopliae* 97

3.3.6 BUTX Lqq1a transcript analysis in *B. bassiana* and *M. anisopliae* 98

3.3.7 Virulence assay 98

3.4 Discussion 100-102

3.5 Conclusion 103

Chapter 3: Tables and Figures 104-121

Chapter 4: Bacterial expression and purification of a fusion protein containing β-BUTX Lqq1a/GNA Lectin and their cytotoxicity assay against insect cell lines

4.1 Introduction 125-126

4.2 Materials and Methods 127-134

4.2.1 Bacterial strain, Cell lines and chemicals 127

4.2.2 β-BUTX Lqq1a and GNA gene synthesis 127

4.2.3 Expression vector construction 128

4.2.4 *E. coli* DH5-α chemical competent cell preparation 128

4.2.4.1 *E. coli* DH5-α transfection 128
4.2.5 GNA and β-BUTX Lqq1a/GNA expression and purification 129
4.2.5.1 Shuffle T7 express LysY chemical competent cells preparation 129
4.2.5.2 GNA and β-BUTX Lqq1a/GNA expression 129
4.2.5.3 GNA and β-BUTX Lqq1a/GNA affinity purification 129
4.2.6 Cell culture and maintenance 130
4.2.7 Cell viability assay 130
4.2.8 Microscopy analysis 131
4.2.9 Mitochondrial membrane potential assay 132
4.2.10 Cell cycle analysis 132
4.2.11 Gene expression analysis by Real-time quantitative PCR 132
4.2.12 Insect bioassay of GNA and β-BUTX Lqq1a/GNA with *S. litura* 133
4.2.12.1 Maintenance of insect cultures 133
4.2.12.2 Intra-hemocoeilic injection bioassay 133
4.2.13 Statistical data analysis 134
4.3 Results 135-139
4.3.1 Cloning GNA and β-BUTX Lqq1a/GNA in pET28a expression vector 135
4.3.2 GNA and fusion protein β-BUTX Lqq1a/GNA expression and purification 135
4.3.3 Cell viability assay 135
4.3.4 Dual staining assay 136
4.3.5 DAPI staining assay 136
4.3.6 Mitochondrial membrane potential assay 137
4.3.7 Flow cytometry analysis 137
4.3.8 Gene expression analysis 138
4.3.9 Insect bioassay with *S. litura* 138
4.4 Discussion 140-144
4.5 Conclusion 145
Chapter 4: Tables and Figures 146-163

Chapter 5: Cloning and expression of β-BUTX Lqq1a, Cyt1Aa and truncated Cry1Ac/GNA in *Metarhizium anisopliae* and insect toxicity assay

5.1 Introduction 167-170

5.2 Materials and Methods 171-180

5.2.1 Microbial strains and Culture conditions 171

5.2.2 Cyt1Aa expression vector construction 171

5.2.2.1 Cyt1Aa amplification 171

5.2.2.2 GPDH promoter (P*gpdh*) amplification 172

5.2.2.2.1 *M. anisopliae* genomic DNA isolation 172

5.2.2.2.2 P*gpdh* amplification 173

5.2.2.3 GPDH promoter (P*gpdh*) fusion with Cyt1Aa 173

5.2.2.4 P*gpdh*-Mcl1sp-Cyt1Aa cloning in pMcl1-BUTX Lqq1a vector 173

5.2.3 Truncated Cry1Ac-GNA expression vector construction 174

5.2.3.1 Cry1Ac truncation 174

5.2.3.2 GNA amplification 175

5.2.3.3 P*gpdh*-Mcl1sp-tCry1Ac/GNA fusion 176

5.2.3.4 P*gpdh*-Mcl1sp-tCry1Ac/GNA Cloning in pMcl1-BUTX Lqq1a vector 176

5.2.4 *Agrobacterium*-mediated transformation of *M. anisopliae* 177

5.2.4.1 Agrobacterium electro-competent cell preparation 177

5.2.4.2 Electroporation 177

5.2.4.3 *Agrobacterium* and *Metarhizium* co-cultivation 177

5.2.5 Genome integration analysis 178

5.2.6 Semi-quantitative RT-PCR analysis 179

5.2.7 Western blot analysis 179

5.2.8 Insect Bioassay 180

5.2.9 Statistical analysis 180

5.3 Results 181-185

5.3.1 pBUTX Lqq1a/Cyt1Aa vector construction 181

5.3.2 pBUTX Lqq1a/tCry1Ac-GNA vector construction 182

5.3.3 Genome integration analysis of BUTX Lqq1a and Cyt1Aa in *M. anisopliae* 182
5.3.4 Genome integration analysis of BUTX Lqq1a and tCry1Ac-GNA 183
5.3.5 Cyt1Aa and BUTX Lqq1a transcript analysis 183
5.3.6 BUTX Lqq1a and tCry1Ac/GNA transcript analysis 184
5.3.7 Western blot analysis of BUTX Lqq1a 184
5.3.8 Insect Bioassay 184
5.4 Discussion 186-189
5.5 Conclusion 190
Chapter 5: Tables and Figures 191-205

Chapter 6: Time of expression analysis of β-BUTX Lqq1a/sGFP in *M. anisopliae*

6.1 Introduction 209-210
6.2 Materials and Methods 211-216
6.2.1 Microbial strains and culture conditions 211
6.2.2 Vector construction 211
6.2.2.1 BUTX Lqq1a gene synthesis 211
6.2.2.2 Synthetic Green Fluorescent Protein (sGFP) coding gene amplification 211
6.2.2.3 Overlap extension PCR 212
6.2.2.4 Gibson assembly reaction 212
6.2.2.5 Colony PCR clone confirmation 213
6.2.2.6 Plasmid isolation 213
6.2.2.7 Clone confirmation by Double digestion 213
6.2.3 *Agrobacterium* mediated transformation 214
6.2.3.1 *Agrobacterium* electro-competent cell preparation 214
6.2.3.2 Electroporation 214
6.2.3.3 Co-cultivation with *M. anisopliae* 214
6.2.4 *M. anisopliae* clonal confirmation 215
6.2.5 Haemolymph induction and Reverse transcription-PCR analysis 215
6.2.5.1 Haemolymph induction 215

6.2.5.2 RNA extraction and transcript analysis	215
6.2.6 Western blot analysis	216
6.2.7 Fluorescence microscopy analysis	216
6.3 Results	217-219
6.3.1 pBUTX Lqq1a/sGFP vector construction	217
6.3.2 Genomic integration analysis	217
6.3.3 Semi-quantitative RT-PCR analysis	218
6.3.4 Western blot analysis	218
6.3.5 Fluorescence microscopy analysis	218
6.4 Discussion	220-221
6.5 Conclusion	222
Chapter 6: Tables and Figures	223-232
References	233-262
Research output	263-264
Vitae	265

List of Tables

Chapter 3

3.1	List of primers used for pMcl1-BUTX Lqq1a vector construction in *B. bassiana*	104
3.2	List of primers used for pMcl1-BUTX Lqq1a vector construction in *M. anisopliae*	104

Chapter 4

4.1	List of primers used for GNA and β-BUTX Lqq1a/GNA fusion	146
4.2	List of Primers used for RT-qPCR analysis	146

Chapter 5

5.1	List of primers used for P*gpdh* and Cyt1Aa cloning	191
5.2	List of primers used for P*gpdh* and tCry1Ac-GNA cloning	191
5.3	List of primers used for semi-quantitative RT-PCR analysis	192

Chapter 6

6.1	List of primers used for BUTX Lqq1a and sGFP fusion	223
6.2	List of primers used for semi-quantitative RT-PCR analysis	223

List of Figures

Chapter 1

1.1	Schematic representation of different life stages of entomopathogen infection on insects	29
1.2	Linearized sodium channel α-subunit with its four domains transmembrane	29
1.3	Predicted β-BUTX Lqq1a structure using QUARK	30
1.4	Crystal structure of Cry1Ac toxin	30
1.5	Schematic representation of *B. thuringiensis* Cry toxins generalized mode of action	31
1.6	Cyt1Aa protein structure	32
1.7	Schematic representation of *B. thuringiensis* subsp. *israelensis* Cyt toxin generalized mode of action	33
1.8	GNA lectin bound with three mannose residue	34
1.9	GNA lectin generalized mode of action on insect mid-gut cells	35

Chapter 2

2.1	Scorpion neurotoxic β-BUTX Lqq1a sequence codon optimization	64
2.2	Plasmid map showing the pUC57 vector harboring β-BUTX Lqq1a gene	64
2.3	Gel purified DNA fragments of β-BUTX Lqq1a and pET28a expression vector	65
2.4	PCR clone confirmation of pET28a-β-BUTX Lqq1a	65
2.5	Schematic representation of recombinant β-BUTX Lqq1a expression and purification	66
2.6	SDS-PAGE analysis of $(His)_6$-β-BUTX Lqq1a protein expression and Ni-NTA affinity purification	67
2.7	Size exclusion chromatography purification of β-BUTX Lqq1a	67
2.8	Schematic representation and SDS PAGE analysis of size exclusion chromatography purified $(His)_6$ β-BUTX Lqq1a protein	68
2.9	MALDI mass spectrometry and western blot analysis purified β-BUTX Lqq1a protein	69
2.10	MTT cell viability assay of purified β-BUTX Lqq1a against *Sf*-21 cell lines	70
2.11	Morphological analysis of β-BUTX Lqq1a treated *Sf*-21 cell lines	71
2.12	Microscopy analysis of β-BUTX Lqq1a treated *Sf*-21 cells using PI	72
2.13	FE-SEM Ultra-structural analysis of β-BUTX Lqq1a treated *Sf*-21 cells	72

2.14	Cell cycle analysis of β-BUTX Lqq1a treated*Sf*-21 cells using FACS	73
2.15	β-BUTX Lqq1a injection bioassay of *Helicoverpa armigera*	74
2.16	β-BUTX Lqq1a injection bioassay *Spodoptera litura*	75

Chapter 3

3.1	Schematic representation of pMcl1-BUTX Lqq1a vector construction	105
3.2	Schematic representation of pMcl1-BUTX Lqq1a-Bar-Mcl1 vector construction for *M.anisopliae* cloning	106
3.3	Schematic representation of *B. bassiana* protoplast preparation and transformation method	107
3.4	Schematic representation of *Agrobacterium*-mediated transformation of *M.anisopliae*	108
3.5	Agarose gel electphoresis analysis of plasmid pUC57 harboring codon optimized 5'UTR Mclsp-BUTX Lqq1a sequence	109
3.6	Agarose gel electphoresis analysis of BUTX Lqq1a PCR amplification	109
3.7	Agarose gel electrophoresis analysis of PMcl1-BUTX Lqq1a cloning in pAL1 vector	110
3.8	Agarose gel electrophoresis analysis pMcl1-BUTX Lqq1a clone confirmation by restriction enzyme digestion	110
3.9	Agarose electrophoresis analysis of pMcl1-BUTX Lqq1a clone confirmation by colony PCR amplification	111
3.10	The schematic representation of the BUTX Lqq1a arrangement in the pMcl1-BUTX Lqq1a vector	111
3.11	Light microscopy studies of *B. bassiana* protoplast preparation	112
3.12	*B. bassiana*-BUTX Lqq1a colonies observed on Czapek Dox agar selection medium	112
3.13	Agarose electrophoresis analysis of gel purified products for *M. anisopliae* vector construction	113
3.14	Agarose electrophoresis analysis of purified plasmids from selected pMcl1-BUTX Lqq1a- Bar-Mcl1 gene clones.	113
3.15	Agarose electrophoresis images of gel purified products for pCAMBIA3300 binary vector cloning	114
3.16	Agarose images of Plasmid DNA isolated from selected *M.anisopliae* pMcl1-BUTX Lqq1a clones	114
3.17	Agarose electrophoresis analysis of pMcl1-BUTX Lqq1a clone confirmation by restriction enzyme digestion.	115
3.18	The schematic representation of the BUTX Lqq1a arrangement in the pMcl-BUTX Lqq1a	115

3.19 Agarose electrophoresis analysis of *B. bassiana* genomic DNA 116

3.20 Agarose electrophoresis analysis of *B. bassian a*clone confirmation by PCR with gene-specific primers 116

3.21 Agarose electrophoresis analysis of *M. anisopliae* genomic DNA isolation and PCR clone confirmation studies 117

3.22 Agarose image of PCR products amplified using *M. anisopliae* clones genomic DNA an PCR confirmation 117

3.23 Agarose gel electrophoresis analysis of total RNA isolated from *B. bassiana* BUTX Lqq1a clones 118

3.24 Agarose gel electrophoresis analysis of total RNA isolated from *M. anisopliae* BUTX Lqq1a clones 118

3.25 Semi-quantitative RT-PCR analysis of cDNA synthesized from *B. bassiana* clones total RNA 119

3.26 Semi-quantitative RT-PCR analysis of cDNA synthesized from *M. anisopliae* clones total RNA 119

3.27 Western blotting analysis of hemolymph induced Bb-wild type and Bb-BUTX Lqq1a strain 120

3.28 Western blotting analysis of hemolymph induced wild type and Ma-BUTX Lqq1a strain 120

3.29 Kaplan-Meier survival plot of *Phyllophaga smithi* 121

3.30 Topical application Bioassay conducted with Ma-BUTX Lqq1a and unmodified wild type strain 121

Chapter 4

4.1 Bacterial codon-optimized Linker GNA sequence 147

4.2 Gel images of pET28a and Linker GNA cloning and its confirmation by PCR 148

4.3 Agarose gel electrophoresis analysis of pET28a-Linker GNA clone confirmation by PCR 148

4.4 Bacterial codon optimized fused β-BUTX Lqq1a and Linker GNA sequence 149

4.5 Agarose gel images of pET28a and β-BUTX Lqq1a/Linker GNA cloning and its confirmation by PCR 150

4.6 Agarose gel electrophoresis analysis of pET28a-BUTX Lqq1a/GNA clone confirmation by double digestion method 150

4.7 Schematic representation of GNA and fusion protein β-BUTX Lqq1a/GNA with N-terminal $(His)_6$ – tag 151

4.8 The SDS-PAGE analysis of Ni-NTA affinity purified Linker GNA protein 151

4.9	The SDS-PAGE analysis of Ni-NTA purified β-BUTX Lqq1a/Linker GNA protein	152
4.10	SDS-PAGE (16% Acrylamide gel in Tris-Glycine buffer) analysis of purified recombinant GNA and fusion protein β-BUTX Lqq1a/GNA	153
4.11	Cytotoxicity assay conducted with purified GNA on the viability of *Sf*-9, *Sf*-21 insect cell lines, and J774a.1 mouse cell lines as determined by MTT assay	154
4.12	MTT cell viability assay conducted purified β-BUTX Lqq1a/GNA on the viability of *Sf*-9, *Sf*-21 insect cell lines, and J774a.1 mouse cell lines	155
4.13	Fluorescence microscopy analysis of recombinant GNA treated *Sf*-9, *Sf*-21, and J774a.1 cell lines stained with FDA and PI	159
4.14	Fluorescence microscopy analysis of recombinant β-BUTX Lqq1a/GNA treated *Sf*-9, *Sf*-21, and J774a.1 cell lines stained with FDA and PI	157
4.15	Fluorescence microscopy analysis of recombinant GNA treated *Sf*-9, *Sf*-21 and J774a.1 cell lines stained with DAPI	158
4.16	Fluorescence microscopy analysis of recombinant β-BUTX Lqq1a/GNA treated *Sf*-9, *Sf*-21 and J774a.1 cell lines stained with DAPI	158
4.17	Mitochondrial membrane potential assay of recombinant GNA treated *Sf*-9, and *Sf*-21 insect cell lines	159
4.18	Mitochondrial membrane potential assay of recombinant β-BUTX Lqq1a/GNA treated *Sf*-9, and *Sf*-21 insect cell lines	160
4.19	Cell cycle analysis of GNA and β-BUTX Lqq1a/GNA treated *Sf*-9 and *Sf*-21 insect cell lines	161
4.20	RT-qPCR based gene expressional analysis of GNA and β-BUTX Lqq1a/GNA treated *Sf*-9 and *Sf*-21 insect cell lines	162
4.21	Injection bioassay performed with purified recombinant proteins in *S. litura*	163

Chapter 5

5.1	Agarose gel electrophoresis analysis of PCR amplified and gel purified products of GPDH promoter, Mcl1sp and Cyt1Aa fusion.	193
5.2	Agarose gel electrophoresis analysis of Colony PCR clone confirmation for the pBUTX Lqq1a/Cyt1Aa clones.	193
5.3	Schematic representation of arrangement of BUTX Lqq1a and Cyt1Aa constructs in the binary vector.	194
5.4	Agarose gel electrophoresis analysis of plasmids isolated from pBUTX Lqq1a/Cyt1Aa clones.	194

5.5	Agarose gel electrophoresis image analysis of PCR amplified and gel purified fragments of truncated Cry1Ac and GNA	194
5.6	Schematic representation of Cry1Ac truncation and fusion with GNA.	195
5.7	Agarose gel electrophoresis analysis restriction enzyme digested plasmids and PCR purified fusion fragments for pCAMBIA cloning	196
5.8	Agarose gel electrophoresis analysis of colony PCR clone confirmation	196
5.9	Agarose gel electrophoresis analysis of pBUTX Lqq1a/tCry1Ac-GNA clone confirmation by restriction enzyme digestion.	197
5.10	Graphical representation of arrangement of pyramided genes in the binary vector pBUTX Lqq1a/tCry1Ac-GNA	197
5.11	Agarose gel electrophoresis analysis of genomic DNA isolated from Ma-BUTX Lqq1a/Cyt1Aa clones.	198
5.12	Agarose gel electrophoresis analysis of BUTX Lqq1a amplification by PCR from Ma-BUTX Lqq1a/Cyt1Aa clones	198
5.13	Agarose gel electrophoresis analysis Cyt1Aa amplification by PCR from Ma-BUTX Lqq1a/Cyt1Aa clones	198
5.14	Agarose gel electrophoresis analysis of genomic DNA isolated from selected Ma-BUTX Lqq1a/tCry1Ac-GNA clones	199
5.15	Agarose gel electrophoresis analysis of BUTX Lqq1a amplification by PCR from Ma-BUTX Lqq1a/tCry1Ac-GNA clones	199
5.16	Agarose gel electrophoresis analysis of tCry1Ac-GNA amplified from Ma-BUTX Lqq1a/tCry1Ac-GNA clones	200
5.17	Agarose gel electrophoresis analysis of P*Mcl1*-BUTX Lqq1a gene amplified from Ma-BUTX Lqq1a/tCry1Ac GNA clones	200
5.18	Semi-quantitative RT-PCR analysis of Cyt1Aa and Cry1Ac transcripts	201
5.19	Semi-quantitative RT-PCR analysis of BUTX Lqq1a transcripts	201
5.20	Semi-quantitative RT-PCR analysis of GNA transcripts	202
5.21	Semi-quantitative RT-PCR analysis of GAPDH transcripts	202
5.22	Western blotting analysis of hemolymph induced Ma-wild type and Ma-BUTX Lqq1a/Cyt1Aa and tCry1Ac-GNA strains	202
5.23	Insect bioassay performed with wild type *M. anisopliae* and Ma-BUTX Lqq1a/Cyt1Aa clones	203
5.24	*Phyllophaga* insect bioassay performed with *M.anisopliae* expressing BUTX-Lqq1a/Cyt1Aa	203
5.25	*Phyllophaga* insect bioassay performed with *M. anisopliae* expressing BUTX Lqq1a/tCry1Ac-GNA	204
5.26	Injection bioassay conducted with *M. anisopliae* spores on *S. litura*	204
5.27	*M. anisopliae* GPDH promoter sequence	205

Chapter 6

6.1	Plasmid map of pUC57 harboring BUTX Lqq1a	224
6.2	Plasmid map of pAL1 harboring sGFP	224
6.3	PCR fragments amplified for BUTX Lqq1a/sGFP cloning into pCAMBIA3300 vector	225
6.4	Colony PCR confirmation for BUTX Lqq1a/sGFP cloning into pCAMBIA vector	225
6.5	Plasmids isolated from the pBUTX Lqq1a/sGFP clones	226
6.6	Clone confirmation by restriction enzyme digestion of pBUTX Lqq1a/sGFP clonal plasmids	226
6.7	Schematic representation of pBUTX Lqq1a/sGFP binary vector	227
6.8	Genomic DNA isolated from *M. anisopliae* carrying BUTX Lqq1a/sGFP	228
6.9	Clonal confirmation by Bar gene amplification for *M. anisopliae* carrying BUTX Lqq1a/sGFP	228
6.10	PCR clonal confirmation by BUTX Lqq1a/sGFP gene amplification from Ma-BUTX Lqq1a/sGFP	229
6.11	PCR clonal confirmation for the P*Mcl1*-BUTX Lqq1a/sGFP gene amplified from Ma-BUTX Lqq1a/sGFP	229
6.12	Semi-quantitative RT-PCR analysis of BUTX Lqq1a transcripts amplification from Ma-BUTX Lqq1a/sGFP clones	230
6.13	Western blot analysis of fusion protein BUTX Lqq1a/sGFP expression from Ma-BUTX Lqq1a/sGFP clones	230
6.14	Time of expressional analysis of BUTX Lqq1a/sGFP from Ma-BUTX Lqq1a/sGFP clones using Fluorescence microscopy	231
6.15	Time of expressional analysis of BUTX Lqq1a/sGFP from Ma-BUTX Lqq1a/sGFP clones using Fluorescence microscopy at 1 hr interval	232
6.16	Time of expressional analysis of BUTX Lqq1a/sGFP from Ma-BUTX Lqq1a/sGFP clones using Fluorescence microscopy at 3 hr interval	232

List of Abbreviations

UNFAO	United nations Food and Agricultural Organization
2,4-D	2,4-Dichlorophenoxyacetic acid
GABA	Gamma-aminobutyric acid
VGSC	Voltage Gated Sodium Channel
VGCC	Voltage Gated Chlorine Channel
DDT	Dichlorodiphenyltrichloroethane
CYPs	Cytochrome P450s
Mtx	Mosquitocidal toxin
Bin	Binary toxin
Bt	*Bacillus thuringiensis*
Cry	Crystal toxin
Cyt	Cytolytic toxin
kbp	Kilo base pair
Vip	Vegetative insecticidal protein
APN	Aminopeptidase N
ALP	Alkaline Phosphatase
AcMNPV	*Autographa californica* multinucleopolyhedrovirus
DNA	Deoxy ribonucleic acid
Cit1a	Cyto-insectotoxin
BmNPV	*Bombyx mori* Nucleopolyhedrovirus
AalT	*Andructonus australis* insect toxin
PKS	polyketide synthase
NRPS	Non-ribosomal peptide synthetases
HYD1	Hydrophobin 1
MAD1	*Metarhizium* Adhesin 1
MAPK	Mitogen-activated protein kinase
CYP52X1	Cytochrome P450 monooxygenase
MrpacC	*Metarhizium robertsi* pH-responsive transcription factor
CHIT1	Chitinase protein
Pr1	Protease
BmChBD	*Bombyx mori* Chitin Binding Domain
BbChBD	*Beauveria bassiana* Chitin Binding Domain
Bbchit1	*Beauveria bassiana* chitinase
CDEP1	Cuticle degrading protease from *Beauveria bassiana*
Bjα IT	*Buthotus judaicus* α-insect toxin

PPAFs	Prophenoloxidase activation factors
Bi-VSP	*Bombus ignitus* venom serine protease
BmK NT1	*Buthus martensii* Karsch Neurotoxin
β-BUTX	β- toxin from Buthidae family scorpion
Lqq1a	*Leuirus quinquestriatus quinquestriatus* toxin 1 a
CAD	Cadherin like proteins
ABC transporters	Adenosine triphosphate (ATP)-binding cassette transporters
IPM	Integrated pest management
Cry1A Mod	Modified Cry1A protein
GalNAc	N-acetyl D- galactosamine
Bti	*Bacillus thuringiensis* subsp. *israelensis*
UDA	*Urtica dioica* agglutinin
GNA	*Galanthus nivalis* agglutinin
Hv1a	*Hadronyche versuta* toxin 1 a
Pl1a	*Pireneitega luctuosa* toxin 1 a
ASAL	*Allium sativum* agglutinin
t-Cry1Ac	Truncated Cry1Ac protein
sGFP	Synthetic Green Fluorescent protein
BTI-TN-5B1-4	*Trichoplusia ni* insect cell line
$(His)_6$	Six Histidine tag
Sf-9	*Spodoptera frugiperda* insect cell line
PBS	Phosphate buffer saline
MTT	3-(4,5-dimethylthiazol-2-yl)-2,5-diphenyl tetrazolium bromide
Na_v	Voltage gated sodium channel
Ca_v	Voltage gated calcium channel
NaCl	Sodium chloride
Ni-NTA	Nickel-Nitrilotriacetic Acid
SDS-PAGE	Sodium Dodecyl Sulfate-Poly Acrylamide Gel electrophoresis
MALDI-TOF	Matrix-assisted laser desorption/ionization time of flight
TBS	Tris Buffered Saline
TNM-FH	*Trichoplusia ni* medium developed by W.F.Hink
FBS	Fetal Bovine Serum
DMSO	Dimethyl sulfoxide
PI	Propidium Iodide
FDA	Fluorescene Diacetate
FACS	Fluorescent activated cell sorter
IPTG	Isopropyl Thiogalactopyranoside
LqhαIT	*Leiurus quinquestriatus hebraeus* insect toxin

Abbreviations

P*Mcl1*	*Metarhizum* collagen like protein promoter
UTR	Untranslated region
Mcl1sp	*Metarhizium* collagen like protein signal peptide sequence
DTT	Dithiothreitol
HEPES	(4-(2-hydroxyethyl)-1-piperazineethanesulfonic acid)
pMcl1-BUTX Lqq1a	Plasmid harbouring P*Mcl1*-BUTX Lqq1a
EDTA	Ethylenediaminetetraacetic acid
cMoL	Coagulant *Moringa oleifera* lectin
ConA	Concanavalin A
PNA	Peanut agglutinin
SFl1	*Segestria florentina*
DlasiL	*Dioclea lasiocarpa* lectin
DAPI	4′,6-diamidino-2-phenylindole
P*gpdh*	Glyceraldehyde 3-phosphate dehydrogenase

SYNOPSIS

INTRODUCTION

The rising population, dietary preferences and urbanization in developed as well as in developing countries require tremendous steps to enhance agriculture production to meet the accretive demand. It can only be met by considerably increasing agricultural yield and modification in the use of inputs. However, agricultural productivity is highly demarked by changes in climatic conditions and continuous attacks by pests. With advent of synthetic and biological insecticides/pesticides, numerous pests gradually developed resistance to most of the insecticides, leading to their resurgence (Sundström et al. 2014). Alternatively, biological organisms such as bacteria, fungi, and virus being sustainably used to control insect pests.

Various fungi genera effectively being employed to lessen the intensity of pest attack. Potentially, *Beauveria* spp. and *Metarhizium* spp. are broad host range environmental friendly entomopathogenic fungi, occur ubiquitously in nature and approved by United States environmental protection agency (US-EPA) for controlling insect pests (Darbro et al. 2011, Roberts and St Leger 2004). These entomopathogens are reported to infect various insect species which belongs to different orders such as Coleoptera (Williams et al. 2013), Diptera (Kim et al. 2014), Lepidoptera (Ramzi and Zibaee 2014), Hemiptera (Lacey et al. 2011), and Thysanoptera (Wu et al. 2013). In India, alone over 200 bio-pesticide formulations reported to be based on *Beauveria* and *Metarhizium*. However, bio-pesticides cover only 5% of Indian Pesticide market (Kumar et al. 2019). Despite the fact that entomopathogens do not required to be ingested to pursue on insect, the major reason for the biological pesticides not being able to compete with other synthetic chemical

pesticide is their ability to make agile response to neutralize the major economic agricultural impact caused by insect pests (Gressel 2001, St Leger et al. 1996).

Advancement in molecular techniques facilitated researchers globally, to enhance fungi virulence by over expressing the endogenous proteins such as chitinase, and proteases (St Leger et al. 1996). In addition, virulence of entomopathogenic fungi heightened by expression of heterologous toxic proteins (Fan et al. 2011, Lu et al. 2008). Major heterologous toxic proteins reported to exploited are from scorpion and spider neurotoxins. These neurotoxins purportedly produced in wake of defense and/or for predation. Neurotoxins are short peptides ranges from 30-80 amino acids mainly targeting ion channels. Long chain peptide which primarily targets sodium ion channel have been classified as excitatory and depressant toxin (Zlotkin et al. 1985).

The β-BUTX Lqq1a is an β-insect toxin 1 from scorpion *Leiurus quinquestriatus quinquestriatus* and this excitatory toxin binds to the receptor site-4 in domain II of insect voltage gated sodium channels (VGSCs). This toxin purified from crude venom caused fast excitatory contraction paralysis in the fly larvae and proven 40 times more toxic than the crude venom (Kopeyan et al. 1990, Zlotkin et al. 1985) and it also shares high degree of similarity with the well-known scorpion β-insect neurotoxin AaIT from *Andructonus australis*. β-BUTX Lqq1a was able to bind competitively with synaptosomal membrane vesicles that were previously treated with AaIT. It has been experimentally proven that β-insect excitatory toxins bind to the voltage sensing module in the extracellular loop of S1-S2 and S3-S4 of domain II and pore forming module of domain III in the VGSCs of insects (Gurevitz 2012)

Other heterologous proteins exploited to modulate the fungal virulence are by the use of plant defense molecule called lectins and bacterial Crystal and Cytolytic toxins.

Synopsis

Lectins are present in both monocot as well as dicot plants, which are reversible carbohydrate binding proteins or glyco-conjugates, that can precipitate polysaccharides and agglutinate cells (Van Damme et al. 1987, Vandenborre et al. 2011). Various types of Lectins are classified based on evolutionarily and structurally related domains. Snowdrop lectin belongs to *Galanthus nivalis* Agglutinin (GNA)-lectin family that is a 13 kDa protein primarily exist as a tetrameric protein which specially binds to α-D mannose residues and readily agglutinates rabbit erythrocytes (Van Damme et al. 1987). Snowdrop lectin reported to exhibit activity against root nod nematodes (Ripoll et al. 2003), sap sucking rice pest (Bharathi et al. 2011), aphids (Birch et al. 1999), mites (McCafferty et al. 2008), and tomato moth (Fitches et al. 1997). Evident activity against insects includes mortality, reduction in feeding, and action on metamorphosis. The exact mode of action of lectins on insect, by binding and blocking the absorption of nutrients by insect midgut epithelial cells. In addition, some of the lectins disrupts and traverse across the midgut peritropic matrix and exert the action in the cavity (Fitches et al. 2001, Fitches et al. 2012).

Bacillus thuringiensis is a gram-positive insect pathogenic bacterium, produces paracrystal inclusions called δ-endotoxins such as Cry and Cyt during sporulation. These Cry toxins are effective against Lepidoptera, Coleoptera and Hymenoptera and Diptera. However, Cyt toxins are active only against Diptera and Coleoptera insects. Cry toxin consist of three domains where domain I contains α-helices which help in pore formation in insect midgut, domain II and III involve in receptor binding and specificity. Contrarily, Cyt toxins need not to bind with the receptors, directly interact with membrane lipids, and exert action by inserting into membrane and forming pores (Bravo et al. 2011, Derbyshire et al. 2001, Gomez et al. 2007).

Gene pyramiding is one of the vital approach to eliminate the problem associated with insect resistance to a particular gene product or specific toxins (Maqbool et al. 2001). However, venom purified β-BUTX Lqq1a reported to be toxic against fly larvae, potential activity against agricultural crop pests remain to be elucidated. Bacterial expression system subsides the hurdle in achieving purification of toxins/proteins in greater amount which avoid the deadening job of purifying specific proteins from the crude venom. Expression and purification of fusion proteins were reported for *Galanthus nivalis* agglutinin with other neurotoxins by using various expression system such as bacteria *Escherichia coli* and *Pichia pastoris* (Down et al. 2006, Fitches et al. 2012).

The present study has been hypothesized that exploitation of scorpion neurotoxin, snowdrop lectin and *B. thuringiensis* Crystal and Cytolytic toxin would enhance the pathogenicity of Entomopathogenic fungi against agricultural crop pests and it might lead to the reduction in development of resistance in insects against particular targeted gene.

OBJECTIVES

The objective of the study was designed to express the insecticidal toxins recombinantly in the bacterial expression system and testing purified recombinant proteins against insect cell lines and insect system. Additionally, expression of these toxin in entomopathogenic fungi, either separately or in combination with other toxins and testing their efficacy against some of the agricultural pest.

1. Expression and purification of β-BUTX Lqq1a toxin and its biological activity against insect cells and agricultural insect pests.
2. Cloning and expression of β-BUTX Lqq1a in *Beauveria bassiana* and *Metarhizium anisopliae* and their insect toxicity assay.
3. Bacterial expression and purification of fusion protein containing β-BUTX Lqq1a/GNA Lectin and their cytotoxicity assay against insect cell lines.
4. Cloning and expression of β-BUTX Lqq1a, Cyt1Aa and t-Cry1Ac/GNA in *Metarhizium anisopliae* and insects toxicity assay.
5. Time expression analysis of β-BUTX Lqq1a/sGFP in *M. anisopliae.*

BRIEF DESCRIBTION ABOUT THE RESEARCH WORK

Chapter 1: Introduction, Review of Literature and Objectives

This chapter describes the importance of food security, agricultural productivity, and crop damage caused by insect pests and application of synthetic chemical pesticides to overcome the challenges dealt with. Effect of synthetic chemical pesticides and the major drawbacks associated with the uses also discussed in detail based on the documented literatures. Chemical pesticide alternative i.e. biological pesticides and its advantage and disadvantages were also considered. Entomopathogenic fungi *M. anisopliae* and *B. bassiana* based biological pesticides, their mode of action and enzyme involved in pathogenesis were also discussed elaborately. Toxins involved in increasing the virulence of biological pesticides were discussed with clearly emphasizing the role of heterologous genes/toxins in increasing the pathogenicity. Finally, methods involved to reduce the development of resistance in insects by gene pyramiding with heterologous proteins with various functional properties also detailed, with relevant to the framed objective of the proposed work.

Chapter 2: Expression and purification of β-BUTX Lqq1a toxin and its biological activity against insect cells and agricultural insect pests.

The chapter was to determine the toxicity of bacterially purified β-BUTX Lqq1a against various insects as well as insect cell line. In the present study cloning, optimized expression, purification of β-BUTX Lqq1a toxin and characterization was performed initially. Further, cytotoxic assessment against insect cell line *Sf*-21 resulted in apoptotic like structures and insect toxicity assessment with *H. armigera* and *S. litura.*

Results:

1.1 Expression, purification of β-BUTX Lqq1a and *S. frugiperda* insect cell (*Sf*-21) toxicity assessment

a) Scorpion neurotoxin β-BUTX Lqq1a was successfully codon optimized and cloned in pUC57 vector resulting in pUC57-β-BUTX Lqq1a

b) PCR amplified β-BUTX-Lqq1a gene was further cloned in expression vector pET28a and protein expression was optimized in Terrific Broth (TB) medium supplemented with 1.5% glycerol and final purification was performed using Ni-NTA affinity chromatography.

c) N-terminal His-Tag was removed by using thrombin protease treatment and final purification was done using Size exclusion chromatography (**Fig. 1**)

d) *Sf*-21 cell viability assay conducted with purified recombinant β-BUTX Lqq1a resulted in significant ($p < 0.002$) dose dependent cytotoxicity (**Fig.2**)

e) Fluorescence microscopy analysis also revealed the cytotoxic activity of β-BUTX Lqq1a on *Sf*-21 cell lines with significant morphological changes such as cell shrinkage, membrane blebbing and apoptotic structures

1.2 *In vivo* entomotoxic assessment of purified β-BUTX Lqq1a

a) β-BUTX Lqq1a toxin intra-hemocoellic injection in *H. armigera* showed significant ($p < 0.0001$) larval mortality with LC_{50}=0.13 µg insect^{-1}, as well as immediate paralysis and reduced feeding were also observed

b) *S. litura* injected with purified β-BUTX Lqq1a toxin resulted initial paralysis, shortening and blackening of insect body, significant death ($p < 0.0001$) and predicted LC_{50}=0.147 µg insect $^{-1}$

Fig. 1

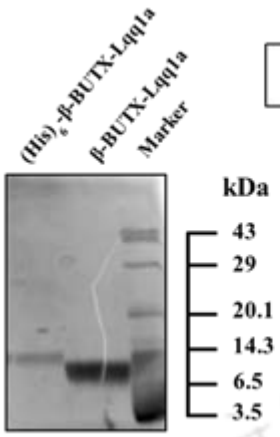

Fig. 2

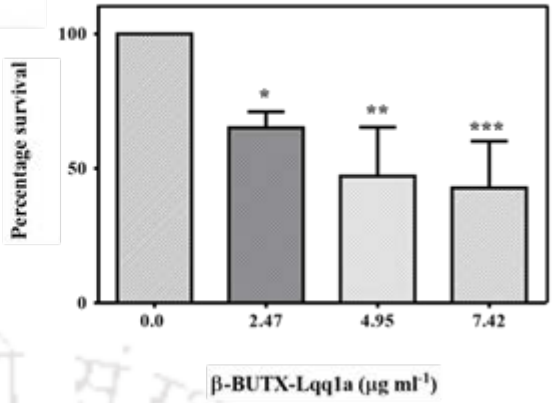

Fig.1 SDS-PAGE (16% acrylamide gel in Tris-glycine buffer) analysis of undigested and digested $(His)_6$-β-BUTX Lqq1a protein after size exclusion chromatography purification. Marker denotes the standard low range protein molecular weight marker.

Fig. 2 Effect of various concentration of purified β-BUTX-Lqq1a toxin on the viability of *Sf*-21 insect cell lines determined by MTT assay.

Chapter 3: Cloning and expression of β-BUTX Lqq1a in *Beauveria bassiana* and *Metarhizium anisopliae* and insects toxicity assay

3.1 Cloning and expression of P*Mcl1*-BUTX Lqq1a in *B. bassiana*

The main objective of this study is to clone BUTX Lqq1a under the control of hemolymph specific inducible promoter *Mcl1* from *M. anisopliae* and directing the toxic protein into hemolymph with the help of Mcl1 signal peptide sequence. After the successful genomic integration of transgene confirmation, it was further experimented on hemolymph inducible characteristics with silk worm hemolymph by western blot and semi quantitative RT-PCR analysis.

Results:

3.1.1 Vector construction and transformation by protoplast cum electroporation method for *B. bassiana*

Mcl1 promoter and BUTX Lqq1a gene was successfully fused by overlap extension PCR method followed by its cloning into double digested pAL1 which resulted in the pMcl1-BUTX Lqq1a expression vector. Optimized protoplast cum electroporation method was followed to transfer the pMcl1-BUTX Lqq1a construct into *B. bassiana*. Optomized lysis buffer containing 20 mM KH_2PO_4, 0.7 M KCl and 0.7 M $(NH_4)_2SO_4$ (pH 6.8) and 1% lysing enzyme (from *Trichoderma harzianum*, Sigma) was used to remove the cell wall and parameters optimized for electroporation was 900 V, 25 µF capacitance and 600 mΩ resistance.

3.1.2 Selection and BUTX Lqq1a expressional analysis by semi-quantitative RT-PCR and Western blot analysis

After, the clonal selection on 300 µg ml^{-1} glufosinate ammonium containing M-100 minimal medium, and genomic DNA integration of BUTX Lqq1a was confirmed by PCR with gene specific primers. Further, the expression of BUTX Lqq1a was analyzed by hemolymph induction and semi-quantitative RT-PCR method.

3.2 Cloning and expression of P*Mcl1*-BUTX Lqq1a in *M. anisopliae* and insect bioassay

The main aim of this part of study is to clone BUTX Lqq1a under the control of MCL1 promoter and transform them into *M. anisopliae*. To encourage the homologous recombination, BUTX Lqq1a was placed between MCL1 promoter and Mcl1 gene from *M. anisopliae* and transformed using *Agrobacterium* mediated transformation. Further

testing the genomically integrated clones on *Phyllophaga smithi* resulted in significant mortality and mycelia engorgement.

Results:

3.2.1 Cloning and expression of BUTX Lqq1a in *M. anisopliae*

Fungal codon optimized BUTX Lqq1a along with 5-UTR region was successfully fused with Mcl1 Promoter (P*Mcl1*) and Mcl1 gene using overlap extension PCR. In addition, fused fragments were then cloned in pCAMBIA 3300 binary vector, which resulted in binary vector pMcl1-BUTX Lqq1a-Mcl1 gene for *Agrobacterium*-mediated transformation.

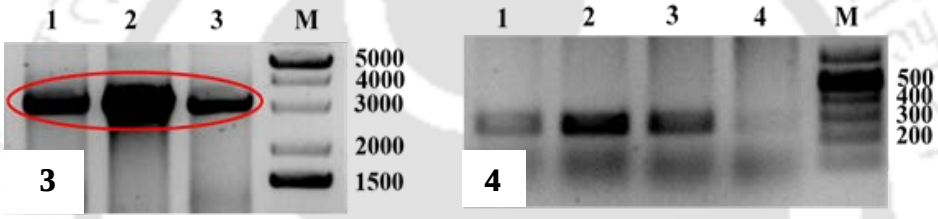

Fig. 3 Agarose gel image of PCR products amplified using *M. anisopliae* clones genomic DNA. **Lane 1, 2, and 3: P*Mcl1*-BUTX Lqq1a** PCR products for *M. anisopliae* clone confirmation (~3 Kbp), Lane M: O' GeneRuler 1 KbPlus DNA Ladder.

Fig. 4 Agarose gel image of PCR products amplified using Ma-BUTX Lqq1a clones genomic DNA. **Lane 1, 2, 3, 4, and 5: BUTX Lqq1a** PCR products of Ma-BUTX Lqq1a clones **(295 bp),** Lane M: O' GeneRuler 1 KbPlus DNA Ladder.

3.2.2 *Phyllophaga smithi* insect bioassay with Ma-BUTX Lqq1a

Insect bioassay conducted with the *M. anisopliae* expressing BUTX Lqq1a on *P. smithi* resulted in significant mortality when compared with control (**Fig. 5A and B**)

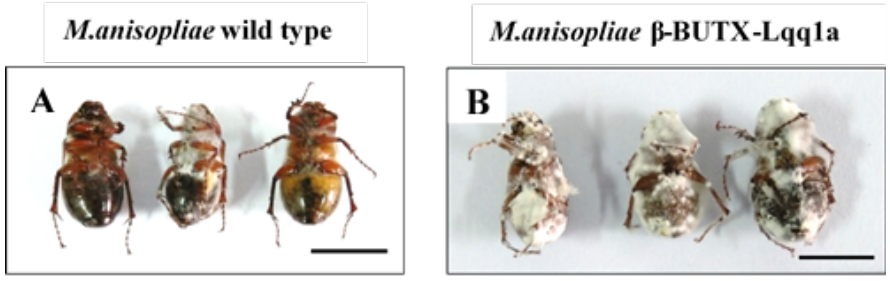

Fig. 5. *Phyllophaga* insect bioassay. **A)** *M. anisopliae* wild type infected *Phyllophaga* and **B)** *M. anisopliae* expressing β-BUTX Lqq1a infected *Phyllophaga* insects. Scale bar represents 1 cm.

Chapter 4: Bacterial expression and purification of fusion protein containing β-BUTX Lqq1a/GNA Lectin and their cytotoxicity assay against insect cell lines

The main objective of this study is to construct the fusion protein containing scorpion neurotoxin β-BUTX Lqq1a and *Galanthus nivalis* agglutinin GNA. Upon successful purification further testing their cytotoxicity potential against various insect cell line and entomotoxicity studies against *S. litura.*

Results:

4.1 GNA and β-BUTX Lqq1a/ GNA cloning and expression

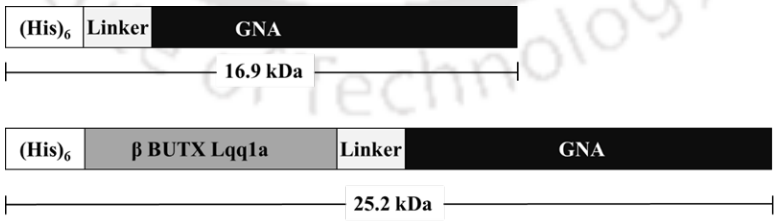

Fig. 6 Schematic representation of GNA as well as fusion protein containing β-BUTX Lqq1a/ GNA

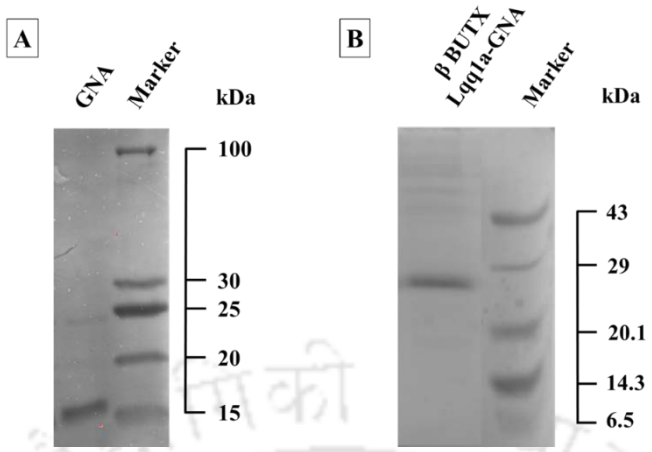

Fig. 7 SDS-PAGE (16% acrylamide gel in Tris-glycine buffer) analysis of purified recombinant proteins. A) Recombinant GNA purified using Ni-NTA affinity chromatography. Lane 1 is GNA, size approximately 16.9 kDA protein. Lane 2 is low range molecular weight marker. B) Recombinant fusion protein β-BUTX Lqq1a/GNA purified using affinity chromatography. Lane 1: fusion protein containing β-BUTX Lqq1a and GNA, predicted theoretical molecular weight is approximately 25.2 kDa.

4.2 Cytotoxicity studies of GNA and fusion protein β-BUTX Lqq1a/GNA treated cell lines:

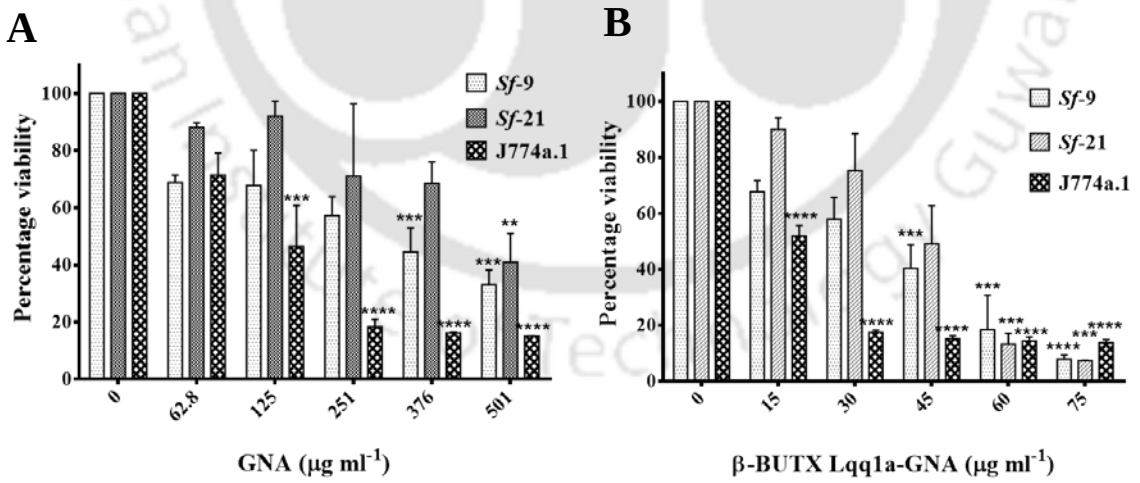

Fig. 8 MTT assay conducted with various concentration of purified recombinant GNA **(A)** and β-BUTX Lqq1a/GNA **(B)** on the viability of *Sf*-9, *Sf*-21 insect cell lines and J774a.1 mouse cell line. One-way ANOVA followed by Dunnett's pairwise multiple comparison analysis indicated that both GNA and fusion protein β-BUTX Lqq1a/GNA had affected cell proliferation in dose dependent manner ($p < 0.0001$) when compared with control.

4.3 Fluorescence microscopy studies of GNA and fusion protein β-BUTX Lqq1a/GNA treated cell lines

Both GNA and β-BUTX Lqq1a/GNA treated cell lines appeared to exhibit deformed nucleus and chromosomal shrinkage when stained with DAPI nuclear stain.

4.4 Flow cytometry and RT-qPCR analysis

Flow cytometry analysis of GNA treated *Sf*-9 and *Sf*-21 cells indicated the accumulation of cells at G2/M phase of cell cycle. Correspondingly, fusion protein treated *Sf*-9 and *Sf*-21 cells also observed to be arrested in G2/M phase of cell cycle. These results are in accordance with other lectin cell cycle arrest, suggesting the possible correlation between DNA damage and apoptosis mediated cell death. Multi-fold relatively expression of Caspase 2 in treated *Sf*-9 and *Sf*-21 cell indicated significant mitochondrial caspase mediated apoptotic death.

Chapter 5: Cloning and expression of β-BUTX Lqq1a, Cyt1Aa and t-Cry1Ac/GNA in *Metarhizium anisopliae* and insects toxicity assay

5.1 Cloning and Expression of β-BUTX Lqq1a and Cyt1Aa in *M. anisopliae*

The main objective of this study is to exploit potency of Cyt1Aa protein from *Bacillus thuringiensis* subsp. *israelensis* in combination with Scorpion neurotoxin β-BUTX Lqq1a when expressed in *M. anisopliae*. β-BUTX Lqq1a was expressed under the control of promoter Mcl1 and Cyt1Aa was driven by GPDH promoter.

Results:

a) Cloning and expression of β-BUTX Lqq1a and Cyt1Aa

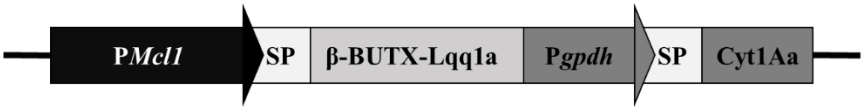

Fig. 9 Schematic representation of expression constructs containing β-BUTX Lqq1a and Cyt1Aa under the control of various promoters

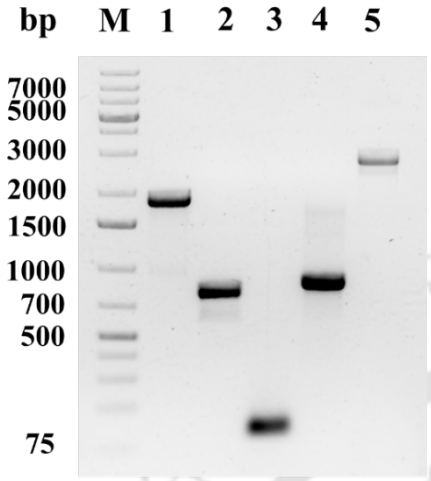

Fig. 10 GPDH, Mcl1Sp and Cyt1Aa fusion

1) GPDH promoter amplified from *M. anisopliae* genomic DNA **(1833 bp)**

2) Bt Cyt1Aa gene product (**810 bp)** from ***Bacillus thuringiensis* HD522**

3) Mcl1 signal peptide **(117 bp) from *M. anisopliae***

4) Bt Cyt1Aa and Mcl1 sp fused product **(867 bp)**

5) GPDH promoter, Bt Cyt1Aa and Mcl1 sp fused product (**2,640 bp**)

M- 1 Kbplus gene ruler

b) Insect bioassay of *M. anisopliae* expressing BUTX Lqq1a/Cyt1A

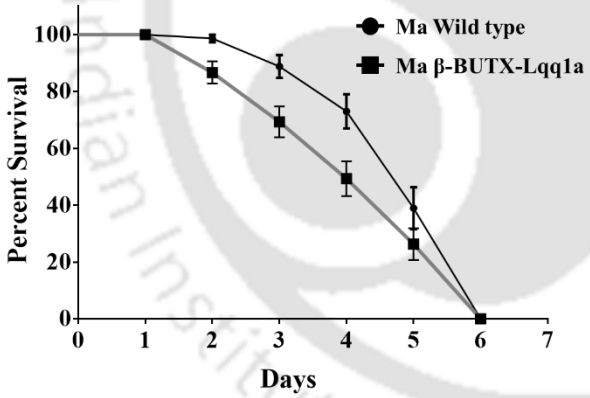

Fig. 11 Kaplan-Meier survival plot of *Phyllophaga smithi* (n=15, Log-rank (Mantel-Cox) test p=0.0082) bioassay conducted with *M. anisopliae* wildtype and *M. anisopliae* BUTX-Lqq1a/Cyt1Aa

5.2 Expression and Insect bioassay of *M. anisopliae* expressing BUTX Lqq1a and truncated Cry1Ac/GNA

The main objective of the study is to develop *M. anisopliae* expressing the fusion protein containing β-BUTX Lqq1a under the control of Mcl1 promoter and GPDH promoter driven truncated Cry1Ac fused with GNA to enhance the carbohydrate binding and entomotoxicity.

Results:

Cloning and expression of BUTX Lqq1a and tCry1Ac/GNA in *M.anisopliae*

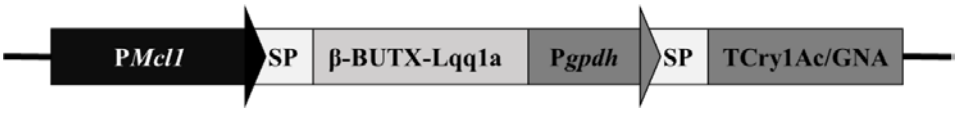

Fig. 12. Schematic representation of expression constructs containing BUTX Lqq1a /tCry1Ac-GNA under the control of various promoters

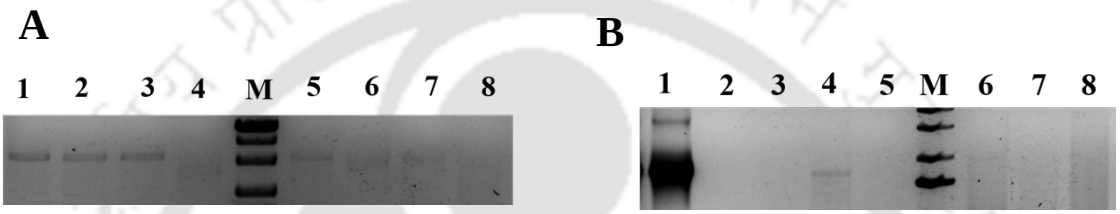

Fig. 13. A) Mcl1 promoter BUTX Lqq1a PCR clone confirmation for the *M. anisopliae* BUTX Lqq1a/tCry1Ac-GNA clones **B)** tCry1Ac-GNA PCR clone confirmation for the *M. anisopliae* BUTXLqq1a /tCry1Ac-GNA clones.

Chapter 6: Time expression analysis of β-BUTX Lqq1a/sGFP in *M. anisopliae*

The aim of this study is to analyze the real time expression of BUTX Lqq1a driven by Mcl1 promoter during the insect pathogenesis by tagging with sGFP.

Results:

a) Cloning and expression of β-BUTX Lqq1a/sGFP in *M.anisopliae*

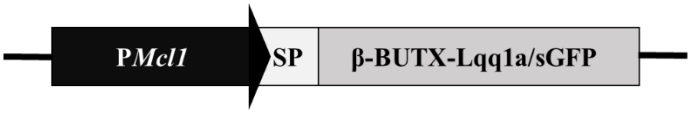

Fig. 14. Schematic representation of expression constructs containing BUTX Lqq1a/sGFP under the control of Mcl1 promoter.

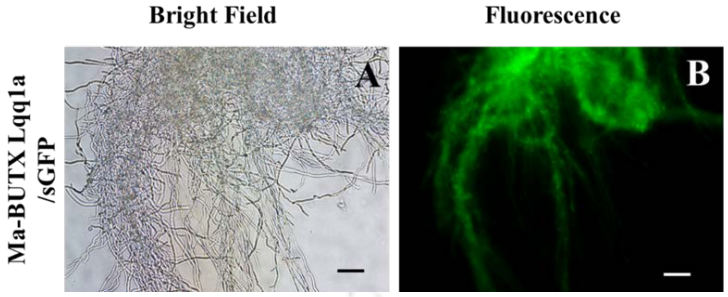

Fig. 15 Time of expressional analysis of BUTX Lqq1a/sGFP from Ma-BUTX Lqq1a/sGFP clones using Fluorescence microscopy at 1 h interval. A and B represents the Ma-BUTX Lqq1a/sGFP induced at 1 h interval in bright field as well as fluorescence field. Scale bar represents 20 µM.

Significant findings:

- Bacterially purified scorpion recombinant protein β-BUTX Lqq1a caused significant reduction in *Sf*-21 cell proliferation and additionally cytotoxicity resulted in severe cell membrane damage, membrane blebbing and apoptosis mediated cell death
- β-BUTX Lqq1a proven to be toxic to *H. armigera* and *S. litura* when injected intra hemocoelly.
- *M.anisopliae* expressing β-BUTX Lqq1a was predicted to be significantly more toxic to *P. smithi* than the wild type.
- Recombinant GNA and fusion protein containing β-BUTX Lqq1a/GNA causes significant reduction in the proliferation and overall G2/M phase cell cycle arrest and caspase mediated apoptotic death of *Sf*-9 and *Sf*-21 insect cell lines
- *M.anisopliae* expressing fusion protein containing β-BUTX Lqq1a/Cyt1Aa exhibit significantly increased larval mortality of *P. smithi* when compared to wild type.
- *M.anisopliae* expressing fusion protein containing β-BUTX Lqq1a/tCry1Ac GNA exhibit significantly increased larval mortality *S. litura* when injected.
- Fluorescence microscopy analysis of real time expression of β-BUTX Lqq1a/sGFP in *M. anisopliae* induced with hemolymph, initial expression was observed at 1 hr and more intense sGFP expression was observed at around 3 hr interval.

Future Prospects:

- Bacterial Expression and purification of fusion protein containing truncated Cry1Ac-GNA and testing its efficacy against various agricultural insect pests
- Testing the efficacy of Ma-BUTX Lqq1a and Bb-BUTX Lqq1a against various agricultural insect pests
- Testing the efficacy of Ma-BUTX Lqq1a/tCry1Ac-GNA against other agricultural insect pests

CHAPTER 1

Introduction, Review of Literature and Objectives

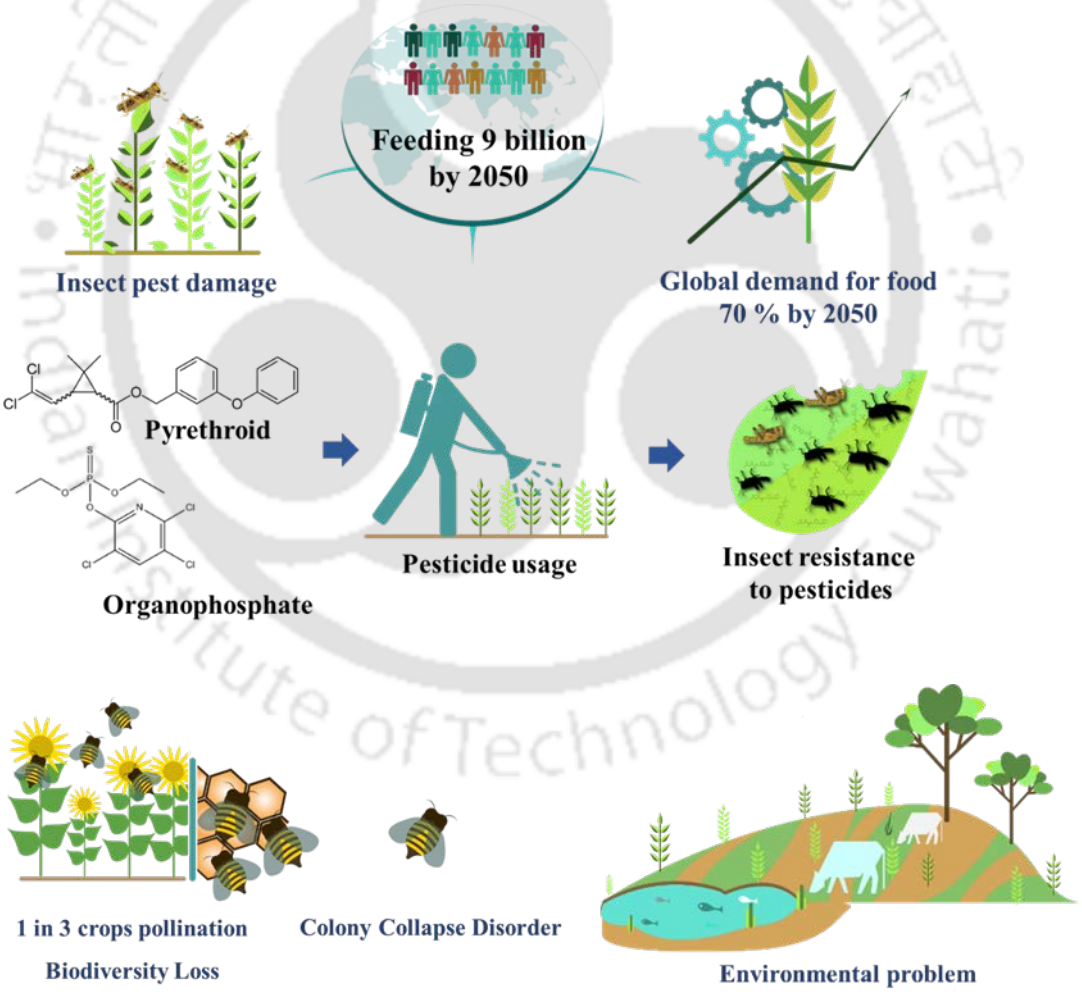

1.1 General introduction

Global population projected to increase to 9 billion, and the worldwide requirement of nutritional food will increase by 70% in 2050 (Godfray et al. 2010). In India alone, it is envisioned to rise to 1.6 billion by 2050 (United Nations 2015). Population acclivitous, availability of nutritious foods, and urbanization in developing countries, especially in India, requires essential steps to enhance the agricultural productivity to cope with the growing necessitate. Various factors govern to influence the sustainable agricultural productivity are uncertain climatic conditions, insect pests damage, storage loss, and insecticide resistance. Genetically modified organisms immensely contribute to the improvement in agricultural production systems, to meet the nutritional requirement of individuals and to fight against insect pest damage, thus the global food security. Also, synthetic chemical pesticides offer an additional advantage to control damages caused by insect pests. Extensive usage of chemical pesticides not only had an impact on pests, slightly significantly affected the non-target organisms and the environment. To avoid the development of insecticide resistance as well as curbing the effect on the non-target organism, biological agents are currently employed as an alternative to control insect pest damage.

Biological organisms are continuously exploited, such as bacteria, fungi, virus, and other natural products which are either naturally parasitic to insects or possess insecticidal property. *Beauveria bassiana* and *Metarhizium anisopliae* are the most widely used environmental friendly entomopathogenic fungi against various insect orders (Roberts and St Leger 2004). In India alone, more than 200 registered biological pesticide formulations based on *B. bassiana* and *M. anisopliae* are being utilized to control insect pest damage. Bacteria and virus need to be ingested by the host to exert the potential action. However, entomopathogenic fungi act by direct penetration of insect cuticle.

Direct penetration of insect cuticle is being facilitated by the fungi secretome, which consists of chitinase, protease, and lipase. However, in spite of intensive efforts these biological pesticides or mycoinsecticides have not fulfilled expectations as biocontrol agents because of evolutionary balance between the host and fungi, relatively slow speed of killing host, requirement for high amount of inoculum, and inconsistent efficacy compared to the synthetic chemical pesticides with which they compete (Gressel 2001, StLeger et al. 1996).

Recent advancements in genetic engineering implicate the use of molecular techniques in enhancing the entomopathogenic potency. Improvement in entomopathogenic fungi virulence and specificity achieved by either overexpression of endogenous genes and heterologous insecticidal genes from plants, bacteria, and arthropod origin. Arthropod species such as scorpion, spider, and wasp produce crude venom as defensive agents. This crude venom contains a mixture of proteins and peptide molecules, which possess insecticidal property, further could be exploited for their potential use as insect pest control. Bacteria such as *Bacillus* sp., are continuously explored for their possible use against insects. *B. thuringiensis* produces crystalline and cytolytic toxins with the potential to cause damage to the insect. Because of the potent insecticidal property of these toxins, a variety of agricultural crops such as cotton, maize, soybean, and brinjal has been expressed with toxins to counter the insect pest damage. The plant produces a variety of primary and secondary metabolites as defense molecule during the insect pest attack. These primary metabolites produced majorly of protein molecules, which exert insecticidal properties. Lectins are the significant component of defense molecule provided by the plant during the herbivore attack. These lectins have proven a toxic effect on major agricultural insect pest.

1.2 Food security challenges associated with agricultural pest and diseases

United Nation Food and Agricultural Organization (UNFAO) has projected that 70% increase in the global demand for food by 2050, and food production has to be doubled to feed the projected growth sustainably. Transformative changes in agriculture and food systems need to occur to achieve a world without hunger and malnutrition. Agricultural productivity is being affected by several factors such as soil health deterioration, climatic changes such as temperature, precipitation, and suitable crop models. Sudden pest and disease breakouts might constrain expansion and productivity. With new agricultural crop protection measures, we can produce only two-third food grains, and the remaining one-third loss occurs due to devastating pest and diseases. Thirty percent of post-harvest loss occurs to the stored foods due to the insect damages, valuing more than 100 billion US dollar (Boyer et al. 2012, Bruce 2012, Godfray et al. 2010). More than 10,000 insect species have found to damage food crops with an estimated annual loss of 13.6% globally and more than 3 million people killed annually by the occurrence of malaria, mosquito-borne disease (Ansari et al. 2014).

Bemisia tabaci (Tobacco whitefly), a polyphagous insect, is one of the significant pest prevailing in 156 countries across the globe followed by *Aphis gossypii* (Cotton aphid) in 153 countries, *Plutella xylostella* (Diamondback moth) and *Helicoverpa armigera* (cotton bollworm) around 135 countries. *H. armigera* is one of the significant polyphagous lepidopteran agricultural pests infesting a broader range of crops such as cotton, maize, and other high valued crops reported globally. In India alone, 1063 pests said to devastating effect on plants (Bebber et al. 2014).

1.3 Global and Indian scenario of insect pest control

Agriculture belongs to 50% of Indians' principle livelihood. Primary concern prevails in the Indian community in sustainability are bound to land resources, rising population, pest associated crop loss, and post-harvest losses. Pesticides immensely used for preventing damage to the agricultural crops by insect pests, thus helping to feed the overgrowing population and playing an essential role in protecting millions of lives from malaria and other insect vector-borne diseases. High incidence of various pests leads to the extensive application of synthetic chemical pesticides. Mancozeb, 2,4-D, acephate, and profenofos are the primary chemical pesticides produced and used to control pest damage in cotton (66.70%) and cereals (64.74%) in India. From crop protection to the managing of vector-borne diseases, pesticides are being applied globally, approximately 4.6 million tonnes (Ansari et al. 2014). Neonicotinoids and fipronil systemic neurotoxic insecticides account for more than one-third of the pesticide market globally to control insect pest damage (Van der Sluijs et al. 2015). Insecticides which are currently being used worldwide mostly target insect receptors such as acetylcholinesterase receptor, Gamma-aminobutyric acid (GABA)-gated chloride receptor, and voltage-gated sodium (VGSC), chloride (VGCC) channels, mitochondrial complex II electron transport system, hormones and the insect feeding behavior (Hardy 2014).

1.4 Development of pesticide resistance in insect pests

Due to the indiscriminate use, in recent past, insect pests acquired resistance to the widely used insecticides such as pyrethroids, organophosphate, DDT, and to other pesticides in different insect pest orders across the globe.

1.4.1 Pre-adaptation hypothesis

Preadaptation is one of the hypotheses of insecticide resistance. Herbivorous insect feed on some of the plants which naturally produces secondary metabolites with higher toxicity and over the time herbivorous insects have exposed to a broader range of secondary metabolites or allelochemicals such as alkaloids, terpenoids, glucosinolates, glucosides, and polyketides. These metabolites involved in membrane disruption, metabolic inhibition, nutrient uptake prevention, ion transport, and signal transduction inhibition, finally distortion in hormonal regulation. Synthetic chemical pesticides function also follows allelochemical mechanisms. The herbivorous insects evolved to degrade the toxic molecules, sequestration, and excretion metabolically, and target site modification of such compounds may lead to pre-adaptation to new generation insecticides. In addition, due to an evolutionary relationship with the host plant, insect pest may change the relative expression of a set of genes, which helps in detoxification of synthetic chemical pesticides (Chen et al. 2018).

1.4.2 Enhanced detoxification mechanism

Most of the insects acquire resistance through the mechanism of enhanced detoxification by cytochrome P450 complex (CYPs), and a mutation in insecticide targeted sites voltage-gated ion channels (Zimmer et al. 2014). A point mutation in VGSC leads to the development of resistance to pyrethroid in European mite *Panonychus ulmi* (Rameshgar et al. 2019). Intensive use of fewer active chemical insecticides has led to stronger selection pressure on insects for the evolution of pesticide resistance (Storkey et al. 2019) . The pollen beetle (*Meligethes aeneus F.*), a significant pest of oilseed rape throughout Europe, reported having high-level resistance to pyrethroid-based insecticides (Zimmer et al. 2014). *B. tabaci* shows a high frequency of resistance to pyrethroid and organophosphate because of mutations in VGSC gene and ACE gene (Gauthier et al.

2014). Frequent exposure of *Spodoptera litura* to profenofos, an acetylcholine esterase inhibitor, developed resistance under laboratory conditions (Abbas et al. 2014) and rice striped stem borer, *Chilo suppressalis* (Walker) acquired resistance to triazophos (Su et al. 2014) . An elevated level of resistance has been identified in the malaria vector, *Anopheles gambiae sensu late* to deltamethrin and Dichlorodiphenyltrichloroethane (DDT) (Nkya et al. 2014).

1.5 Environmental and human health risks associated with insecticides

For centuries, human society has benefitted by cultivating essential food crops. The green revolution gave rise to agricultural production increase but also contributed to a concomitant increase in environmental and health concerns. Although tonnes of insecticides used globally, the potential threats they brought to non-target organisms and the environment are immeasurable (Enserink et al. 2013). Overuse of synthetic chemical pesticides could lead to the contamination of freshwater ecosystems (Deknock et al. 2019). A recent evaluation of the usage of pesticides in Europe and Australia revealed a significant effect on species and family richness in stream invertebrate regional biodiversity (Beketov et al. 2013). It has been found that increased exposure of insecticide carbaryl to the developing larvae of green frogs (*Lithobates clamitans*), can influence the brain development and could affect the meta-morphogenesis of anurans (Boone et al. 2013). Persistence risk of organochlorine pesticides in the soil ecosystem reported due to the extensive usage (Helou et al. 2019). Loss of biodiversity in beneficial organisms such as natural predators of crop pests, pollinators, and soil microbes. Habitat loss and toxic chemical pesticide use threaten the ability of ecosystems to maintain the ecological functions and equilibrium between natural flora and fauna.

1.5.1 Negative impact on pollinators

Pollinators are the key components in maintaining biodiversity and ecosystem stability. The decline in the pollinator population, negatively influences the terrestrial ecosystem stability, crop production, food security, and ultimately, human welfare (Potts et al. 2010). The United Nations Food and Agriculture Organization (FAO 2008) reported that bees are responsible for the pollination of 71 out of 100 crops, and the annual estimated value of those crops are more than 200 billion US dollars. Application of insecticides negatively affects honeybees and other non-target insects' survival, even nonlethal exposure to thiamethoxam insecticide, impair honeybees returning to their hives (Henry et al. 2012). The realistic field level exposure of Bumblebee to neonicotinoid pesticide, imidacloprid significantly reduced the colony growth rate and observed an 85% reduction in new queen bee production (Whitehorn et al. 2012). Use of cholinergic pesticides clothianidin, coumaphosoxon, causes depolarization block of neuronal firing in brain cells of honeybee (Palmer et al. 2013). Considering the risks associated, there is a necessity to reduce the chemical synthetic pesticides use and its effect on non-target organisms and particularly to the environment.

1.6 Biological pesticides

Bio-pesticide is defined as "Any molecules from the biological origin, whole organism or product derived from them" (Villaverde et al. 2014). Different classes of bio-pesticide are naturally occurring, such as biochemical, microbial entomopathogens, and plant-based active ingredients (Ruiu 2018). Current global bio-pesticide in total crop protection market is $ 3 billion and expected to reach beyond $ 4.5 billion by 2023 (Damalas and Koutroubas 2018). Fifteen microbial agents are currently employed to control agricultural crop pest based on 970 commercial formulations. Indian bio-pesticide

market covers only 4.2% global bio-pesticide market. In India alone, 14 registered bio-pesticides are in use, for reliably sustainable and environmentally friendly options and India has seen around the 14-fold increase in bio-pesticide use since 1996–2016 (Kumar et al. 2019). Delayed or absence of resistance development to the biological control agents is an added advantage (Gao et al. 2017).

1.6.1 Bacteria as insect biological control agent

Few bacterial species have been reported to pathogenic to insect pest which is designated as Entomopathogenic bacterium. The most widely reported entomopathogenic bacteria belong to *B. thuringiensis* subspecies affect mostly Lepidopteran insects. However, some other insect pathogenic bacteria have also been reported, such as *Lysinibacillus (Bacillus) sphaericus, Serratia spp.* and *Paenibacillus spp*. *L. sphaericus* is a Gram-positive soil bacterium, formerly known as *Bacillus sphaericus* produces spherical spores and various insecticidal toxins such as sphaericolysin a cholesterol-dependent cytolysin toxin, mosquitocidal toxins (Mtx1 and 2) and Binary prototoxins (Bin) (Berry 2012, Kellen et al. 1965). *L. sphaericus* have been reported to effects mainly Dipteran insects such as *Culex* and *Anopheles* species (Santana-Martinez et al. 2019). *Serratia spp.* causes amber disease in *Costelytra giveni* one of the New Zealand grass grub that is highly specific to the host (Jackson et al. 1991). It has been reported to cause a reduction in feeding as well as insecticidal activity against Scarabaeidae insects such as *Polyphylla olivieri*, *C. giveni* (Bidari et al. 2018, Hurst et al. 2018).

1.6.1.1 *Bacillus thuringiensis*

Bacteria *B. thuringiensis* (*Bt*) is a soil-borne insect pathogen, secretes crystal δ-endotoxins (Cry), cytotoxins (Cyt), and vegetative insecticidal proteins (Vip) (Yang et al. 2019). It kills host by effectively binding to insect midgut receptors such as cadherin,

aminopeptidase N (APN), and alkaline phosphatase (ALP), leading to the formation of pores in the epithelial cells residing on midgut (Bravo et al. 2011). *B. thurigiensis* based formulations have been used to control *Ostrinia nubilalis* Hubner (Lepidoptera: carmbidae), a major pest of corn in temperate regions (Crava et al. 2014), *S. exigua* (Beet armyworm) (Naimov et al. 2014) and combination of toxins also used against *S. littoralis* and *Ephestia kuehniella* (Elleuch et al. 2014).

1.6.2 Baculovirus as biocontrol agents

Baculovirus is a pathogenic insect virus, having circular double-stranded, rod shaped DNA molecule with 80-180 kbp size range (van Oers and Vlak 2007). It has potential use as bioinsecticide because of their high specificity towards insects and which considered as safe to vertebrates and plants (Rao et al. 2015, Shrestha et al. 2018). *Autographa californica* nucleopolyhedrovirus (AcMNPV) is one of the completely studied Baculovirus contains circular, double stranded DNA with approximate size of 130 kbp, which is packaged within the nucleocapsid and highly pathogenic to many Lepidopteran insect species. This virus enters into epithelial cells based on endocytosis and receptor mediated internalization and causes death of infected insects (Au et al. 2016, Hodgson et al. 2019, Peng et al. 2010, Qin et al. 2018). Similar to AcMNPV, other nuclear polyhedroviruses also been reported from various lepidopteran insects such as *H. armigera* and *S. litura* (Ali et al. 2018, Bayramoglu et al. 2018, Chen et al. 2019, Cuartas et al. 2015, Ginting et al. 2018, Gross et al. 1994, Ilinsky et al. 2018, Kelly et al. 1983, Wang et al. 2019). Fusion protein containing insect specific cyto-insectotoxin (Cit1a) from spider *Lachesana tarabaevi* and polyhedrin when recombinantly expressed in BmNPV and AcNPV significantly reduced the median lethal time (Ali et al. 2015). Fusion of Bt toxins to the baculovirus expression system improves virulence against

diamondback moth *P. xylostella* (Chang et al. 2003), and also expression of insect-specific neurotoxin AalT along with Cry toxin resulted in high-level insecticidal activity against *P. xylostella* larvae and reduced lethal time against *S. exigua* (Shim et al. 2009).

1.6.3 Fungi as biological control agents

The most significant potential of using entomopathogenic fungi as biopesticide is their environmental safety. *Beauveria bassiana* (Balsamo) Vuillemin, *Metarhizium anisopliae* (Metschnikoff) Sorokin, *Isaria fumosorosea* ((wize) Brown and Smith) and *Lecanicillium lecanii* (Zimmermann) (formerly *Verticillium lecanii*) are naturally occurring entomopathogenic fungi, which are being used to control crop pests and vectors of disease-causing insects (de Faria and Wraight 2007, Wang and Feng 2014). Entomopathogenic fungi are virulent against various insect orders including Coleoptera (Williams et al. 2013, Long-Wa Zhang et al. 2011), Diptera (Kim et al. 2014), Hemiptera (Lacey et al. 2011), Lepidoptera (Oliveira et al. 2012, Ramzi and Zibaee 2014), Siphonaptera (Mnyone et al. 2012), Thysanoptera (Wang et al. 2013, Wu et al. 2013) and also against non-insects Acari (Fernandes et al. 2011, Ren et al. 2011).

1.7 Entomopathogenic fungi *Metarhizium anisopliae* and *Beauveria bassiana*

1.7.1 *Metarhizium anisopliae*

Metarhizium species have been widely accepted and best-studied fungi at molecular level with a greater potential as a biological control agent against wider range of arthropod insects. Initial experimental studies conducted by Metschnikoff (1879) to control wheat grain beetle *Anisoplia austriaca* using *M. anisopliae* hence the name *anisopliae*. It is also being called as ‘green muscardine fungi’ due to the green color sporulation. *Metarhizium* is the first reported fungi to be bulk produced and utilized against insect pests (Krassilstschik 1888). *Metarhizium sp.* has been reported to be

pathogenic to more than 200 insects but not toxic to mammals. It may not be from insect habitats; however, studies suggest that it may be from soil root inter-phase where it grows by the influence of root metabolites (Roberts and St Leger 2004).

The taxonomic classification of *Metarhizium* is

Kingdom: Fungi
Division: Ascomycota
Class: Sordarimycetes
Order: Hypocreales
Family: Clavicipitaceae
Genus: *Metarhizium*
Species: *M. anisopliae*

Along with *M. anisopliae*, other species such as *M. flavoviridae* and *M. acridum* are among the most abundant entomopathogens. This fungus reportedly cause infection in the range of agricultural pests and vectors of disease-causing agents including from Lepidopteran (*S. litura, H. armigera, H. zea, S. frugiperda, P. xlyostella*), Hemipteran (*Aphis craccivora, Nilaparvatha lugens*), Homopteran (*Myzus persicae, A. gossypii*) (Correa-Cuadros et al. 2016, Jaber et al. 2018, Mweke et al. 2018, Ramanujam et al. 2018, Rivero-Borja et al. 2018, Sahayaraj et al. 2018, Silva et al. 2008, Tahir et al. 2019, Tang et al. 2019).

Metarhizium secretes various secondary metabolites in response to the different ecological growth conditions (Rios-Moreno et al. 2016). These secondary metabolites play an essential role in determining the virulence of the fungi against various insect pest (Lozano-Tovar et al. 2015). Apart from the insecticidal property, they exhibit antibacterial (Kao et al. 2015, Tian et al. 2016), antifungal (Lozano-Tovar et al. 2017), and cytotoxic potential against various cancerous cell lines (Molnar et al. 2010). These secondary metabolites produced by the entomopathogenic fungi are clustered together as

biosynthetic gene clusters such as polyketide synthase (PKS), and non-ribosomal peptide synthetases (NRPS). Destruxin is one of the secondary metabolite produced by *Metarhizium* that is a cyclic hexadepsipetide compound coded by polyketide synthase clusters (Sbaraini et al. 2016). This peptide possess the ability to suppress the drug resistant cancerous cells (Wu et al. 2018). Swainsonine is an important metabolite being produced by *Metarhizum* (Singh and Kaur 2014b). It inhibits Golgi α-mannosidase-II proteins of the cancerous cells as well as exhibits antil-eukaemic activity (Singh and Kaur 2014a).

1.7.2 *Beauveria bassiana*

In early 1770s an Italian Scientist Agostino Bassi discovered the appearance of white powdery structures devastating the silkworm industry which was later identified as *Beauveria bassiana,* a causative agent of white muscardine fungal disease. At the same time Giuseppe Gabriel Balsamo-Crivelli (1800-1874) also identified the fungus as *bassiana.* Later the fungus was named as *Beauveria bassiana* in 1912, in honor of the French scientist Jean Beauverie by Jean Paul Vuillemin (1861-1932) (Paul Vuillemin 1912). This fungus occurs naturally in soil as white covered mycelium and conidiophores are clustered together and appears in dentriculate pattern.

The taxonomic classification of *B. bassiana* is as follows:

Kingdom: Fungi
Division: Ascomycota
Class: Sordariomycetes
Order: Hypocreales
Family: Cordycipitaceae
Genus: *Beauveria*
Species: *B. bassiana*

Secondary metabolites and secretary enzymes play an essential role in determining the virulence of this fungus. Secretary enzymes such as chitinase, cuticle degrading proteases, metalloproteases and other enzymes are the primary metabolites in determining the virulence. Additionally, secondary metabolites such as beauvetetraones, bassiatin, beauverolides, beauvericin, dipicolinic acid, bassianolide, bassianin, oxalic acid, tenellin, basiacridin, and oosporin are also produced by the *B. bassiana* and among these metabolites beauvericin, bassianolide, oxalic acid and dipicolinic acid exhibits insecticidal activity (Lee et al. 2019). Apart from the insecticidal property of these secondary metabolites some exert antifungal, antibacterial and anticancer activity also (Lee et al. 2016). These active metabolites are coded by the biosynthetic gene clusters such as polyketide synthase and non-ribosomal peptide synthetase present in the *B. bassiana* genome (Molnar et al. 2010).

B. bassiana has been reported to infect more than 700 insect species from various insect orders including from Lepidoptera (*S. litura, H. armigera, Chillo partellus* and *P. xylostella*), Orthoptera (*Locusta migratoriaa manilensis*), Coleoptera (*Dendroctonus rufipennis*), Hemiptera (*B. tabaci, and A. craccivora*), Diptera (*Drosophila suzukii*) and Thysanoptera (*Frankliniella occidentalis*) (Batcho et al. 2018, Davis et al. 2018, Dhar et al. 2019, Jaber and Araj 2018, Mweke et al. 2018, Rhodes et al. 2018, Sangbaramou et al. 2018, Sufyan et al. 2019, Tahir et al. 2019).

1.7.3 Entomopathogenic fungi life cycle

Unlike bacteria and virus, which need specialized routes to be ingested, to act upon insects, these fungi do not need to be ingested because of their direct penetrating ability into insects. **Fig. 1.1** represents the various infection stages of entomopathogenic fungi. These fungal infections follow different life stages within insect host. Initial

physical contact between the fungal spore and cuticle, it recognizes host, which lead to spore germination and production of cuticle penetration structure called appressorium (highly specialized cell). In *B. bassiana* hydrophobins (HYD1, HYD2) and adhesins (MAD1, MAD2) play a distinct role in cell surface hydrophobicity, adhesion to insects respectively (Wang and St Leger 2007a, Shizhu Zhang et al. 2011). Mitogen-activated protein kinase (MAPK) is reported being responsible for appressorium formation and insect cuticle penetration (Zhang et al. 2010). Epicuticle contains a mixture of lipids, fatty acids, and wax ester layers, which protect insects from desiccation and microbial attack. Cytochrome P450 monooxygenase (CYP52X1) from *B. bassiana* helps in the degradation of specific epicuticular wax of insect (Pedrini et al. 2013).

MrpacC, a pH-responsive transcription factor from *M. roberstii* contributes to the fungal virulence by penetrating insect cuticles, mycosis of insect cadavers and evasion of host immunity (Huang et al. 2015). Cuticle degradation is accomplished by enzymes such as chitinases (CHIT1) (Fang et al. 2005), proteases (Prl and Pr2) (Bagga et al. 2004, St Leger et al. 1987), carboxypeptidases, metalloproteases, aminopeptidases, and possibly lipases (Cho et al. 2006, St. Leger 1995). Once inside the insect, the fungi turn into blastospores that bud and spread through and invade the hemolymph of insects. Upon the death of insect host, hyphae reemerge to cover the corpse and produce a massive number of conidia to infect a new host.

1.8 Major drawbacks associated with entomopathogenic fungi

One of the significant drawbacks in exploiting these fungi to be used as a biopesticide is their slow speed of killing the host even after infection. Use of more virulent strain takes 3-10 days to kill the host which would allow the insects to make major crop damage even after the infection. Abiotic stress such as temperature, humidity,

and UV radiation also influence the virulence. Therefore, effective strategies are required to increase the virulence and abiotic stress tolerance and by doing so, the pathogen could reduce the median lethal time (LC_{50}) and the dose (LD_{50}) required in achieving the high mortality. This may be accomplished by manipulating the fungi genetically through transgenic approaches (Leger and Wang 2010, Thomas and Read 2007).

1.9 Strategies used to improve the virulence of entomopathogenic fungi

1.9.1 Endogenous genes overexpression

The most attractive candidate for this approach could be the proteins expressed by entomopathogenic fungi during host infection, which includes proteases, chitinases, lipases, esterase, and metalloproteases. StLeger et al. (1996) developed a method to improve the virulence by overexpressing a toxic protease Pr1 in *M. anisopliae*, which exhibited a decrease in median lethal time to 25%. Insect cuticles are mainly consisting of a network of insoluble polysaccharide chitin and proteins. Expression of endochitinase gene Bbchit in *B. bassiana* significantly reduced the level of lethal time to 50% and dose to 50% compared to that of wild type strain (Fang et al. 2005). The fusion of chitin binding domain BmChBD from *Bombyx mori* with chitinase from *B. bassiana* Bbchit1 increases specific binding to the chitin polymer targets in insects (Fan et al. 2007, Fan et al. 2011). Construction of hybrid protease by fusion of a chitin binding domain BbChBD from *B. mori* to the C-terminal end of CDEP-1, subtilisin-like protein from *B. bassiana* increased the ability to bind chitin (Fan et al. 2010). It has been observed that transformants overexpressing *B. bassiana* Pr1A homolog (CDEP1) and Bbchit1 exhibited a 24.9% reduction in LT_{50} and 60.5% reduction in LC_{50} value (Fang et al. 2009).

1.9.2 Heterologous genes overexpression

1.9.2.1 Scorpion toxins overexpression

Although endogenous genes mostly used by research communities, an approach considered to be an enormous potential is, to engineer the entomopathogenic fungi with genes from the heterologous origin. Initially, baculovirus was engineered to express AaIT1, a neurotoxin from *Andructonus australis*, which acts explicitly on insect Na+ channel (Stewart et al. 1991). Wang and Leger, (2007) also used the same gene to express in *M. anisopliae* specifically in insect hemolymph using *Metarhizium* collagen-like (Mcl1) promoter, which further increased fungal toxicity 22-fold against tobacco hornworm caterpillars and adult yellow fever mosquitoes (Wang and St Leger 2007b). Expression of AaIT along with protease Pr1A from *M. anisopliae* in *B. bassiana* reduced the LT_{50} value to 40 % against the larvae of pine caterpillar *Dendrolimus punctatus* (Lu et al. 2008). *M. acridum* genetically modified to express BjαIT, an insect-selective neurotoxin from *Buthotus judaicus*, resulted in increased virulence against locusts *L. migratoria manilensis* (Peng and Xia 2015).

1.9.2.2 Overexpression of other heterologous proteins

Melanization is a rapid response of insect immune systems towards invading pathogens. During that, a series of serine proteases expressed which in turn activate prophenoloxidase (proPO) activation factors (PPAFs). This factor catalyzes the conversion of prophenoloxidase to phenoloxidase, which helps in the production of melanin. Bumblebee (*Bombus ignitus*) venom serine protease (Bi-VSP) induces the lethal melanization in beet armyworm has also been expressed in *B. bassiana* (Kim et al. 2013). Cloning and expression of the vegetative insecticidal protein (Vip3Aa1) from

B. thuringiensis increased 23-35% virulence against *S. litura* and higher *per os* toxicity (Qin et al. 2010) and against *P. xylostella* (Liu et al. 2013).

1.10 Scorpion and spider toxins

Venom is one of the essential tools for scorpions to predate and exercise self-defense. These toxins or crudes are comprised of proteins ranging from 30-80 amino acid residues, mainly targeting ion channels. It has been classified based on size, short peptides that target K+ channels, and long chains peptides (α-toxins and β-toxins) which target Na+ channels. BmK NT1 is a 65 amino acid long peptide produced by scorpion *Buthus martensii* Karsch that primarily act on voltage-gated sodium channel (Zou et al. 2016). It is further classified as a depressant toxin (blocking the action potentials) and excitatory toxin (repetitive firing of the neuron) (Ji et al. 2002, Leipold et al. 2012).

1.10.1 Voltage-gated channels

Voltage-gated channels are integral membrane proteins that function as a gateway to the passage of sodium, potassium, and calcium ions across the biological membranes. Voltage-gated sodium channels (VGSC) generate and propagate action potential in neurons (Bosmans and Tytgat 2007). **Fig. 1.2** represents the linearized sodium channel α-subunit structure. It is composed of one α-subunit (220-260 kDa) and one or two β-subunits. The α-subunit of sodium channels consists of four homologous domains; each contains six hydrophobic transmembrane α-helices (S1-S6) segments connected by intra and extracellular loops. The loop between S5 and S6 segments form a pore, and S4 part in each domain contains positively charged amino acid residues at every third position, which believed to play a vital role in channel activation by opening pore. The interloop connecting domain S3 and S4 mainly consist of hydrophobic residues; act as inactivation gate in VGSCs (Bosmans and Tytgat 2007, Catterall et al. 2007). Scorpion α-toxins bind

to receptor site 3 (extracellular loops S1-S2 and S3-S4 at DIV and S5-S6 at DI) on sodium channels which blocks the channel activation. Whereas β-toxins bind to receptor site 4 (extracellular loops S1-S2 and S3-S4 at DII and S5-S6 at DIII) and trap inactivation channels which induce repetitive firing of action potentials (Cestèle and Catterall 2000, Gurevitz 2012).

1.10.2 BUTX-Lqq1a toxin

The β-BUTX-Lqq1a is an excitatory insect-selective toxin from Buthidae family scorpion *Leuirus quinquestriatus quinquestriatus* that contains 70 amino acids including eight half-cysteine residues at the positions 16-37, 22-42, 26-44, 38-64 and devoid of methionine and tryptophan amino acids. **Fig. 1.3** represents predicted secondary structure of β-BUTX-Lqq1a toxin (unpublished, this study). This toxin causes flaccid paralysis in insects by inducing repetitive firing in the VGSCs (Kopeyan et al. 1990, Zlotkin et al. 1985). It closely resembles insect β-toxin AaIT1 from *A. australis* (Hector), which has been already proven non-toxic to mammals (Ji et al. 2002).

1.11 *Bacillus thuringiensis* Cry and Cyt toxins

*Bacillus thuringiensis*is a soil born gram-positive insect pathogenic bacterium, produces paracrystal inclusions called δ-endotoxins during sporulation. It provides two different multigenic forms of endotoxins, which are Crystal (Cry) and Cytolytic (Cyt) toxins. Cry toxins are effective against Lepidoptera, Coleoptera, Hymenoptera and Diptera. Cyt toxins are active against Diptera and Coleoptera. They are highly insect specific and innoxious to human and animals. Initially, *B. thuringiensis* used as a formulation for pest management. Later it has been introduced within the plants to counter the insect pests effectively. Until now, 2.3 billion hectares of genetically engineered crops cultivated throughout the world since 1996. The United States of

America is the largest producer of biotech plants in the world, planting 39.4% of global hectares with engineered maize topping the list. India stands 5th among the top countries growing biotech crops, particularly *B. thuringiensis* gene engineered transgenic cotton, where cotton cultivation covers 11.4 million hectares of land (Briefs 2017). Due to commercial exploitation, the use of chemical pesticide is substantially reduced. Among Cry toxins, Cry1A related toxins mostly integrated into transgenic crops to minimize the insect pests attack. These cry toxins consist of three domains, where domain I contain α-helices, which helps in pore formation in insect mid-gut, domain II, and III involve in receptor binding and specificity. Receptors for these proteins are catherin like proteins (CAD), aminopeptidase N (APN), alkaline phosphatases (ALP), and ABC transporters. In insect mid-gut Cry toxin solubilization occur due to the alkaline environment, resulting in the inactivated toxin. The toxin oligomerization occurs in the insect midgut with the help of Cadherin receptors promoting pore formation in the midgut epithelial cells leading to the death of the insects. Meanwhile, due to improper integrated pest management (IPM) - refuge method and awareness related to the transgenic crops, insect pests developed resistance against these mostly used Cry toxins. Strategies to overcome resistance are to either modify the toxin so that binding specificities will be altered or stacking two to three different toxins together so that the development of resistance to these toxins can be slowed down. Delaying the pest adaptation and broader insecticidal potential could be done by fusing one or two different proteins with various activity (Zhao et al. 2017). Oligomeric structure formation is the intermediate step in the creation of pores in the mid-gut of the insects, which is mediated by the binding of toxins to the receptor-like cadherin. However, the Cry1A Mod proteins are devoid of helix α-1 which can form oligomers in the absence of cadherin receptors. These modified toxins have been reported

to kill insects, which express the cadherin receptor at a low level, thus paving the way to eliminate the insect resistance (Gómez et al. 2015, Muñóz-Garay et al. 2009).

1.11.1 General aspects of Cry1Ac toxin and insect resistance development

Cry1Ac is one of the toxin produced by *B. thuringiensis* subsp. *kurstaki* HD-73 strain. It is a 3-domain Cry toxin, which is a staggeringly studied and characterized pore-forming toxin, primarily acts by forming pores in the insect mid-gut epithelial cells leading to increase in turgor pressure within the cell, cell burst and death of mainly lepidopteran insects. Cry1Ac contains 579 amino acids with three different domain structure (**Fig. 1.4**). Region 18-221 amino acids belong to endotoxin N or delta-endotoxin N-terminal domain rich in helices. Region 223-431 composed mainly of β-sheets called as endotoxin M and region 433-579 called as C-terminal domain or endotoxin N, which contains β-sheets throughout the domain (Derbyshire et al. 2001). Cry1Ac Domain III loop regions exhibit the lectin-like properties, which in turn recognize and binds to carbohydrate N-acetyl D-galactosamine (GalNAc) attached to aminopeptidase receptor. GalNAc binding induces relative conformational modification, which further enhances the membrane insertion of an oligomeric prepore structure (Derbyshire et al. 2001). Cry1Ac profitable activity on various lepidopteran insects, led to engineer the plant system to counter against important agricultural pest such as *H. armigera* (Chakraborty et al. 2016, Dourado et al. 2016, Ghosh et al. 2017, Liu et al. 2019), *H. zea* (Carriere et al. 2018, Knight et al. 2015) and *S. litura* (Bernardi et al. 2014, Selvi et al. 2012).

Fig. 1.5 represents the generalized mode of action of Cry toxins. Initial proteolytic processing of crystal and binding to a series of proteins in the insect mid-gut brush border membrane, further causes pore formation, ultimate paralysis, and eventual death. Alkaline phosphatase (ALP), aminopeptidase N (APN), cadherin (CAD) and the several ABCC

transporters have all been reported as putative receptors for Cry1Ac in various insect pests (Bernardi et al. 2014, Carriere et al. 2018, Dourado et al. 2016, Liu et al. 2019). The main relative interaction between the Cry1Ac and membrane-bound receptors may substantially reduce the insect susceptibility to toxin thus developing into resistant against Bt toxin (Fabrick et al. 2009, Fabrick et al. 2019, Guo et al. 2019, Zhang et al. 2019).

1.12 Cytolytic toxin structure overview

B. thuringiensis subsp. *israelensis* (Bti) produces crystalline (Cry4Aa, Cry4Ba, Cry10Aa, and Cry11Aa) as well as many cytolytic (Cyt1Aa and Cyt2Ba) toxins during sporulation. These toxins have proven insecticidal activity against major agricultural pests as well as vectors of disease-causing agents such as mosquitoes (Bravo et al. 2018, Elleuch et al. 2015, Kang et al. 2018, Torres-Quintero et al. 2018). Unlike Cry toxins, Cytolytic toxins do not require to bind to the specific receptors present on the brush border membrane. However, it acts by nonspecific interaction. **Fig. 1.6** represents the Cyt1Aa toxin, which follows the α/β domain structure with inner core rich in β-sheets, whereas the outer layer consists of α-helices.

The β-sheets around the inner core of the protein forms β-barrel structure during the membrane insertion (Cohen et al. 2011, Li et al. 1996).After the processing and activation of Cyt toxins in the insect mid-gut, mature oligomer toxin inserts into the lipid membrane without any receptor-mediated interaction. **Fig. 1.7** represents the Cyt toxins mode of action. Initially, β-strands (β6-β8) located at the C-terminal domain of Cyt toxin, form a core structure of β-barrel, which further perforate the membrane (Promdonkoy and Ellar 2003, Rodriguez-Almazan et al. 2011). This event causes the osmotic lysis of cells, with increased water influx and cell swelling (Li et al. 1996). Cyt1Aa act synergistically as a membrane-bound receptor for other Cry toxins where loop β6-αE and β7 of Cyt1Aa

interact directly with Cry11Aa (Perez et al. 2005). Synergistic expression of Cyt1Aa along with other Cry toxins (Cry11Aa, Cry1Ac, and Cry3Aa) reported to alleviate the resistance mechanism and enhance the activity (Federici and Bauer 1998, Perez et al. 2005, Pérez et al. 2007, Sayyed et al. 2001).

1.13 General aspects of Lectins

In nature, plants evolved numerous defense mechanisms against phytophagous insects using morphological, structural, and by the chemical defense. Among the chemically synthesized compounds, peptides and proteins, particularly lectins, are one of them. It has proven to be toxic to major agricultural insect pests belonging to various insect order such as Lepidoptera (Sadeghi et al. 2009), Coleoptera (Dowd et al. 2003, Melander et al. 2003, Murdock et al. 1990), Diptera (Zhou et al. 2000), Hemiptera (Beneteau et al. 2010) and Homoptera (Sauvion et al. 2004). The word lectin originated from the Latin word called “Legere,” which means “to select” because of their ability to bind selectively and reversibly to specific mono and oligosaccharides. Plant lectins are a heterogeneous group of proteins that recognize and bind reversibly to the carbohydrate moieties (Van Damme et al. 2008).

Initially, lectins were classified based on their agglutination of red blood cells, and later it was no longer used since some of the lectins possess catalytic domain other than carbohydrate binding domain. Lectins were classified as merolectins, hololectins, chimerolectins, and superlectins based on the presence of sugar binding domain and a catalytic domain. Merolectins contain single carbohydrate binding domain and do not exhibit agglutination property. Hololectins possess multivalent carbohydrate binding domains, thus demonstrate agglutinating characteristics. Chimerolectins consist of other catalytic domain with distinct biological activity in addition to carbohydrate binding

domain such as *Urtica dioica* agglutinin (UDA) (Does et al. 1999, Van Damme et al. 2008). Superlectins binds non-specific sugar molecules with two or more carbohydrate binding domains.

Apart from carbohydrate binding properties, some lectins reported to exert coagulant in nature (de Oliveira et al. 2011, Gidrol et al. 1994), some involve in transport of glycoproteins (Banerjee et al. 2007) and act as regulators of intracellular signaling mechanisms in plant (Lannoo and Van Damme 2010). Midgut epithelium of most of the insects contains physical barrier peritrophic matrix, which consists of chitin fibrils held together by chitin binding domain and glycoproteins such as peritrophins (Hegedus et al. 2009). These glycoproteins and chitin fibrils are the targets of lectins. Seven lectins have proven to be toxic to insects, that include *Galanthus nivalis* agglutinin (GNA)-related lectins, legume lectins, Hevein-related lectins, Nictaba-related lectins, Ricin related lectins, Amaranthins and Jacalins (Vandenborre et al. 2011). Toxicity of lectins may be attributed to a reduction in the survival of larvae, loss of weight, reduction in the ability of feeding, deformation in the pupae, and delay in adult emergence (Fitches et al. 2012).

1.13.1 GNA Lectin

The best studied, GNA lectin (**Fig. 1.8**) is produced by the plant Snowdrop which belongs to Amaryllidaceae family. This plant lectin extracted from bulbs specifically binds to high mannose containing N-glycan residues which are present abundantly within the insect cuticle. GNA contains tetrameric identical subunit protein with three well-conserved binding sites for to α-1, 3 linked terminal mannose residues. Each subunit contains three conserved domains, which are highly folded antiparallel four stranded β-sheets (Hester et al. 1995, Wright and Hester 1996). Successfully introduced GNA into variety of plants such as cotton (Liu et al. 2019), potato (Mi et al. 2017), rice (Rao et al.

1998) and wheat (Liang et al. 2004, Miao et al. 2011, Shah et al. 2005, Stoger et al. 1999) exhibited insecticidal property against various insect pests, primarily on sap-sucking hemipteran insect pests (Liu et al. 2016).

In addition, a fusion of lectins to neurotoxin or peptide venom acts as a carrier to transport peptides or toxins across the gut epithelium and delivering it to the target sites. **Fig. 1.9** represents the generalized mode of action of Lectins in the insect mid-gut. Insecticidal spider neurotoxin SFl1 from *Segestria florentina* fused with GNA was tested against the rice brown planthopper *Nilaparvata lugens* (Stal) and peach potato aphid *Myzus persicae* (Sulzer) which slowed the development and reproductive capacity (Down et al. 2006). The spider venom peptide ω-hexatoxin-Hv1a targets insect voltage-gated ion channel, fused with snowdrop lectin GNA, mediated the transport of Hv1a across the gut epithelium and delivered the toxin to the site of action (Fitches et al. 2012). Amautobitoxin (Pl1a) / GNA tested against housefly *Musca domestica* and pea aphid *Acrythosiphon pisum*, which caused mortality when delivered orally (Yang et al. 2014). *Bt* Cry1Ac fused with *Allium sativum* agglutinin (ASAL) caused 100% mortality in *H. armigera* and *Pectinophora gossypiella* (Tajne et al. 2014).

1.13 Lacunae and scope of work

As it is evident from the literature, there are scarce reports available on the expression and purification of arthropod toxins in bacterial system, that are insecticidal in nature as well as their expression in entomopathogenic fungi to improve the virulence to tackle against economically important agricultural pests. Less popularity in the use of fungal biocontrol agents stems from their lower virulence, less tolerance to abiotic stress conditions as well as mere field persistence ability, which is all being substantiated by use of chemical pesticides. Intensified chemical pesticide applications led to resistance development in insects and un-controllable impact on non-target organisms. However, biocontrol agents display added advantages by delaying the process of resistance development. The use of heterologous proteins offers a reliable solution to increase the tolerance to abiotic stress and to magnify the virulence factor towards specific insect pests. Combinatorial effect of multi-functional proteins needs to be addressed to dynamically improve the virulence of entomopathogenic fungi and thus agricultural productivity.

1.14 Objectives

To increase the virulence of entomopathogenic fungi towards agricultural pest, strategies devised based on the literature studies are as follows:

1. Expression and purification of β-BUTX Lqq1a toxin and its biological activity against insect cells and agricultural insect pests.
2. Cloning and expression of β-BUTX Lqq1a in *Beauveria bassiana* and *Metarhizium anisopliae* and their insect toxicity assay.
3. Bacterial expression and purification of fusion protein containing β-BUTX Lqq1a/GNA Lectin and their cytotoxicity assay against insect cell lines.
4. Cloning and expression of β-BUTX Lqq1a, Cyt1Aa and t-Cry1Ac/GNA in *Metarhizium anisopliae* and insect toxicity assay.
5. Time expression analysis of β-BUTX Lqq1a/sGFP in *M. anisopliae.*

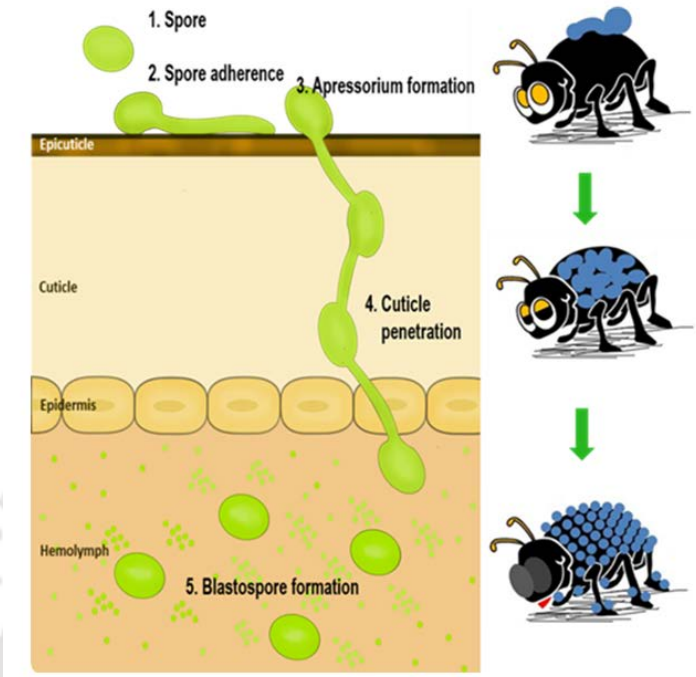

Fig. 1.1 Schematic representation of different life stages of entomopathogen infection on insects (Adapted from (Thomas and Read 2007)).

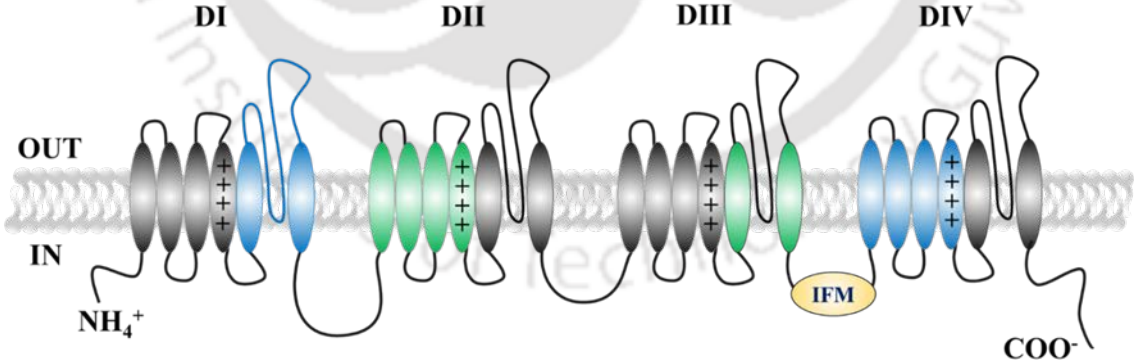

Fig. 1.2 Linearized sodium channel α-subunit with its four domains transmembrane with each containing six cylindrical α-helices (Adapted from (Gurevitz 2012)).

Fig. 1.3 Predicted β-BUTX Lqq1a structure using QUARK (Xu and Zhang 2012, Xu and Zhang 2013).

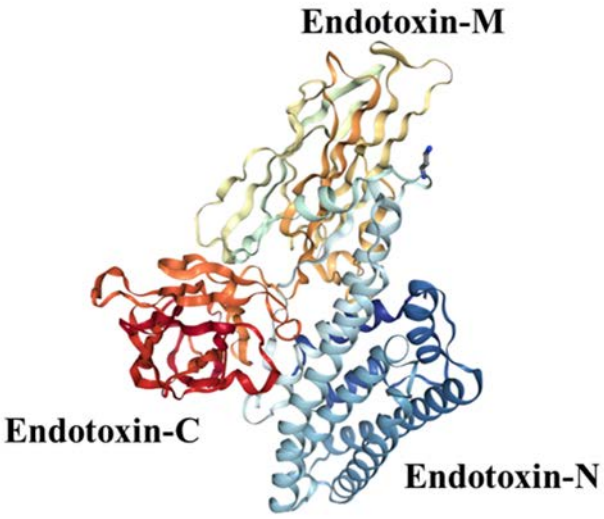

Fig. 1.4 Crystal structure of Cry1Ac toxin (PDB:4ARX) (Derbyshire et al. 2001)

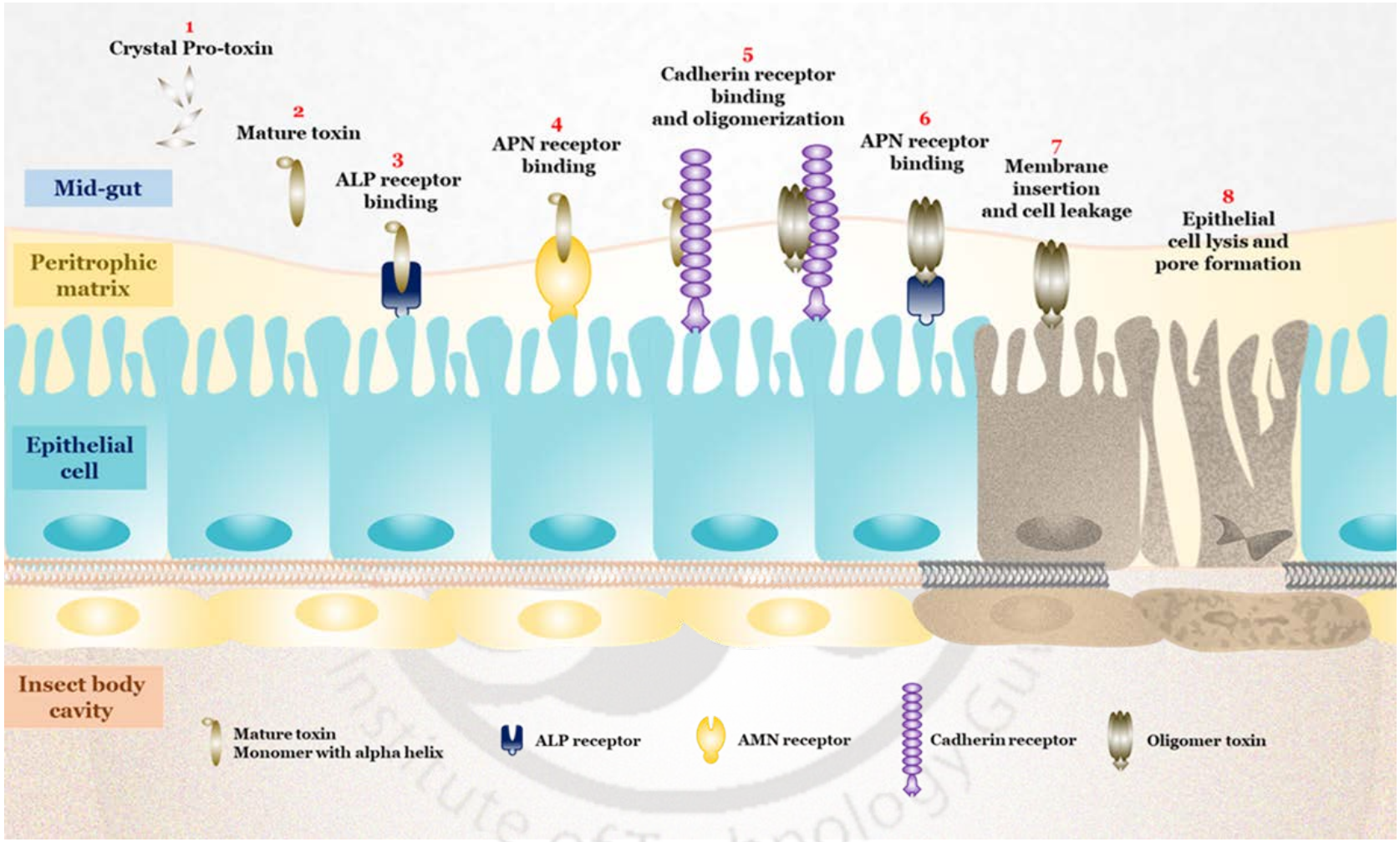

Fig. 1.5 Schematic representation of *B. thuringiensis* Cry toxins generalized mode of action (Adapted from (Pardo-Lopez et al. 2013))

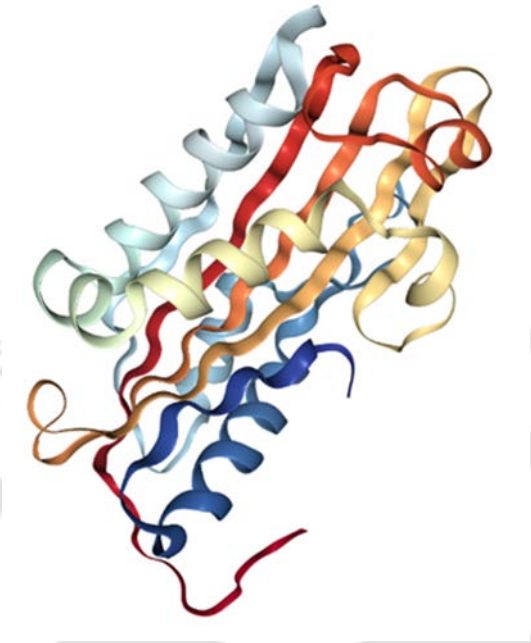

Fig. 1.6 Cyt1Aa protein structure (PDB**:** 3RON, (Cohen et al. 2011))

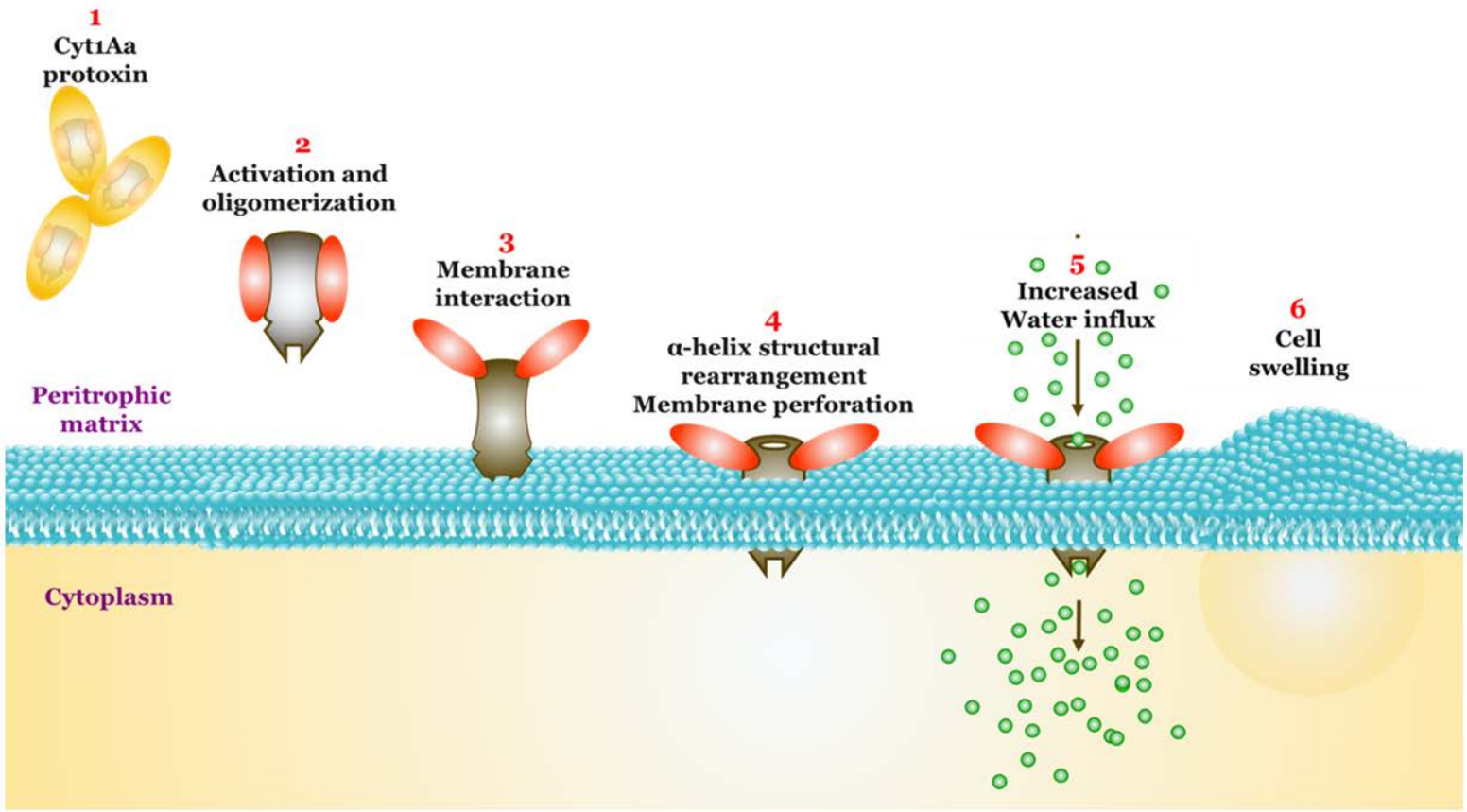

Fig. 1.7 Schematic representation of *B. thuringiensis* subsp. *israelensis* Cyt toxin generalized mode of action

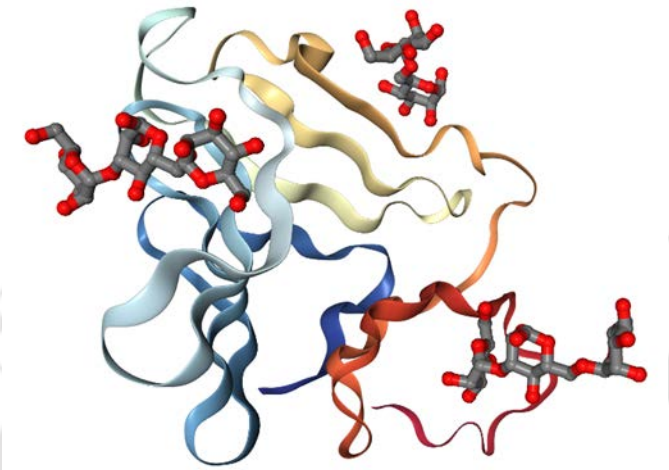

Fig. 1.8 GNA lectin bound with three mannose residue (PDB:1JPC, (Wright and Hester 1996))

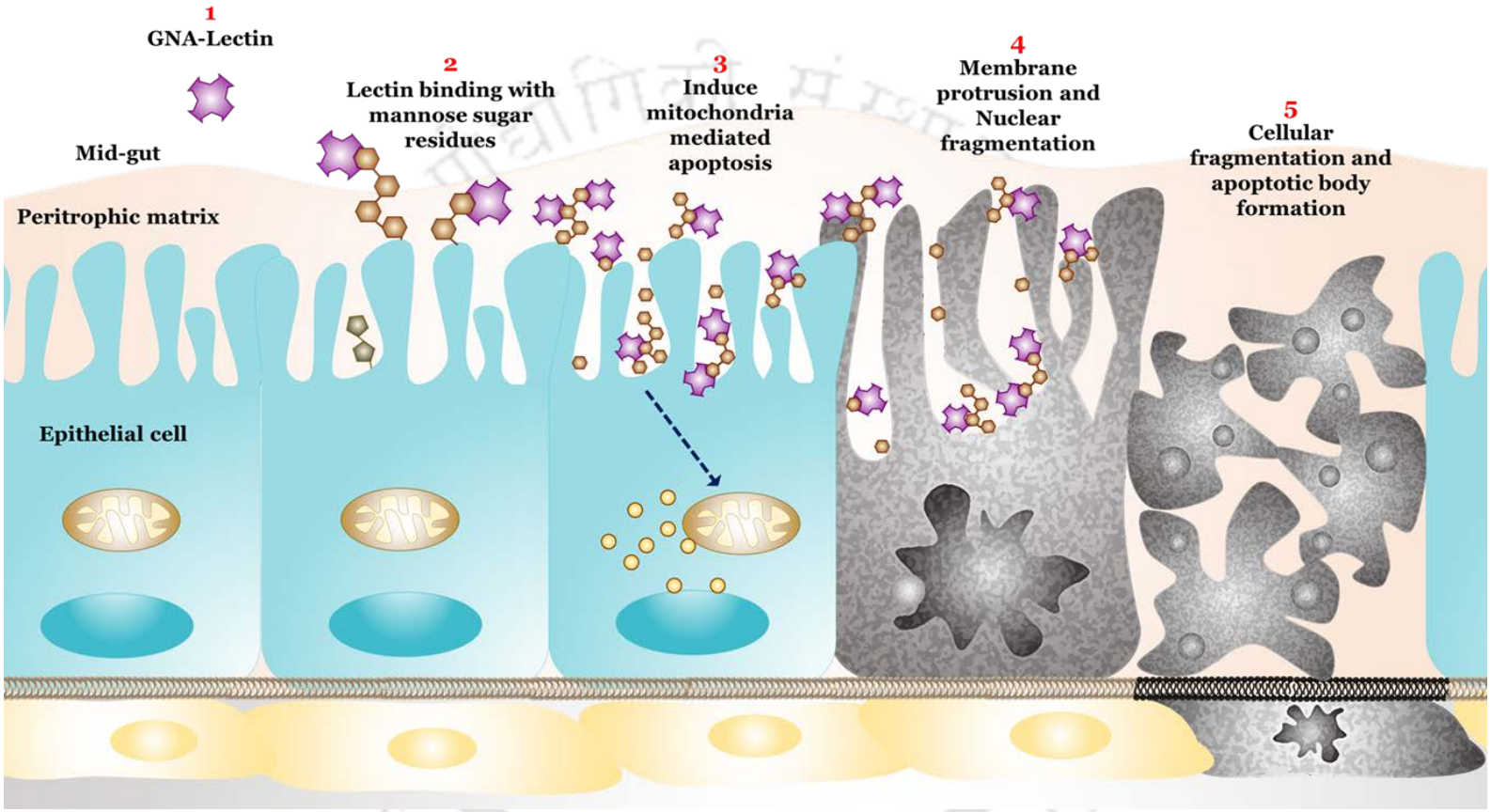

Fig. 1.9 GNA lectin generalized mode of action on insect mid-gut cells (Adapted from (Napoleão et al. 2019))

CHAPTER 2

Expression and purification of β-BUTX Lqq1a toxin and its biological activity against insect cells and agricultural insect pests

---

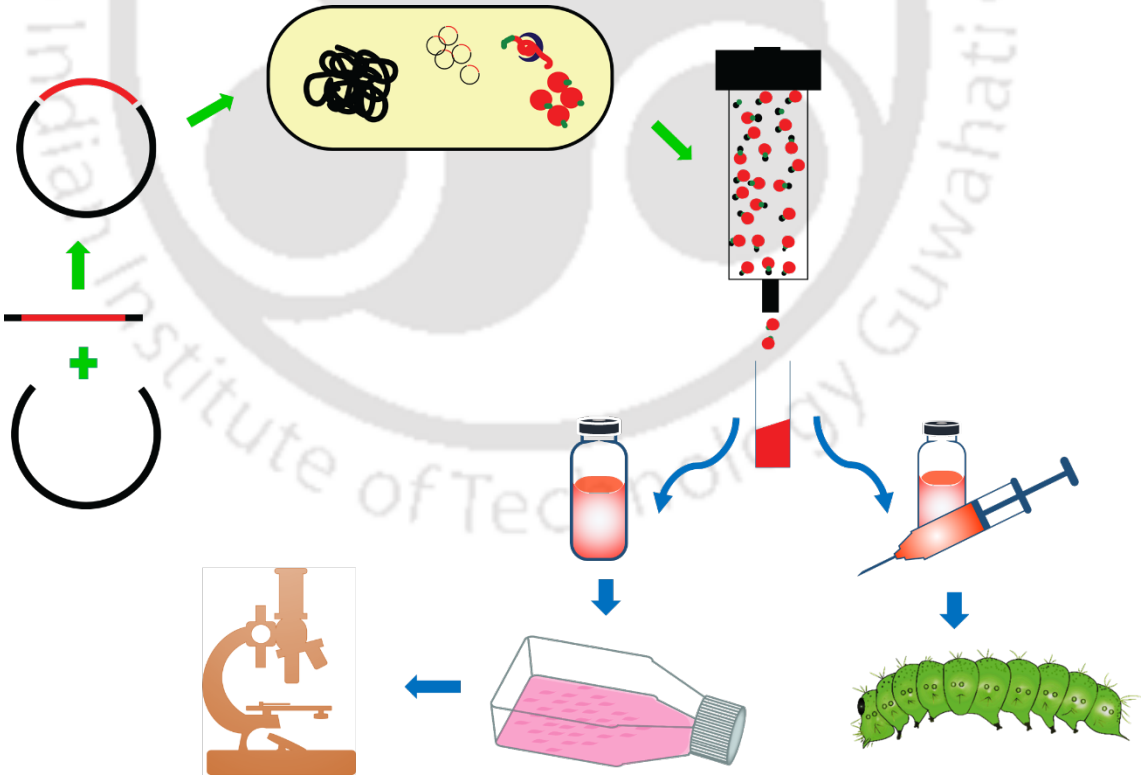

2.1 Introduction

The rising population, dietary preferences, and urbanization in developed as well as in developing countries require tremendous steps to enhance agriculture production to meet the increasing demand. It can only be achieved by considerably increasing agricultural yield and modification in the use of input resources. However, agricultural productivity is highly demarked by changes in climatic conditions and continuous attacks by pests. With the advent of synthetic and biological insecticides/pesticides, the pests gradually developed resistance to most of the insecticides, leading to their resurgence (Sundstrom et al. 2014). Among the resistant insect pests, tobacco caterpillar, *Spodoptera litura*, is one of the most destructive agricultural pest damaging more than 100 crops in Asian countries. It has developed resistance to a wide variety of insecticides, particularly organophosphates and pyrethroids (Pattapu et al. 2018, Saleem et al. 2015, Sparks and Nauen 2015). Similarly, cotton and other crops are profoundly affected by the presence of *Helicoverpa armigera* (Bird 2018, Kukanur et al. 2018). Worldwide, more than 6 billion tonnes of pesticides have been used since the last decade, to control the insect pests. Although synthetic pesticides offer a significant advantage in controlling the pest population, the appearance of resistance in insects, hazards associated with human health and environmental persistence, trigger the need to find suitable alternatives (Vontas et al. 2011, Zimmer et al. 2014).

Usage of bio-insecticides, along with integrated pest management strategies, have been recently employed, aiming to control the pests attack with minimal risks to health and environment. Spider and scorpion produce toxins in secreted venom in the wake of defense and predation. These biologically active compounds contain mixture of small peptides and proteins with targeted action on neuronal ion channels such as voltage-gated

sodium channels (Na_v) (Yang et al. 2014, Zlotkin et al. 2000), calcium channels (Ca_v) (Khan et al. 2006, Pal et al. 2013), neuronal receptors located on cell membrane and presynaptic receptors. Because of selectivity, specificity, and biodegradability, these peptides have proven to be agriculturally essential to be used as bio-insecticides (Gershburg et al. 1998, Ji et al. 2002, Kopeyan et al. 1974, Tianpei et al. 2014).

β-BUTX Lqq1a is a β-insect toxin one from scorpion *Leiurus quinquestriatus quinquestriatus*, and this excitatory toxin binds to the receptor site-4 in domain II of insect voltage-gated sodium channels (VGSCs). This toxin purified from crude venom caused fast excitatory contraction paralysis in the fly larvae and proven 40 times more toxic than the crude venom (Kopeyan et al. 1990, Zlotkin et al. 1985), and it shares a high degree of similarity with the well-known scorpion β-insect neurotoxin AaIT1 from *Andructonus australis*. β-BUTX Lqq1a was able to bind competitively with synaptosomal membrane vesicles that were previously treated with AaIT1 (Loret et al. 1990). It has been experimentally proven that β-insect excitatory toxins bind to the voltage sensing module in the extracellular loop of S1-S2 and S3-S4 of domain II and pore-forming module of domain III in the VGSCs of insects (Song et al. 2011).

Being one of the most potential candidates which could be used as bio-insecticides and there are no reports mentioning the expression of β-BUTX Lqq1a toxin in other species, for efficient purification of the toxin in bacteria. The present study is the first report demonstrating the expression and purification of β-BUTX Lqq1a toxin protein in *Escherichia coli*. The current research focuses on the development of purified recombinant β-BUTX Lqq1a and its toxicological effects on cotton bollworm *H. armigera* and tobacco cutworm *S. litura.* Cytotoxicity assays were also conducted to study the activity of the purified recombinant β-BUTX Lqq1a against lepidopteran insect

cell lines. Thus, the present study displays an efficient and economical way of toxin production, providing a novel insight into the development of bio-insecticides.

2.2 Materials and Methods

2.2.1 Bacterial strains and reagents

The *E. coli* DH5-α strain was used for maintenance of cloning and expression vectors. SHuffle T7 Express Lys competent cell (New England Biolabs, USA) was used for the expression of β-BUTX Lqq1a. All restriction enzymes, Phusion DNA polymerase, and ligation enzymes were purchased from New England Biolabs, USA. Integrated DNA Technologies, USA, synthesized all the primers. Plasmid DNA and gel extraction kits were purchased from Macherey Nagel, GmBH.

2.2.2 β-BUTX-Lqq1a gene synthesis

The protein sequence of β-BUTX Lqq1a was obtained from National Center for Biotechnology Information (NCBI) database with the accession number: P19856.1 followed by its reverse translation into DNA sequence using European Molecular Biological Laboratory (EMBL)-EMBOSS Backtranseq software (Rice et al. 2000). The reverse translated DNA sequence β-BUTX-Lqq1a was codon optimized for bacterial expression. Further, the codon-optimized DNA sequence was synthesized and cloned in plasmid-pUC57 flanking EcoRI and HindIII restriction sites (Genscript, USA).

2.2.3 Expression cassette construction

Primers were designed to clone β-BUTX Lqq1a N-terminally along with the His-Tag and thrombin cleavage site in pET28a bacterial expression vector. β-BUTX Lqq1a DNA sequence was amplified with specific primer set Lqq-FP (5'- CGC **CAT ATG** AAG AAA AAC GGT TAT GCG GTG G -3') and Lqq-RP (5'- CGC **GGA TCC** TTA GTT AAT GGT CAC GAA ATC GC -3') using plasmid pUC57 β-BUTX-Lqq1a as a template. Amplification conditions: initial denaturation for 4 min at 94°C, denaturation at 94°C for 30 sec, annealing at 61°C for 30 sec, extension at 72°C for 45 sec, the cycle was

repeated for 25 times, and then final extension was at 72°C for 10 min. Polymerase Chain Reaction (PCR) amplified β-BUTX Lqq1a sequence, and pET28a expression vector was digested with NdeI and BamHI restriction enzymes at 37ºC followed by their purification using Takara gel purification kit (Takarabio, Japan)

2.2.4 *E. coli* chemical competent cell preparation

The $CaCl_2$ based chemical competent cells were made according to the protocol by Cohen et al. (1972) with little modifications. Initially, 5 ml of LB medium was used to inoculate single DH5α colony and incubated overnight at 37ºC at 200 rpm in rotatory incubator shaker. Next day, 0.1% of overnight grown culture was used to inoculate 500 ml of LB broth and incubated at 37ºC until the optical density of the culture to reach up to OD_{600} 0.3-0.5. Post-incubation, cells were collected by centrifugation at 8000 rpm for 15 min at 4ºC. The collected cells were washed once with 100 mM $CaCl_2$ and incubated in ice-cold 100 mM $CaCl_2$ for 30-45 min. After the incubation, centrifugation was performed to obtain the cell pellet and again resuspended in 1.5 ml of ice-cold 200 mM $CaCl_2$ prepared with 30% glycerol. A 50 µl cell aliquots were made, flash frozen in liquid nitrogen and stored in -80ºC freezer until further use.

2.2.4.1 *E. coli* DH5α transfection

Ligation of the restriction enzyme digested pET28a and β-BUTX Lqq1a purified fragments was performed using T4 DNA ligase at 16ºC for 16 hr. Ligated products were then transformed into bacterium *E. coli* DH5α using calcium chloride ($CaCl_2$) chemical competent transformation method, and the selection was carried out using antibiotic kanamycin (50 µg ml^{-1}). Positive clones were further confirmed by PCR with gene-specific primers. PCR confirmed positive clones were further used for plasmid DNA

isolation. Isolated plasmids were analyzed by using a 1% Agarose gel electrophoresis system, and for imaging, Bio-rad ChemiDoc gel documentation system was employed.

2.2.5 Protein β-BUTX Lqq1a expression and purification

2.2.5.1 Shuffle T7 express LysY chemical competent cells preparation

Chemical competent cells of Shuffle T7 express LysY cells were made according to the protocol followed in **section 2.2.4 of chapter 2**. The pET28a-BUTX Lqq1a (1 µg) was transformed into bacterial protein expression strain SHuffle T7 Express LysY using chemical competent transformation method. The selection was carried out on LB medium supplemented with kanamycin (50 µg ml^{-1}) and incubated at 37ºC for overnight. The colonies were confirmed for the presence of the plasmid and the BUTX Lqq1a gene by PCR based screening method.

2.2.5.2 The $(His)_6$ β-BUTX Lqq1a toxin expression

A single colony Shuffle T7 Express carrying the pET28a-BUTX Lqq1a was used to inoculate 5 ml of LB broth and incubated overnight at 37ºC at 200 rpm. One percent of overnight grown culture was utilized to inoculate into the expression medium. The β-BUTX Lqq1a protein expression was carried out using Terrific Broth (TB) medium (Tryptone 12 g l^{-1}, yeast extract 24 g l^{-1}, K_2HPO_4 12.54 g l^{-1}, KH_2PO_4 2.31 g l^{-1}) with limited modification in medium composition. Instead of recommended glycerol (0.4%) concentration in the TB medium, 1.0 – 2.0% glycerol was used. Initially, bacterial culture was grown until OD_{600} to reach 0.6 at 30ºC and then the culture was induced with 0.5 mM isopropyl thiogalactopyranoside (IPTG) and incubated for 16 hr at 16°C in a refrigerated incubator shaker at 200 rpm.

2.2.5.3 The $(His)_6$ β-BUTX-Lqq1a toxin affinity purification

Post-incubation, the culture was centrifuged at 10,000 rpm for 30 min at 4ºC, and cell pellet was re-suspended in binding buffer A (20 mM Tris-Cl, 300 mM NaCl, 20 mM Imidazole, 10% Glycerol, 5 mM Benzamidine HCl, 2 mM DTT), followed by its lysis using Vibra cell Sonicator with 2 sec pulse ON and 30 sec pulse OFF conditions. The lysate was centrifuged at 13,000 rpm for 1 hr at 4ºC, and the clarified supernatant solution was loaded into Nickel- Nitrillo Triacetic Acid (Ni-NTA) affinity chromatography pre-equilibrated with binding buffer A. Different fractions were eluted with binding buffer A containing 300-400 mM imidazole and analyzed by using 16% Sodium Dodecyl Sulfate-Poly Acrylamide Gel electrophoresis (SDS-PAGE). Gel images were captured using a Biorad Gel Doc EZ gel documentation system and analyzed with Image Lab software 4.0 from Biorad.

2.2.5.4 The $(His)_6$ tag removal and size exclusion chromatography purification

Protease thrombin (Sigma, USA) digestion was carried out at 23ºC overnight incubation to cleave the N-terminal $(His)_6$-tag fragment from the affinity-purified $(His)_6$-β-BUTX Lqq1a protein. Further purification of β-BUTX Lqq1a was performed using Size Exclusion Chromatography System (AKTA purifier) with Superdex 75 columns 10/300 GL (GE, USA) to remove the thrombin protease and cleaved $(His)_6$-tag fragments with phosphate buffer saline pH 7.2 supplemented with 5% glycerol. Finally, β-BUTX Lqq1a protein was concentrated using Amicon ultra-15 centrifugal filter unit with ultracel-3 membrane. Quality of the purified fragments were analyzed by using 16% Sodium Dodecyl Sulfate-Poly Acrylamide Gel electrophoresis (SDS-PAGE) followed by Silver staining the gel. Gel images were captured using a Biorad Gel Doc EZ gel documentation

system and analyzed with Image Lab software 4.0 from Biorad. Quantification analysis of purified β-BUTX-Lqq1a protein was performed using Bradford assay.

2.2.6 MALDI-TOF molecular mass determination

The molecular mass of the purified β-BUTX Lqq1a was validated and analyzed via mass spectrometry through matrix-assisted laser desorption/ionization time of flight (MALDI-TOF/TOF, Bruker Daltonics, Germany). The purified protein was mixed with sinapic acid in various (1:1, 2:1, 4:1) proportions and analyzed. The mass spectrum was processed using Flex Analysis 2.4 software (Bruker Daltonics, Germany). Based on fragment ion calculators, β-BUTX Lqq1a theoretical *m/z* value was calculated and compared with the experimentally determined *m/z* value of β-BUTX Lqq1a.

2.2.7 Western blot analysis

The purified neurotoxin β-BUTX Lqq1a and $(His)_6$-β-BUTX Lqq1a was evaluated by western blot analysis. The highly specific antigenic peptide was chosen from Lqq1a toxin using OptimumAntigen™ Design Tool, and polyclonal antibodies were generated in mouse (Genscript, USA), and anti-mouse IgG secondary antibody which is conjugated with alkaline phosphatase was purchased from Genscript, USA. Final purified protein concentration was quantified using the Bradford method. Protein sample 10-20 µg were separated on a 12-15% SDS-PAGE gel electrophoresis. After the SDS-PAGE separation, proteins were transferred onto 0.45 µM Nitrocellulose membrane (Bio-Rad) using the Invitrogen power blotter system (Thermo Scientific, USA). The membrane was then incubated in blocking buffer (Tris-buffered saline with 3% Bovine serum albumin) for 1 hr at room temperature and further incubated with primary antibody diluted in blocking buffer (1:500 and 1:1000) at 4ºC overnight. Post incubation, the membrane was washed 3-4 times in TBS containing Tween-20 wash buffer for 5 min each. The diluted secondary

antibody in blocking buffer was incubated with the membrane for 1 hr at room temperature and then washed with washing buffer. Finally, the detection was performed using the Clarity™ Western ECL substrate (Bio-rad, India), and imaging was carried out using a ChemiDoc XRS™ gel documentation system (Bio-rad, USA).

2.2.8 Cytotoxicity assay of purifiedβ-BUTX Lqq1a with *Sf*-21 insect cell lines

2.2.8.1 MTT assay

The biological activity of purified β-BUTX Lqq1a was tested with Lepidopteran insect cell line *Sf*-21 isolated from *Spodoptera frugiperda* ovaries, obtained from National Center for Cell Science (NCCS), Pune, India. The *Sf*-21 cell lines were maintained in TNM-FH (*Tricoplusia ni*) modified Grace inset cell culture medium with 10% Fetal Bovine Serum (FBS, Gibco, USA), final pH 6.2 at 27°C with the aerated condition. For β-BUTX-Lqq1a cytotoxicity assay 5 µl of *Sf*-21 cells were seeded (1×10^5 cells ml^{-1}) in 96 well plates with a final volume of 200 µL Stock solutions of purified β-BUTX Lqq1a were made in serum-free TNM-FH medium and was added in three different (2.47, 4.95 and 7.42 µg ml^{-1}) concentrations and incubated for 48 hr to obtain IC_{50} value. Only the serum-free medium was used as control. After the incubation period, 5 µl MTT (5 mg ml^{-1}, Sigma) solution was added and then incubated for 4-6 hr in dark condition at 27°C or until the formation of purple color crystals. Crystals were further pelleted by centrifugation at 1000×g for 15 min and then solubilized in 100 µl of dimethyl sulfoxide (DMSO). Absorbance was recorded using a Tecan multiplate reader (infinite M200pro) with the dual wavelength at A_{590} and A_{660} as the reference wavelength. The experiment was conducted twice with each concentration in triplicates.

2.2.8.2 Light microscopy analysis

Sf-21 cell morphological changes were observed using Inverted light microscope (Nikon TiS, Japan). *Sf*-21 cells were seeded in 24 well plates (5×10^4 cells ml^{-1}) and treated with 4.95 µg ml^{-1} β-BUTX Lqq1a protein for 24 and 48 hr for determination of action of toxin on a various time interval. Zeocin antibiotic (10 µM) was used as a positive control. Post-incubation, cells were centrifuged at 300×g for 10 min and washed with phosphate buffered saline (PBS) pH 7 and observed under an inverted fluorescence microscope (Nikon Ti-S) at 40×magnification. All the images were processed through NIS elements 4.50 analysis software (Nikon, Japan)

2.2.8.3 Fluorescence microscopy analysis

Propidium Iodide (PI, Sigma) binds to DNA by intercalation between the bases. It is commonly used to detect the dead cells in a population since it is not permeable to living cells. PI has maximum excitation and emission wavelength at 535 and 617 nm respectively. Here, in the present study, utilizing the property of PI to evaluate the cytotoxic effect of the purified β-BUTX Lqq1a protein on *Sf*-21 insect cell lines was undertaken. To study the effect, initially *Sf*-21 cells were treated for 24 and 48 hr with higher concentration of toxic protein at 27ºC in aerated static incubator. Post-treatment, cells were collected by centrifugation at 300×g for 10 min at 4ºC and washed with 1 X PBS (pH 7.4) buffer and stained with PI (1 mg ml^{-1}). The cells were visualized under Inverted Fluorescence Microscopy (Nikon Ti-S, Japan) and obtained image was processed with NIS elements 4.50-image analysis software.

2.2.8.4 Ultra-structural analysis using Field Emission Scanning Electron Microscopy

Field Emission-Scanning Electron Microscopy was used to analyze the morphology of treated *Sf*-21 cell lines. For FESEM analysis, cells were treated with 4.2 µg ml^{-1} β-BUTX Lqq1a protein for 24 hr. After treatment, cells were washed with phosphate buffered saline and then fixed by using 4% paraformaldehyde and 2.5% glutaraldehyde for 24 hr at 4°C. After the fixation, cells were centrifuged at 300×g for 10 min and washed with phosphate buffered saline. Finally, cells were dehydrated using an ethanol gradient series of 10, 30, 50, 70, and 100% for 10 min each. Before sample analysis, cells were sputter-coated with gold film (SC7620 "Mini," Polaron Sputter Coater, Quorum Technologies, England) and probed with 2.00 KV electron high tension (EHT) in-Lens secondary detectors using FE-SEM, Carl Zeiss, SIGMA VP, USA.

2.2.8.5 Flow cytometry analysis

Cell cycle analysis was performed using flow cytometer to evaluate the effect of purified recombinant β-BUTX Lqq1a on *Sf*-21 insect cell line. For flow cytometry analysis, cells with a concentration of 2×10^6 cells ml^{-1} were seeded and incubated for 24 hr at 27°C. PBS was taken as control, and for treatment 4.1 and 8.2 µg of β-BUTX Lqq1a toxin was taken. Post-incubation, ice-cold 70% ethanol was added dropwise to fix the cells at 4°C overnight. After the fixation, centrifugation at 2000 rpm for 10 min was done to remove the residual ethanol. Pelleted cells were again re-suspended in phosphate buffered saline (PBS, pH 7.4) and Ribonuclease A (RNase A) treatment was done at 37°C for 1 hr. The cells were then stained by using propidium iodide (1 mg ml^{-1}) for 10 min and analysed using BD FACS Caliber flow cytometer.

2.2.9 Bioassay of β-BUTX Lqq1a with *H. armigera* and *S. litura*

2.2.9.1 Maintenance of insect cultures

H. armigera and *S. litura* insect cultures were procured from National Bureau of Agricultural Insect Resources (NBAIR), Bangalore, India. Both the insects were maintained at 16:8 hr light and dark conditions at 25±3ºC with 60-70% relative humidity (RH) on natural castor leaves diet.

2.2.9.2 Intra-hemocoeilic injection bioassay

Intra-hemocoel injection bioassay was performed using 4th to 5th instar larvae of *H. armigera,* and *S. litura*. Various β-BUTX Lqq1a protein (5 µl) concentrations (2.0, 1.0, and 0.2 µg insect^{-1}) were used for injection in *H. armigera* and for injection in *S. litura* (2.0, 1.0, 0.5 and 0.2 µg insect^{-1}) concentrations were used. PBS (Phosphate Buffered Saline, pH 7.4) was taken as a control for the insects. For each dose, twenty *H. armigera* and thirty *S. litura* larvae were injected with 5 µl of β-BUTX Lqq1a protein and mortality rates were scored at 12, 24, 36, 48, and 72 hr post injection time including control. All the insects were starved for 2 hr pre-injection and chilled at 4ºC until torpid and before injection. Injected insects were supplied with natural castor leaves diet only. All the experiments were conducted at 25-28ºC with 60-70% RH level with 16:8 hr light and dark photoperiod.

2.2.10 Statistical data analysis

Data analysis were conducted using GraphPad Prism software (version 6.0). The values are expressed as mean with standard deviation. For the MTT assay, the data were compared using a one-way analysis of variance (ANOVA) test with Dunnett's multiple comparisons test. Differences were considered statistically significant when the $p < 0.05$. The IC_{50} value was calculated using GraphPad Prism software with the normalized

absorbance percentage vs. log concentration. Kaplan-Meier survival plots were constructed using GraphPad Prism software (version 6.0), and comparison of survival curve was done using Log-rank (Mantel-Cox) test, and LC_{50} value was calculated based on Probit analysis (Finney 1952).

2.3 Results

2.3.1 Cloning in pET28a expression vector

In this study, initially, β-BUTX Lqq1a gene sequence was codon optimized with higher codon adaptation index (CAI=0.97) **(Fig. 2.1)** to maximize the soluble expression in *E. coli* SHuffle T7 Express LysY cells and further cloning into pUC57 vector resulted in pUC57-β-BUTX Lqq1a (**Fig.2.2**) Initially, β-BUTX Lqq1a gene was successfully amplified using the gene-specific primers from pUC57-β-BUTX Lqq1a with the calculated size of 210 base pair (bp) and pET28a double digested fragments were also purified (**Fig. 2.3**). This amplified fragment was further ligated with pET28a vector and cloned in DH5-α cells which has been confirmed by PCR (**Fig. 2.4**).

2.3.2 Expression and purification using Ni-NTA affinity chromatography

The β-BUTX Lqq1a expressional studies were performed in *E. coli* SHuffle T7 Express LysY cells. **Fig. 2.5** indicates the overall schematic representation of steps involved in β-BUTX Lqq1a protein expression and purification. Initial expression studies with various media such as LB, TB and Auto Induction Medium suggested that Terrific broth supplemented with 1.5% glycerol resulted in soluble expression of recombinant protein. Successful purification of $(His)_6$-β-BUTX Lqq1a using Ni-NTA affinity chromatography was achieved using the binding buffer added with 10% glycerol which enhanced the stability of the recombinant protein as analyzed by SDS-PAGE (**Fig. 2.6**). The calculated molecular mass of the purified $(His)_6$-β-BUTX Lqq1a was 10.5 kDa. Reducing the growth temperature to 16ºC after the IPTG induction, resulted in significant improvement in the soluble protein fraction in the supernatant, however overall biomass obtained was comparatively less than higher temperature growth. Large scale purification helps to alleviate the problem with reduced biomass.

2.3.3 N-Terminal $(His)_6$ tag removal using Thrombin Protease

The presence of $(His)_6$ tag at the N-terminal region of the protein would enhance the stability and solubility of the recombinant protein as reported by Esen et al. (2019). However, N-terminal presence may interfere with the biological activity of the recombinant protein. In order to remove the N-Terminal $(His)_6$-tag along with the vector sequence (2 kDa) associated with scorpion toxin, thrombin protease treatment was performed. Thrombin preferentially recognize the LVPRGS amino acid sequence and cleaves between Arg and Gly residues. After initial affinity purification, N-terminal $(His)_6$-tag was removed from $(His)_6$-β-BUTX Lqq1a by incubating with protease thrombin. Based on the sequence analysis using Protparam (Gasteiger et al. 2005), it has been predicted that four extra amino acids (Gly, Ser, His, Met) have added to the N-terminal region of β-BUTX Lqq1a protein.

2.3.4 Size exclusion chromatography

Size exclusion chromatography has become an inevitable technique in the protein purification studies as the desired protein separates based on the size. Purification of soluble and functional cysteine rich neurotoxic proteins from the aggregated counterparts when it is expressed in heterologous expression system and separation from the crude venom, gel separation chromatography has played an essential role in many studies (Kuzmenkov et al. 2016, Oukkache et al. 2015, Rojas-Azofeifa et al. 2019).

In the present study, 2 kDa N-terminal peptide part containing $(His)_6$ tag was initially removed by thrombin digestion. Fractions consisting of $(His)_6$ tag and recombinant protein β-BUTX Lqq1a were further separated and purified to homogeneity using size exclusion chromatography system. **Fig. 2.7** shows the resulted size exclusion chromatogram from the purification where prominent peak 2 shows the $(His)_6$-β-BUTX

Lqq1a protein separation from the aggregated protein (peak 1) and other protein debris, i.e., peak 3 and 4. Analysis of digested and undigested protein using SDS-PAGE followed by silver staining method indicated the removal of N-terminal $(His)_6$ tag and the homogeneity of the purified β-BUTX Lqq1a. **Fig. 2.8A** represents the schematic diagram of the construct $(His)_6$-β-BUTX Lqq1a with predicted molecular mass. In **Fig. 2.8B** Lane 1 shows the undigested protein fraction, i.e. $(His)_6$-β-BUTX Lqq1a, and the approximate calculated molecular weight of 10.05 kDa. Lane 2 shows the N-terminal $(His)_6$ tag removed β-BUTX Lqq1a protein, and the theoretically calculated molecular weight being 8.25 kDa.

2.3.5 Mass spectrometry and Western blot analysis

MALTI-TOF mass spectrometry is an inexpensive and effective tool in identification of bacteria, fungi and virus (Calderaro et al. 2014, Cornut et al. 2019, Hinse et al. 2011, Sonthayanon et al. 2019, Wieser et al. 2012). Apart from organismal identification, this technique also helps in comprehensive proteomic analysis of various crude venom extracted from arthropod insects that has huge potential of clinical as well as biotechnological applications (Huang et al. 2015, Khamessi et al. 2018, Oukkache et al. 2015). Similar studies conducted with purified recombinant protein using MALDI-TOF mass spectrometry analysis further confirmed successful purification of β-BUTX Lqq1a with a molecular mass of 8255.95 Da as compared to the predicted theoretical mass of 8255.81 Da, as shown in **Fig. 2.9A**. Further western blotting analysis also indicated the shift in the molecular weight of the N-terminal His tag removed BUTX Lqq1a recombinant toxin **(Fig. 2.9B).**

2.3.6 Cytotoxicity analysis of treated *Sf*-21 insect cell line using MTT assay

To detect the potential action of toxins purified from various sources on either bacterial, or cancerous cell line, one should be able to detect the metabolic activity of the cell of interest upon treatment. Studies conducted with various peptide with different potential was tested against microbes as well as cancerous cells indicated the use of MTT cell viability assay to assess the anti-proliferative activity (Almaaytah et al. 2012). Here in this study, Cytotoxic activity of purified β-BUTX Lqq1a protein towards *Sf*-21 insect cell population was studied using MTT dye-reduction method. Data analysis revealed a significant reduction ($p < 0.002$) in the cell proliferation and viability of the insect cell lines in a dose-dependent manner (**Fig. 2.10A**). After the data normalization, mean IC_{50} value was observed to be 1.70 to 3.01 µg ml^{-1} with 95% confidence interval (n=12, df=10) **(Fig. 2.10B)**.

2.3.7 Morphological assessment using Light microscopy

To further assess the cytotoxicity of treated cells concerning changes in the cell morphology, qualitative analysis using inverted bright field microscopy was performed. In PBS treated control (**Fig. 2. 11 a and d**), the cells were observed to be healthy, regular, circular and grainy in structure with no morphological changes, whereas in zeocin antibiotic treatment (positive control) (**Fig. 2. 11 b and e**), most of the cells were irregularly shaped depicting disintegration of membrane and formation of apoptotic bodies. Correspondingly, insect cells lines treated with β-BUTX Lqq1a toxin (**Fig. 2.11 c and f**) showed significant morphological changes such as blebbing of the membrane, irregularly shaped cells, cell bulging as well as the formation of apoptotic cell structures.

2.3.8 Fluorescence microscopy analysis

Propidium iodide based cytotoxic analysis is one of the rapid and highly sensitive method to detect the cellular damage caused by particular toxic proteins or metabolites particularly membrane damage (Wrobel et al. 1996). This cell membrane impermeable dye binds to DNA with the cell membrane impairment. As shown in **Fig. 2.12** control cells treated with only PBS pH (7.4) exhibited little or no morphological aberrations which resulted in insignificant uptake of Propidium iodide and almost 90% cells showed negative for PI staining in both 24 and 48 hr treatment. However, *Sf*-21 cells treated with scorpion recombinant protein β-BUTX Lqq1a resulted in profound uptake of propidium iodide in both 24 as well as 48 hr treatment intervals.

2.3.9 Ultra structural analysis using FE-SEM

In addition to it, ultra-structural analysis of insect cell lines upon treatment with the β-BUTX Lqq1a was experimented using FE-SEM. While the PBS treated (control) cells appeared regular and smooth (**Fig. 2.13a**), upon treatment with the toxin, cell lines showed cell shrinkage and shape deformities (**Fig. 2.13b**).

2.3.10 Flow Cytometry analysis

Chromosomal DNA damage could result from oxidative damage caused by the external stimuli which possibly affects the cell cycle progression. The effect of purified β-BUTX Lqq1a toxin was studied by treating the *Sf*-21 cells followed by flow cytometry analysis. ModFit a program was used to analyze the percentage of cells in each phase (G1, S and G2) along with control population. As shown in **Fig. 2.14**, in untreated control population, percentage of cells observed in G1, S, and G2 phase were 42.61, 46.13, and 11.26% respectively. However, *Sf*-21 cells treated with β-BUTX Lqq1a (4.1 and 8.2 µg) exhibited, increased accumulation of cells in G1 phase, 54.61% and 63.78% respectively

and only 19.18% and 14.52% cells were observed in S phase of treated population. We could observe the increment in G1 population of cells treated with increasing concentration of recombinant protein, depicting the dose dependent action.

2.3.11 Insect bioassay

2.3.11.1 *Helicoverpa armigera*

Biological activity of β-BUTX Lqq1a toxin was examined against two lepidopteran insects, *H. armigera* and *S. litura*. Injecting *H. armigera* insect with recombinant β-BUTX Lqq1a toxin resulted in significant larval mortality, which occurred during the initial 24 hr as shown in **Fig. 2.15A**, Kaplan-Meier percentage survival analysis of three different treatments affected the survival of larvae in a dose-dependent manner (Log-rank (Mantel-cox test) χ^2=61.74, df=3, and p<0.0001). Compared to the control group, 60% of mortality was observed in the treated population after 24 hr of injection. Moreover, an increase in the mortality rate was observed after 48 hr. The control population injected with only PBS were able to survive even after 72 hr post injection. The calculated LD_{50} value (R^2=0.99, df=3, p=0.0023) for the treated *H. armigera* was found to be 0.13 µg 175 mg^{-1} or 0.74 µg g^{-1} of larval body mass. Visual observation on toxin treated *H. armigera* showed partial paralysis and sluggish food intake in the initial period of treatment followed by stiffening of the body. Within 36 hr, complete paralysis with gradual melanization of the body was observed, ultimately leading the death of the insects. The control insects (PBS treated) appeared to be healthy and normal, as seen in **Fig. 2.15B.**

2.3.11.2 *Spodoptera litura*

Mortality of *S. litura* larvae injected with various doses of recombinant β-BUTX Lqq1a protein showed significant differences (Log-rank (Mantel-cox test) χ^2=140.4, df=4,

and $p<0.0001$) in the survival rate. Kaplen-Meier survival percentage analysis revealed (**Fig. 2. 16A**) 30-40% reduction in the survival of larvae within 24 hr. More than 90% of the population showed larval mortality 36 hr post injection. On the other hand, the control population was able to reach the normal pupation stage. Complete death of the *S. litura* was observed after 48 hr of post-injection. The calculated ($R^2=0.93$, df=3, $p=0.0005$) LD_{50} value for the treated *S. litura* was 0.147 µg 210 mg^{-1} that is 0.7 µg g^{-1} of insect body mass. Both the insect's cultures showed paralysis immediately after the injection along with skin blackening, shortened body, and reduced feeding, as shown in **Fig. 2.16B**.

2.4 Discussion

The present study is the first report documenting the expression and purification of scorpion based β-BUTX Lqq1a neurotoxin in the bacterial system and its putative application as a bio-insecticide. β-BUTX Lqq1a consists of four intrinsic disulfide bond that bridges together the protein in an adequately folded three-dimensional structure. This folding allows for more natural interaction with insect sodium channels. Codon optimization of the gene of interest, solubilization tag, and expression host selection all are an essential strategy for obtaining properly folded protein in soluble form. To achieve this, when the eukaryotic β-BUTX Lqq1a gene codon optimized for the bacterial expression system, it enhanced the solubility and expression of scorpion toxin. However, most of the spider or scorpion neurotoxins expressed in heterologous systems such as *E. coli* produced as inclusion bodies because of improper folding and absence of oxidized or reduced environment (Dai et al. 2012, Down et al. 2006, Dutra et al. 2008, Fitches et al. 2004, Yang et al. 2018).

Moreover, obtaining a reasonable amount of accurately folded soluble protein is vital to structural and functional studies, especially when the molecule of research is to dealt with *in vivo* experiments. A similar toxin such as AaIT expressed in bacterium resulted in inclusion bodies formation (Ji et al. 2002). However, when β-BUTX Lqq1a toxin was expressed by using SHuffle T7 express LysY strain, which favored the formation of disulfide bonds in the cytoplasm itself, easing out to purify the protein in soluble form. In addition to it, purification of β-BUTX Lqq1a toxin in its proper folded way was achieved by using size exclusion chromatography, aiding its usage in the cytotoxicity and insect bioassays.

MTT assay is one of the vital approaches to quantify the metabolically active cells, which can cleave tetrazolium salts into insoluble purple formazan crystals. The amount of crystals formed is directly proportional to the activity of the proliferation of cells. MTT assay with the purified β-BUTX Lqq1a toxin on insect cell line *Sf*-21 resulted in a dose-dependent decrease in the viable cell population. Ji et al. (2002) conducted cytotoxicity studies with recombinant Aa IT1 toxin on insect cell line *Sf*-9, resulted in reduced cell viability with deficient concentration and the LC_{50} value determined to be 0.13 µM (i.e., 0.913 µg ml^{-1}). Although the β-BUTX Lqq1a toxin reduced the viability of *Sf*-21 cells, calculated IC_{50} value is moderately higher (1.70-3.01 µg ml^{-1}) than Aa IT1 toxin. The difference in the concentration may be due to a small degree of variation (10%) in the amino acids sequence between the two recombinant proteins. In addition, the cytotoxic study of similar neurotoxin Aa IT1 from *A. australis* on *Sf*-9 cell line demonstrated that small intrusion in the plasma membrane caused the cells to swell and resulting in membrane blebbing (Ji et al. 2002). It may be due to binding of Aa IT1 do the putative sodium channel protein present in the plasma membrane increasing the influx of sodium ions. When *Trichoplusia ni* insect cell line (BTI-TN-5B1-4) was treated with the venom purified from *Nasonia vitripennis*, it allowed more flow of sodium ions and also increased the permeability of plasma membrane (Rivers et al. 2002). Similar morphological changes like membrane blebbing, the formation of apoptotic structures, and cell shrinkage were observed in the present study when β-BUTX Lqq1a treated *Sf*-21 insect cell lines were observed microscopically. Therefore, this study suggests that apoptosis could be a causative nature of the cytotoxic activity of β-BUTX Lqq1a.

MTT cell viability assay offers a quantitative estimation of proliferating cells in the particular cell population. However, membrane compromised cells could not be

detected using the MTT assay. Cellular staining which provide detailed information about the damage caused by the other proteins would offer an added advantage. Various stains interact with the chromosomal DNA such as propidium iodide, DAPI not only reveal the membrane impairment, and fragmentation of the nucleus also can be studied. Several studies have reported the use of PI staining principle in studying the effect of secondary metabolites, proteins, and various nanoparticles action on cancerous cell lines through fluorescence microscopy, spectrophotometry as well as flow cytometry analysis (Dengler et al. 1995, Jones and Senft 1985, Şahin et al. 2018). Present study, β-BUTX Lqq1a treated *Sf*-21 cells stained with PI revealed initial membrane impairment. In addition to that, it also clearly suggested the presence of apoptotic bodies and fragmented nucleus in the treated population.

Recombinant β-BUTX Lqq1a showed insecticidal activity on injection into *H. armigera* and *S. litura* with paralysis and mortality symptoms. The intra-hemocoelic injection caused initial flaccid paralysis in *H. armigera* immediately after the injection. Recovery from paralysis was observed after 2 hr of post-injection; however, the feeding behavior completely stopped after 24 hr. Similar studies by Khan et al. (2006) reported that topical application of bacterially expressed spider neurotoxin ω-ACTX-Hv1a toxin (Hvt) from *Hadronyche versuta* onto *H. armigera* resulted in severe mortality within 24 hr post application. It required only 4 pmol $g^{-1}$of body weight to kill the population. Whereas, in the present study, the needed recombinant β-BUTX Lqq1a only 0.074 µg 100 mg^{-1} of larval weight. Upon treatment with Hvt toxin, behavioral symptoms such as lack of coordination and head shaking were noticed in *H. armigera*. However, with an intra-hemocoelic injection of β-BUTX Lqq1a, complete lack of coordination, movement, and feeding were observed. This action probably may be due to the different mode of action

of Hvt, which acts preferably on calcium channel, and β-BUTX Lqq1a effect on voltage-gated sodium channels of *H. armigera.* In similar studies with insect depressant scorpion neurotoxin from *Buthus martensii* Karsch insect toxin 4 (BmK IT4) showed treated larvae with significantly reduced weight and mortality in cotton bollworm. Though it took 98 hr to kill 50% of the bollworm population, 77% mortality was achieved with an almost negligible amount of feeding (Jiang et al. 2001). Nevertheless, within 48 hr of treatment, nearly 90% of the bollworm larvae died due to β-BUTX Lqq1a toxicity. Hence, β-BUTX Lqq1a could be one of the useful tools in controlling the cotton bollworm population despite the appearance of resistance due to synthetic chemical insecticides.

β-BUTX Lqq1a affected the survival of *S. litura* in a dose dependent manner. After toxin injection, average larvae weight increased to a range of 0.9 - 17.4% from the initial average weight. Whereas in control population, 25.97% increase was observed within 24 hr of injection. In the treated population after 24 hr, there was no increase in the average weight of the insect due to complete lack of feeding, whereas in PBS treated control, regular feeding was observed, and also the insects were able to attain pupation or continued with the normal life cycle. Biological activity of δ-palutoxins (Pl1a) from *Paracoelotes luctuosus* tested against *S. litura* resulted in a significant increase in the mortality rates. The LD_{50} value was reported to be 0.95 to 4.48 µg 100 mg^{-1} of insect body weight (Corzo et al. 2000). In the present study, the recombinant β-BUTX Lqq1a required only 0.7 µg g^{-1} of insect body mass to kill 50% population within 36 hr injection. Recombinant β-BUTX Lqq1a is 12 times more potent when compared with reported δ-palutoxins or Pl1a (Corzo et al. 2000). These experiments suggest that β-BUTX Lqq1a was biologically active against *Sf*-21 insect cell lines as well as the two major significant agricultural pests viz., *H. armigera* and *S. litura.*

2.5 Conclusion

Aa IT is the most widely studied neurotoxin from *A. australis,* which has been expressed in various microorganisms such as baculovirus and entomopathogenic fungi and being used or tested as a potential biopesticide (Khan et al. 2006, Zlotkin et al. 2000). Likewise, the present study demonstrated the molecular cloning, soluble expression, and purification of recombinant β-BUTX Lqq1a in a bacterial system. Moreover, the successful application of purified β-BUTX Lqq1a toxin on *Sf*-21 insect cell lines also suggested the possible cytotoxicity. Due to the high potency, if this toxin can express via a suitable delivery system such as *Metarhizium anisopliae, Beauveria bassiana,* and other entomopathogenic fungi into the insect circulatory system, it could turn out to be a potential alternative to the synthetic chemical insecticides.

5'AAGAAAAACGGTTATGCGGTGGACAGCAGCGGCAAGGCGCCGGAGTGCCTGCTGA

GCAACTACTGCTATAACGAATGCACCAAGGTTCACTACGCGGATAAAGGTTATTGCT

GCCTGCTGAGCTGCTACTGCGTGGGCCTGAGCGACGATAAGAAAGTTCTGGAGATCA

GCGACGCGCGTAAGAAATATTGCGATTTCGTGACCATTAAC**3'**

Fig. 2.1 Scorpion neurotoxic β-BUTX Lqq1a sequence codon optimization. Gene sequence codon optimized using commercially available Optimumgene™ codon optimization analysis tool. Optimized gene sequence length is 210 bp with codon adaptation index (CAI) value 0.97.

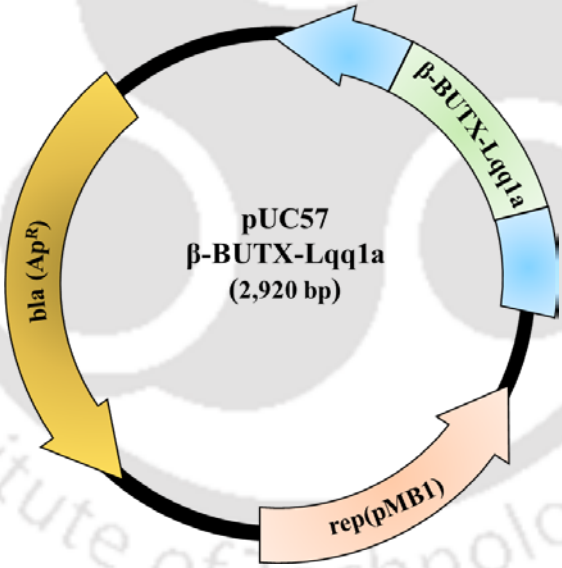

Fig.2.2 Plasmid map showing the pUC57 vector harboring β-BUTX Lqq1a gene.

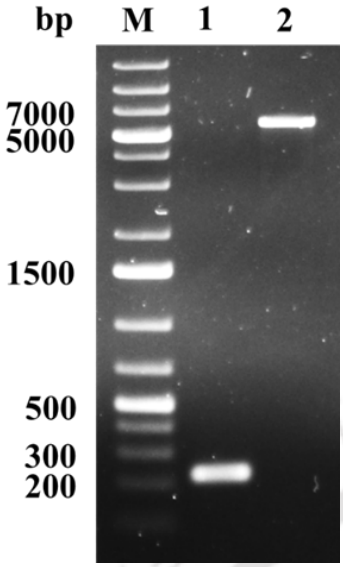

Fig. 2.3 Agarose gel electrophoresis analysis of Gel purified DNA fragments of 1) β-BUTX Lqq1a gene (210 bp), 2) pET28a expression vector (5369 bp) and M- 'O'GeneRuler 1 Kbplus DNA ladder (Fermentas, USA). Both the vector and gene sequence were digested with NdeI and EcoRI restriction enzymes overnight at 37ºC. Gel purified fragments were analyzed on 0.8% agarose gel electrophoresis

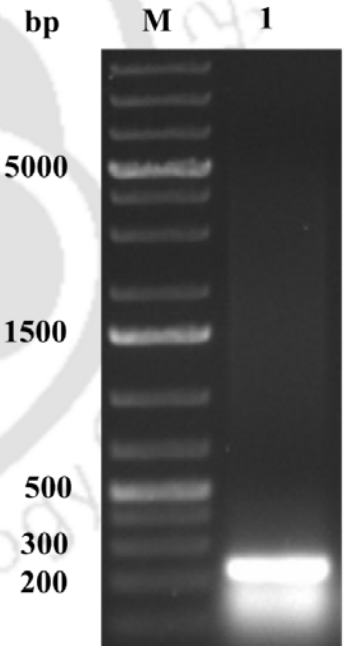

Fig. 2.4 Agarose gel electrophoresis analysis of clone confirmation of pET28a-β-BUTX Lqq1a using polymerase chain reaction with gene specific primers. M is O GeneRuler 1 Kbplus DNA ladder (Fermentas, USA) and 1) β-BUTX Lqq1a gene (210 bp) amplified using the pET28a-β-BUTX Lqq1a colony.

.

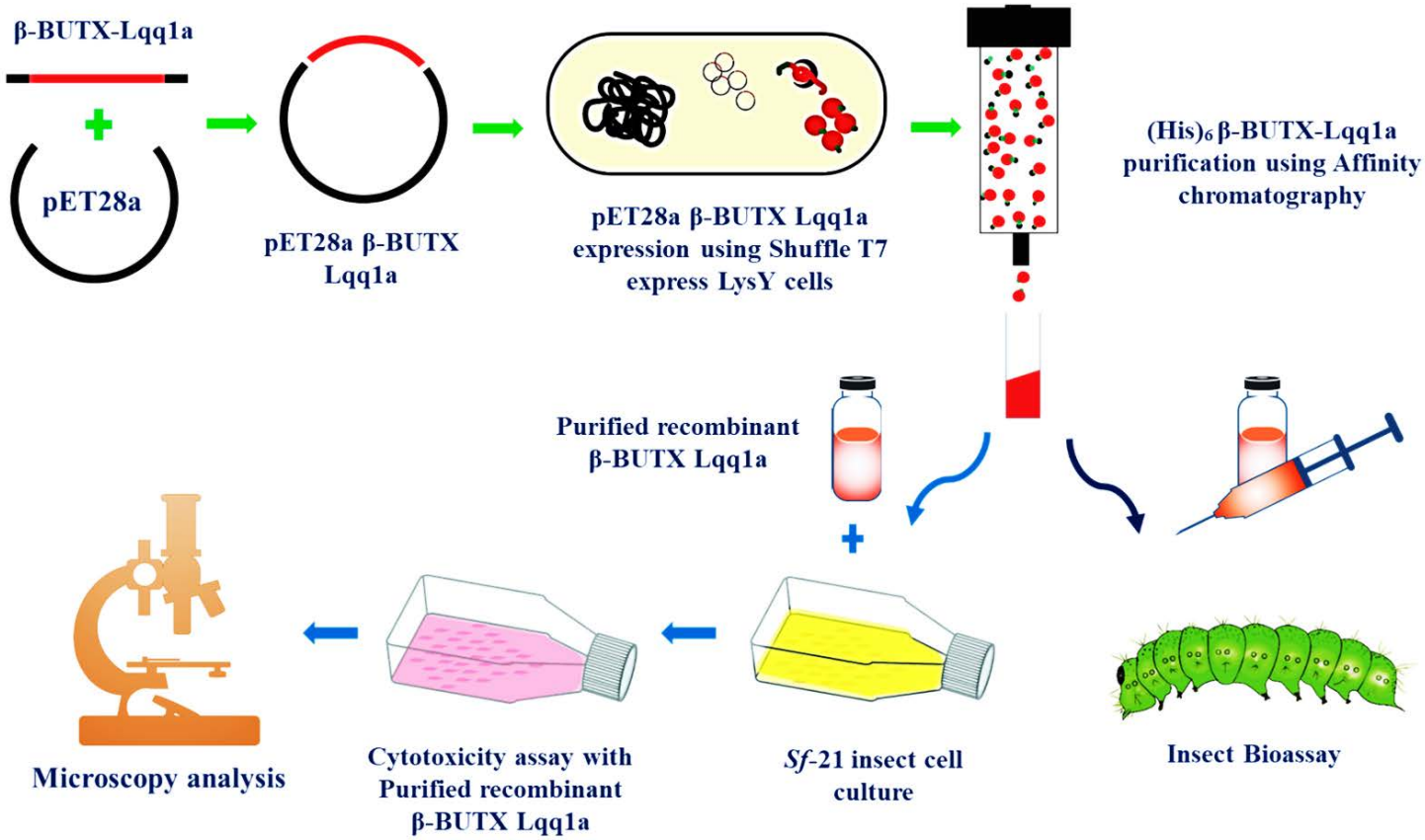

Fig. 2.5 Schematic representation of recombinant β-BUTX Lqq1a expression and purificati

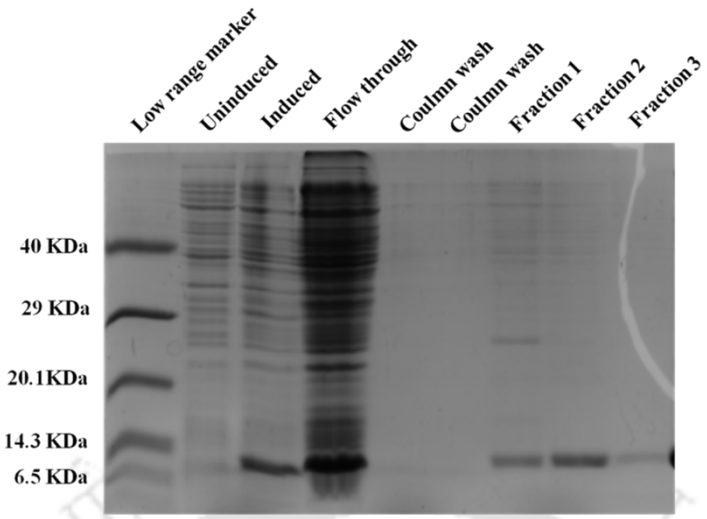

Fig. 2.6 SDS-PAGE analysis of $(His)_6$-β-BUTX Lqq1a protein expression and Ni-NTA affinity purification. $(His)_6$-β-BUTX Lqq1a protein expression was successfully optimized in TB medium supplemented with 1% glycerol with 0.5 mM IPTG at 16ºC for 16 hr at 200 rpm in refrigerated shaking incubator and subsequently purified using Ni-NTA affinity chromatography. Initial affinity purified fractions were analyzed in 18% Tris-Glycine buffer based SDS-PAGE gel electrophoresis. $(His)_6$-β-BUTX Lqq1a protein size is approximately 10.08 kDa. Fraction 1, 2, and 3 shows the near homogeneity-purified protein.

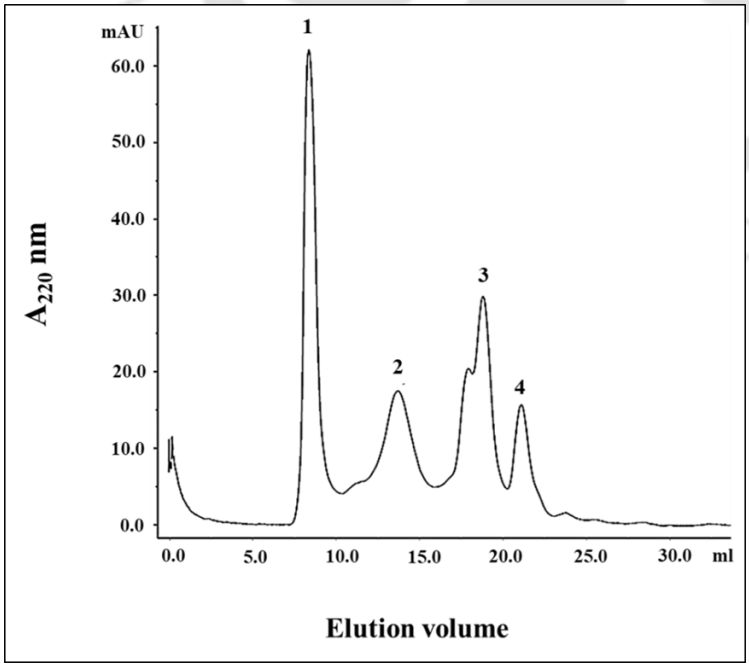

Fig. 2.7 Typical chromatogram from size exclusion chromatography purification of β-BUTX Lqq1a protein using column Superdex 75 10/300 GL Chromatogram indicates the differentially eluted protein fractions against absorbance at 220 nm.

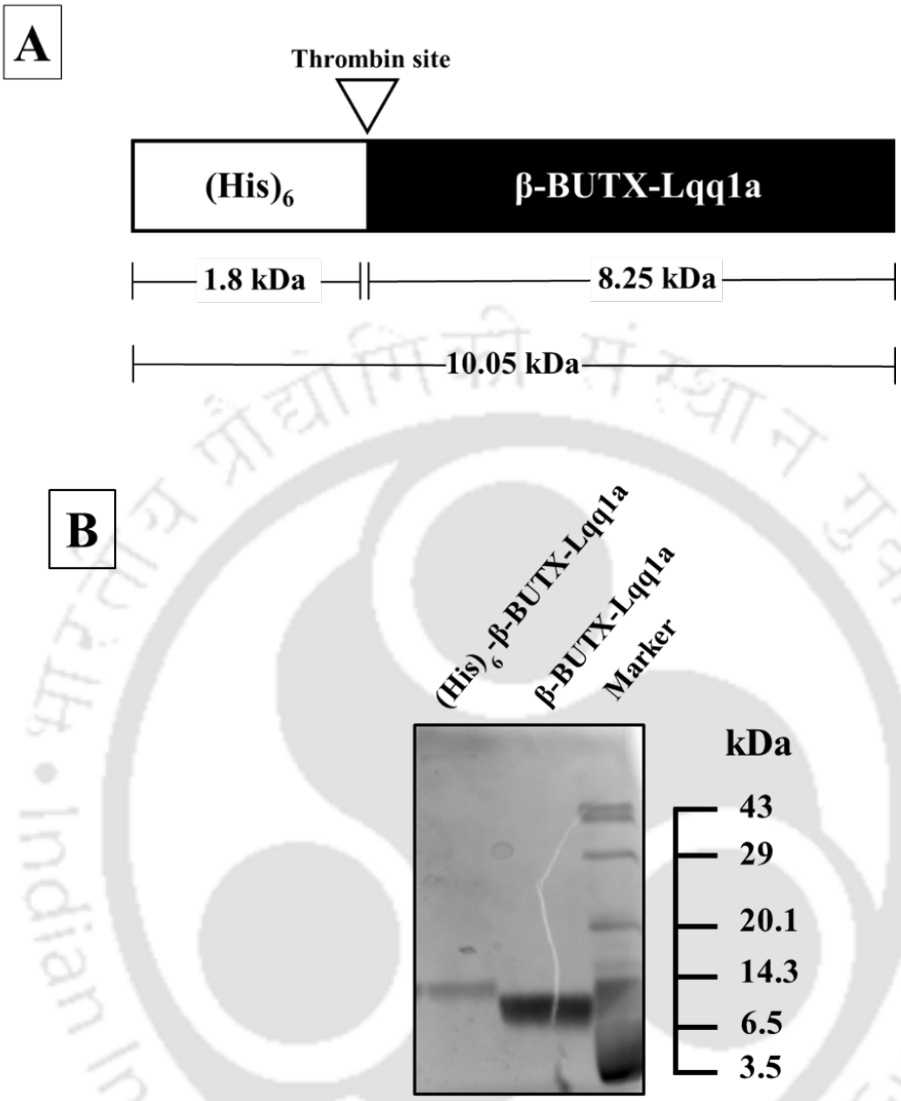

Fig. 2.8 Purification of recombinant $(His)_6$-β-BUTX Lqq1a A) Schematic representation of construct showing predicted molecular mass of $(His)_6$ tag and β-BUTX Lqq1a as well as the total $(His)_6$ β-BUTX Lqq1a mass. B) SDS-PAGE (16% acrylamide gel in Tris-Glycine buffer) analysis of undigested and digested $(His)_6$-β-BUTX Lqq1a protein after size exclusion chromatography purification. Marker denotes the standard low range protein molecular weight marker.

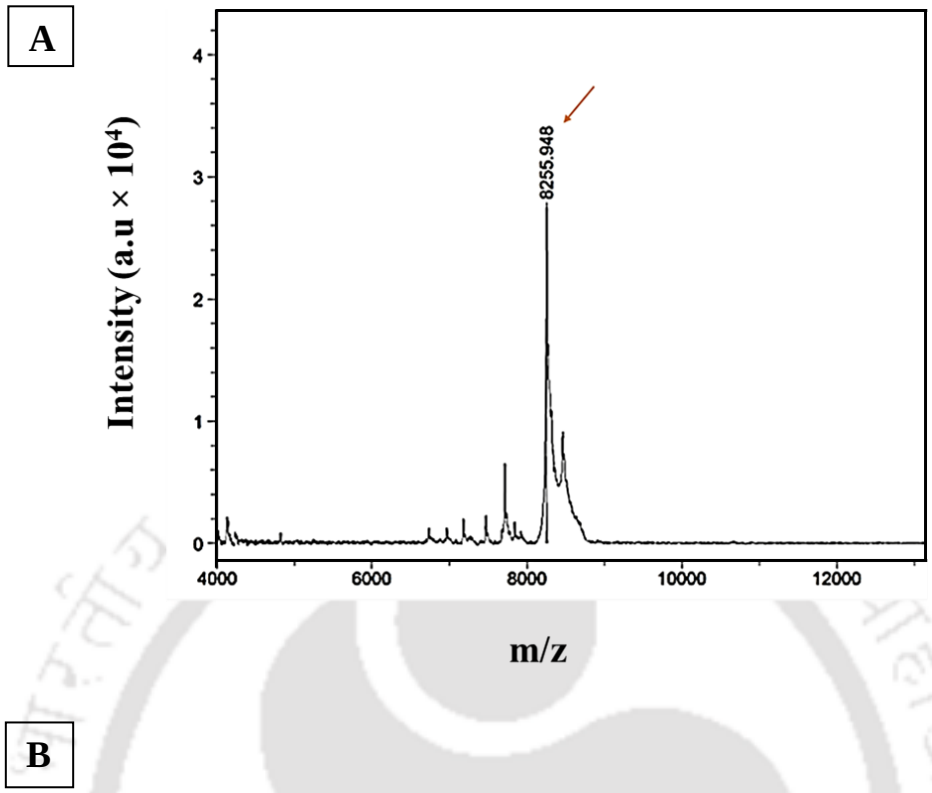

Fig. 2.9 MALDI mass spectrometry **(A)** and Western blot analysis **(B)** of purified β-BUTX Lqq1a protein. Arrow indicates the average mass of column purified β-BUTX Lqq1a protein.

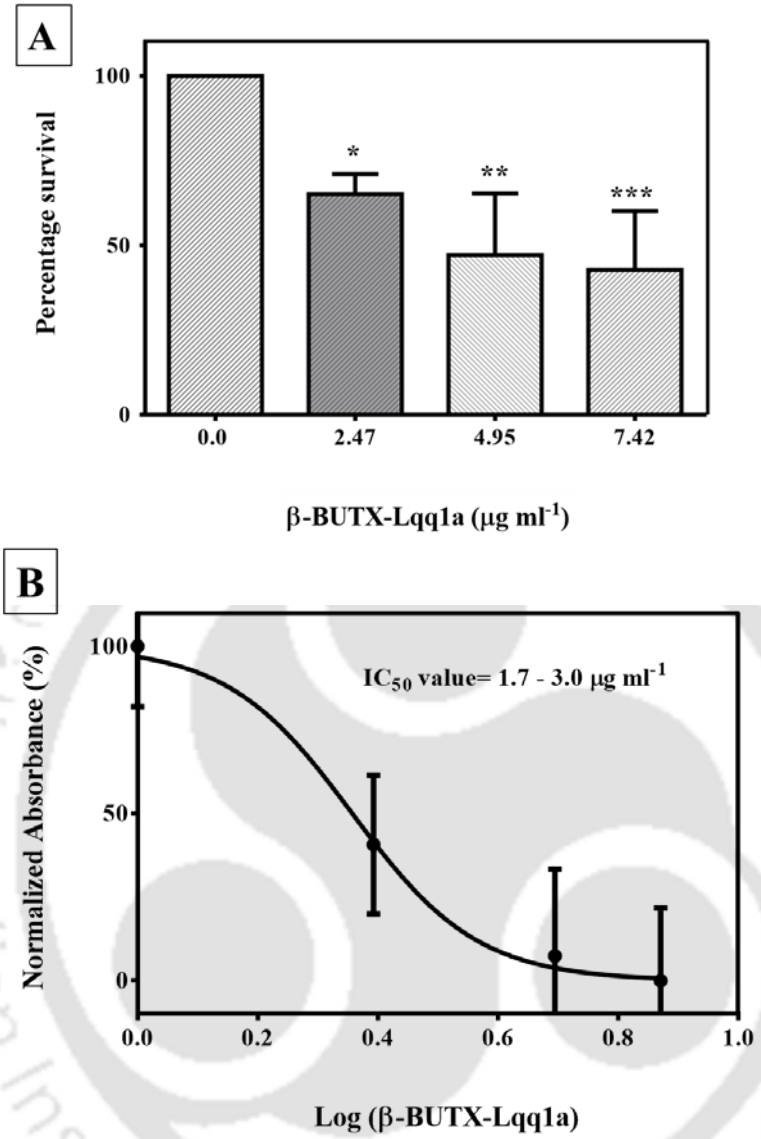

Fig. 2.10 Effect of various concentration of purified β-BUTX Lqq1a toxin on the viability of *Sf*-21 insect cell lines determined by MTT assay A) One-way ANOVA followed by Dunnett's pairwise multiple comparison analysis indicated that β-BUTX Lqq1a affected cell viability in dose dependent manner ($p < 0.002$) when compared with control. Asterisks indicate the results that were significantly different from the control. *, $p < 0.027$, **, $p < 0.002$ and ***, $p < 0.001$. All data are the average of three independent experiments with three replications for each along with standard deviation (±SD). B) Nonlinear fit of normalize transform data was performed to deduce the IC_{50} value purified β-BUTX Lqq1a toxin on the viability of *Sf*-21 insect cell lines determined by MTT assay.

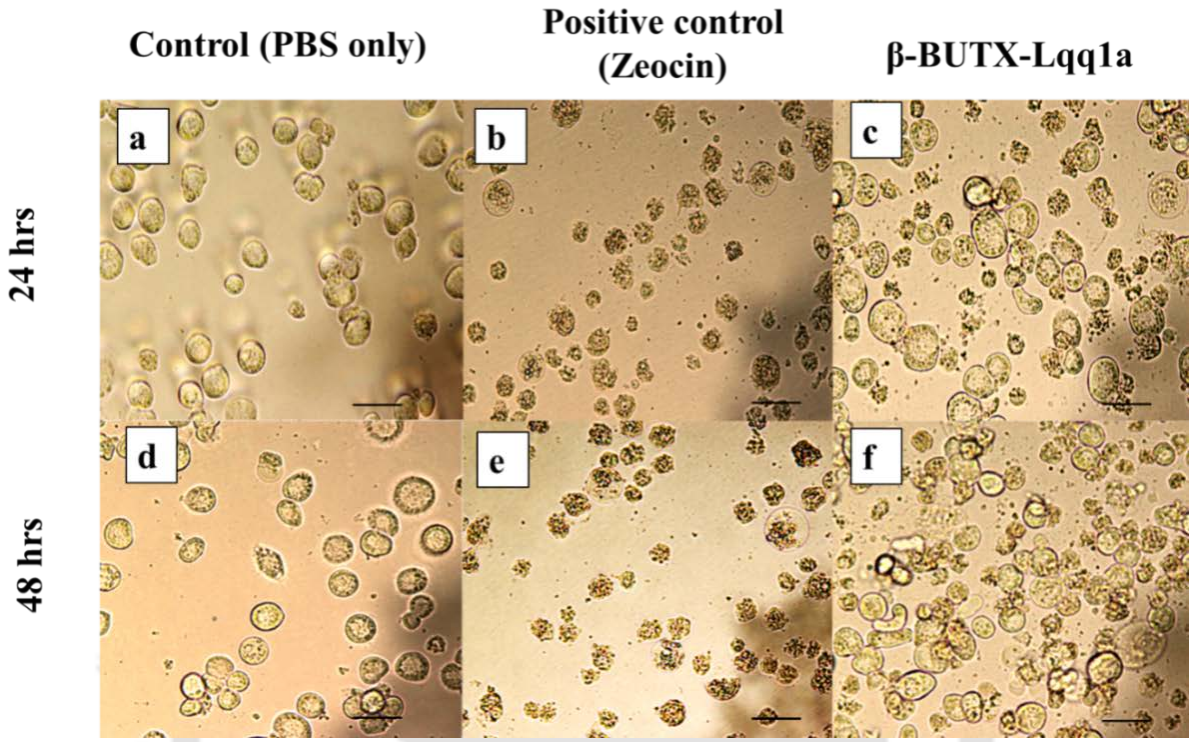

Fig. 2.11 Morphological analysis of treated *Sf*-21 cell lines at 24 and 48 hr time interval Inverted microscopy used for observing the cells under 40 X magnification. The bar represents 50 µM.

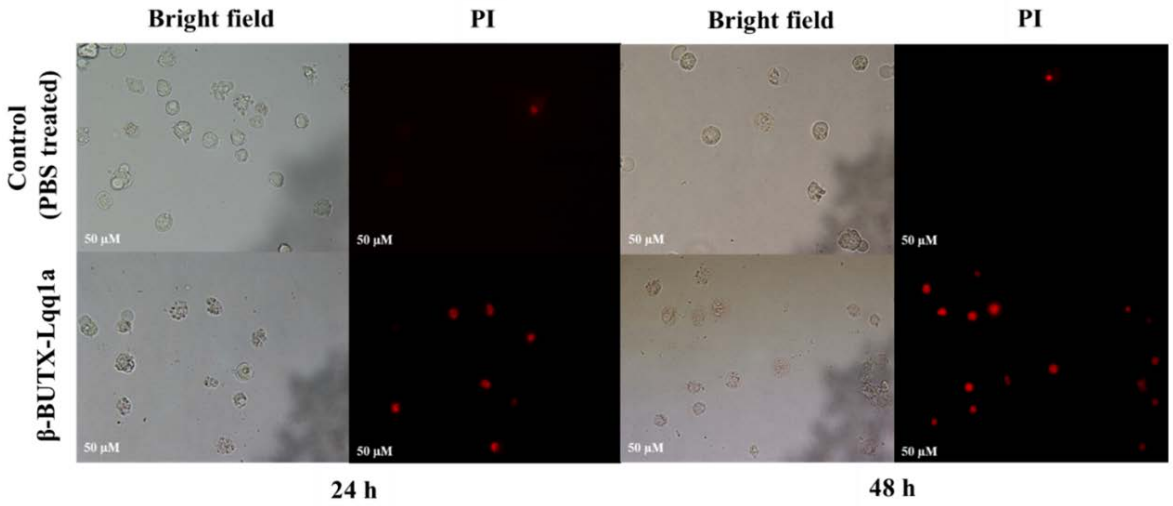

Fig. 2.12 Fluorescence Microscopy analysis of *Sf*-21 cells treated with β-BUTX Lqq1a for 24 and 48 hr respectively and further stained with PI. Images were taken in both bright field and fluorescence for the control (only PBS treated) and β-BUTX Lqq1a treatment at 40 X magnification.

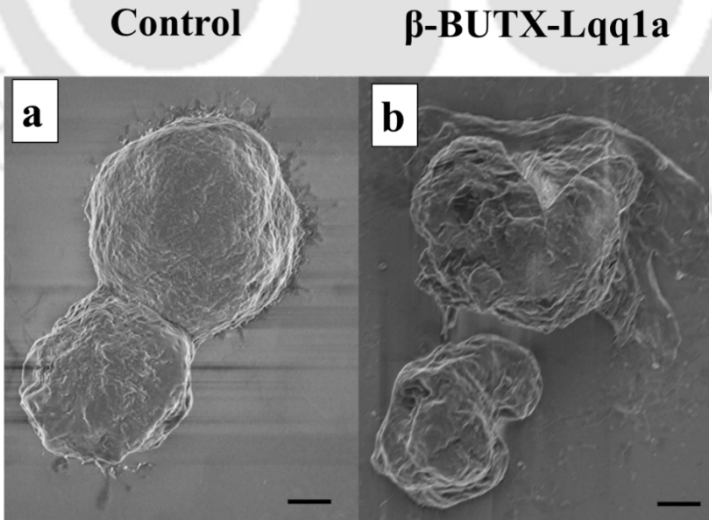

Fig. 2.13 Ultra structural analysis of β-BUTX Lqq1a treated *Sf*-21 insect cell lines using scanning electron microscopy. The bar represents 2 µM for control a and 3 µM for b.

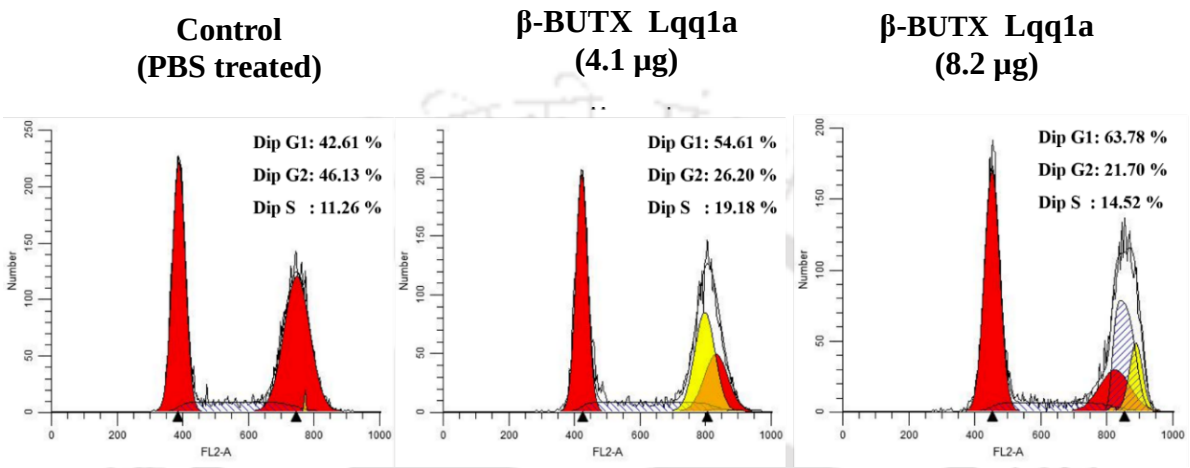

Fig. 2.14 Cell cycle analysis of β-BUTX Lqq1a treated *Sf*-21 insect cell line using ModFit analysis software. Control cells were treated only with PBS (pH 7.4), and two various concentrations of β-BUTX Lqq1a treated *Sf*-21 insect cell line. Data represents three independent experiments with standard deviation (SD)

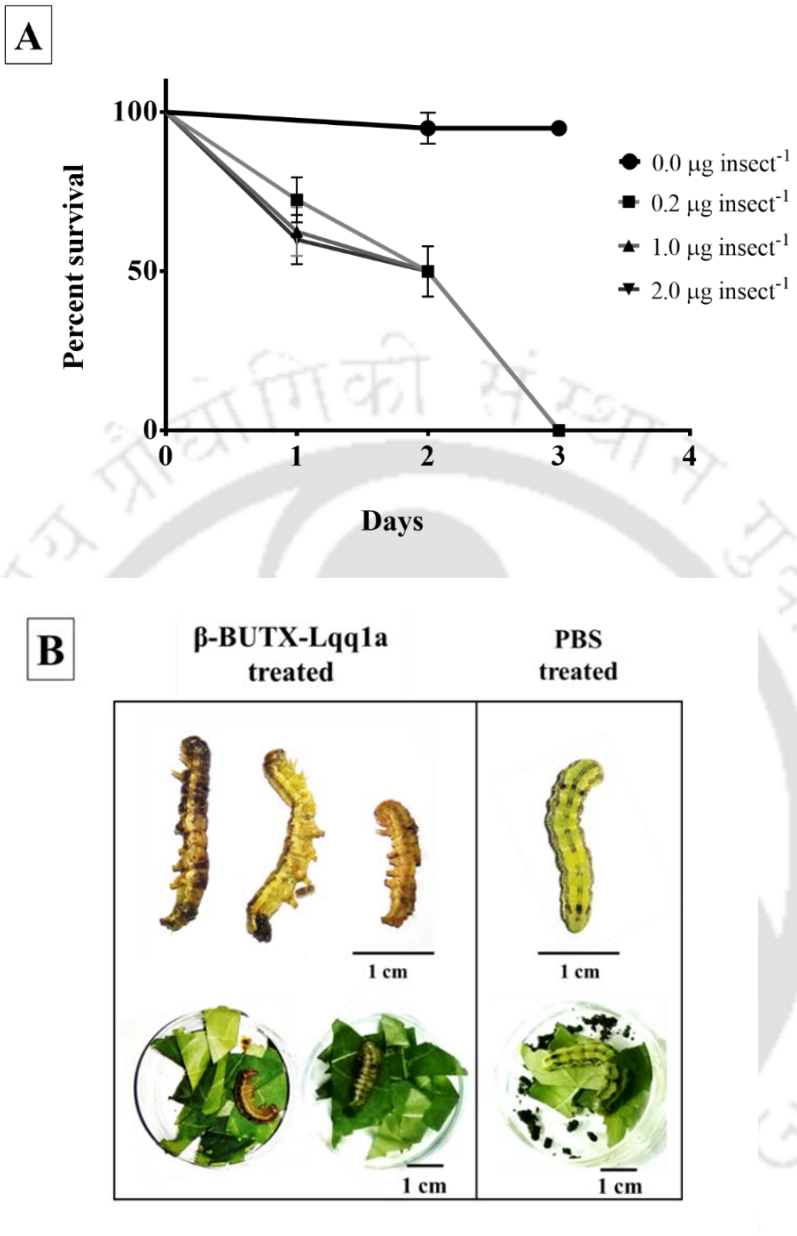

Fig. 2.15 Injection bioassay of *Helicoverpa armigera* A) Kaplan-Meier survival plot of *H. armigera* (n=20) injected with β-BUTX Lqq1a at the stated doses. Only PBS buffer used for injecting the control population. B) Photographic image shows the β-BUTX Lqq1a toxin treated and PBS treated *H. armigera* larvae

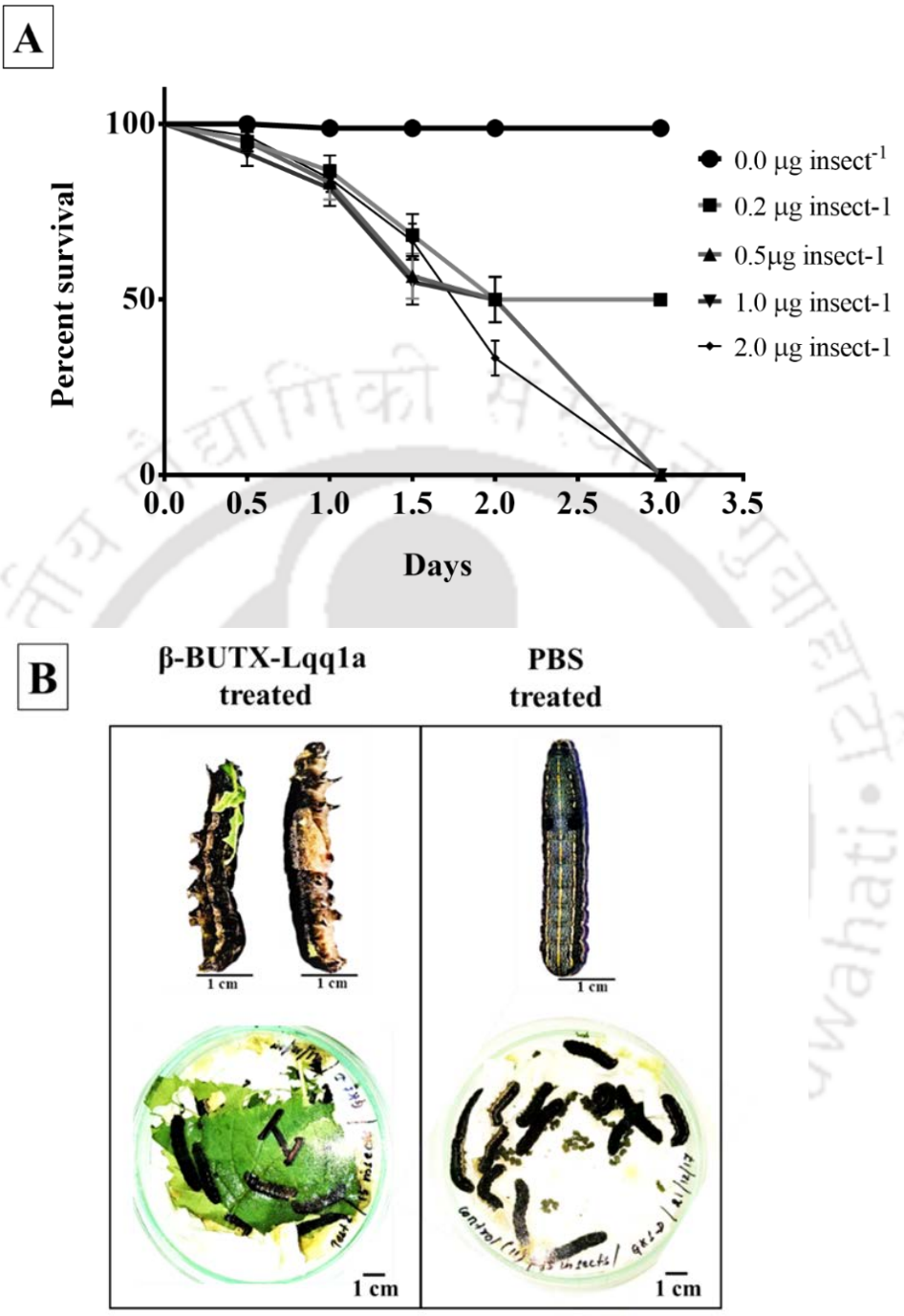

Fig. 2.16 Injection bioassay *Spodoptera litura* A) Kaplan-Meier survival plot of *S. litura* (n=30) injected with β-BUTX Lqq1a at the stated doses. Only PBS buffer used for injecting the control population. B) Photographic image shows the β-BUTX Lqq1a toxin treated and PBS treated *S. litura* larvae.

CHAPTER 3

Cloning and expression of β-BUTX Lqq1a in *Beauveria bassiana* and *Metarhizium anisopliae* and insect bioassay

---

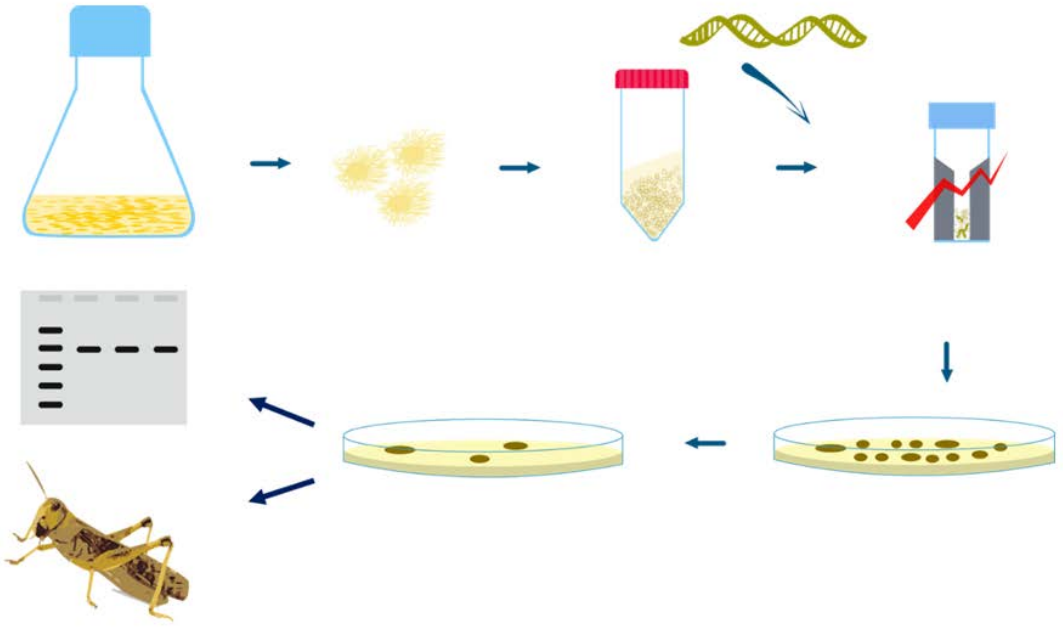

3.1 Introduction

Scorpion and spider possess untapped repository of biologically active molecules in the venom which is being predominantly used as defense molecule and for predation. In recent past, these biologically active molecules incessantly exploited for their immense potential for the control of major agriculturally important insect pests and vectors of the disease-causing agent. These arthropod insect toxins classified into α and β toxins based on the peptide sequence length where 30-40 amino acid containing peptides are called as α-toxins, whereas 70-80 amino acid containing peptides called as β-toxins. These toxins further classified into excitatory and depressant toxin based on their action on voltage-gated sodium channels, voltage-gated calcium channels, calcium- voltage-activated potassium channels, and chloride channels.

AaIT is a 70 amino acid neurotoxic peptide produced by Buthid scorpion *Andructonus australis.* Physio-chemical studies revealed that this toxin binds to voltage-gated sodium channel causing repetitive firing of motor neurons and ultimately causes flaccid paralysis in insects (Zlotkin et al. 2000). Similarly, another insect-selective neurotoxic peptide ω-atracotoxin-Hv1a from funnel web spider *Hadronyche versuta* also caused blockage in voltage-gated calcium channel (Ca_v) leading to acute toxicity in house cricket insect as a result of flaccid paralysis (Chong et al. 2007). LqhαIT is an insect-specific α-toxin from Israeli desert scorpion, *Leiurus quinquestriatus hebraeus* primarily acts on voltage-gated sodium (Na_v) channel (Peng and Xia 2014).

For the control of insect pests and vectors of disease-causing agents, synthetic chemical insecticides being perpetually employed against various insect pests (Saeed et al. 2019, Shah et al. 2019). Pesticide persistence in the environment causes considerable damage to aquatic ecosystems, humans, and animals. Effect of neonicotinoid pesticides

on butterflies, caused a reduction in survival, interruption in the feeding behaviour as well as abnormalities in ovipositional response (Mulé et al. 2017). Beneficial predatory mite, *Neoseiulus fallacis* exposure to carbaryl insecticide caused high mortality with a shortest lethal period (Jamil et al. 2019). Arthropod pesticide resistance database reported that field-evolved resistance in *H. armigera, S. litura,* and *S. exigua* for almost all the neonicotinoid insecticides with a higher incidence of *S. litura* resistant population. Availability of fewer chemically active ingredients led to intense selection pressure for the evolution of pesticide resistance. Use of biological organisms to control insect pest population necessitated to reduce the impact of synthetic chemical pesticides and to avoid resistance development. *B. bassiana* and *M. anisopliae* are most widely used biocontrol agents against a broad range of agricultural pest population (Alikhani et al. 2019, Deng et al. 2019, Gindin et al. 2006, Jiang et al. 2019, Lo Verde et al. 2015, Mahot et al. 2019, Song et al. 2019, Tuncer et al. 2019).

In spite of the general usage of entomopathogenic fungi, limited shelf life, slow speed of kill, and lack of field persistence due to a higher temperature and UV-radiation pose major constraint in competing with chemical pesticides. Due to the intrinsic property of the neurotoxins, some of the toxins has further been expressed in and delivered using entomopathogenic fungi such as *Metarhizium* spp, *Beauveria* spp and in plants systems. AaIT expressed in *M. anisopliae* under the control of hemolymph specific promoter increased the fungal toxicity towards insect pest tobacco hornworm *Manduca sexta* (Wang and St Leger 2007). Similarly, AaIT expressed in *B. bassiana*, which increased the insecticidal efficiency of entomopathogen against mosquito, *Aedes albopictus* adults (Deng et al. 2017). Hv1a neurotoxin caused severe mortality against sucking pests Aphids, *Acyrthosiphon pisum* and *Myzus persicae* when delivered orally as well as when

expressed in plant system (Nakasu et al. 2014, Pal et al. 2013). *M. acridum* expressing $LqhIT_2$ insect toxin exhibited increased virulence against Locusts *Locusta migratoria manilensis* (Peng and Xia 2014).

In the present study, *B. bassiana* and *M. anisopliae* have been exploited to express heterologous insect-specific Buthid scorpion neurotoxin β-BUTX Lqq1a from *Leiurus quinquestriatus quinquestriatus*. This toxin shares higher homology to the thoroughly studied AaIT toxin. Upon successful expression of the toxic protein, bioassay with engineered fungi was performed to evaluate the potential efficacy against *H. armigera*, *S. litura*, and white grub *Phyllophaga smithi*.

3.2 Materials and Methods

3.2.1 Strains and culture conditions

For bacterial cloning and maintenance of plasmids, *Escherichia coli* DH5-α cells were used and maintained in Luria Bertani (LB) medium at 37ºC. *Agrobacterium tumifaciens* EHA 105 strain was grown in LB medium supplemented with Rifampicin (10 µg ml^{-1}). *B. bassiana* (MTCC 984) and *M. anisopliae* (MTCC 892) cultures were procured from Microbial Type Culture Collection and Gene Bank (MTCC, India) and maintained on SDA (Sabroud Dextrose Agar) and PDA (Potato Dextrose Agar) medium respectively at 28ºC.

3.2.1.1 Fungal spore collection

Initially, both *B. bassiana* and *M. anisopliae* spores (1×10^6 ml^{-1}) were inoculated in 100 ml Sabroud Dextrose Agar (pH 5.6) and Potato Dextrose agar (pH 5.6) respectively and incubated for 7-10 days at 25±2ºC in an orbital shaker incubator. Post-incubation, plates containing spores were flooded with 0.05% Triton X-100 solution and collected using a pipette. Finally, spores were counted using Neubauer-haemocytometer and stored at 4ºC until further use.

3.2.2 Gene synthesis

The β-BUTX Lqq1a protein sequence was retrieved from the NCBI database (P19856.1) and followed by the reverse translation using EMBL-EMBOSS Backtranseq software (Rice et al. 2000). The reverse translated sequence was then codon-optimized for the expression in *M. anisopliae* and *B. bassiana*. Along with β-BUTX Lqq1a codon-optimized sequence, 5'-untranslated region, and *Metarhizium* collagen-like promoter signal sequence (Mcl1-sp) was added and cloned in pUC57 vector harboring ampicillin-resistant marker (Genscript, USA).

3.2.3 Vector construction

Two different strategies were followed for the development of expression vector to transfer into *B. bassiana* and *M. anisopliae.*

3.2.3.1 Vector construction for *B. bassiana*

For the cloning of neurotoxic β-BUTX Lqq1a, fungal expression vector pAL1 was used and obtained from Fungal genetic stock center (FGSC, USA) and maintained in *E. coli* DH5-α supplemented with ampicillin (100 µg ml^{-1}). **Fig. 3.1** indicates the schematic representation of *B. bassiana* vector construction method.

3.2.3.1.1 Overlap extension PCR

For the expression vector construction initially, β-BUTX Lqq1a gene along with 5'-UTR and Mcl1sp was amplified using pUC57-BUTX Lqq1a as a template with gene-specific primers with overhangs for pAL1 vector and promoter sequence (**Table 3.1**). The final 50 µL amplification reaction mixture contains 1x HF buffer, 1 µl of 10 mM dNTPs (200 µM) 2.5 µl of 10 µM Forward primer (500 nM), 2.5 µl of 10 µM Reverse primer (500 nM), 1.5 µl of DMSO (3%), 1 µl of plasmid DNA (20 ng), and 1 unit of Phusion DNA Polymerase (ThermoScientific, USA). The amplification conditions are initial denaturation at 98ºC for 3 min, denaturation at 98ºC for 20 sec, annealing at 60-70ºC for 45 sec and extension for 90 sec at 72ºC and cycles were repeated for 25-30 times. The final extension was performed at 72ºC for 10 min. Similarly, *Metarhizium* collagen-like promoter (P*Mcl1*) was amplified using *M. anisopliae* genomic DNA as a template with specific primers with an annealing temperature of 60ºC designed to include vector and Lqq1a overhangs (**Table 3.1**). Plasmid pAL1 vector digested with NcoI and EcoRI restriction enzymes in NEB cutsmart buffer at 37ºC for 3-4 hr and gel purified using TAKARA gel purification kit (Takarabio, Japan)

P*Mcl1* and β-BUTX Lqq1a gene along with 5'-UTR and Mcl1sp were fused using overlap extension polymerase chain reaction (PCR) with the following reaction mixtures 1x HF buffer, 1 µl of 10 mM dNTPs (200 µM) 2.5 µl of 10 µM pAL1 overhang Mcl1pro Forward primer (500 nM), 1.5 µl of PCR purified 5'UTR Mcl1sp-BUTX Lqq1a fragment as reverse primer, 1.5 µl of DMSO (3%), 1 µl gel-purified P*Mcl1* fragment (20 ng) as template and 1 unit of Phusion DNA Polymerase (ThermoScientific, USA). PCR amplified fragments were further gel purified using Takara gel purification kit (TAKARA, Japan). Both the purified vector and insert fragments were analyzed by using agarose gel electrophoresis (1%) and visualized using a ChemiDoc XRS™ gel documentation system (Bio-rad, USA).

3.2.3.1.2 *E. coli* chemical competent cell preparation and transfection

E. coli chemical competent cell was prepared, as mentioned in **chapter 2 section 2.2.4**. and stored at -80ºC until further use. Gibson assembly reaction was performed to clone 5'UTR Mcl1sp-BUTX Lqq1a into the digested pAL1 vector at 50ºC for 45-60 min. Post incubation, the whole reaction mixture was transformed into chemically competent *E. coli* DH5-α cells, and positive clones screened on LB agar supplemented with ampicillin (100 µg ml^{-1}).

3.2.3.1.3 Colony PCR

PCR confirmation of the positive clones was performed by the colony PCR based method with gene-specific primers. The overnight grew culture was transferred into 5 µl of nuclease-free H_2O, and PCR was performed with Taq DNA polymerase with 1x standard Taq DNA polymerase buffer with β-BUTX Lqq1a gene-specific primers. Final amplified PCR products were analysed using 1% Agarose gel electrophoresis.

3.2.3.1.4 Plasmid DNA isolation

Plasmid DNA was isolated according to Bimboim and Doly (1979) modified alkaline lysis method with modifications. Colony PCR confirmed clones were inoculated in 5 ml of LB broth and incubated overnight at 37ºC at 180 rpm in an orbital shaker incubator. Overnight grown cultures were then centrifuged at 10,000 rpm for 30 sec, at 4ºC to collect the cells. The pelleted cells were resuspended in 200 µl Resuspension buffer (50 mM glucose, 25 mM Tris-Cl (pH 8.0), 10 mM EDTA (pH 8.0), and 200 µl lysis solution (0.2 N NaOH, 1% (w/v) SDS) was added and further incubated for 2 min or until clear lysis. Then the suspension was neutralized using 300 µl Neutralization buffer (5 M potassium acetate, glacial acetic acid) and incubated at room temperature for 5-10 min. The lysate was centrifuged at 12,000 rpm, for 10 min at 4ºC and the upper aqueous layer was treated with RNase A and Proteinase K at 37ºC for 30-60 min. post-treatment, 200 µl of ice-cold Chloroform was added and vortexed briefly and further centrifuged to remove the chloroform. The upper aqueous layer was added with 1 volume of ice-cold isopropanol and centrifuged at 12,000 rpm, for 10 min at 4ºC, and the DNA pellet was washed once with 70% ice-cold ethanol. The finally obtained plasmid DNA pellet was dissolved in nuclease-free water and analysed on 1% Agarose gel electrophoresis.

3.2.3.1.5 Clone confirmation by double digestion

Double digestion was performed in NEB cutsmart buffer with NcoI and EcoRI-HF restriction enzymes with 2 µg of isolated plasmid DNA at 37ºC for 2 hr and digested fragments were analyzed on 1% Agarose Gel electrophoresis, and imaging was performed in ChemiDoc XRS™ gel documentation system (Bio-rad, USA).

3.2.3.2 Vector construction for *M. anisopliae*

3.2.3.2.1 Cloning Mcl1 gene downstream of β-BUTX Lqq1a gene

To clone P*Mcl1* and β-BUTX Lqq1a along with Mcl1 gene into pAL1 vector, P*Mcl1*-BUTX Lqq1a-Bar was PCR amplified from previously cloned plasmid pMcl1-BUTX Lqq1a using gene-specific primers flanking overhangs for the Mcl1 gene and pAL1 vector (**Table 3.2**). **Fig. 3.2** indicates the schematic representation of the vector construction procedure followed for *M. anisopliae.* The amplification reaction mixture contains 1x HF buffer, 1 µl of 10 mM dNTPs (200 µM) 2.5 µl of 10 µM pAL1 overhang Mcl1pro forward primer (500 nM), 2.5 µl of 10 µM Mcl1 gene overhang Bar gene reverse primer (500 nM), 1 µl of pMcl1-BUTX Lqq1a (20 ng), and 1 unit of Q5 DNA polymerase (New England Biolabs, USA). The P*Mcl1*-BUTX Lqq1a-Bar gene amplification conditions were initial denaturation was performed at 98ºC for 3 min, denaturation at 98ºC for 20 sec, annealing at 60-70ºC for 45 sec and extension for 150 sec at 72ºC and cycles were repeated for 25-30 times. The final extension was performed at 72ºC for 10 min. Similarly, Mcl1 gene was amplified from the genomic DNA (50 ng) isolated from *M. anisopliae* using High Fidelity Phusion Polymerase in 50 µl amplification reaction containing 500 nM Mcl1 gene-specific primers carrying pAL1 vector and bar gene overhangs (**Table 3.2**). The annealing temperature of the primers was 60ºC. Both the PCR amplified fragments were separated on 1.5% Agarose gel electrophoresis system and extracted using TAKARA gel purification kit.

Gibson assembly reaction was performed with purified P*Mcl1*-BUTX Lqq1a-Bar gene fragment, Mcl1 gene fragment, and double digested pAL1 vector at 50ºC for 45-60 min. Post incubation, the reaction mixture was used to transfect *E. coli* TOP10 chemical competent cells. Colony PCR experiment was conducted to identify the positive clones

using gene specific primers, and further plasmid pMcl1-BUTX Lqq1a-Bar-Mcl1 was isolated from the PCR confirmed clones using Alkaline lysis method.

3.2.3.2.2 pCAMBIA cloning

The binary vector pCAMBIA3300 was digested with EcoRI and HindIII restriction enzymes in NEB cutsmart buffer at 37ºC for 3-4 hr and gel purified using TAKARA gel purification kit. P*Mcl1*-BUTX Lqq1a-Bar-Mcl1 gene fragment was PCR amplified from the plasmid pMcl1-BUTX Lqq1a-Bar-Mcl1 using the specifically designed primers flanking the vector overhangs. Both the purified vector pCAMBIA3300 and insert fragments (P*Mcl1*-BUTX Lqq1a-Bar-Mcl1 gene) were analysed by using agarose gel electrophoresis (1%) and visualized using a ChemiDoc XRS™ gel documentation system (Bio-rad, USA).

3.2.3.2.3 *E. coli* chemical competent cell preparation and transfection

E. coli chemical competent cell was prepared as mentioned in **chapter 2 section 2.2.4**. and stored at -80ºC until further use. Both the digested pCAMBIA vector and insert were fused using Gibson assembly reaction at 50ºC for 45-60 min. Post incubation, the whole reaction mixture was transformed into chemically competent *E. coli* DH5-alpha cells, and positive clones were screened on LB agar supplemented with kanamycin (50 µg ml^{-1}). PCR further confirmed positive clones with P*Mcl1*-B-BUTX Lqq1a gene-specific primer and plasmid double digestion.

3.2.3.2.4 Colony PCR

PCR confirmation of the positive clones was done by the colony PCR based method with P*Mcl1*-B-BUTX Lqq1a gene-specific primers as mentioned in the **section 3.2.3.1.2.**

3.2.3.2.5 Plasmid isolation

Plasmid DNA was isolated from the selected clones as mentioned in the **section 3.2.3.1.3** and further analyzed by using 1% Agarose gel electrophoresis

3.2.3.2.6 Double digestion

Restriction enzyme digestion was performed in NEB cutsmart buffer with EcoRI-HF enzyme with two µg of isolated plasmid pCAMBIA3300 P*Mcl1* β-BUTX-Lqq1a at 37ºC for 2 hr and digested fragments were analyzed in 1% Agarose Gel electrophoresis, and imaging was performed in ChemiDoc XRS™ gel documentation system (Bio-rad, USA)

3.2.4 Protoplast based transformation of *B. bassiana*

3.2.4.1 *B. bassiana* protoplast preparation

B. bassiana protoplast were prepared according to Pfeifer and Khachatourians (1987) with modifications. For protoplast preparation (**Fig. 3.3**), spores were collected from 15 days old culture grown on Potato Dextrose Agar (PDA), pH 5.6 and counted using Neubauer hemocytometer. Spores (2×10^6 ml^{-1}) were inoculated in 100 ml of PDB and incubated for 30-40 hr at 28°C. Post incubation, cultures were collected by centrifugation at 10,000 rpm for 15 min and washed twice with sterile water and phosphate buffer (pH 7.4). Initially, fungal mycelium was treated with 10 mM Dithiothreitol (DTT) for 30 min and washed twice with phosphate buffer (20 mM). DTT treated mycelium was further re-suspended in 20 ml of buffer containing 20 mM KH_2PO_4, 0.7 M KCl and 0.7 M $(NH_4)_2SO_4$ (pH 6.8) and 1% lysing enzyme (from *Trichoderma harzianum*, Sigma) and incubated at 28°C for 4-5 hr on rotatory incubator shaker at 100 rpm. Protoplast formation was periodically observed under a light microscope. After consistent protoplast formation, protoplast was removed from cell

debris and collected using centrifugation at 5,000 rpm for 15 min. Collected protoplast were then washed twice with 1M sorbitol. Finally, 200 µl aliquots were made and used for electroporation.

3.2.4.2 *B. bassiana* protoplast electroporation

Vector pMcl1-B-BUTX Lqq1a (3-10 µg) was mixed with 150 µl of *B. bassiana* protoplasts (1×10^8 protoplast ml^{-1}) and incubated on ice for 15-30 min in 0.2 cm electroporation cuvette. Then, 700-1000 V was applied using Biorad Gene PulserXcell™ electroporation system. Immediately, 1 ml of 1 M sorbitol was added and incubated for 3 hr at 28°C in static condition. Later this was plated on Czapek Dox Agar (K_2HPO_4 1 g l^{-1}, $FeSO_4.7H_2O$ 0.01 g l^{-1}, $MgSO_4.7H_2O$ 0.5 g l^{-1}, KCl 0.5 g l^{-1}, $NaNO_3$ 3 g l^{-1}, Sucrose 30 g l^{-1}, 0.7 M $(NH_4)_2SO_4$) with 300 µg ml^{-1} Glufosinate ammonium (Sigma, USA) as selection agent. Initial 12 hr post-incubation at 28°C, Czapek dox soft agar containing glufosinate-ammonium (300 µg ml^{-1}) was poured as top agar. Transformants appeared on selective medium after 10-12 day post-incubation, and were transferred and sub-cultured for three consecutive generations to obtain mitotically stable transformants.

3.2.5 *Agrobacterium*-mediated transformation of *M. anisopliae*

3.2.5.1 Electro-competent cell preparation

A. tumifaciens EHA105 (*At*-EHA105) strain was used for electro-competent cell preparation (Shaw 1995) and *M. anisopliae* transformation. A single colony of *At*-EHA105 cells was grown in LB broth containing rifampicin (10 µg ml^{-1}) at 28ºC in an orbital shaker at 200 rpm. Overnight grown culture (1 ml) was further inoculated into 200 ml of LB broth and grown for 4-5 hr until OD_{600} ~0.8. Cells were collected by centrifugation at 5,000 rpm for 10 min. Cell pellets were washed in 10 mM HEPES buffer (pH 7.0) twice and finally, cells were resuspended in 10% glycerol and stored at -80 ºC.

3.2.5.2 Electroporation

Plasmid pCAMBIA3300 harboring P*Mcl1*-B-BUTX Lqq1a construct was mixed with *At*-EHA105 electro-competent cells and electroporated at following conditions 1200 V, 25 µF, 600 Ω using Biorad Gene Pulser Xcell™ electroporation apparatus. Electroporated cultures were then mixed with LB broth and incubated for 2 hr at 28ºC in 200 rpm shaking conditions. Post incubation *At*-EHA105 cells were plated on LB Agar containing rifampicin (20 µg ml^{-1}) and kanamycin (50 µg ml^{-1}) and then incubated for two days at 28ºC in static condition. The plasmid was isolated from the randomly selected clones and gene-specific PCR and restriction digestion based confirmation was carried out on (1%) agarose gel electrophoresis system.

3.2.5.3 *Agrobacterium* and *Metarhizium* co-cultivation

Agrobacterium-mediated transformation was carried out according to the protocol by Sevim et al. (2012) with little modifications. **Fig. 3.4** represents the schematic diagram for the *Agrobacterium*-mediated transformation procedure. Initially, *Agrobacterium* harboring P*Mcl1*-B-BUTX Lqq1a was grown in LB medium supplemented with kanamycin (50 µg ml^{-1}, Sigma, USA) and rifampicin (20 µg ml^{-1}, Himedia, India) for two days at 28ºC on orbital incubator shaker (200 rpm). Optical density (OD_{600}) of grown culture was adjusted to 0.17 with induction medium (dos Reis et al. 2004) containing 200 µM acetosyringone (Sigma, USA) and incubated for 4-5 hr at 28ºC until OD_{600} ~0.45. *M. anisopliae* (2×10^7 Spores ml^{-1}) was mixed with an equal volume of *Agrobacterium* pMcl1-BUTX Lqq1a (OD600 ~0.4-0.5) and incubated for 2 hr at 28ºC. Then, cultures were spread on sterile nitrocellulose filter paper, which further was placed on Induction medium containing Acetosyringone (200 µM) and co-cultivated for two days at 28ºC in static conditions. Post-co-cultivation, the filter paper was transferred to M-100 minimal

medium (Stevens 1974) supplemented with glufosinate ammonium (300 µg ml^{-1} Sigma, USA) and cefotaxime (50 µg ml^{-1} Himedia, India) and incubated for 5-10 days at 28ºC until colony formation.

Transformants were sub-cultured for two consecutive generations without any selection pressure and then confirmed for P*Mcl1*-BUTX Lqq1a genomic DNA integration. For confirmation of genomic DNA integration, spores were grown for two days in PDA broth at 28ºC with 180 rpm shaking conditions. Mycelial biomass was obtained by centrifugation and used for genomic DNA isolation. PCR was done using isolated genomic DNA from transformants with gene-specific primers.

3.2.6 Clone confirmation by isolating genomic DNA

Both *B. bassiana and M. anisopliae* carrying P*Mcl1*-BUTX Lqq1a were confirmed by genomic DNA isolation followed by PCR confirmation with gene-specific primers. For genomic DNA isolation, both fungi spores were inoculated in 20 ml of potato dextrose broth and grown for 48 hr to obtain mycelial biomass. The grown culture was centrifuged at 4000 rpm for 30 min to remove the supernatant from the mycelial biomass. Then the whole biomass was ground using 1 ml of lysis buffer containing 40 mM Tris-HCl, 600 mM NaCl, and 2 mM EDTA. After the lysis 200 µl of 10% SDS, 5 µl Proteinase K (1 mg ml^{-1}) and 5 µl RNase A (10 mg ml^{-1}) were added and incubated at 60ºC for 1 hr. Post incubation, 150 µl of 6M NaCl was added thoroughly mixed by vortex for the 30 sec followed by centrifugation for 30 min at 13,000 rpm at 4ºC. Recovered supernatant was mixed with 200 µl phenol: chloroform: isoamyl alcohol and centrifuged for 15 min at 13,000 rpm at 4ºC. Chloroform treatment was done to remove any residual phenol from the supernatant. Genomic DNA was precipitated by adding ice-cold isopropanol and incubated for 30-60 min in -20ºC. Post incubation, DNA precipitate was

collected by centrifugation at 10,000 rpm for 10 min at 4ºC. DNA pellet was then washed with 70% ethanol once and air-dried. Qualitative and quantitative analysis was done by Agarose gel electrophoresis and NanoDrop method.

3.2.7 Haemolymph induction and Reverse transcription-PCR analysis

Initially, inoculum culture (*B. bassiana* and *M. anisopliae*) was grown in Sabouraud Dextrose Broth (SDB) for two days at 28ºC in orbital incubator shaker. Post-growth, wet culture (1 g) was transferred onto 10 ml of silkworm hemolymph. Hemolymph was extracted from 5th instar Eri silkworm and stored in phosphate buffer (PBS, pH 7.2) containing 2 mM EDTA. After culturing at 28ºC for 12 hr, mycelium was collected by centrifugation for RNA extraction, and the filtrate was stored in -20ºC for further western blot analysis. Total RNA was extracted using RNAiso Plus kit (Takara, Japan) and genomic DNA contamination was removed by using DNAse I treatment (Promega). One microgram of total RNA was used for cDNA synthesis (SuperScript™ III first-strand synthesis system, Invitrogen, USA). Synthesized cDNA was used for semi-quantitative RT-PCR analysis based on BUTX Lqq1a specific primers.

3.2.8 Western blot analysis

The neurotoxin BUTX Lqq1a expression in *M. anisopliae* isolates was evaluated by western blot analysis. The highly specific antigenic peptide was chosen from BUTX Lqq1a toxin using OptimumAntigen™ Design Tool, and polyclonal antibodies were generated in mouse (Genscript, USA), and anti-mouse IgG secondary antibody which is conjugated with alkaline phosphatase was purchased from Genscript, USA. Initially, for the crude protein sample preparation, wild type *M. anisopliae* and Ma-BUTX Lqq1a strains as well as wild type *B. bassiana* and Bb-BUTX Lqq1a strains were grown in potato dextrose broth for two days at 28ºC. Post-incubation, 1 g of wet mycelial biomass

was transferred into 10 ml of Eri silkworm hemolymph and further grown overnight at 27ºC in shaking conditions. Post-incubation, the supernatant was collected, and protein concentration was quantified using the Bradford method and crude protein sample 10-20 µg were separated on a 12-15% SDS-PAGE gel electrophoresis. After this, proteins were transferred onto 0.45 µM Nitrocellulose membrane (Bio-Rad) using the Invitrogen power blotter system (ThermoScientific, USA). The membrane was then incubated in blocking buffer (Tris-buffered saline with 3% Bovine serum albumin) for 1 hr at room temperature and further incubated with primary antibody diluted in blocking buffer (1:500 and 1:1000) at 4ºC overnight. Post incubation, the membrane was washed 3-4 times in TBS containing Tween-20 wash buffer for 5 min each. The diluted secondary antibody in blocking buffer was incubated with the membrane for 1 hr at room temperature and then washed with washing buffer. Finally, the detection was performed using the Clarity™ Western ECL substrate (Bio-rad, India), and imaging was carried out using a ChemiDoc XRS™ gel documentation system (Bio-rad, USA).

3.2.9 Insect bioassay

Insect bioassay was conducted to study the efficacy of recombinant *M. anisopliae* harboring P*Mcl1*-BUTX Lqq1a constructs. Insect culture *Phylophaga smithi* adults were collected locally from Indian Institute of Technology Guwahati, Guwahati, Assam, India and maintained on 10% sucrose solution. Dipping or topical application method was performed with 2×10^7 Spores ml^{-1} for recombinant and wild type control strain for the bioassay. The excess liquid on each insect was removed by placing them on dry sterile tissue paper and placed on natural castor leaves diet with 16:8 hr light and dark condition at 25-28ºC with 60-70% relative humidity level. Insect mortality was recorded every 24 hr.

3.2.10 Statistical data analysis

Data analysis was conducted using GraphPad Prism software (version 6.0). The values are expressed as mean with standard deviation. The p-value $< .05$. was considered statistically significant data and the Kaplan-Meier survival plots were constructed using GraphPad Prism software (version 6.0), and comparison of survival curve was made using Log-rank (Mantel-Cox) test, and LT_{50} value was calculated based on Probit analysis (Finney 1952).

3.3 Results

3.3.1 pMcl1-B-BUTX Lqq1a vector construction for *B. bassiana*

In the present study, BUTX-Lqq1a was successfully codon optimized with higher codon adaptation index (CAI= 9.0) using OptimumGene-Codon Optimization tool for both *B. bassiana* and *M. anisopliae*. Along with BUTX Lqq1a, 5'-Untranslational region and *Metarhizium* collagen like protein signal peptide sequence was also codon-optimized successfully and cloned in pUC57 vector which resulted in pUC57-5'UTR Mclsp-BUTX Lqq1a plasmid which has been further confirmed by restriction enzyme digestion (**Fig. 3.5**) and PCR amplification of BUTX Lqq1a gene sequence (**Fig. 3.6**).

After the successful codon optimization and cloning, 5'UTR Mclsp-BUTX Lqq1a fragment was amplified (**Fig. 3.7**), and fused downstream of *Metarhizium* collagen-like promoter (P*Mcl1*) to express the BUTX Lqq1a protein in soluble form in *B. bassiana* when induced with hemolymph conditions. Further to deliver the protein into the insect cavity during the infection process, BUTX Lqq1a was tagged N-terminally with *Metarhizium* collagen-like protein signal peptide sequence (Mcl1-sp) along with 5' Untranslated region (5'UTR). Initially, BUTX Lqq1a along with Mcl1-sp and 5'UTR regions were successfully amplified and fused downstream of the MCL1 promoter region and theses fragments were successfully cloned in a pAL1 expression vector which have been confirmed by restriction enzyme digestion (**Fig. 3.8**) and PCR confirmation (**Fig. 3.9**). This cloning led to development of pMcl1-BUTX Lqq1a expression system for *B. bassiana*. **Fig. 3.10** indicates the schematic representation of the BUTX Lqq1a arrangement in the pMcl1-BUTX Lqq1a vector.

3.3.2 pMcl1-BUTX Lqq1a transformation into *B. bassiana*

Initially, *B. bassiana* protoplast was successfully prepared using the 40 hr old grown mycelia which resulted better yield, as well as a significantly higher number of the protoplasts (5×10^9 ml^{-1}), was obtained when treated with lytic enzymes for 3 hr in mild agitation conditions **(Fig. 3.11).** The DTT treatment improved the efficiency of protoplast formation when compared to the untreated mycelia. The plasmid carrying P*Mcl1*-BUTX Lqq1a was efficiently transferred into *B. bassiana* using protoplast cum electroporation mediated transformation. A Nine hundred voltage was found to be more efficient in transferring the plasmid DNA into protoplast. Colony growth observed after 10 day post-selection plating in Czapek Dox agar containing 300 µg ml^{-1} resulted in a significantly higher number of colonies (**Fig. 3.12**).

3.3.3 pMcl1-BUTX Lqq1a binary vector construction for *M. anisopliae*

Initially, pMcl1-Lqq1a construct alone was used to transform *M. anisopliae*. However, the reduced transformation efficiency and absence of complete P*Mcl1*-BUTX Lqq1a construct in the genome prompted to design another transformation strategy to integrate the whole construct into the genome of *M. anisopliae*.

In the present study, P*Mcl1*-BUTX Lqq1a, along with *bar* gene was successfully amplified using pMcl1-BUTX Lqq1a vector, which was designed to transform into *B. bassiana*. To create a vector which enhances homologous recombination, Mcl1 gene was successfully amplified from the *M. anisopliae* genomic DNA and designed to place downstream of BUTX Lqq1a gene. The resulted two fragments were successfully cloned in pAL1 expression vector (**Fig. 3.13**), which lead to the development of homologous recombination plasmid (pMcl1-BUTX Lqq1a-Bar-Mcl1) (**Fig. 3.14**).

To further enhance the integration of BUTX Lqq1a into *M. anisopliae*, P*Mcl1*-BUTX Lqq1a-Bar-Mcl1 fragment was amplified and cloned in *Agrobacterium* binary vector pCAMBIA3300 (**Fig. 3.15**) which resulted in pCAM P*Mcl1*-BUTX Lqq1a binary vector (**Fig. 3.16**). Restriction enzyme digestion of the resulted plasmid revealed the presence of 3 kbp fragment, P*Mcl1*-BUTX Lqq1a (**Fig.3.17**). Schematic arrangement of P*Mcl1*-BUTX Lqq1a-Mcl1 gene in the binary vector is represented in **Fig. 3.18.**

3.3.4 Genomic integration of BUTX Lqq1a analysis in *B. bassiana*

To continuously express the BUTX Lqq1a within the hemolymph of insect, the gene of interest along with the Promoter should integrate into the genome of the fungi since *B. bassiana* does not possess any extra-chromosomal DNA. The integration of the gene of interest could be assessed by PCR with gene-specific primers or Southern blotting analysis. In the present study, the genomic combination of BUTX Lqq1a using PCR with primers designed to amplify the gene of interest was evaluated. For the amplification, genomic DNA was successfully isolated using optimized extraction procedure from *B. bassiana* clones which appeared in the glufosinate-ammonium selection medium (**Fig. 3. 19**). Upon successful isolation, genomic DNA was used as a template to amplify the gene of interest, BUTX Lqq1a. Successful amplification of BUTX Lqq1a from *B. bassiana* clones further showed the significant integration of BUTX Lqq1a within the genome **(Fig. 3.20**).

3.3.5 Genomic integration of BUTX Lqq1a analysis in *M. anisopliae*

The scorpion gene BUTX Lqq1a integration into the genome of *M. anisopliae*was assessed in a similar method to the BUTX Lqq1a genomic DNA integration analysis in *B. bassiana.* Initially, genomic DNA was successfully isolated from selected *M. anisopliae* clones, which were growing on glufosinate ammonium screening medium

(**Fig. 3. 21**). Isolated genomic DNA was further tested for the presence of complete P*Mcl1*- B-BUTX Lqq1a construct within the genome using PCR with the promoter and gene-specific primers. The P*Mcl1*-BUTX Lqq1a amplified fragment from the genomic DNA, further confirms the presence of genomically integrated BUTX Lqq1a (**Fig. 3.22**)

3.3.6 BUTX Lqq1a transcript analysis in *B. bassiana* and *M. anisopliae*

Successful integration of BUTX Lqq1a transgene into the genomic DNA was also tested by analyzing the inducible expression of the transgene in hemolymph using semi-quantitative RT-PCR and western blot. For RT-PCR analysis, initially total RNA was successfully isolated from the PCR confirmed clones of Bb-BUTX Lqq1a (**Fig. 3.23**) and Ma-BUTX Lqq1a (**Fig. 3.24**). After the successful isolation, total RNA has been converted into cDNA, and further semi-quantitative RT-PCR analysis resulted in the presence of the significant amount of BUTX Lqq1a transcript (**Fig. 3.25** Bb-BUTX Lqq1a and Fig. **3.26** Ma-BUTX Lqq1a). The western blot analysis also revealed the presence of expressed BUTX Lqq1a protein in the hemolymph induced fraction of Bb-BUTX Lqq1a (**Fig. 3.27** and Ma-BUTX Lqq1a clones (**Fig. 3.28**). These RT-PCR and western blot analysis results indicate that the scorpion gene BUTX Lqq1a integrated into the genome of *B. bassiana* and *M. anisopliae* and could be inducible with insect hemolymph, and significant expression also could be achieved.

3.3.7 Virulence assay

The wildtype and Ma-BUTX Lqq1a strain virulence was assessed based on the half-maximal lethal time (LT_{50}) value. Topical application bioassay of white grub *P. smithi* with Ma-BUTX Lqq1a had significantly lower survival than the white grub infected with Ma-Wildtype strain (**Fig. 3.29)**, Kaplan-Meier survival plot (n=15, Log-rank (Mantel-Cox) test p=0.0009)). The calculated LT_{50} value for the Ma-Wildtype was

4.5 days (R^2=97.38) and for the Ma-BUTX Lqq1a, it was3.4 days (R^2 =96.63). Fungal mycelia emergence was observed two days of post-treatment and MaLqq1a growth was more vigorous when compared to wild type strain. Also, the blackening of the whole insect was found as a result of fungal infection (**Fig. 3.30**).

3.4 Discussion

To deliver the recombinant DNA, the development of a suitable transformation system is very much crucial in fungal genome modification. Several transformation methods were developed for *B. bassiana*, such as Protoplast mediated (Eley et al. 2007, Kosir et al. 1991, Pfeifer and Khachatourians 1987, Pfeifer and Khachatourians 1992), blastospore mediated (Chen et al. 2017, Ying and Feng 2006), blastospore cum restriction enzyme-mediated integration, electroporation-based transformation (Jiang et al. 2007, Lee et al. 2015), and *Agrobacterium*-mediated transformation (dos Reis et al. 2004, Fang et al. 2004, Leclerque et al. 2004, Wu et al. 2008). Pfeifer and Khachatourians (1987) reported the protoplast preparation using blastospore and mycelia, yielded 100% efficient protoplast from 24 hr old culture. However, *B. bassiana* protoplast prepared from 40 hr old mycelia with 1% lytic enzymes from *T. harzianum* generated 100% protoplast within 3 hr post-treatment (**Fig. 3.11)**. The use of stabilizers such as $(NH_4)_2SO_4$ and KCl at 0.7 M concentration increased the stability of protoplast. To transfer the DNA into the protoplast physical method such as electroporation and chemical method such as Poly Ethylene Glycol (PEG) mediated processes were employed (Eley et al. 2007, Pfeifer and Khachatourians 1992, Ying and Feng 2006). In the present study, optimized Protoplast cum electroporation mediated transformation was employed to transfer the P*Mcl1*-BUTX Lqq1a construct into *B. bassiana*. A voltage at 900 V was found to be capable of transferring the construct into *B. bassiana* using electroporation.

Previous reports suggested that homologous recombination improves the efficiency of gene integration into genome of the filamentous fungi *Metarhizium* (Lin et al. 2011, Michielse et al. 2005, Staats et al. 2007, Z. X. Wang et al. 2019, Xie et al. 2019, Xu et al. 2014). In the present study, to increase the frequency and efficiency of the BUTX Lqq1a gene integration into *Metarhizum*, homologous recombination strategy was

followed. Mcl1 gene (~1.5 Kbp fragment) was amplified from *M. anisopliae* genomic DNA and placed downstream of P*Mcl1*-Lqq1a construct, which resulted in P*Mcl1*-BUTX Lqq1a-Mcl1 gene. *Agrobacterium* offers reliable transformation method in various filamentous fungi because of simplicity and efficiency (Duarte et al. 2007, Fang et al. 2006, Goettel et al. 1990, Hu and Xia 2019, Kanjo et al. 2019, Zhang et al. 2019). After the successful construction, P*Mcl1*-BUTX Lqq1a-mcl1 gene was transferred into *Metarhizium* using the optimized *Agrobacterium*-mediated transformation method. Putative transformants, which showed optimal growth in the selection medium containing glufosinate ammonium, were selected for further analysis.

Stable integration of the transgene into the chromosome is very much essential to investigate the stable expression of the transgene. Previous studies reported that the transgene integration using protoplast mediated transformation was less efficient compared to other transformation methods (Bogo et al. 1996, Goettel et al. 1990). However, the number of transformants obtained was comparatively higher using protoplast cum electroporation mediated transformation. *M. anisopliae* transformed using *Agrobacterium* yielded a higher number of transformants after 7-10 days of incubation. In spite of the laborious nature of this method, it is one of the superior technique opted for gene transfer because of higher frequency of T-DNA integration (Gao et al. 2019, Hu and Xia 2019, Z. K. Wang et al. 2019, Zhang et al. 2019). All the putative transformants from *B. bassiana* and *M. anisopliae* were subcultured for five consecutive generations without glufosinate ammonium. PCR confirmed BUTX Lqq1a gene integration with gene-specific primer using genomic DNA isolated from the selected clones. The results obtained from the *B. bassiana* and *M. anisopliae* genomic DNA isolation and clone confirmation suggested that the occurrence of BUTX Lqq1a integration in the genome.

AaIT1 expressed under the control of hemolymph specific MCL1 promoter increased amount of transcripts significantly when exposed to hemolymph containing medium as experimented by RT-PCR (Wang and Leger, 2006, 2007). The RT-PCR analysis of the *B. bassiana* clones carrying the BUTX Lqq1a when exposed to hemolymph isolated from Muga silkworm resulted in significant detection of transcript expression. Similarly, semi-quantitative RT-PCR analysis performed with cDNA synthesized from total RNA isolated using hemolymph induced *M. anisopliae* carrying transgene, resulted in significant presence of BUTX Lqq1a transcripts in the hemolymph induced fraction. Western blot analysis of 3-day old *M. anisopliae* expressing BUTX Lqq1a also indicated the secretion of toxin in the hemolymph

LqhIT2 expression enhanced the virulence of *M. acridum* and exhibited reduced half-maximal lethal time (29.6%) towards Locust (Peng and Xia 2014). High-level expression of insect-specific neurotoxin AaIT1 in *M. anisopliae* increased the virulence against tobacco hornworm (22-fold) and *A. aegypti* (9-fold) (Wang and St Leger 2007). Furthermore, *M. anisopliae* expressing various channel acting hybrid toxins also synergistically work with AaIT to kill the mosquitoes and required 45% fewer spores compared to wild type strains (Bilgo et al. 2017). Similarly, expression of BUTX Lqq1a in *M. anisopliae* reduced the lethal time to 24.4% when compared to genetically unmodified wild type strain, suggesting that BUTX Lqq1a possess immense potential to increase the virulence of *M. anisopliae*.

3.5 Conclusion

In conclusion BUTX Lqq1a was successfully cloned and transformed using protoplast cum electroporation mediated transformation in *B. bassiana* as well as in *M. anisopliae* and the expression of neurotoxin was further confirmed by semi-quantitative RT-PCR analysis. Future studies with the genetically modified Bb-BUTX Lqq1a clones against various agricultural insect pests would pave the way to the development of novel biological pesticide.

Furthermore, expression of BUTX Lqq1a in *M. anisopliae* showed that neurotoxin increased the virulence the against white grub. These findings suggest that genetically engineered *M. anisopliae* might render a relatively cost-effective solution to counter the damage caused by *P. smithi* and other insect pests.

Table 3.1 List of primers used for pMcl1-BUTX Lqq1a vector construction in *B. bassiana*

Primer	5'----------3'
MCl1Pro FP NcoI pAL1 OH	CCAGTTCCGCCCATTCTCCGCCCCATGGAATCATGCAGCGCTATGAGAGC
MCl1 SP RP Lqq1a OH	CAGCGTAGCCGTTCTTCTTTGCCGACGCCAGGGCCAGC
Lqq1a FP MCl1 SP OH	GCTGGCCCTGGCGTCGGCAAAGAAGAACGGCTACGCTG
Lqq1a RP EcoRI pAl1 OH	CGGTATCGATAAGCTTGATATCGAATTCTTAGTTGATGGTGACAAAGTCG

Table 3.2 List of primers used for pMcl1-BUTX Lqq1a vector construction in *M. anisopliae*

Primer	5'----------3'
PtrpC OH-XbaI-HR mcl1 FP	CATTCAATATCATCTTCTGTCGAGTCTAGACAGGATCCTGCCGCCCTGCTCAAC
pAL OH-Xba1-HR mcl1 RP	GCACAGAGGCCGCAGAATGTGCTCTAGAGGCATCAGAGCCAGCACCGGTG
Ptrpc-RP-XbaI-HR Mcl1 OH	GTTGAGCAGGGCGGCAGGATCCTGTCTAGACTCGACAGAAGATGATATTGAATGCC
pCAM OH-EcoRI-Mcl1Pro-FP	GGAAACAGCTATGACCATGATTACGAATTCAATCATGCAGCGCTATGAGAGC
pCAM OH-HindIII-mcl1 gene-RP	CGTTGTAAAACGACGGCCAGTGCCAAGCTTGGCATCAGAGCCAGCACCGGTG
LqqIT1 RP HindIII pCAM OH	CGTTGTAAAACGACGGCCAGTGCCAAGCTTATTGTTGATGGTGACAAAGTCGC

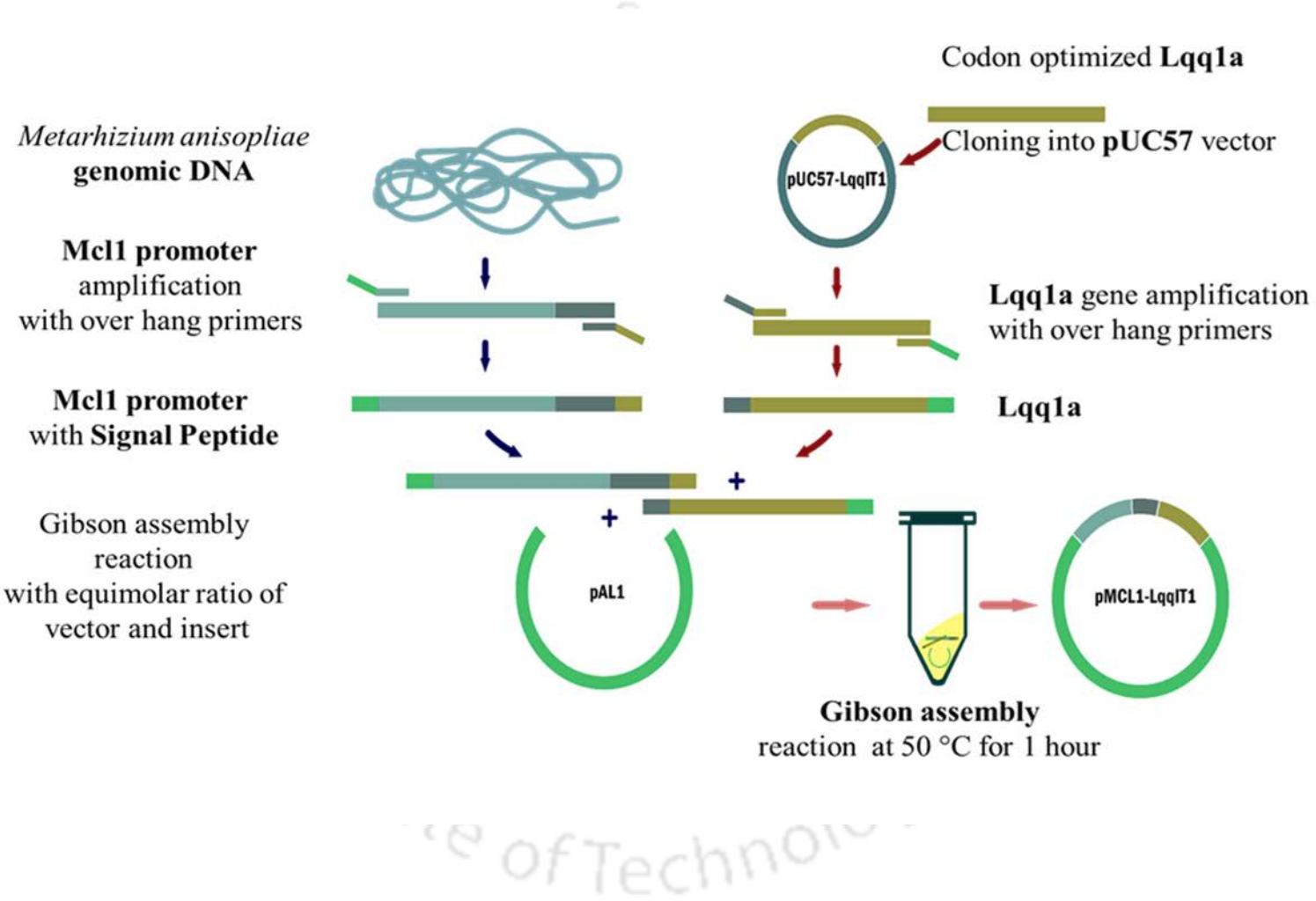

Fig.3.1 Schematic representation of pMcl1-BUTX Lqq1a vector construction

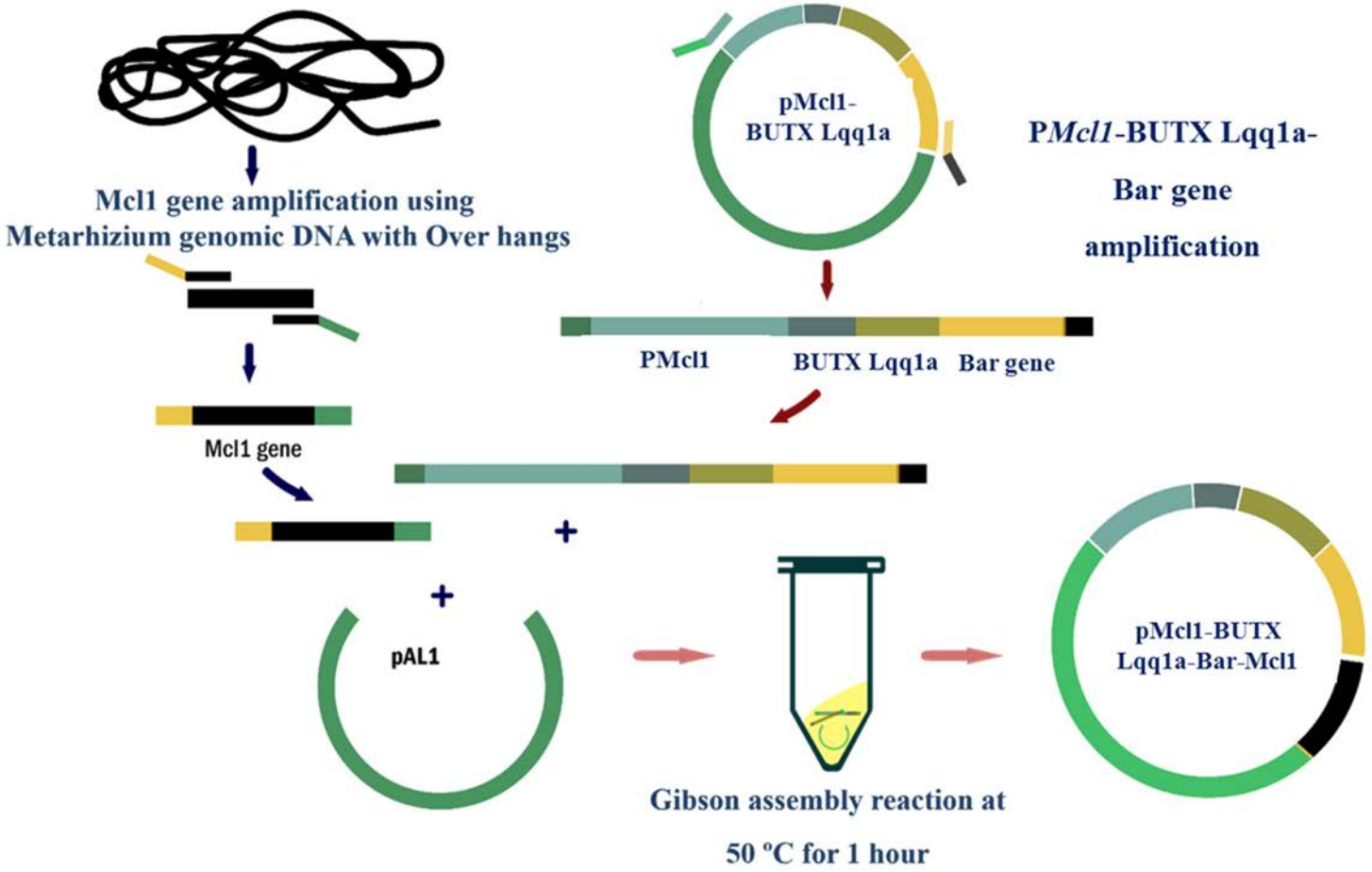

Fig.3.2 Schematic representation of pMcl1-BUTX Lqq1a-Bar-Mcl1 vector construction for *M. anisopliae* cloning

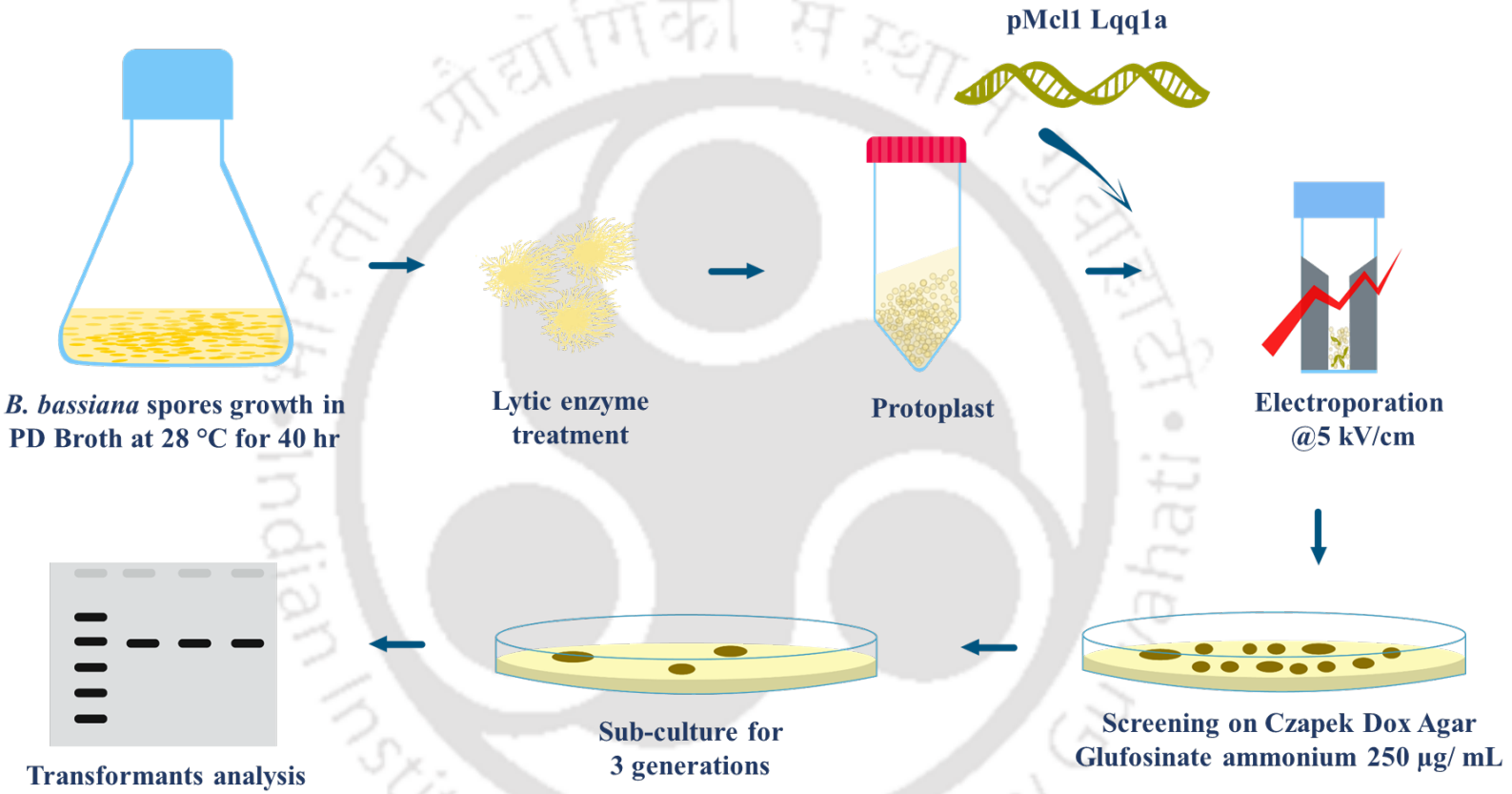

Fig. 3.3 Schematic representation of *B. bassiana* protoplast preparation and transformation method.

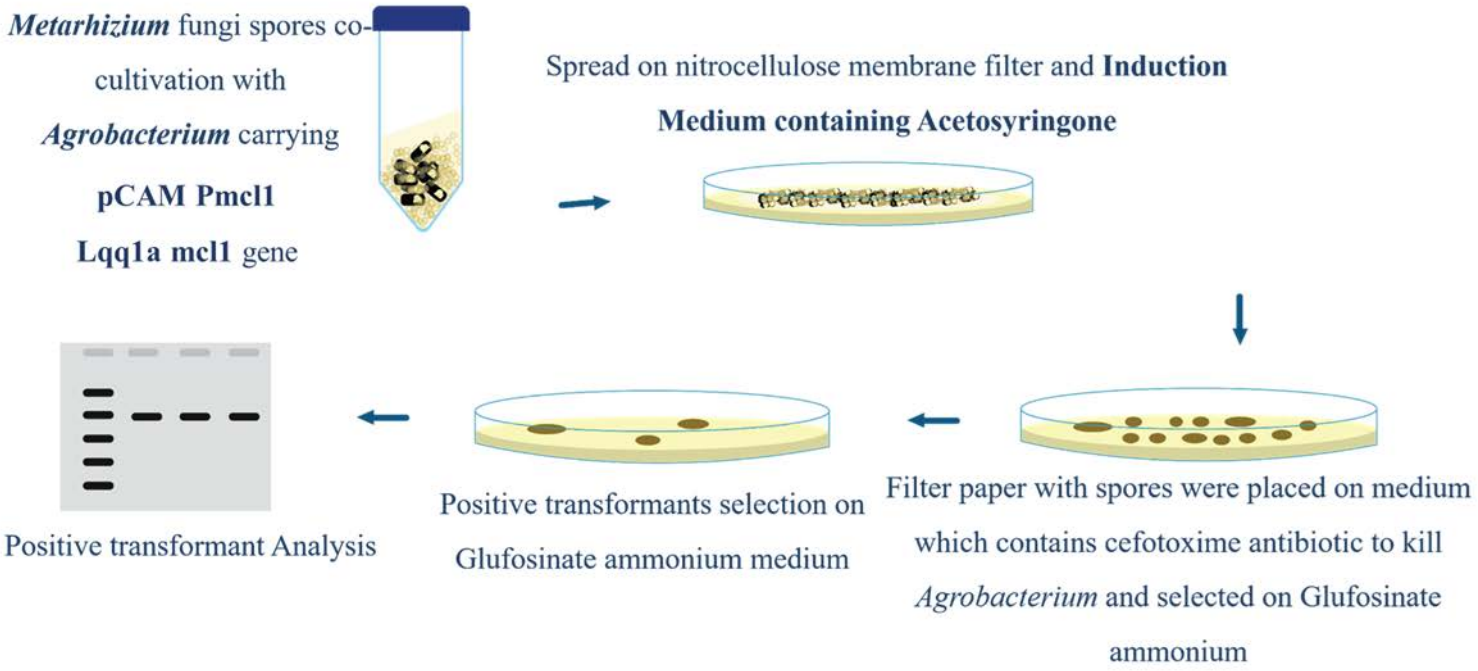

Fig. 3.4 Schematic representation of *Agrobacterium*-mediated transformation of *M. anisopliae*.

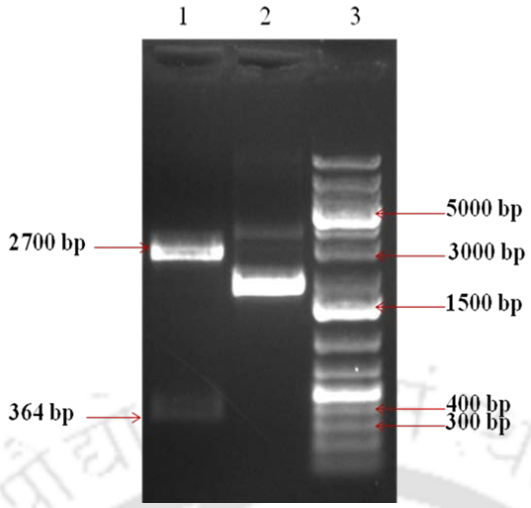

Fig. 3.5 Agarose gel electrophoresis analysis of plasmid pUC57 harboring codon optimized 5'UTR Mclsp-BUTX Lqq1a sequence. Lane 1: Restriction enzyme digested results yielding pUC57 vector backbone (2700 bp) and the insert (364 bp). Lane 2: Undigested pUC57 5'UTR Mclsp-BUTX Lqq1a (3064 bp) and Lane 3: 1Kb plus gene ruler.

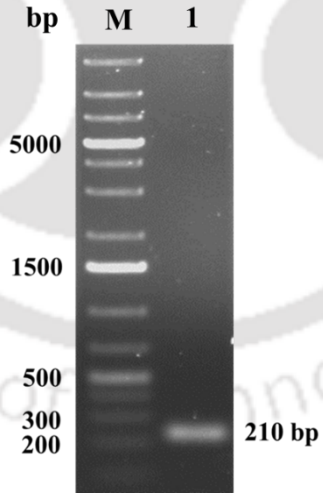

Fig. 3.6 Agarose gel electrophoresis analysis of BUTX Lqq1a PCR amplification from plasmid pUC57 harboring codon optimized 5'UTR Mclsp-BUTX Lqq1a sequence. Lane 1:1Kbplus Gene O Ruler and Lane 2: PCR amplified BUTX Lqq1a product (210 bp).

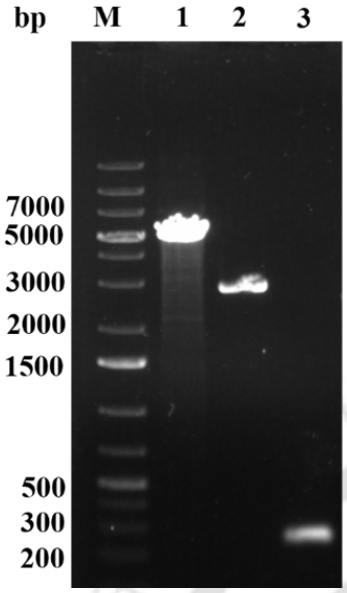

Fig. 3.7 Agarose gel electrophoresis analysis of P*Mcl1*-BUTX Lqq1a cloning in pAL1 vector. Lane 1: plasmid pAL1 digested (4830 bp) Lane 2: P*Mcl1* (*Metarhizium* collagen-like Promoter 1 (2854 bp), Lane 3- Mcl1sp-BUTX Lqq1a (295 bp)**,** and Lane M: O GeneRuler 1Kb plus DNA Ladder

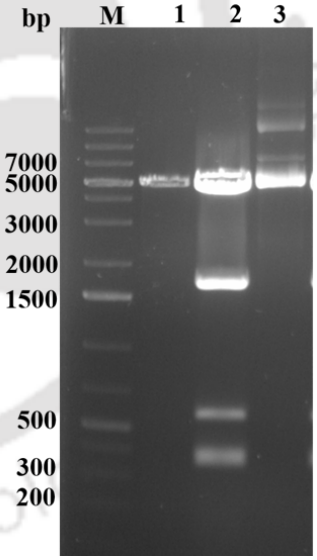

Fig. 3.8 Agarose gel electrophoresis image of clone confirmation analysis by restriction enzyme digestion. Double digestion confirmation of pMcl1-BUTX Lqq1a clone. Lane 1: Digested empty pAL1 vector (4830 bp), Lane 2: Clone digested with NcoI and EcoRI enzymes (Size 4830 bp, 1709 bp, 569 bp, 391 bp and 359 bp (391 and 359 bp are not differentiable)), and Lane 3: Undigested clone (size 7866 bp). Lane M: O GeneRuler 1Kb plus DNA Ladder

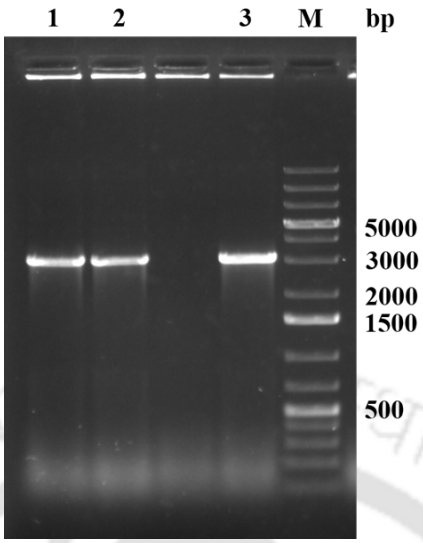

Fig. 3.9 Agarose electrophoresis analysis of pMcl1-BUTX Lqq1a clone confirmation by colony PCR amplification. Lane M: Marker 1 kbp plus Gene Ruler, and Lane 1,2 and 3: PCR amplified product of P*Mcl1*-BUTX Lqq1a (Size 3092 bp).

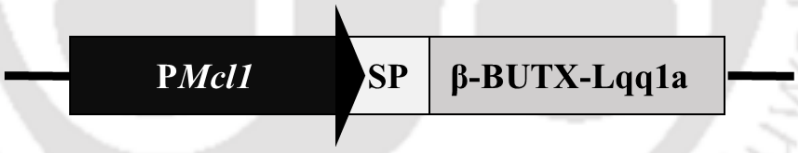

Fig. 3.10 The schematic representation of the BUTX Lqq1a arrangement in the pMcl1-BUTX Lqq1a vector

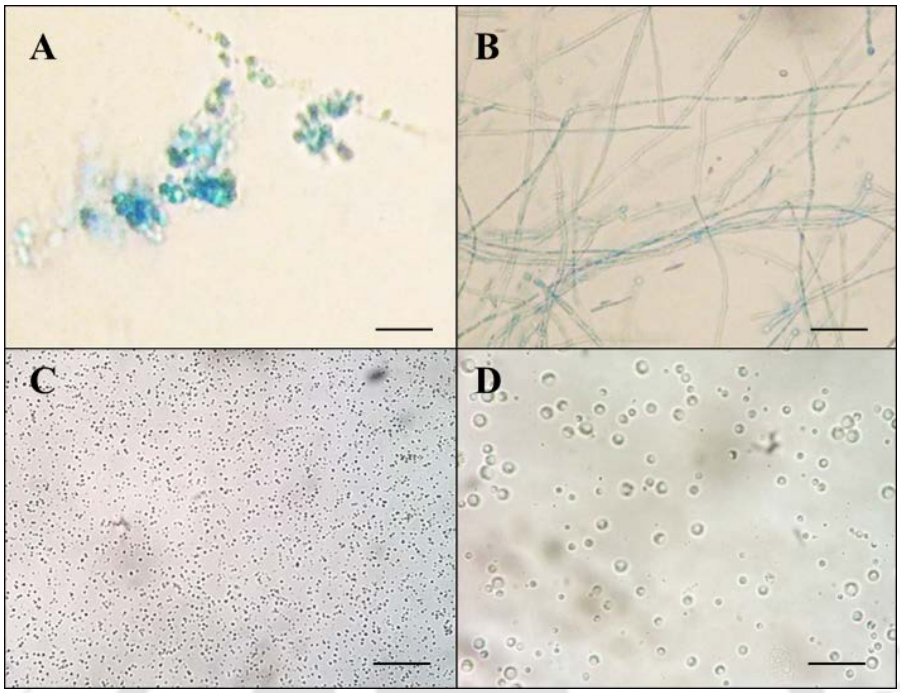

Fig. 3.11 Light microscopy studies of *B. bassiana* protoplast preparation. **A)** *B. bassiana* spores, **B)** 40 hr grown mycelium and **C** and **D)** protoplast. *B. bassiana* BUTX Lqq1a transformants. The Bar represents 50 µM scale.

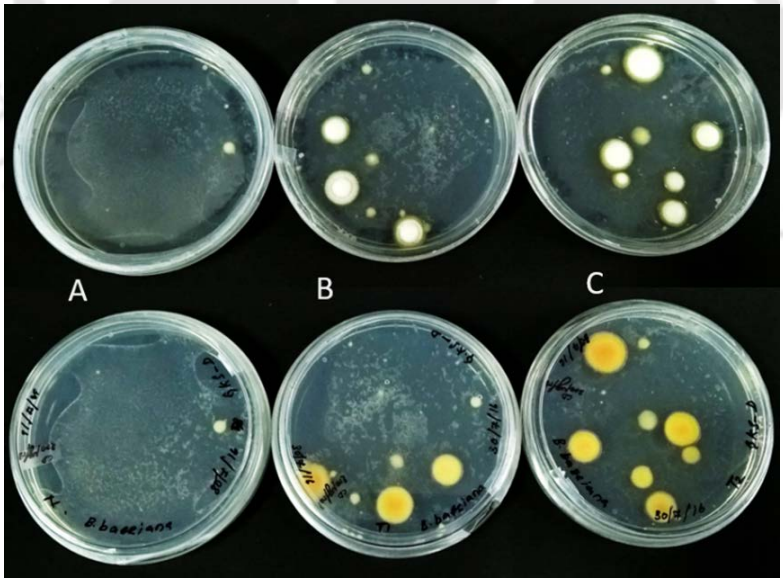

Fig. 3.12 *B. bassiana* BUTX Lqq1a clones observed on Czapek Dox agar with (300 µg ml^{-1}) glufosinate ammonium selection media. A) Negative control, B and C are *B. bassiana* clones.

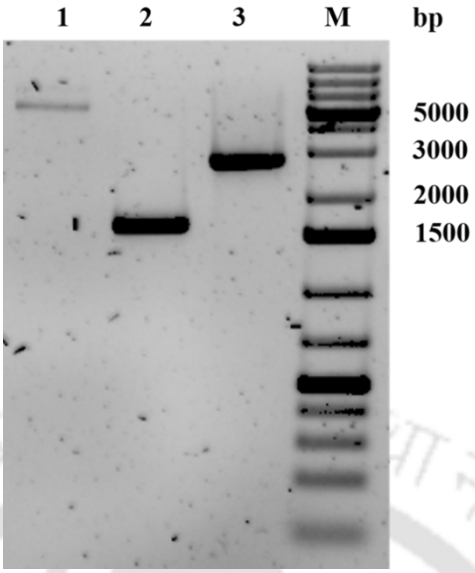

Fig. 3.13 Agarose gel electrophoresis analysis of gel purified products for *M. anisopliae* vector construction. Lane 1: P*Mcl1*-BUTX Lqq1a-Bar (5059 bp), Lane 2: Mcl1 gene (1560 bp), Lane 3: pAL1 digested with NcoI and XbaI (2650 bp), Lane M: O GeneRuler 1Kb plus DNA Ladder

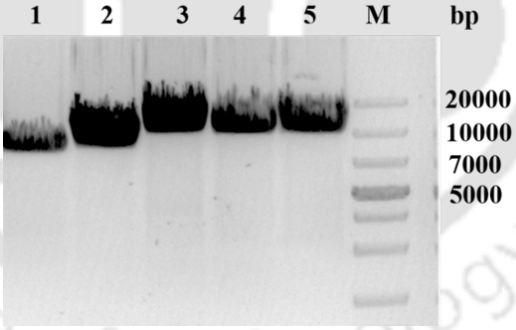

Fig. 3.14 Agarose gel electrophoresis analysis of purified plasmids from selected pMcl1-BUTX Lqq1a- Bar-Mcl1 gene clones. Lane 1: pMcl1-BUTX Lqq1a clone alone (7991 bp), Lane 2,3,4,5: pMcl1-BUTX Lqq1a-Bar-Mcl1 clones (~10 000 bp), Lane M: O GeneRuler 1Kb plus DNA Ladder.

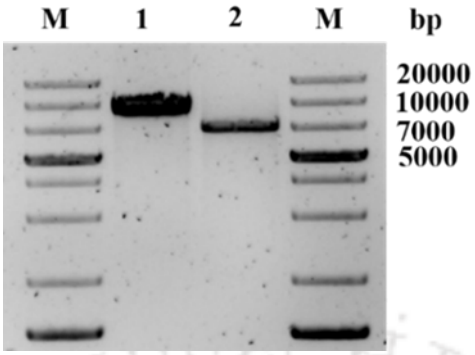

Fig. 3.15 Agarose gel electrophoresis images of gel purified products for pCAMBIA3300 binary vector cloning. Lane 1: pCAMBIA3300 digested with EcoRI and HindIII (8378 bp), Lane 2: P*Mcl1*-BUTX Lqq1a-Bar-Mcl1 fragment (~6.9 kbp).

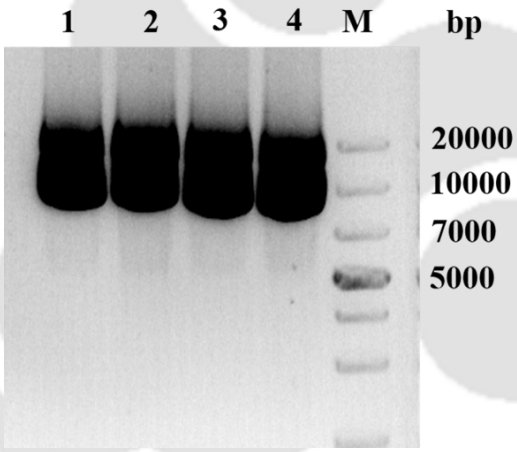

Fig. 3.16 Agarose gel images of Plasmid DNA isolated from selected pMcl1-BUTX Lqq1a clones. **Lane 1, 2, 3, 4**: pMcl1 BUTX Lqq1a clones **(~15 kbp)**, **M:** 1 Kb O Plus Gene Ruler

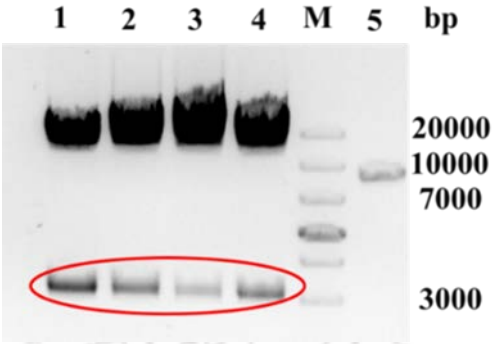

Fig. 3.17 Agarose gel electrophoresis analysis of pMcl1-BUTX Lqq1a clone confirmation by restriction enzyme digestion. **Lane 1, 2, 3, 4:** pMcl1-BUTX Lqq1a clones digested with EcoRI, **Lane 5:** pCAMBIA3300 empty vector.

Fig. 3.18 The schematic representation of the BUTX Lqq1a arrangement in the pMcl1-BUTX Lqq1a

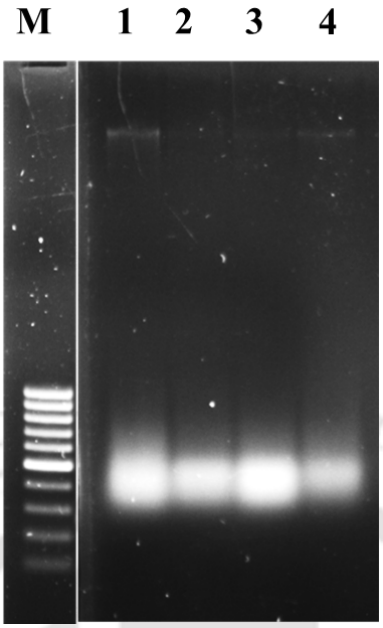

Fig. 3.19 Agarose gel electrophoresis analysis of *B. bassiana* genomic DNA isolation. Lane M: 100 bp DNA marker, Lane 1,2,3 and 4: Genomic DNA isolated from selected clones.

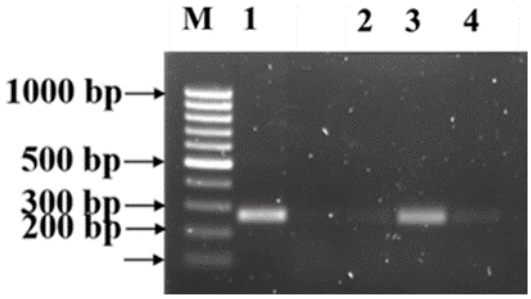

Fig. 3. 20 Agarose gel electrophoresis analysis of *B. bassiana* clone confirmation by PCR with gene-specific primers. The calculated size of the gene was 257 bp. Lane M: 100 bp DNA marker, Lane1: Positive control (BUTX Lqq1a amplicon), Lane 2, 3, and 4 observed amplicons with positive selected *B. bassiana* BUTX Lqq1a clones.

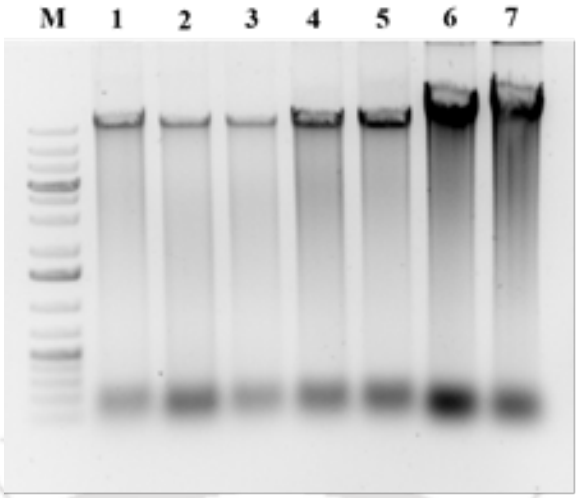

Fig. 3.21 Agarose gel electrophoresis analysis of *M. anisopliae* genomic DNA isolation and PCR clone confirmation studies. Lane 1, 2, 3, 4, 5, 6, and 7: selected Ma-BUTX Lqq1a clones genomic DNA isolated and Lane M: O'GeneRuler 1Kb Plus DNA ladder.

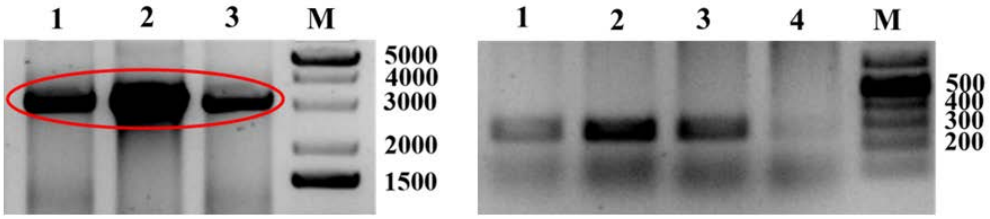

Fig. 3.22 Agarose gel image of PCR products amplified using *M. anisopliae* clones genomic DNA. **A)** Full length construct amplification. Lane 1, 2, and 3: P*Mcl1*-BUTX Lqq1a PCR products for *M. anisopliae* clone confirmation (~3 Kbps).

B) Agarose gel image of PCR products amplified using Ma-BUTX Lqq1a clones genomic DNA. Lane 1, 2, 3, and 4: BUTX Lqq1a PCR products of Ma-BUTX Lqq1a clones (295 bp) and Lane M: O'GeneRuler 1Kb Plus DNA ladder.

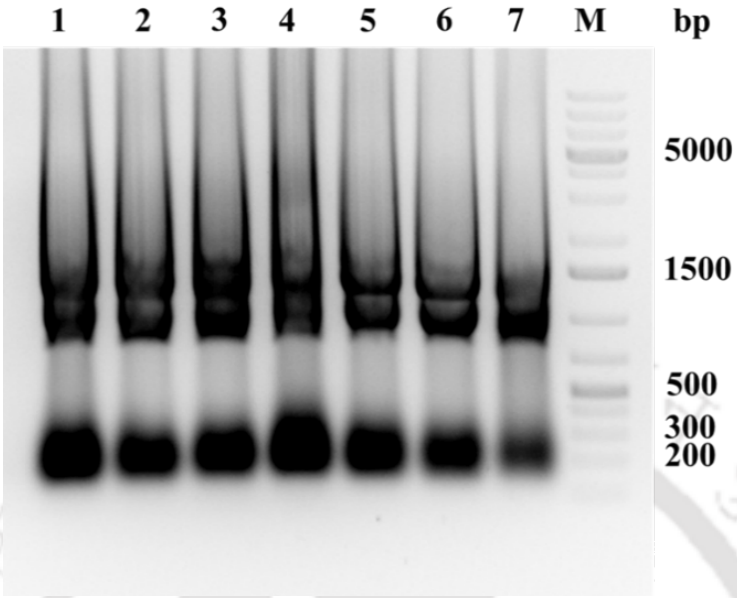

Fig. 3.23 Agarose gel electrophoresis analysis of total RNA isolated from *B. bassiana* BUTX Lqq1a clones. Lane 1 to 7: Bb-BUTX Lqq1a total RNA, Lane M: O' GeneRuler 1 Kb Plus DNA ladder.

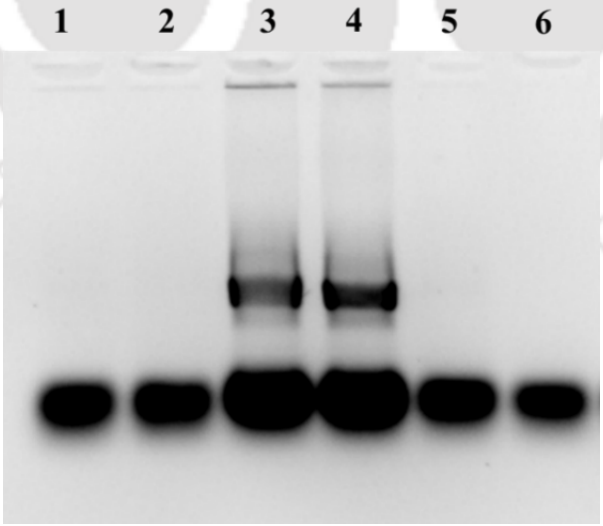

Fig. 3.24 Agarose gel electrophoresis analysis of total RNA isolated from *M. anisopliae* BUTX Lqq1a clones. Lane 1 to 6: Ma-BUTX Lqq1a total RNA.

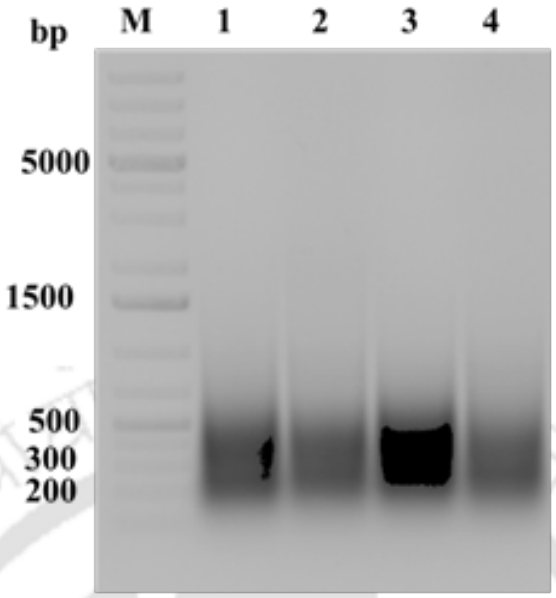

Fig. 3.25 Semi-quantitative RT-PCR analysis of cDNA synthesized from *B. bassiana* clone totals RNA. Lane 1,2,3,4: BUTX Lqq1a PCR products from cDNA synthesized from Bb-BUTX Lqq1a clones Lane M: O'geneRuler 1 Kb Plus DNA Ladder.

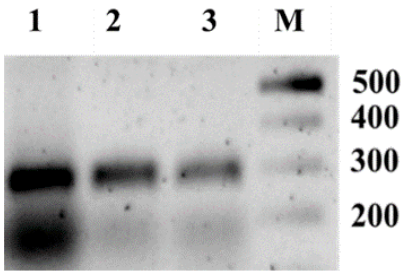

Fig. 3.26 Semi-quantitative RT-PCR analysis. Agarose gel image of BUTX Lqq1a PCR products amplified using cDNA synthesized from *M. anisopliae* clones. Lane 1,2, and 3: BUTX Lqq1a PCR products (295 bp) from cDNA synthesized from Ma-BUTX Lqq1a clones, M: O'GeneRuler 1 Kb Plus DNA ladder.

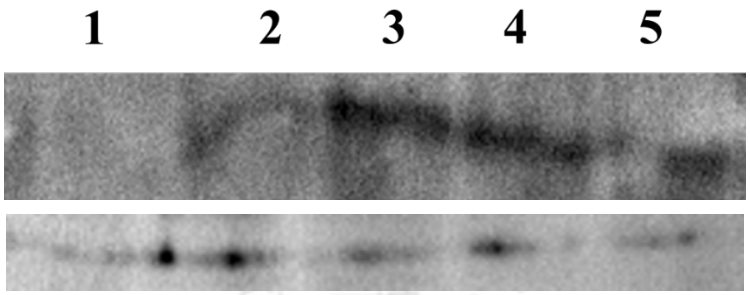

Fig. 3.27 Western blotting analysis of hemolymph induced Bb-wild type and Bb-BUTX Lqq1a strain and Loading control (β-tubulin). Lane 1: shows the unmodified wild type *B. bassiana* and Lane 2, 3,4 and 5 indicates the Bb-BUTX Lqq1a.

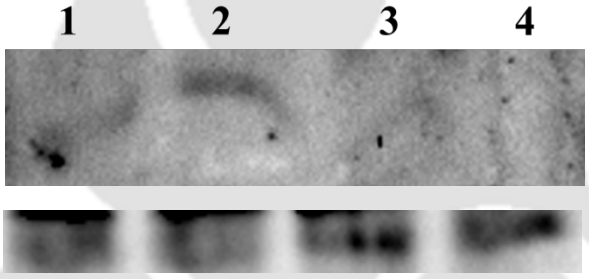

Fig. 3.28 Western blotting analysis of hemolymph induced wild type and Ma-BUTX Lqq1a strain and Loading control (β-tubulin). Lane 1, 2, and 3 indicates the Ma-BUTX Lqq1a and Lane 4 shows the unmodified wild type *M. anisopliae.*

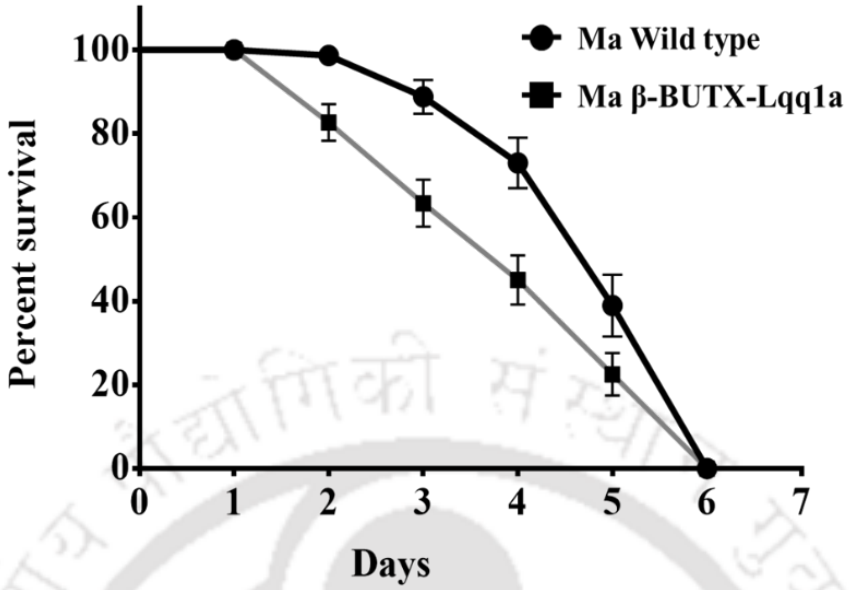

Fig. 3.29 Kaplan-Meier survival plot of *Phyllophaga smithi* (n=15, Log-rank (Mantel-Cox) test p=0.0009) bioassay conducted with *M. anisopliae* wildtype and Ma-BUTX-Lqq1a strain.

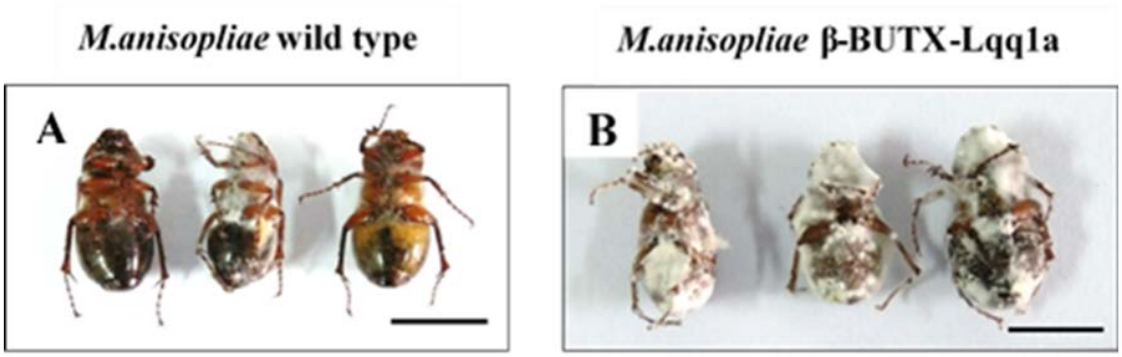

Fig. 3.30 Topical application Bioassay conducted with Ma-BUTX Lqq1a and unmodified wild type strain. Scale bar represents 1 cm.

CHAPTER 4

Bacterial expression and purification of a fusion protein containing β-BUTX Lqq1a/GNA Lectin and their cytotoxicity assay against insect cell lines

---

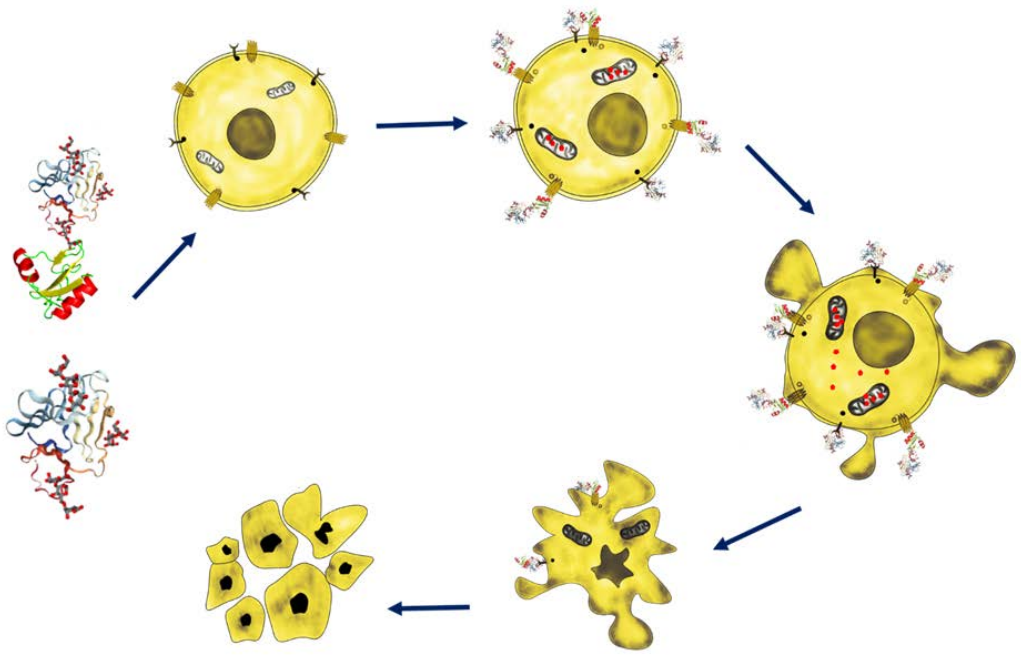

4.1 Introduction

Plants execute an arsenal of defense strategies against herbivory attack by producing defense-related peptides and proteins. Lectin is one of the primary defense protein produced by both monocot as well as dicot plants, and it binds reversibly to carbohydrate-containing proteins or glycol-conjugates. Lectin binding leads to the polysaccharides precipitation as well as agglutination of cells rich in receptors containing carbohydrate moieties (Vandamme et al. 1991). *Galanthus*, which is a bulbous perennial herbaceous plan produces active lectin or agglutinin as one of the defensive protein in the bulb. This GNA is a 13-kDa tetramer and bind specifically to α-D mannose residues and readily agglutinates rabbit erythrocytes (Vandamme et al. 1987).

Due to the intrinsic mannose-binding property, GNA lectin exhibited insecticidal activity against various pests including sap sucking brown planthopper, aphids, mites, tomato pests (Bharathi et al. 2011, Birch et al. 1999, Fitches et al. 1997, McCafferty et al. 2008) and also nematicidal activity against plant parasitic root-knot nematode (Ripoll et al. 2003). The exact mode of action of mannose lectins in insect is attributed to binding and blocking the absorption of nutrients by mid-gut epithelial cells (Agra-Neto et al. 2014). Also, GNA lectin disrupts and traverse across insect mid-gut barrier peritrophic matrix and exert action in the hemolymph (Powell et al. 1998). Besides, insecticidal activity, GNA lectin demonstrated activity against various cancerous cells (Gondim et al. 2017). Anti-tumor activity of lectin may be associated with DNA synthesis inhibition (Karasaki et al. 2001), reduction in the mitochondrial membrane potential (MMP) and caspase-dependent induction of apoptosis and autophagy (Liu et al. 2009). Oxidative stress and release of a cascade of apoptosis-related proteins were evident in lectin cytotoxicity (de Andrade Luz et al. 2017). It has proven potential activity against human

immune deficiency virus-HIV1 (Ye et al. 2001) and influenza virus H1N1-2009 (Sato et al. 2011). Lectin inhibited the entry of HIV-1 into the cells by binding to envelope protein. It also exhibited anti-influenza activity by directly binding to the viral envelope, thus blocking entrance (Sato et al. 2011).

In recent past, GNA combined with other neurotoxic peptides from either spider or scorpion is being exploited for their immense potential as an alternative to synthetic chemical pesticide. Liu et al. (2016) expressed GNA fused with *Andructonus australis* insect toxin (AaIT) in tobacco, which exhibited a potential increase in toxicity towards *Helicoverpa armigera*. Also, another recombinant fusion protein Hv1A/GNA containing spider toxin from *Hadronyche versuta* reduced the survival of aphid *Myzus persicae* (Nakasu et al. 2014). Though GNA/GNA fusion proteins were effectively utilized to control the agricultural pests, their mode of action on insect cell line is yet to be exploited. Buthidae family excitatory insect toxin β-BUTX Lqq1a, from Scorpion *Leiurus quinquestriatus quinquestriatus* exhibited cytotoxic as well as insecticidal potential towards *H. armigera* and *S. litura* (Kopeyan et al. 1990, Murugan and Saini 2019). This toxin is a cysteine-rich peptide which binds to the voltage sensing module in the extracellular loop of S1-S2 and S3-S4 of domain II and pore-forming module of domain III in the voltage-gated sodium channels (VGSC) of insects (Song et al. 2011).

The present study pioneers in analyzing the potential of both the neurotoxin Lqq1a and GNA action on *Spodoptera* and mouse macrophage cell line. Cytotoxicity studies by various bioassays and basic cytotoxic mechanisms were also evaluated for both the proteins.

4.2 Materials and Methods

4.2.1 Bacterial strain, Cell lines and chemicals

For bacterial cloning and maintenance, *Escherichia coli* DH5α strain and for protein expression, *E. coli* SHuffle T7 express LysY strain was employed (New England Biolabs, USA). Luria Bertani medium was used to maintain bacterial cultures at 37ºC. All restriction enzymes, Phusion DNA polymerase, and ligation enzymes were purchased from New England Biolabs, USA. Integrated DNA Technologies, USA, synthesized all the primers. Plasmid DNA and gel extraction kits were purchased from Macherey Nagel, GmBH. Thiazolyl Blue Tetrazolium Bromide-MTT, Propidium Iodide, and Fluorescein diacetate (FDA) were purchased from Sigma Aldrich Inc, USA.

4.2.2 β-BUTX Lqq1a and GNA gene synthesis

The protein sequence of β-BUTX Lqq1a was retrieved from National Center for Biotechnology Information (NCBI) database with the accession number: P19856.1 followed by its reverse translation into DNA sequence using European Molecular Biological Laboratory (EMBL)-EMBOSS Backtranseq software (Rice et al. 2000). The reverse translated DNA sequence β-BUTX Lqq1a was codon optimized for bacterial expression. Further, the codon-optimized DNA sequence was chemically synthesized and cloned in pUC57 vector flanking EcoRI and HindIII restriction sites (Genscript, USA). The protein sequence of GNA lectin and flexible Linker sequence (17 amino acid residue) was obtained from Longstaff et al. (1998) and Chen et al. (2013) respectively and then reverse translated into DNA sequence using (EMBL)-EMBOSS Backtranseq software (Rice et al. 2000). The reverse translated DNA was further codon-optimized for bacterial expression. Then codon optimized Linker GNA DNA sequence was synthesized and cloned in pUC57 vector flanking NdeI and EcoRI restriction sites (Genscript, USA).

4.2.3 Expression vector construction

Overlap extension PCR was performed to clone GNA along with N-terminal His-Tag in pET28a bacterial expression vector, and for fusing the β-BUTX Lqq1a with GNA. The primers used for the fusion are listed in the **Table 4.1**. Both PCR amplified DNA fragments, pET28a expression vector was digested with NdeI, and EcoRI restriction enzymes and gel purified using Takara gel purification kit. Ligation of the purified fragments was performed using T4 DNA ligase (NEB, USA) at 16ºC for 16 hr duration.

4.2.4 *E. coli* DH5α chemical competent cell preparation

The $CaCl_2$ based chemical competent cells were made according to the protocol Cohen et al. (1972) with little modifications. Initially, 5 ml of LB medium was used to inoculate single DH5α colony and incubated overnight at 37ºC at 200 rpm in rotatory incubator shaker. Next day, 0.1% of overnight grown culture was used to inoculate 500 ml of LB broth and incubated at 37ºC until the optical density of the culture reached up to OD_{600} 0.3-0.5. Post-incubation, cells were collected by centrifugation at 8000 rpm for 15 min at 4ºC. The collected cells were washed once with 100 mM $CaCl_2$ and incubated in ice-cold 100 mM $CaCl_2$ for 30-45 min. After the incubation, centrifugation was performed to obtain the cell pellet and again resuspended in 1.5 ml of ice-cold 200 mM $CaCl_2$ prepared with 30% glycerol. The volume of 50 µl cell aliquots was made, flash-frozen in liquid nitrogen and stored in -80ºC freezer until further use.

4.2.4.1 *E. coli* DH5-α transfection

Ligated products were then transformed into *E. coli* DH5-α using calcium chloride ($CaCl_2$) chemical competent transformation method, and the selection was carried out using antibiotic kanamycin (50 µg ml^{-1}). Positive clones were further confirmed by PCR with gene-specific primers. PCR confirmed positive clones were further used for plasmid

DNA isolation. Isolated plasmids were analyzed by using a 1% Agarose gel electrophoresis system, and for imaging, Bio-rad ChemiDoc gel documentation system was employed.

4.2.5 GNA and β-BUTX Lqq1a/GNA expression and purification

4.2.5.1 Shuffle T7 express LysY chemical competent cells preparation

Chemical competent cells of Shuffle T7 express LysY cells were according to the protocol followed in **section 2.2.4 of chapter 2**. The plasmid pET28a β-BUTX Lqq1a/GNA and pET28a GNA were transformed into bacterial protein expression strain SHuffle T7 Express LysY using chemical competent transformation method. The selection was carried out on LB medium supplemented with kanamycin (50 µg m^{-l}) and incubated at 37ºC for overnight. Again the colonies were confirmed for the presence of the plasmid and the BUTX Lqq1a gene by PCR based screening method.

4.2.5.2 GNA and β-BUTX Lqq1a/GNA expression

The recombinant β-BUTX Lqq1a/GNA and GNA protein expression were carried out using Terrific Broth (TB) medium (Tryptone 12 g l^{-1}, yeast extract 24 g l^{-1}, K_2HPO_4 12.54 g l^{-1}, KH_2PO_4 2.31 g l^{-1}) supplemented with 1.0% glycerol. Initially, bacterial culture was grown until OD_{600} to reach 0.6 at 30ºC and then it was induced with 0.5 mM isopropyl thiogalactopyranoside (IPTG) and incubated for 16 hr at 16°C in a refrigerated incubator shaker at 200 rpm.

4.2.5.3 GNA and β-BUTX Lqq1a/GNA affinity purification

Post-incubation, the culture was centrifuged, and cell pellet was re-suspended in binding buffer A (20 mM Tris-HCl, 300 mM NaCl, 20 mM Imidazole, 10% Glycerol, 5 mM Benzamidine HCl, 2 mM DTT), followed by lysis using Vibra cell Sonicator with 2

sec pulse ON and 30 sec pulse OFF conditions. Further, the crude lysate was centrifuged at 13,000 rpm for 1 hr at 4ºC, and the filtered supernatant solution was loaded into Nickel-Nitrillo Triacetic Acid (Ni-NTA) affinity chromatography column pre-equilibrated with binding buffer A. Different fractions were eluted with binding buffer A containing 300-400 mM imidazole and buffer exchanged with phosphate buffered saline (PBS, pH 7.4) using Amicon ultra-cell centrifugal filter (3000 kDa Molecular weight cutoff, Merck millipore). Concentrated fractions were further analysed by using 16% Sodium Dodecyl Sulfate-Poly Acrylamide Gel electrophoresis (SDS-PAGE). Gel images were captured using a Biorad Gel Doc EZ gel documentation system and analysed with Image Lab software 4.0 from Biorad. Quantification analysis of purified β-BUTX-Lqq1a/GNA and GNA protein was performed using Bradford assay.

4.2.6 Cell culture and maintenance

Spodoptera frugiperda insect cell line *Sf*-9 and *Sf*-21 and Mouse Macrophage cell line J774a.1 (National Centre for Cellular Science, India) were used to evaluate the cytotoxicity of purified recombinant proteins. Insect cell lines were maintained in *Trichoplusia ni* (TNM-FH) medium (Sigma, USA) supplemented with 10% Fetal Bovine Serum (FBS) in an aerated incubator at 27ºC. Mouse cell lines were grown in RPMI-1640 (Roswell Park Memorial Institute medium, Sigma, USA) medium supplemented with 10% FBS at 37ºC with 5% CO_2.

4.2.7 Cell Viability Assay

The viability of *Sf*-9, *Sf*-21, and J774a.1 cell were evaluated by MTT (3-(4,5-Dimethylthiazol-2-yl)-2,5-diphenyl tetrazolium bromide) based colorimetric assay. Healthy cells with more than 95% viability were chosen for the cell viability experiment. Initially 1×10^6 cells from *Sf*-9 and *Sf*-21 cultures were incubated in TNM-FH insect

medium, and subsequently different concentrations of GNA (62.8, 125, 252, 376, 501 µg ml^{-1}) and β-BUTX Lqq1a/GNA (15, 30, 45, 60, 75 µg ml^{-1}) was added and incubated for 6-12 hr at 27ºC under aerated conditions. Also, for J774a.1 cells, cultures were incubated in RPMI-1649 medium with various concentrations of GNA and β-BUTX Lqq1a/GNA for 24 hr at 37ºC under 5% CO_2 conditions. PBS (pH 7.4) was taken as a control treatment for both the cell lines. After the respective incubation period, 10 µl of MTT solution was added and incubated at least 4-5 hr. MTT along with medium was removed by centrifugation at 2000×g for 30 min. Then the crystals were dissolved in 100% DMSO (Dimethyl Sulfoxide), and absorbance at 570 nm with reference 660 nm was measured using Tecan Multiplate reader (Infinite Pro 200, Austria).

4.2.8 Microscopy analysis

For microscopy analysis, initially, *Sf*-9 and *Sf*-21 cells with more than 95% viability were chosen. Then 1×10^6 cells from *Sf*-9 and *Sf*-21 cultures were incubated in TNM-FH insect medium, and subsequently, GNA and β-BUTX Lqq1a/GNA were added at higher concentration and incubated for 24-48 hr at 27ºC under aerated conditions. Also, for J774a.1 cells, cultures were incubated in RPMI-1640 medium with higher concentration of GNA and β-BUTX Lqq1a/GNA for 24-48 hr at 37ºC under 5% CO_2 conditions. Insect and mouse cell lines treated with PBS (pH 7.4) were taken as control. Dual staining method using Fluorescein Diacetate (FDA) and Propidium Iodide (PI) was performed to differentiate the live cells from dead cells. DAPI (4′,6-diamidino-2-phenylindole) staining was also performed to visualize the chromosomal DNA damage of treated as well as control cells. Imaging was performed with the help of Inverted Fluorescence Microscope (Nikon-Ti-S, Japan).

4.2.9 Mitochondrial membrane potential assay

Mitochondrial membrane potential analysis was performed using Rhodamine 123 based fluorescence microscopy assay. Initially *Sf*-9 and *Sf*-21 cells at a density of 2×10^6 cells ml^{-1} were seeded along with the GNA and β-BUTX Lqq1a/GNA and incubated for 12 hr at 27°C in an aerated incubator and only PBS (pH 7.4) treated cells were taken as control. Post-incubation, treated and control cells were centrifuged at 500×g for 5 min at 4ºC and Rho 123 was added at a final concentration 50 nM in PBS (pH 7.4) and incubated for 15 min. Treated and untreated cells were washed twice with PBS (pH 7.4) and analysed by using Inverted Fluorescence Microscope (Nikon-Ti-S, Japan).

4.2.10 Cell cycle analysis

Cell cycle analysis was performed using flow cytometer to evaluate the effect of purified GNA and β-BUTX Lqq1a/GNA on the insect cell line. For flow cytometry analysis, cells with a concentration of 2×10^6 cells ml^{-1} were seeded along with the GNA and β-BUTX Lqq1a/GNA and incubated for 24 hr at 27°C aerated incubator. Post-incubation, ice-cold 70% ethanol was added dropwise to fix the cells at 4°C overnight. After the fixation, centrifugation at 2000 rpm for 10 min was done to remove the residual ethanol. Pelleted cells were again re-suspended in phosphate buffered saline (PBS, pH 7.4) and Ribonuclease A (RNase A) treatment was done at 37°C for 1 hr. Then, cells were stained by using propidium iodide (1 mg ml^{-1}) for 10 min and analyzed using BD FACS Caliber flow cytometer.

4.2.11 Gene expression analysis by Real-time quantitative PCR

The RT-qPCR analysis was carried out using complementary DNA (cDNA) synthesized from total RNA which was isolated from the treated as well as untreated control cells to assess the differential expression of genes in the wake of GNA and

β-BUTX Lqq1a/GNA treatment in *Sf*-9 and *Sf*-21 cells. The *Sf*-9 and *Sf*-21 cells (2×10^6 cells ml^{-1}) were seeded with GNA and β-BUTX Lqq1a/GNA, incubated for 24-48 hr at 27°C in an aerated incubator. Total RNA was isolated using RNAisoPlus kit (Takara, Japan) according to the manufacturer protocol and converted into cDNA using Primescript 1st strand cDNA synthesis kit (Takara, Japan). After cDNA synthesis, RT-qPCR was performed with a set of primers (**Table 4.2**) using PowerUp SYBR Green master mix (Applied Biosystems, USA) using ABI7500 RT-PCR system.

4.2.12 Insect bioassay of GNA and β-BUTX Lqq1a/GNA with *S. litura*

4.2.12.1 Maintenance of insect cultures

S. litura insect eggs were procured from National Bureau of Agricultural Insect Resources (NBAIR), Bangalore, India and maintained in a 16:8 hr light and dark photoperiod conditions at 25±3ºC in natural castor leaves diet at 60-70% relative humidity (RH).

4.2.12.2 Intra-hemocoeilic injection bioassay

Intra-hemocoel injection bioassay was performed using 5th instar larvae of *H. armigera*, and *S. litura*. A 10 µl of GNA and β-BUTX Lqq1a/GNA protein (10 µg $insect^{-1}$) was used for injection in *S. litura* (n=30). PBS (pH 7.4) was taken as a control for the injection. All the insects were starved for 2 hr pre-injection and chilled at 4ºC until torpid before injection. Injected insects were supplied with natural castor leaves diet only. All the experiments were conducted at 25-28ºC with 60-70% RH level with 16:8 hr light and dark photoperiod.

4.2.13 Statistical data analysis

Data analysis were conducted using GraphPad Prism software (version 6.0). The values are expressed as mean with standard deviation. For the MTT assay, the data were compared using a one-way analysis of variance (ANOVA) test with Dunnett's multiple comparisons test. Differences were considered statistically significant when the p-value < 0.05. The IC_{50} value was calculated using GraphPad Prism software with the normalized absorbance percentage vs. log concentration. Microscopy images were processed with the help of NIS element analysis 4.5 (Nikon, Japan). Cell cycle data analysis was carried out using FCS Express (6.0) software and threshold cycle (C_T) values for control *gpdh*, and other genes were determined using ABI 7500 system software, and $2^{-\Delta\Delta CT}$ values were determined based on Livak and Schmittgen (2001) method.

4.3 Results

4.3.1 Cloning GNA and β-BUTX Lqq1a/GNA in pET28a expression vector

In the present study, initially codon optimized GNA (**Fig. 4.1**) was successfully amplified and cloned in pET28a expression vector yielding pET28a GNA (**Fig. 4.2**). Further PCR with gene specific primers also confirmed the presence of GNA (**Fig. 4.3**). Later codon optimized β-BUTX Lqq1a (**Fig. 4.4**) was successfully fused with the upstream end of GNA using overlap extension PCR and cloned in expression vector pET28a yielding pET28a β-BUTX Lqq1a/GNA (**Fig. 4.5**). Cloning was further confirmed by digestion with restriction enzymes (**Fig. 4.6**).

4.3.2 GNA and fusion protein β-BUTX Lqq1a/GNA expression and purification

In the present study, both the GNA and β-BUTX Lqq1a were codon optimized to maximize the soluble expression in *E. coli* SHuffle T7 express LysY system. For fusion, GNA was C-terminally fused with β-BUTX Lqq1a toxin with the help of flexible linker sequence (AEAAAKEAAAKEAAAKA) by PCR based fusion method (**Fig. 4.7**). After the successful confirmation, GNA (**Fig. 4.8**) and fusion protein β-BUTX Lqq1a/GNA (**Fig. 4.9**) were successfully expressed and purified using Ni-NTA affinity chromatography system. Finally, both the purified proteins were analysed by using SDS-PAGE and molecular weight was confirmed to be 16.9 kDa and 25.2 kDa, respectively (**Fig. 4.10 A and B**).

4.3.3 Cell viability assay

MTT dye-reduction method was performed to evaluate the effect of recombinant GNA and β-BUTX Lqq1a/GNA action on *Sf*-9, *Sf*-21, and J774a.1 cell lines. As seen in **Fig. 4.11**, GNA significantly affected the cell proliferation of *Sf*-9 ($p < 0.0001$) and J774a.1 ($p < 0.0001$) in dose-dependent manner except for the *Sf*-21 insect cell line.

Significant effect (p = 0.01) was found for the *Sf*-21 cell only at higher concentration of recombinant GNA. The calculated IC_{50} value for the *Sf*-9, *Sf*-21, and J774a.1 cell lines were 106.3, 187.5, and 89.5 µg $ml^{-1,}$ respectively. Cell viability assay conducted with various concentrations of recombinant fusion β-BUTX Lqq1a/GNA also significantly ($p \leq 0.0001$) affected the cell proliferation in a dose-dependent manner in all the three cell lines (**Fig. 4.12**). The calculated normalized mean IC_{50} value of *Sf*-9, *Sf*-21, and J774a.1 cell lines were 26.5, 39.6, and 14.2 µg $ml^{-1,}$ respectively.

4.3.4 Dual staining assay

To evaluate the cytotoxicity, *Sf*-9, *Sf*-21, and J774a.1 cells were exposed to a higher concentration of recombinant GNA and fusion protein β-BUTX Lqq1a/GNA. As seen in **Fig. 4.13**, the control cells were positive for the FDA, and an almost negligible amount of PI-positive cells was observed. However, in GNA treated cells lines, all the cells detected to be PI positive. Also, an insignificant number of cells exposed to FDA were positive. The **Fig. 4.14** represents the fusion protein β-BUTX Lqq1a/GNA treatment with *Sf*-9, *Sf*-21 and J774a.1 cells and stained with live cell stain FDA and nuclear stain PI. Untreated control cells were able to metabolize the FDA and resulted in green fluorescence. Whereas in the treated population, all the cells observed to have stained with nuclear stain PI, indicating the damage caused by the combined action of fusion protein β-BUTX Lqq1a/GNA.

4.3.5 DAPI staining assay

The change in chromosomal DNA pattern was analysed by staining the treated and untreated cells using a nucleic acid stain DAPI. As seen in **Fig. 4.15** GNA treated insect and mouse cell lines exhibited aberration in chromosomes or nucleus structure when compared with untreated or PBS treated control cells. Similarly, fusion protein β-

BUTX Lqq1a/GNA treatment in *Sf*-9, *Sf*-21, and J774a.1 cells indicated the chromosomal alteration when compared to PBS treated control (**Fig. 4.16**)

4.3.6 Mitochondrial membrane potential assay

The membrane electrochemical potential generated in mitochondria using proton gradient was assessed by Rho 123 fluorescence quenching. Initial staining of untreated cells exhibited higher Rho 123 fluorescence both in *Sf*-9 and *Sf*-21 cells (**Fig. 4.17 and 4.18**). However, in the GNA and β-BUTX Lqq1a/GNA treated insect cell population, reduction in the fluorescent intensity was observed due to quenching in Rho 123 fluorescence by reactive oxygen species. This indicate the cytotoxic activity of both GNA and fusion protein in insect cell lines.

4.3.7 Flow cytometry analysis

To determine the effect of purified recombinant GNA and β-BUTX Lqq1a/GNA on cell cycle progression, flow cytometry analysis was performed with treated and untreated *Sf*-9 and *Sf*-21 insect cell lines. As shown in **Fig.4.19,** purified GNA treated *Sf*-9 cells (**Fig. 4.19C**) accumulated in the G2 phase with a significant increase in the cell number as compared to control. Also, GNA treated *Sf*-21 cells (**Fig. 4.19D**) also showed a substantial increase in the G2 population as compared to *Sf*-21 control. Correspondingly, the number of cells in the G2 and S phase was significantly reduced. Similar effects were observed with the *Sf*-9 (**Fig. 4.19E**) and *Sf*-21(**Fig. 4.19F**) cells treated with purified fusion protein β-BUTX Lqq1a/GNA, where significantly increased number of cells accumulated in the G2 phase of the cell population. The corresponding reduction in cell numbers was observed in G1 and S phase of treated cells.

4.3.8 Gene expression analysis

RT-PCR analysis was performed to study the GNA and β-BUTX Lqq1a/GNA induced effects on the expressional gene level, with the selected set of caspase-dependent and caspase-independent genes. The relative expression of Caspase 2 in GNA treated *Sf*-9 cell increased to 1.1 fold more when compared to control (**Fig. 4.20A**). Similarly, Caspase 5, AIF, IAP, and Survivin expression increased to 6.2, 0.2, 5.0, and 1.9 fold, respectively. While *Sf*-21 cells treated with GNA observed for the increased relative fold expression in Caspase 2 (1.1), Caspase 5 (0.1) and IAP (7.8). However, the relative expression of AIF (0.2) and Survivin (0.4) were lower when compared to control.

When the expression of caspase-dependent and independent genes of β-BUTX Lqq1a-GNA treated *Sf*-9 and *Sf*-21 cell were evaluated, a significant increase in the interpretation of Caspase 2, Caspase 5 and IAP was observed (**Fig. 4.20B**) The expression of AIF and Survivin was not substantial in treated *Sf*-21 cells compared to control. Overall, both GNA and β-BUTX Lqq1a/GNA had significantly affected the insect cell line survival.

4.3.9 Insect bioassay with *S. litura*

Insect bioassay was performed with 5th instar stage *S. litura* larvae, to evaluate the insecticidal toxicity of the purified recombinant proteins. Insects injected with purified recombinant GNA and β-BUTX Lqq1a/GNA exhibited significant mortality in the 5th instar larvae with initial reduction in the feeding, and mortality of the injected insects. More than 60% reduction in survival was observed within 24 hr post-injection and complete mortality was observed after 48 hr. Severe melanization of insect body was associated with insect mortality in hemocoilic injected insects. Fusion protein showed relatively immediate death of *S. litura* larvae than GNA treated larvae. However, the PBS treated insect population observed to be healthier and reached the pupation stage. This

assay suggests that both the GNA and β-BUTX Lqq1a/GNA could cause severe insect morality in *S. litura* (**Fig. 4.21**)

4.4 Discussion

The present study, details the GNA and fusion protein β-BUTX Lqq1a/GNA expression and purification using optimized codon sequence in SHuffle T7 express LysY bacterial system, which allows the disulfide bonding within the cytoplasm. The first report on native GNA purification directly from Snowdrop plant was done by Vandamme et al. (1987) followed by the recombinant expression and purification of GNA using *E. coli* as the host system (Longstaff et al. 1998, Luo et al. 2005). Recombinant GNA purified from *E. coli* reportedly expressed as inclusion bodies, due to the richness in cysteine amino acid (Longstaff et al. 1998, Luo et al. 2005). However, soluble expression of GNA was achieved using the optimized expression method, which includes the addition of 1.0% glycerol in growth medium and by reducing the growth temperature to 16ºC. Numerous studies have reported the use of fusion protein containing GNA with other spider or scorpion neurotoxin for the control of insect pests by overexpression in plants (Down et al. 2006, Fitches et al. 2002, Fitches et al. 2004, Fitches et al. 2010, Fitches et al. 2012, Liu et al. 2016, Trung et al. 2006, Yang et al. 2015, Yang et al. 2014). In the present study, GNA lectin was C-terminally fused to the scorpion toxin via linker sequence that is rich in Alanine and Lysine amino acids, which makes the linker to be more rigid and further increases the stability and folding of the fusion protein (Takamatsu et al. 1990). The fusion β-BUTX Lqq1a/GNA protein was successfully expressed in SHuffle T7 expression system in a soluble form and purified using single step Ni-NTA affinity chromatography. However, all the reported fusion proteins were tested for oral toxicity towards agriculturally important insect pests, a detailed study on the mechanism of fusion protein action on the cellular level was requisite.

MTT cell viability assay demonstrated that both GNA and fusion protein β-BUTX Lqq1a/GNA affected the viability of *Sf*-9, *Sf*-21, and J774a.1 cells in a dose-dependent manner. Susceptibility of *Sf*-21 cells towards GNA was 1.7 fold higher than *Sf*-9 and two-fold higher than J774a.1 cell lines. Differential susceptibility of various cell lines toward GNA lectin may be attributed to the availability of mannose residues on the cell membrane surface. *Sf*-21 sensitivity towards GNA may be due to the presence of less number of mannose residues compared to *Sf*-9, albeit it is a parental cell line. Liu et al. (2009) showed that mannose/glucose binding lectin ConA anti-proliferative activity correlated with the carbohydrate binding activity and lead to autophagy-mediated death of human melanoma cells. Coagulant *Moringa oleifera* lectin (cMoL) and peanut agglutinin (PNA) exhibited potential cytotoxic activity against various cancerous cell lines despite the non-significant action on healthy cells (de Andrade Luz et al. 2017, Mukhopadhyay et al. 2014). Correspondingly, GNA also exhibited prospective cytotoxic as well as anti-proliferative action on insect and macrophage cells.

Fusion protein β-BUTX Lqq1a/GNA showed dose-dependent activity against a variety of cell lines with the possible mechanism of cytotoxicity. A fusion protein containing ButaIT/GNA from Buthidae family, *Mesobuthus tamulus* insect toxin and Snowdrop caused severe mortality when fed orally to a variety of insect belongs to Lepidopteran, Dipteran, and Coleopteran insects (Fitches et al. 2010). Likewise, SFI1 protein from *Segestria florentina* showed increased mortality when fused with GNA against tomato pests, *Lacanobia oleracea* (Fitches et al. 2004). Both studies represented that either neurotoxin or GNA alone could not exhibit significant mortality. However, when combined, mortality increased to a considerable level. Recombinant GNA alone required higher concentration to exert the cytotoxic activity, however, when fused with

neurotoxin β-BUTX Lqq1a, dosage against *Sf*-9 reduced almost four-fold, 4.7 fold against *Sf*-21 and 6.3 fold against J774a.1 with increased activity.

Dual staining with FDA-PI offers a reliable, consistent, and rapid method of determining the cellular viability where live cell would be able to metabolize the non-fluorescent FDA into green fluorescein molecule due to the action of esterase present in the metabolically active cell. Whereas dead cell would be able to take up more amount of cell-impermeable DNA binding PI dye, due to the damages in the cellular membrane (Jones and Senft 1985). Moringa coagulant lectin (cMoL) treated melanoma cells stained with Annexin V and PI, clearly indicated more population of PI-stained cells than Annexin stained cells. Moreover, the visible damages of cMoL on melanoma cells were the appearance of nuclear fragmentation and reduction in the cellular volume, chromosomal condensation and plasma membrane blebbing (de Andrade Luz et al. 2017). Similar observations were made in the *Sf*-9, S*f*-21 and J774a.1 cells treated with both GNA and β-BUTX Lqq1a/GNA, where treated cells were able to take up PI whereas control cells were able to metabolize the FDA. Initial membrane blebbing and DNA fragmentation were evident for the cells treated with both the recombinant protein. These experiments suggested the possible binding of GNA to the mannose residues present on the cell surface receptors, reducing or blocking the transport of essential nutrients across the membrane or induction of cascade of the signalling pathway, which lead to the production of ROS with associated DNA damage. The action of GNA and fusion protein on mouse cell line at lower dosage signifies the presence of mannose residues on the cellular surface, as confirmed by the high agglutinated population in the treatment than the untreated population. Reduction in the fusion protein dosage may be attributed to the presence of GNA binding mannose residues and putative voltage-gated sodium ion channel.

Cytotoxic activity may lead to oxidative damage of a cell, which in turn causes chromosomal DNA damage and ultimately affects the cell cycle progression (AshaRani et al. 2009). Gondim et al. (2017) demonstrated the activity of *Dioclea lasiocarpa* lectin (DlasiL) against A2780 ovarian cancer cell lines where it caused arrest in G2/M phase cell cycle. Another mannose-binding lectin from *Sophora flavescens* caused cell cycle arrest at G2/M phase and lead to caspase-dependent apoptosis of tumor cell (Liu et al. 2008). Recombinant GNA demonstrated significant G2 phase cell cycle arrest in treated *Sf*-9 and *Sf*-21 cells. Correspondingly, fusion protein treated *Sf*-9, and *Sf*-21 cells were also observed to be arrested in the G2/M phase of the cell cycle. These results are by other lectin mechanism of cell cycle arrest, suggesting the possible correlation between DNA damage and apoptosis mediated cell death.

Lectin induces programmed cell death by caspase-mediated apoptotic pathway (Kim et al. 1993). It's binding to the cell surface may produce the intracellular signals that may modulate the cell to express the proteins which are related to programmed cell death (Lichtenstein and Rabinovich 2013). *Moringa* lectin (cMoL) caused caspase 3 and 8 mediated cell death in B6-F10 cancerous cells where it has been postulated that binding of cMoL to glycans present on the cell surface triggered endocytosis by the cell and ultimate deregulation of homeostasis, which resulted in activation of caspase and ROS production (de Andrade Luz et al. 2017). Complexing of a high mannose-binding lectin from *S. flavescens* with cell surface receptors of HeLa cells triggered the recruitment of procaspase eight protein, resulted in caspase 8 activation (Liu et al. 2008). Caspase 2 expression may be attributed to stress-induced apoptosis, where it complexed with a cascade of other caspase-related proteins and induced cell death (Lopez-Cruzan et al. 2016, Tinel and Tschopp 2004). Similar findings were observed in the present study

where expression of Caspase 2 in GNA, as well as β-BUTX Lqq1a/GNA, treated insect cells suggest that both the proteins induced cell death by caspase-dependent manner. In the case of human tumor cell lines, more expression of survivin, which is an inhibitor of apoptosis, related protein correlated with reduced apoptosis (Garg et al. 2016). However, in the case of *Sf*-9 treated with GNA as well as β-BUTX Lqq1a-GNA appeared to overexpress survivin in the wake of stress. Contrarily, the expression of survivin in *Sf*-21 was lesser compared to *Sf*-9 cells. These results suggested that binding of lectin and fusion protein would trigger either the endocytosis mediated pathway where simultaneously inducing other caspase-dependent signalling molecules, ultimately led to the death of treated cells for biocontrol of insect pests.

4.4 Conclusion

Successfully purified GNA and fusion β-BUTX Lqq1a/GNA were adequately tested for the cytotoxic activity against insect as well as mouse cell lines. MTT assay resulted in a dose-dependent reduction of cell viability and fluorescence microscopy analysis also revealed the possible effects on a cell such as membrane damage, DNA fragmentation, and cell shrinkage. Cell cycle progression and the qRT-PCR report suggested the caspase-dependent death of GNA and β-BUTX Lqq1a/GNA treated insect cell lines. Insect bioassay with purified protein also resulted in significant mortality in treated larvae. Because of the higher potency of the fusion protein, when expressed in the proper host such as plants and entomopathogenic fungi, it could be a potential insecticidal candidate protein for biocontrol.

Table 4.1 List of primers used for GNA and β-BUTX Lqq1a/GNA fusion

Primer Name	5’----------3’
Bac-LqqIT1-RP-Linker OH	CGCTTCTTTAGCAGCCGCTTCAGCGTTAATGGTCACGAAATCGC
Bac-Linker FP-LqqIT1 OH	TATTGCGATTTCGTGACCATTAACGCTGAAGCGGCTGCTAAAGAAGCG
Bac-GNA RP-EcoRI OH	GCTTATTTAATTACCTGCAGGGAATTCTTAGTGGTGATGGTGATGGTGGTG

Table 4.2 List of Primers used for RT-qPCR analysis

Primer	5’----------3’
Sf-caspase-2-RT-F	TAGCAGCAATAATGGAGGACGC
Sf-caspase-2-RT-R	CTCGGTACTTGTGGTTGGTGTTG
Sf-caspase-5-RT-F	GATACTGGGACTTGGTGCGTGAT
Sf-caspase-5-RT-R	TGCGTGTTGTTTCTGTTGGGTT
Sf-IAP-RT-F	AAAACCGACAACCACGACACC
Sf-IAP-RT-R	CCCTCCACCCACCTCATAATCT
Sf-Survivin-RT-F	TTGGGCGGAGCACAAAAGC
Sf-Survivin-RT-R	GCACTGCCTTTGCCTTCTCATC
Sf-GAPDH-RT-F	TTGACGGACCCTCTGGAAAA
Sf-GAPDH-RT-R	ACGTTAGCAACGGGAACACG
Sf-AIF1-RT-F	CAAGCACTACACGCACCAGAG
Sf-AIF1-RT-R	CTGCCGAGAAGACACCCACT

GCT GAA GCG GCT GCT AAA GAA GCG GCG GCT AAA GAA GCG GCT GCT AAA GCGTCC TGC CTG AGC GAT AAC ATC CTG TAT TCC GGC GAA ACC CTG AGC ACC GGC GAG TTC CTG AAC TAC GGT AGC TTC GTT TTC ATC ATG CAA GAG GAC TGC AAC CTG GTG CTG TAC GAC GTT GAT AAG CCG ATT TGG GCC ACC AAC ACC GGC GGT CTG AGC CGT AGC TGC TTC CTG AGC ATG CAG ACC GAT GGC AAC CTG GTT GTC TAC AAC CCG AGC AAC AAG CCG ATC TGG GCG AGC AAC ACC GGC GGT CAG AAC GGT AAC TAC GTC TGC ATT CTG CAA AAG GAC CGT AAC GTG GTC ATT TAC GGC ACC GAC CGC TGG GCT ACC GGCCAC CACCAC CAT CAC CAT CAC CACTAA

Linker sequence

#GNA sequence

C-terminal His tag sequence

Stop codon

Fig. 4.1 Codon-optimized Linker GNA sequence to be expressed in a bacterium with CAI index of 0.88.

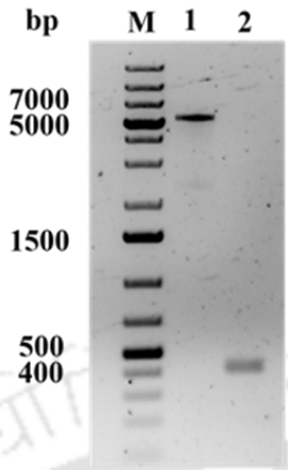

Fig. 4.2 Gel images of pET28a and Linker GNA cloning and its confirmation by PCR. A) pET28a and Linker GNA cloning Lane 1: pET28a expression vector (5369 bp), Lane 2: Linker GNA DNA sequence (417 bp) and M- O GeneRuler 1 Kb plus DNA ladder (Fermentas, USA). Both the vector and gene sequence was digested with NdeI and EcoRI restriction enzymes overnight at 37ºC. Gel purified fragments were analyzed on 0.8% agarose gel electrophoresis.

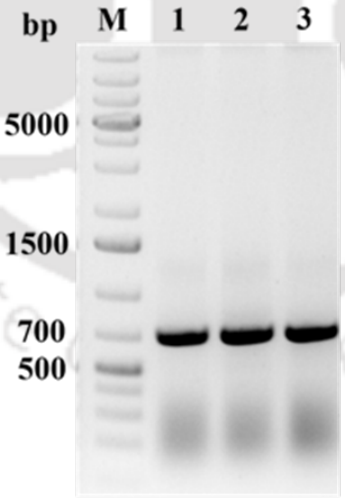

Fig. 4.3 Agarose gel electrophoresis analysis of pET28a-Linker GNA clone confirmation by PCR. Linker GNA amplified using pET FP and T7 RP. Lane 1-3 are the Linker GNA amplified sequence (Calculated Size 688 bp) and M: O GeneRuler 1 Kb plus DNA ladder (Fermentas, USA).

AAG AAA AAC GGT TAT GCG GTG GAC AGC AGC GGC AAG GCG CCG GAG

TGC CTG CTG AGC AAC TAC TGC TAT AAC GAA TGC ACC AAG GTT CAC

TAC GCG GAT AAA GGT TAT TGC TGC CTG CTG AGC TGC TAC TGC GTG

GGC CTG AGC GAC GAT AAG AAA GTT CTG GAG ATC AGC GAC GCG CGT

AAG AAA TAT TGC GAT TTC GTG ACC ATT AACGCT GAA GCG GCT GCT

AAA GAA GCG GCG GCT AAA GAA GCG GCT GCT AAA GCGTCC TGC CTG

AGC GAT AAC ATC CTG TAT TCC GGC GAA ACC CTG AGC ACC GGC GAG

TTC CTG AAC TAC GGT AGC TTC GTT TTC ATC ATG CAA GAG GAC TGC

AAC CTG GTG CTG TAC GAC GTT GAT AAG CCG ATT TGG GCC ACC AAC

ACC GGC GGT CTG AGC CGT AGC TGC TTC CTG AGC ATG CAG ACC GAT

GGC AAC CTG GTT GTC TAC AAC CCG AGC AAC AAG CCG ATC TGG GCG

AGC AAC ACC GGC GGT CAG AAC GGT AAC TAC GTC TGC ATT CTG CAA

AAG GAC CGT AAC GTG GTC ATT TAC GGC ACC GAC CGC TGG GCT ACC

GGCCAC CACCAC CAT CAC CAT CAC CACTAA

β-BUTX Lqq1a sequence

Linker sequence

#GNA sequence

C-terminal His tag sequence

Stop codon

Fig. 4.4 Bacterial codon optimized fused β-BUTX Lqq1a and Linker GNA sequence with C-terminal His tag and stop codon

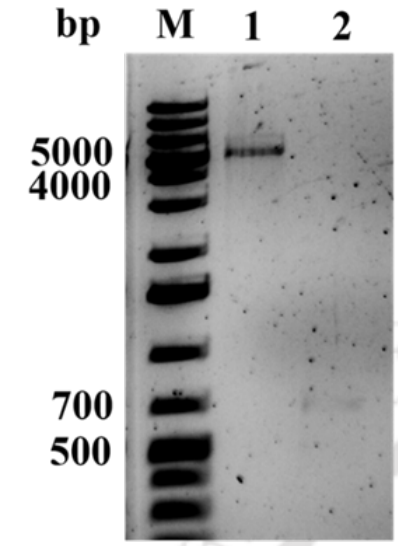

Fig. 4.5 Agarose gel images of pET28a and β-BUTX Lqq1a/Linker GNA cloning and its confirmation by PCR. The pET28a and β-BUTX Lqq1a/Linker GNA cloning Lane 1: pET28a expression vector (5369 bp), Lane 2: Fused β-BUTX Lqq1a/Linker GNA DNA sequence (650 bp) and Lane M: O GeneRuler 1 Kb plus DNA ladder (Fermentas, USA). Both the vector and gene sequence was digested with NdeI and EcoRI restriction enzymes overnight at 37ºC. Gel purified fragments were analysed on 0.8% agarose gel electrophoresis

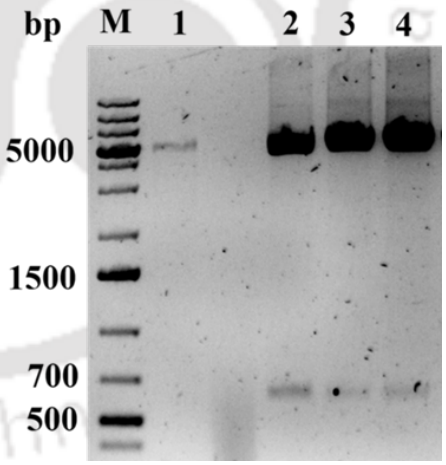

Fig. 4.6 Agarose gel electrophoresis analysis of pET28a-BUTX Lqq1a/GNA clone confirmation by double digestion method. Lane 1: Linearized empty pET28a vector (5369 bp), Lane 2-4: pET28a-BUTX Lqq1a/GNA digested with NdeI and EcoRI restriction enzymes (5369 bp+650 bp) and Lane M: O GeneRuler 1 Kb plus DNA ladder (Fermentas, USA).

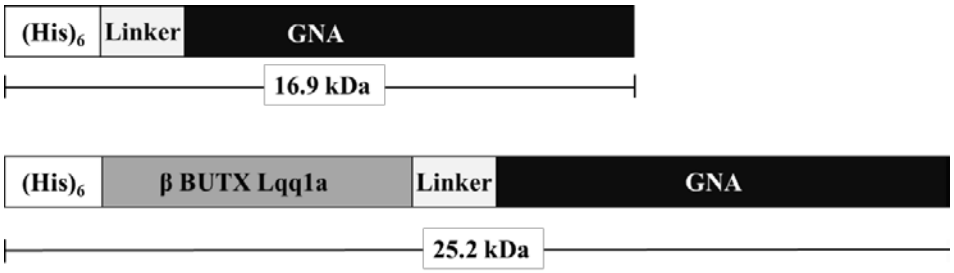

Fig. 4.7 Schematic representation of GNA and fusion protein β-BUTX Lqq1a/GNA with N-terminal $(His)_6$ – tag.

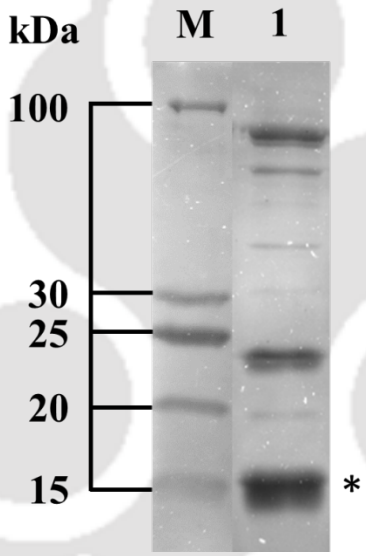

Fig. 4.8 The SDS-PAGE analysis of Ni-NTA affinity purified Linker GNA protein. Linker GNA protein expression was successfully optimized in TB medium supplemented with 1% glycerol with 0.5 mM Isopropyl thiogalactopyranoside at 16ºC for 16 hr at 200 rpm in refrigerated shaking incubator and subsequently purified using Ni-NTA affinity chromatography. Initial affinity purified fractions were analyzed in 16% Tris-Glycine buffer based SDS-PAGE gel electrophoresis. M-protein marker low range from Thermofisher scientific. **Linker GNA protein size is approximately 16.9 kDa.**

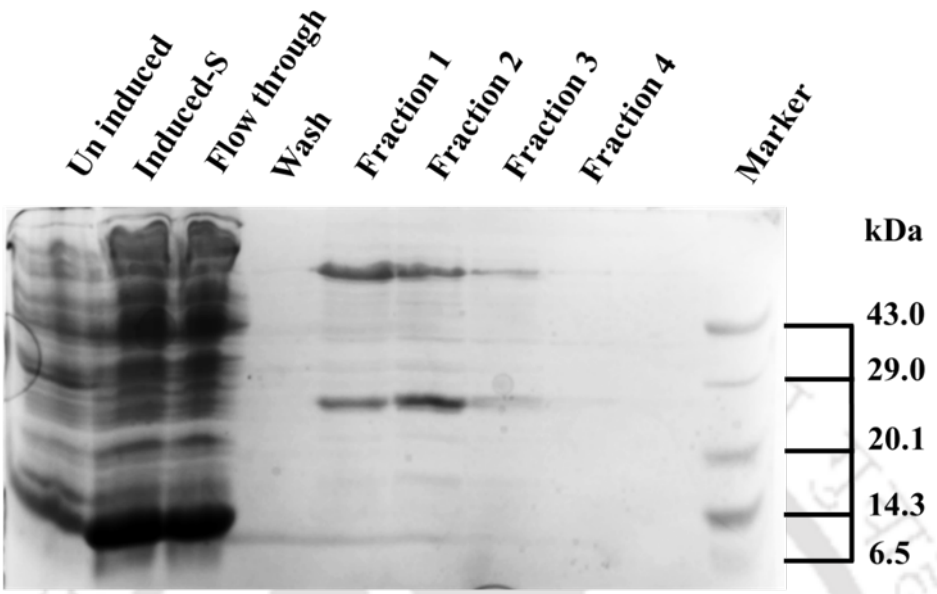

Fig. 4.9 The SDS-PAGE analysis of Ni-NTA purified β-BUTX Lqq1a /Linker GNA protein. β-BUTX Lqq1a/Linker GNA protein expression was successfully optimized in TB medium supplemented with 1% glycerol with 0.5 mM IPTG at 16ºC for 16 hr at 200 rpm in refrigerated shaking incubator and subsequently purified using Ni-NTA affinity chromatography. Initial affinity purified fractions were analyzed in 16% Tris-Glycine buffer based SDS-PAGE gel electrophoresis. M-protein marker low range from Thermofisher scientific. β-BUTX Lqq1a /Linker GNA protein size is approximately 25.2 kDa.

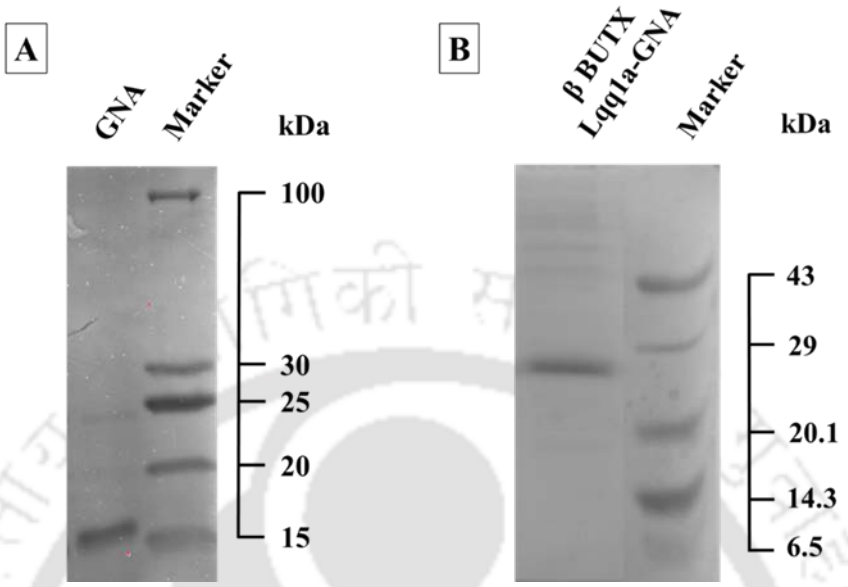

Fig. 4.10 SDS-PAGE (16% Acrylamide gel in Tris-Glycine buffer) analysis of purified recombinant GNA. A) Recombinant GNA purified using Ni-NTA affinity chromatography. Lane 1 is GNA, size approximately 16.9 kDa protein. Lane 2 is a low range molecular weight marker. B) Recombinant fusion protein β-BUTX Lqq1a/GNA purified using affinity chromatography. Lane 1: fusion protein containing β-BUTX Lqq1a and GNA predicted theoretical molecular weight is approximately 25.2 kDa.

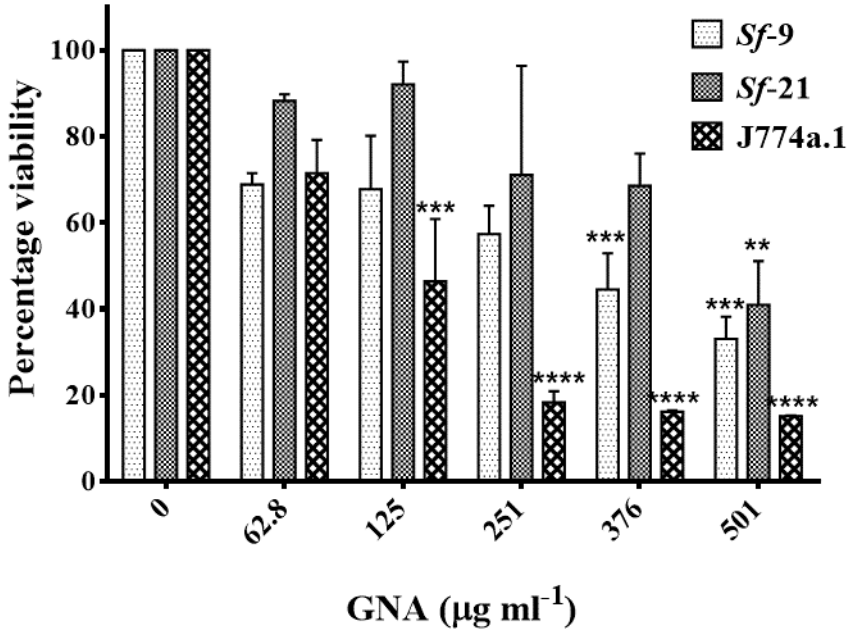

Fig. 4.11 Cytotoxicity assay on the various concentration of recombinant purified GNA on the viability of *Sf*-9, *Sf*-21 insect cell lines, and J774a.1 mouse cell lines as determined by MTT assay. One-way ANOVA, followed by Dunnett's pairwise multiple comparison analysis, indicated that GNA had affected cell proliferation in a dose-dependent manner ($p < 0.0001$) when compared to control. Asterisks indicate the results that were significantly different from the control. **, $p< 0.01$, ***, $p = 0.0001$ and ****, $p< 0.0001$. All data are the average of two independent experiments with three replications for each along with standard deviation (±SD).

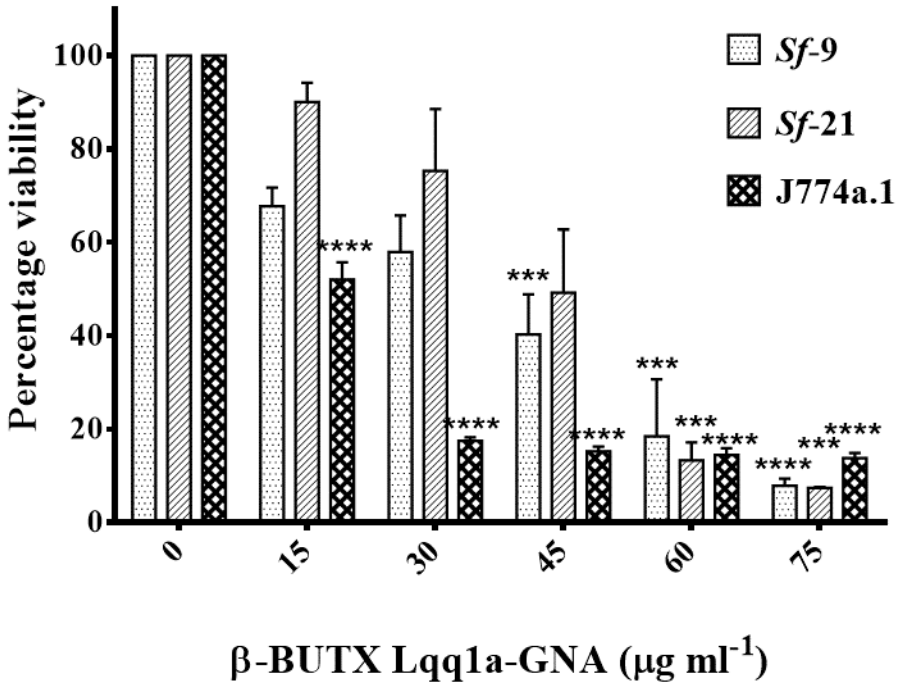

Fig. 4.12 Cell viability assay with various concentration of recombinant purified β-BUTX Lqq1a/GNA on the viability of *Sf*-9, *Sf*-21 insect cell lines, and J774a.1 mouse cell lines as determined by MTT assay. One-way ANOVA, followed by Dunnett's pairwise multiple comparison analysis, indicated that β-BUTX Lqq1a/GNA had affected cell proliferation in a dose-dependent manner ($p < 0.0001$) when compared with control. Asterisks indicate the results that were significantly different from the control. ***, $p = 0.0001$ and ****, $p < 0.0001$. All data are the average of two independent experiments with three replications for each along with standard deviation (±SD).

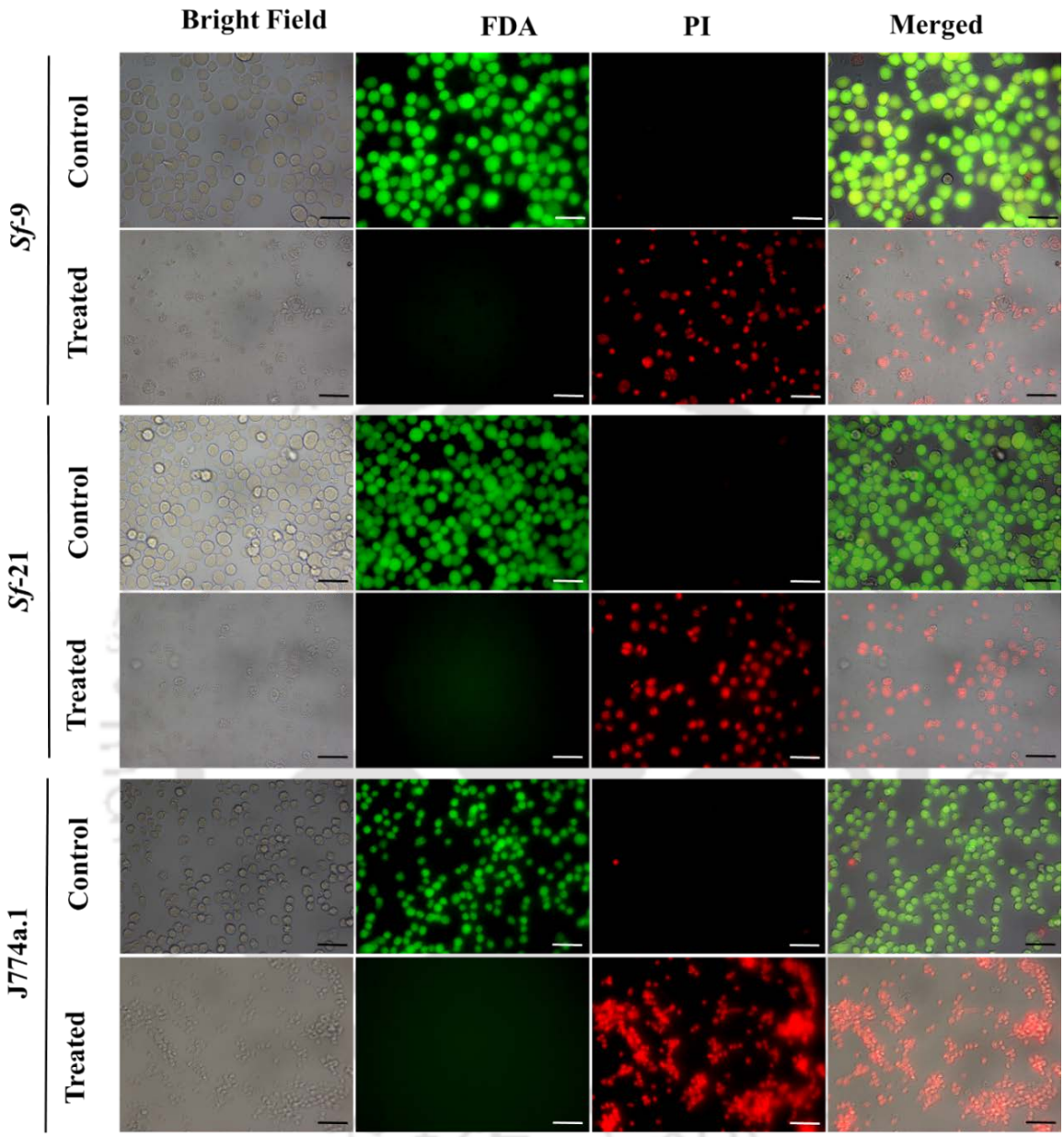

Fig. 4.13 Fluorescence microscopy analysis of recombinant GNA treated *Sf*-9, *Sf*-21, and J774a.1 cell lines stained with FDA and PI. Images were representative of two independent experiments. The bar represents 50 µM.

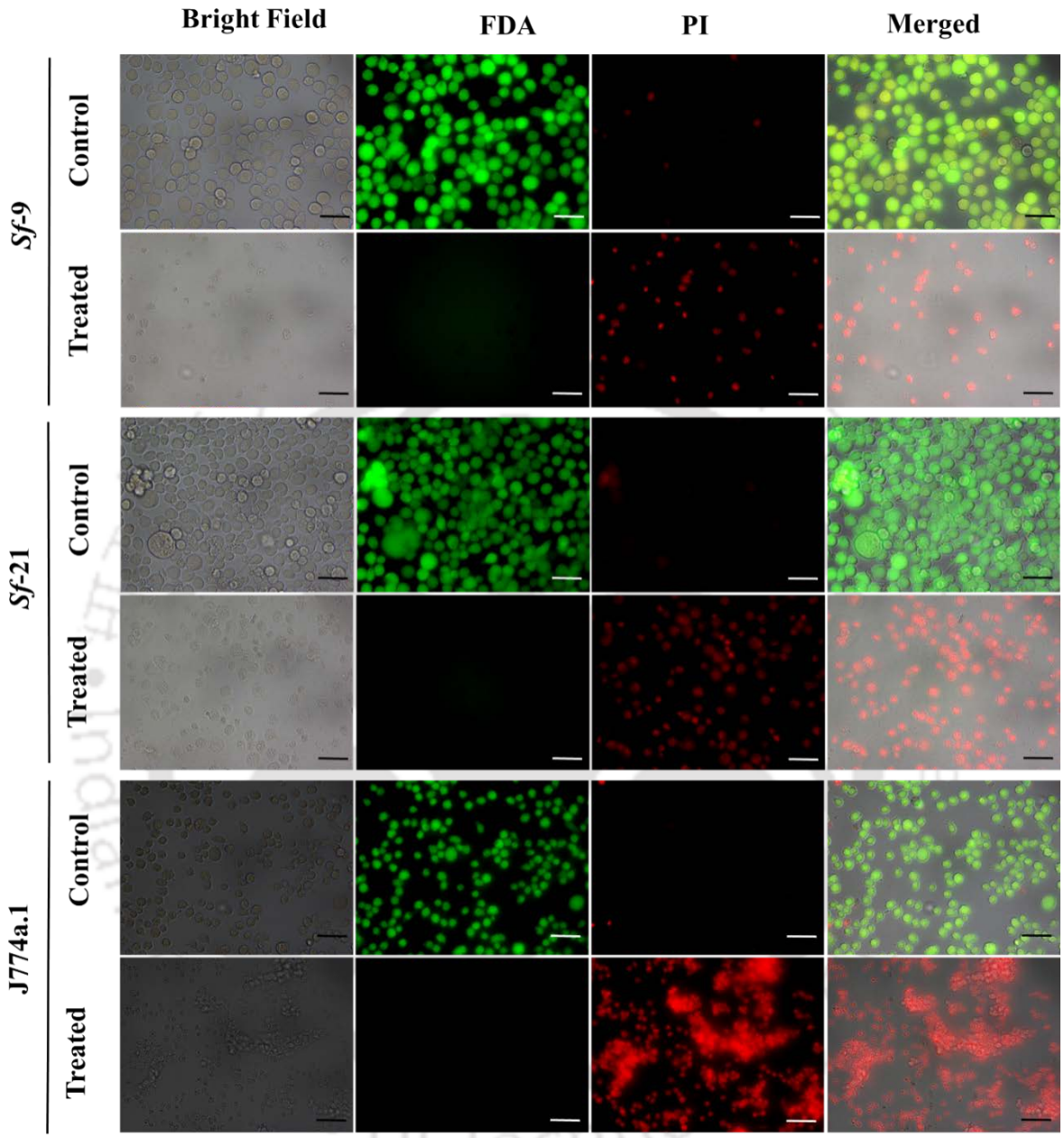

Fig. 4.14 Fluorescence microscopy analysis of recombinant β-BUTX Lqq1a/GNA treated *Sf*-9, *Sf*-21, and J774a.1 cell lines stained with FDA and PI. Images were representative of two independent experiments. The bar represents 50 µM.

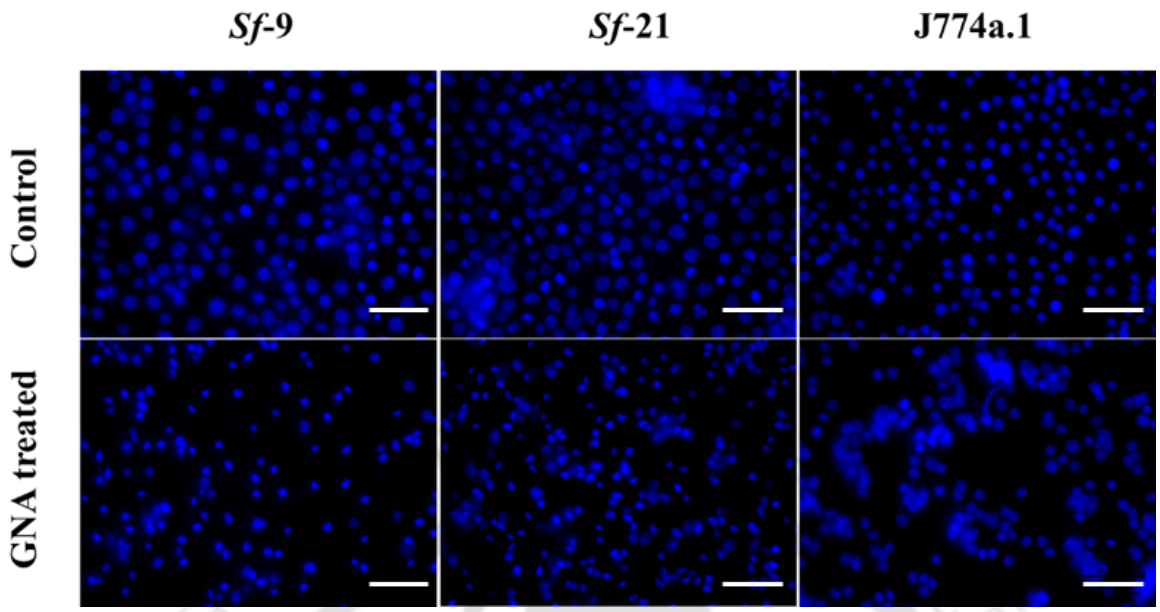

Fig. 4.15 Fluorescence microscopy analysis of recombinant GNA treated *Sf*-9, *Sf*-21 and J774a.1 cell lines stained with DAPI. Images were representative of two independent experiments. The scale bar represents 50 µM.

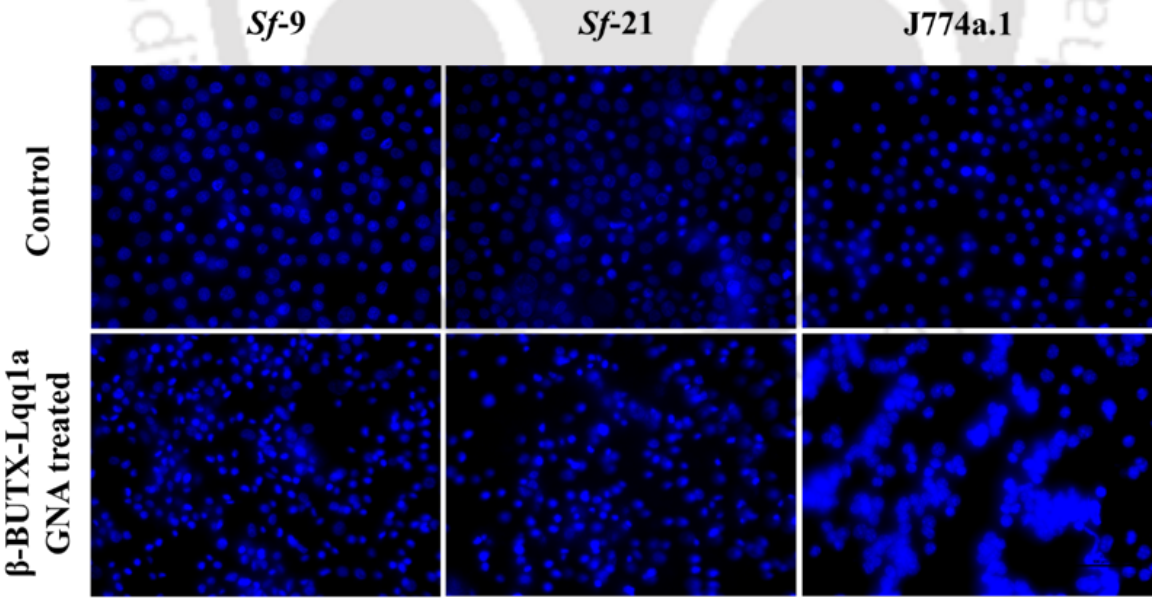

Fig. 4.16 Fluorescence microscopy analysis of recombinant β-BUTX Lqq1a/GNA treated *Sf*-9, *Sf*-21 and J774a.1 cell lines stained with DAPI. Images were representative of two independent experiments. The scale bar represents 50 µM.

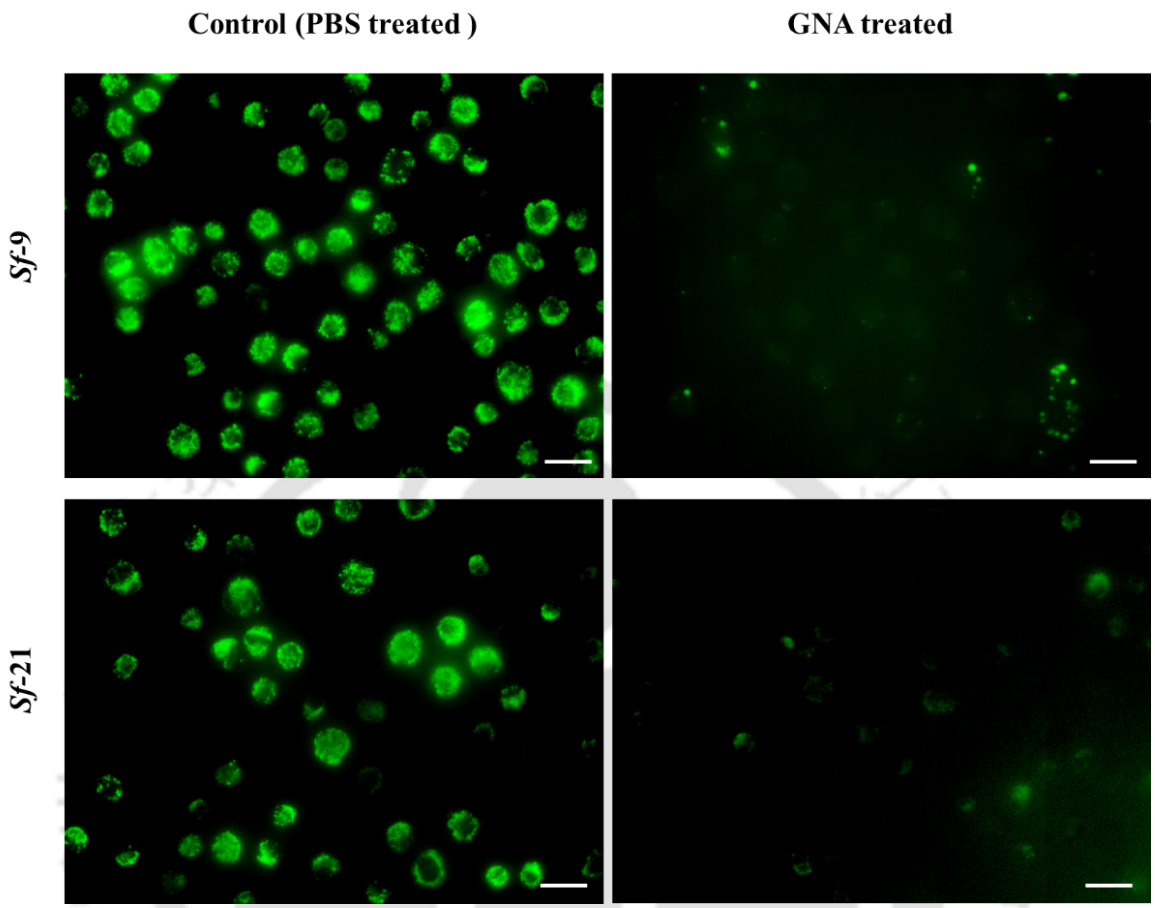

Fig. 4.17 Mitochondrial membrane potential assay of recombinant GNA treated *Sf*-9, and *Sf*-21 insect cell lines. Images were representative of two independent experiments. The scale bar represents 50 µM.

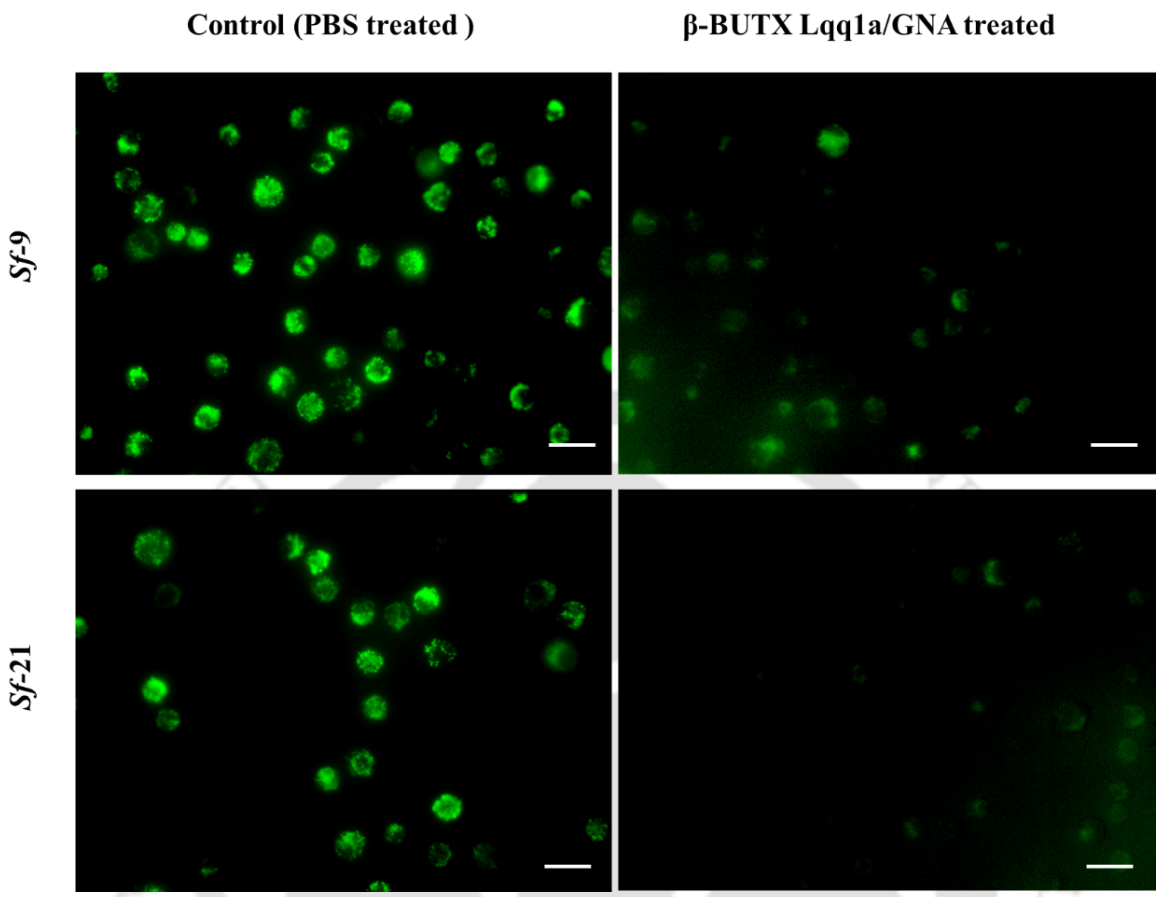

Fig. 4.18 Mitochondrial membrane potential assay of recombinant β-BUTX Lqq1a/GNA treated *Sf*-9, and *Sf*-21 insect cell lines. Images were representative of two independent experiments. The scale bar represents 50 µM.

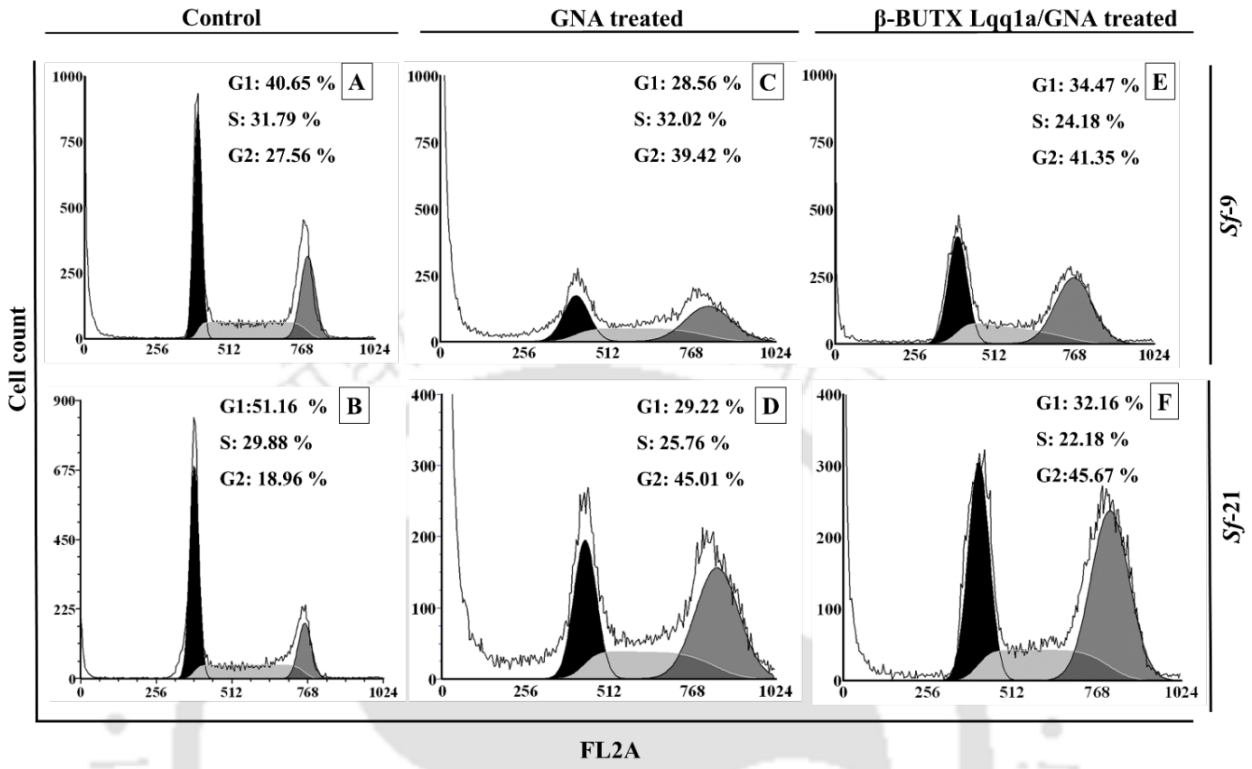

Fig. 4.19 Cell cycle analysis of GNA and β-BUTX Lqq1a/GNA treated *Sf*-9 and *Sf*-21 insect cell lines. A) *Sf*-9, B) *Sf*-21 Control cells, C) *Sf*-9, D) *Sf*-21 cells treated with GNA and E) *Sf*-9, F) *Sf*-21 cells treated with β-BUTX Lqq1a/GNA fusion protein. Data represent the average of two independent experiments.

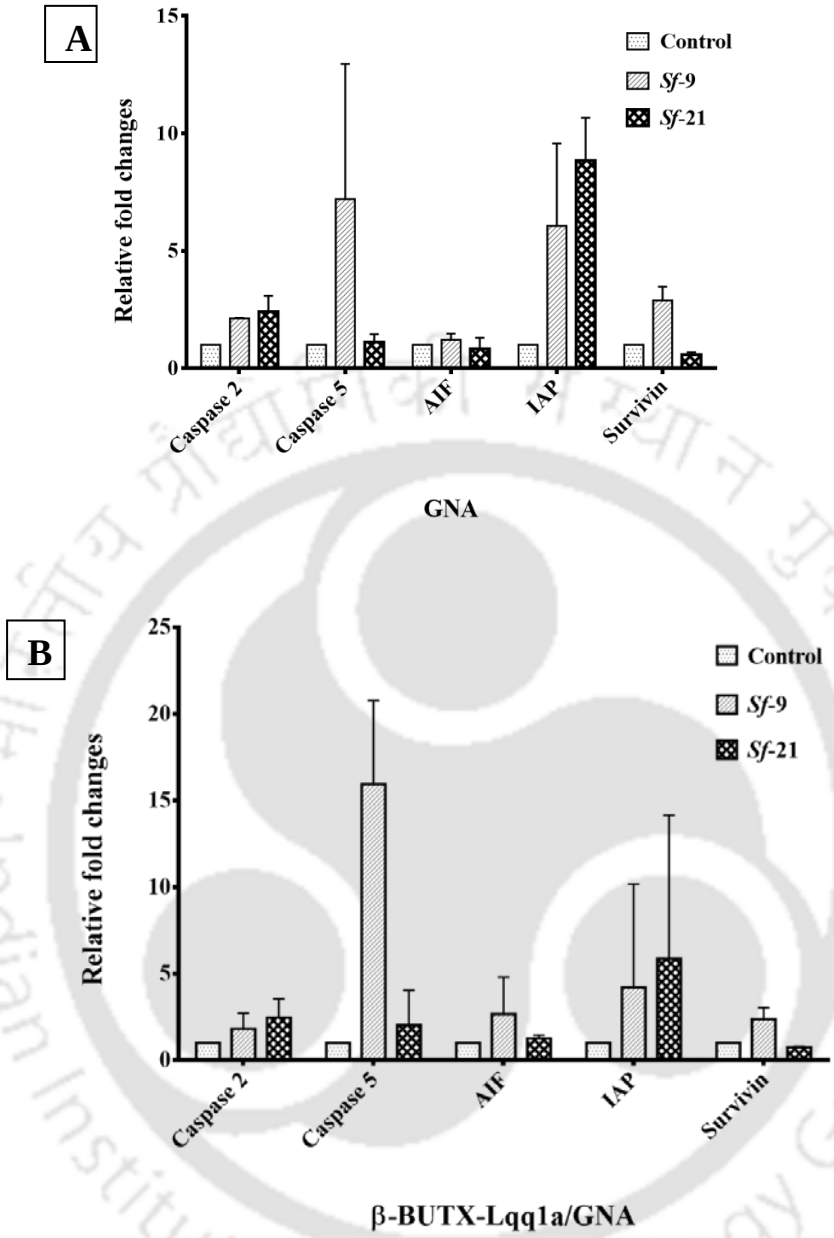

Fig. 4.20 RT-qPCR based gene expressional analysis of treated insect cell lines. **A**) Represents *Sf*-9 and *Sf*-21 cells treated with recombinant GNA. **B**) Graphical representation of *Sf*-9 and *Sf*-21 cells treated with recombinant β-BUTX Lqq1a/GNA fusion protein. Data represent two independent experiments with three replications, each with a mean± standard deviation.

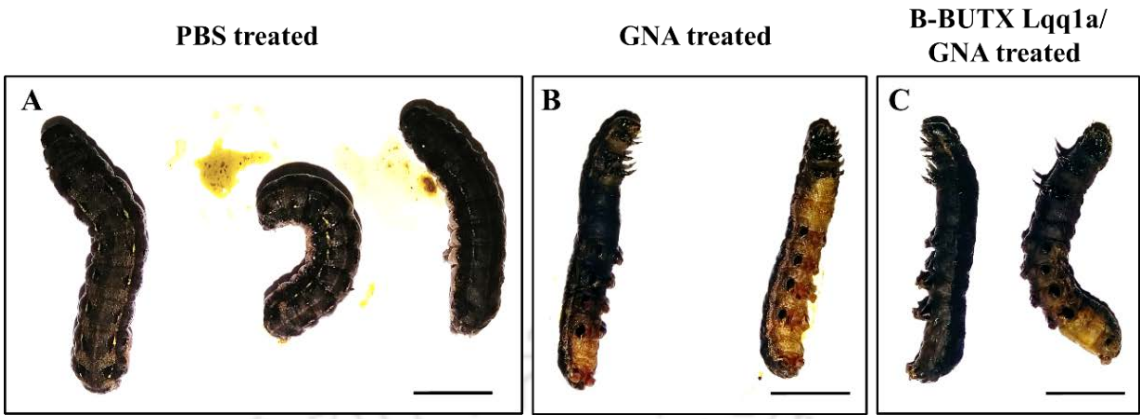

Fig. 4.21 Injection bioassay performed with purified recombinant proteins in *S. litura*. A) Only PBS buffer used for injecting the control population. B) Represents GNA treated larvae and C) indicates the β-BUTX Lqq1a/GNA toxin treated *S. litura* larvae. The scale bar represents 1 cm in length.

CHAPTER 5

Cloning and expression of β-BUTX Lqq1a, Cyt1Aa and truncated Cry1Ac/GNA in *Metarhizium anisopliae* and insect toxicity assay

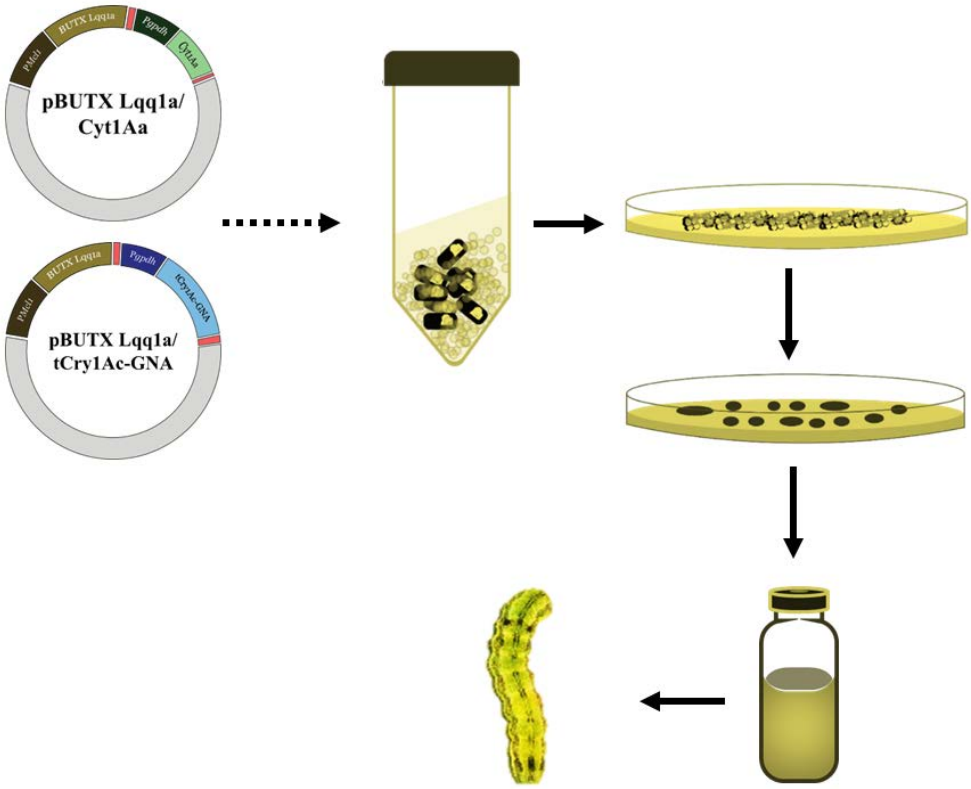

5.1 Introduction

Bacillus thuringiensis is a Gram-positive soil bacterium and produces para-sporal inclusion bodies during sporulation. This inclusion contains Crystalline (Cry) toxins called δ-endotoxins, and Cytolytic (Cyt) toxins. Besides this toxin, other Vegetative insecticidal proteins (Vip) are also produced during the vegetative stage of the bacterial growth (Lee et al. 2006). These Cry and Cyt toxins gained momentum across the scientific community because of its specific insecticidal activity against various agriculturally important insect pests. Among the Cry toxins, Cry1Ac is the most widely expressed protein in broader crops against major economically important pests such as *Trichoplusia ni*, *Helicoverpa armigera*, *H. zea*, *Heliothis viresens*, and *Spodoptera litura* and one of the advantages is that they do not harm the non-target organisms (Ba et al. 2018, Hernandez and Ferre 2005, Marques et al. 2018, Rukarwa et al. 2014, Tian et al. 2018, Wang et al. 2019, Xing et al. 2019, Yu et al. 2014, Zhang et al. 2019).

Primarily, crystalline protoxin is solubilized in the insect mid-gut protease environment releasing the active toxin. This active toxin then binds to a series of mid-gut membrane receptors, forming functional oligomeric structure which then perforates the mid-gut epithelial layer, causing osmotic lysis and ultimate death of the insect. Receptors reported to be involved in the Cry1Ac binding are alkaline phosphatase (ALP), aminopeptidase N (APN), cadherin (CAD) and ABC transporters (Ocelotl et al. 2017, Qiu et al. 2017, Qiu et al. 2015, Ren et al. 2016, Wang et al. 2016, Wei et al. 2016, Zhang et al. 2019). Reduced binding, reduced expression, reduced toxin activation and mutations in the receptor binding site reported to cause the development of resistance in various insect species (Fabrick et al. 2019, Jakka et al. 2015, Nakaishi et al. 2018, Zhang et al. 2019). Indirect modulation by transcriptional factors and signalling mechanisms alter the

expression of mid-gut receptors and thus susceptibility and resistance to Cry toxins (Guo et al. 2015, Mi et al. 2017). Modification in the protoxin and binding improves the insect susceptibility to Cry toxins. In a subsequent interaction with mid-gut cadherin receptors, N-terminal region of the Cry toxin is involved in oligomeric structure formation. Other receptors such as GPI-anchored ALP and APN is necessary for the oligomer membrane insertion. Modification of Cry toxins by removing N-terminal helix α-1 improved the susceptibility of Cadherin mediated resistant insects toward Cry toxins (García-Gómez et al. 2013, Gómez et al. 2015, Munoz-Garay et al. 2010, Soberon et al. 2007).

Unlike Cry, Cyt toxins act directly on the insect mid-gut lipid membrane, not requiring of binding with receptors sequentially, causing increased water influx and cell swelling. This Cyt1Aa produced by *B. thuringiensis* subsp. *israelensis* (Bti) acts specifically against Dipteran insect species. Cyt1Aa toxin acts as a receptor for Cry toxins, which further enhances toxin oligomerization and pore formation. Synergistic interaction with other Cry toxin such as Cry1Ac, Cry2Aa, Cry3Aa, Cry4a, Cry10a, and Cry11A increases the susceptibility of single toxin-resistant insects (Bideshi et al. 2013, Elleuch et al. 2015, Federici and Bauer 1998, Perez et al. 2007, Sayyed et al. 2001, Wirth et al. 2005). The Modified Cyt1Aa hybrid toxins, which carry domain II loop 3 part from Cry1Ab increases the specificity of Cyt1Aa to Lepidopteran insects (Torres-Quintero et al. 2018). Delayed resistance, lack of receptors, and synergistic effect with other Cry toxins offer Cyt1Aa as a potential candidature protein in insect pest management.

Modification in the protoxin activation, mid-gut enzyme-mediated processing, receptor binding, oligomer formation could potentially improve the susceptibility of resistant insects toward Bt Cry toxins. Modification of Cry1Ab and Cry1Ac toxin binding site in cadherin receptor by removing the N-terminal and α-1 helix of domain I, enhanced

the toxicity against *Manduca sexta* (Munoz-Garay et al. 2010, Soberon et al. 2007). Apart from deletions, domain swapping is becoming an essential approach in countering insect resistance and enhancing the toxicity (Bosch et al. 1994). Hybrid toxin constructed by fusing Cry1Ab domain I and II with Cry1C domain III resulted in magnified toxicity than the wild type toxin (de Maagd et al. 2000). Similar domain swapping studies with Cry1Ia (I, II) and Cry1Ba (III), as well as Cry3Aa (I, II) and Cry1Ab (III) improved the hybrid Cry proteins toxicity against various pests (Hibbard et al. 2011, Naimov et al. 2001, Walters et al. 2010). In the three-domain Cry1Ac toxin, domain III is a δ-endotoxin C which contains carbohydrate binding module (CBM) 6, CBM35 and CBM36 like sites. These modules are non-catalytic, usually associated with catalytic glycoside hydrolase domain (Madej et al. 2014). Replacement of domain III of Cry1Ac with *Allium sativum* carbohydrate-binding lectin module (ASAL) enhanced the toxic effect of the fusion protein against Lepidopteran and Hemipteran insects (Boddupally et al. 2018).

The carbohydrate binding lectins present in the plant are primarily produced during the herbivore attack. *Galanthus nivalis* (Snowdrop plant) synthesize a 52 kDa tetrameric protein present in a higher amount within bulbs, that bind specifically to α-D mannose sugar residues. Red blood cells agglutinated readily by incubating with the GNA but not human red blood cells (Vandamme et al. 1987). This GNA when delivered orally, it has been proven toxic to many Lepidopteran, Dipteran, Homopteran and Hymenopteran insects (Bell et al. 1999, Li and Romeis 2009, Nagadhara et al. 2004, Ripoll et al. 2003, Wang et al. 2005). Functional expression of GNA in rice and wheat caused antifeedant activity in brown planthopper *Nilaparvata lugens* and reduction in the fecundity of grain aphids (Powell et al. 1995, Stoger et al. 1999). In addition to the insecticidal property,

GNA also helps in delivering the protein across the mid-gut peritrophic matrix to hemolymph of insects (Fitches et al. 2002, Fitches et al. 2004, Fitches et al. 2001).

The present study reports the fusion of GNA with the truncated Cry1Ac and cloning and expression in *M. anisopliae* along with β-BUTX Lqq1a neurotoxic peptide. In addition, Cyt1Aa along with β-BUTX Lqq1a was also fused and expressed in *M. anisopliae*. *M. anisopliae* expressing these pyramided toxins were further tested for its effect on agricultural insect pests.

5.2 Materials and Methods

5.2.1 Microbial strains and Culture conditions

For bacterial cloning and maintenance of plasmids, *Escherichia coli* DH5-α cells were used and maintained in Luria Bertani (LB) medium at 37ºC. *Agrobacterium tumifaciens* EHA 105 strain was grown and maintained in LB medium supplemented with Rifampicin (10 µg ml^{-1}). *M. anisopliae* (MTCC 892) culture was procured from Microbial Type Culture Collection and Gene Bank (MTCC, India) and maintained in Potato Dextrose Agar at 28±2ºC.

5.2.2 Cyt1Aa expression vector construction

5.2.2.1 Cyt1Aa amplification

Bacillus thuringiensis subsp. *israelensis* strain was procured from Bacillus Genetic Stock Centre (BGSC-4Q1), Ohio State University, Columbus, USA and maintained in Nutrient Agar at 30ºC. For amplification of Cyt1Aa, gene-specific primers (**Table 5.1**) were designed (Integrated DNA Technologies, Malaysia) based on the reference sequence number obtained from NCBI: LC128536.1. Reaction components such as Phusion Polymerase and dNTPs were purchased from ThermoFisher, USA and New England Biolabs, USA respectively.

The total DNA was extracted by mixing small loop full of culture in sterile MilliQ water and boiled for 5 min at 98ºC and further clarified by centrifuging at 13,000 rpm for 5 min. The clarified supernatant was used as template for Cyt1Aa amplification with following reaction conditions step 1: Initial denaturation 98ºC for 3 min, step 2: Denaturation 98ºC for 15 sec, step 3: Annealing 60ºC for 45 sec, step 4: Extension 72ºC for 1 min and step 5: Final extension 72ºC for 10 min. After the Cyt1Aa amplification, PCR products were separated on 1% Agarose gel electrophoresis system (Amersham,

USA) and extracted using Takara Bio gel purification kit by following manufacturer protocol. Finally, purified fragments were analyzed on 1% Agarose gel electrophoresis and quantified using NanoPhotometer (Implen, USA).

5.2.2.2 GPDH promoter (P*gpdh*) amplification

5.2.2.2.1 *M. anisopliae* genomic DNA isolation

Initially, *M. anisopliae* genomic DNA was isolated using the following modified protocol. *M. anisopliae* spores (1×10^7 ml^{-1}) was inoculated in 20 ml of Potato Dextrose broth (PDB, pH 5.6±0.2), and incubated at 27ºC for 48 hr in a rotatory incubator shaker. Post incubation, mycelial biomass was harvested by centrifugation at 5,000 rpm for 10 min at 4ºC. Mycelial biomass (500 mg) was homogenized with ice-cold pestle and mortar added with DNA extraction buffer (Tris-Cl 40 mM, NaCl 150 mM, Ethylene Diamine Tetra Acetic acid (EDTA) 2 mM). After the thorough homogenization, 200 µl of 20% SDS was added with brief vortex for 30 s and incubated for 1-2 hr at 60ºC. Post incubation, 150 µl of 6M NaCl and 200 µl of Phenol: Chloroform: Isoamyl alcohol (25:24:1) was added and thoroughly mixed extracts were further clarified by centrifugation at 13,000 rpm for 30 min at 25ºC. The clarified supernatant was further treated with RNase A (20 mg ml^{-1}) and Proteinase K (1 mg ml^{-1}) at 37ºC for 1 hr. Final removal of proteins and other debris was performed by adding 200 µl of chloroform and centrifuged at 13,000 rpm for 15-30 min. To the clarified supernatant, an equal volume of ice-cold isopropanol was added and incubated at -20ºC for 30 min. Precipitated DNA was washed once with 70% Ethanol, and air dried DNA was finally dissolved in nuclease-free water (Ambion, Invitrogen, USA). DNA quality and quantity were analyzed by using 0.8% Agarose Gel electrophoresis and NanoPhotometer, respectively.

5.2.2.2.2 P*gpdh* amplification

The promoter *gpdh*, promoter-specific primers were designed (IDT, Malaysia) with Cyt1Aa and pCAMBIA3300 vector overhangs (**Table 5.1**). Genomic DNA isolated from *M. anisopliae* was used as a template. Following reaction conditions were set up to amplify the P*gpdh* using Phusion polymerase, step 1: Initial denaturation 98ºC for 3 min, step 2: Denaturation 98ºC for 15 sec, step 3: Annealing 60ºC for 45 sec, step 4: Extension 72ºC for 1 min and step 5: Final extension 72ºC for 10 min. Post-amplification, P*gpdh* PCR products were separated in 1% Agarose gel electrophoresis system (Amersham, USA) and extracted using Takara Bio gel purification kit by following manufacturer protocol. Finally, the DNA fragments were analyzed again on 1% Agarose gel electrophoresis and quantified using NanoPhotometer (Implen, USA).

5.2.2.3 GPDH promoter (P*gpdh*) fusion with Cyt1Aa

Metarhizium collagen-like protein signal peptide (Mcl1sp) sequence was fused upstream of Cyt1Aa to secrete the Cyt1Aa outside the cell and placed downstream of P*gpgh*. Apart from Cyt1Aa and gpdh promoter, Mcl1sp was also amplified from the genomic DNA of *M. anisopliae* using primer designed (**Table 5.1**) with overhangs for Cyt1Aa and *gpdh* promoter region. Initially, Cyt1Aa was fused with Mcl1sp using overlap extension PCR and gel purified. This fused gel purified fragment was then fused with P*gpdh* using the overlap extension PCR (annealing temperature: 62ºC). P*gpdh*-Mcl1sp-Cyt1Aa fragment was finally gel purified and quantified using NanoPhotometer.

5.2.2.4 P*gpdh*-Mcl1sp-Cyt1Aa cloning in pMcl1-BUTX-Lqq1a vector

Initially, pMcl1-BUTX-Lqq1a vector was digested with BamHI and HindIII restriction enzymes at 37ºC for 3-4 hr and gel extracted using Takara gel purification kit. Both P*gpdh*-Mcl1sp-Cyt1Aa and double digested pMcl1-BUTX-Lqq1a was taken in

equal molar concentration and mixed with homemade Gibson assembly master mix, and the reaction was performed at 50ºC for 45-60 min. Following Gibson assembly reaction, 5 µl of the reaction was used to transfer into the chemically competent *E. coli* cells and selection was carried out in LB medium supplemented with 50 µg ml^{-1} kanamycin antibiotic and incubated at 37ºC. Putative transformants were selected and confirmed using colony PCR. For colony PCR, loop full of cultures were used as a template for amplification. Also, putative transformants were grown in 5 ml of liquid LB medium supplemented with 50 µg ml^{-1} kanamycin and plasmids were isolated using TakaraBio plasmid isolation kit. Restriction enzyme confirmation was done for the plasmid DNA (**pBUTX-Lqq1a/Cyt1Aa**) isolated from putative transformants. Both colony PCR products and digested plasmids were separated on 1% Agarose Gel electrophoresis, and images were taken using Bio-rad Gel Doc™ XR gel documentation system.

5.2.3 Truncated Cry1Ac-GNA expression vector construction

5.2.3.1 Cry1Ac truncation

The *B. thuringiensis* subsp. *kurstaki* HD73 (4D1) was procured from BGSC, Columbus, USA, and maintained in Nutrient agar medium. Loopful of a bacterial culture grown for two days was used to isolate total DNA by boiling at 98ºC for 5 min in nuclease-free water. Cellular debris was removed by centrifuging boiled culture at 12,000 rpm for 15-30 min. The clarified supernatant was used as a source for Cry1Ac amplification. Based on the bioinformatics analysis, the Cry1Ac sequence was retrieved from NCBI GenBank with the following accession number: NC_020249.1, which corresponds to the Cry1Ac gene located in the plasmid pH73 of *B. thuringiensis* ssp. *kurstaki* str. HD73 (4D1). From the conserved domain structure study, primers were designed with vector and GNA overhangs to amplify the Endotoxin-N and -M domain

excluding the 141 bp from the Endotoxin-N as well as the whole Endotoxin-C domain (**Table 5.2**). Truncated Cry1Ac (tCry1Ac) amplification reaction conditions were step 1: Initial denaturation 98ºC for 4 min, step 2: Denaturation 98ºC for 15 sec, step 3: Annealing 60ºC for 45 sec, step 4: Extension 72ºC for 1.5 min and step 5: Final extension 72ºC for 10 min. Post-amplification, tCry1Ac PCR products were separated in 1% Agarose gel electrophoresis system (Amersham, USA) and extracted using Takara Bio gel purification kit by following manufacturer protocol. Finally, fragments were analyzed again in 1% Agarose gel electrophoresis and quantified using NanoPhotometer (Implen, USA).

5.2.3.2 GNA amplification

The protein sequence of GNA lectin was retrieved from Longstaff et al., (1998) and then reverse translated into DNA sequence using (EMBL)-EMBOSS Backtranseq software (Rice et al. 2000). The reverse translated DNA was further codon-optimized for fungal expression. Then codon optimized DNA was chemically synthesized and cloned in pUC57 vector flanking NdeI and EcoRI restriction sites (Genscript, USA) and used as a template for GNA amplification with primers (**Table 5.2**) designed with Cry1Ac and vector over-hangs. GNA was amplified with the following reaction conditions, step 1: Initial denaturation 98ºC for 4 min, step 2: Denaturation 98ºC for 15 sec, step 3: Annealing 60ºC for 45 sec, step 4: Extension 72ºC for 1.5 min and step 5: Final extension 72ºC for 10 min. Post-amplification, GNA PCR products were separated in 1% Agarose gel electrophoresis system (Amersham, USA) and extracted using Takara Bio gel purification kit by following manufacturer protocol. Finally, PCR fragments were analyzed again on 1% Agarose gel electrophoresis and quantified using NanoPhotometer (Implen, USA).

5.2.3.3 P*gpdh*-Mcl1sp-tCry1Ac/GNA fusion

To fuse all four fragments overlap extension PCR was performed with fragments bearing extension of one another gene fragment either at 3' or 5' end. Initially, P*gpdh* along with Mcl1 signal sequence was amplified from previously cloned pMcl1-Lqq1a-Cyt1Aa vector with over-hang for the pCAMBIA3300 and Cry1Ac gene. Secondly, overlap extension PCR was performed to fuse tCry1Ac and GNA bearing vector and Mcl1sp over-hangs. Finally, these two fragments were fused, which resulted in P*gpdh*-Mcl1sp-tCry1Ac/GNA.

5.2.3.4 P*gpdh*-Mcl1sp-tCry1Ac/GNA Cloning in pMcl1-BUTX Lqq1a vector

Initially, pMcl1-BUTX Lqq1a vector was digested with BamHI and HindIII restriction enzymes at 37ºC for 3-4 hr and gel extracted using Takara gel purification kit. Both P*gpdh*-Mcl1sp-tCry1Ac/GNA and double digested pMcl1-BUTX Lqq1a was taken in equal molar concentration and mixed with homemade Gibson assembly master mix, and the reaction was performed at 50ºC for 45-60 min. Following Gibson assembly reaction, 5 µl of the reaction was used to transfer the chemically competent *E. coli* cells and selection was carried out in LB medium supplemented with 50 µg ml^{-1} kanamycin and incubated at 37ºC. Putative transformants were selected and confirmed using colony PCR. A loopful of cultures used as a template for colony PCR amplification. Also, liquid LB medium supplemented with 50 µg ml^{-1} kanamycin antibiotic was used to grow putative transformants and plasmids were isolated using TakaraBio plasmid isolation kit. Plasmid DNA (**pBUTX-Lqq1a/tCry1Ac-GNA**) isolated from putative transformants was confirmed based on restriction enzyme digestion analysis. Both colony PCR products and digested plasmids were separated on 1% Agarose Gel electrophoresis, and images were taken using Bio-rad Gel Doc™ XR gel documentation system.

5.2.4 *Agrobacterium*-mediated transformation of *M. anisopliae*

5.2.4.1 *Agrobacterium* electro-competent cell preparation

For electro-competent cell preparation, *A. tumifaciens* EHA105 (*At*-EHA105) strain was used (Shaw 1995). A single colony of *At*-EHA105 cells was grown in LB broth containing rifampicin (10 µg ml^{-1}) at 28ºC in an orbital incubator shaker at 200 rpm. Overnight grown culture (1 ml) was further inoculated in 200 ml of LB broth and grown for 4-5 hr until OD600 ~0.8. Cells were collected by centrifugation at 5,000 rpm for 10 min, and the cell pellets were washed in 10 mM HEPES buffer (pH 7.0) twice. Finally, cells were resuspended in 10 % glycerol and stored at -80 ºC.

5.2.4.2 Electroporation

Plasmids **pBUTX-Lqq1a/Cyt1Aa and pBUTX-Lqq1a/tCry1Ac-GNA** construct was mixed with *At*-EHA105 electro-competent cells and electroporation was performed at following conditions 1200 V, 25 µF, 600 Ω using Biorad Gene PulserXcell™ electroporation apparatus. Electroporated cultures were then mixed with LB broth and incubated for 2 hr at 28ºC in 200 rpm shaking conditions. Post incubation, *At*-EHA105 cells were plated on LB Agar containing rifampicin (20 µg ml-1) and kanamycin (50 µg ml^{-1}) and then incubated for two days at 28ºC in static condition. The plasmid was isolated from the randomly selected colonies to confirm the clones, and gene-specific PCR and restriction digestion based confirmation were carried out on (1%) agarose gel electrophoresis system.

5.2.4.3 *Agrobacterium* and *Metarhizium* co-cultivation

Agrobacterium-mediated transformation was carried out according to the protocol by Sevim et al. (2012) with little modifications. Initially, *Agrobacterium* harbouring **pBUTX-Lqq1a/Cyt1Aa and pBUTX-Lqq1a/tCry1Ac-GNA** was grown in LB medium

supplemented with kanamycin (50 µg ml^{-1}, Sigma, USA) and rifampicin (20 µg ml^{-1}, Himedia, India) for two days at 28ºC on orbital incubator shaker (200 rpm). Optical density (OD600) of grown culture was adjusted to 0.17 with induction medium (dos Reis et al., 2004) containing 200 µM acetosyringone (Sigma, USA) and incubated for 4-5 hr at 28ºC until OD600 ~0.45. *M. anisopliae* (2×10^7 Spores ml^{-1}) was mixed with an equal volume of *Agrobacterium* **pBUTX-Lqq1a/Cyt1Aa and pBUTX-Lqq1a/tCry1Ac-GNA** (OD600 ~0.4-0.5) and incubated for 2 hr at 28ºC. Then cultures were spread on sterile nitrocellulose filter paper, which were further placed on Induction medium containing Acetosyringone (200 µM) and co-cultivated for two days at 28ºC in static conditions. Post-co-cultivation, the filter paper was transferred to M-100 minimal medium (Stevens R., 1974) supplemented with glufosinate ammonium (300 µg ml^{-1} Sigma, USA) and cefotaxime (50 µg ml^{-1} Himedia, India) and incubated for 5-10 days at 28ºC until colony formation.

Transformants were sub-cultured for two consecutive generations without any selection pressure and then confirmed for P*Mcl1*-BUTX Lqq1a genomic DNA integration. For confirmation of genomic DNA, integrations spores were grown for two days in PDA broth at 28ºC with 180 rpm shaking conditions. Mycelial biomass was obtained by centrifugation and used for genomic DNA isolation. PCR was done using isolated genomic DNA from transformants with gene-specific primers.

5.2.5 Genome integration analysis

Integration of T-DNA containing fusion genes BUTX-Lqq1a/Cyt1Aa and BUTX-Lqq1a/tCry1Ac-GNA into the chromosomal DNA of *M. anisopliae* is essential to express the pyramided genes. Putative transformants growing on glufosinate ammonium supplemented medium was randomly selected and sub-cultured for at least five

consecutive generations. Randomly selected clones were inoculated in 20 ml of Potato dextrose broth and incubated for 48 hr. Post incubation genomic DNA was isolated as mentioned in materials and methods (**5.2.2.2.1** *M. anisopliae* genomic DNA isolation). After the genomic DNA isolation, DNA agarose gel electrophoresis was performed to test the genomic DNA integrity. Isolated DNA was used as a template for PCR to confirm the Genomic DNA integration, both Cyt1Aa and tCry1Ac/GNA clones.

5.2.6 Semi-quantitative RT-PCR analysis

Initially, inoculum culture (Ma-BUTX Lqq1a/Cyt1Aa and Ma-BUTX Lqq1a/tCry1Ac-GNA) was grown in Potato Dextrose Broth (SDB) for two days at 28ºC in orbital incubator shaker. Post-growth, wet culture (1 g) was transferred onto 10 ml of silkworm hemolymph. Hemolymph was extracted from 5th instar Eri silkworm and stored in phosphate buffer containing 2 mM EDTA. After culturing at 28ºC for 12 hr, mycelium was collected by centrifugation for RNA extraction, and the filtrate was stored at -20ºC for further western blot analysis. Total RNA was extracted using RNAiso Plus kit (Takara, Japan) and genomic DNA contamination was removed by using DNAse I treatment (Promega). One microgram of total RNA was used for cDNA synthesis (SuperScript™ III first-strand synthesis system, Invitrogen, USA). Synthesized cDNA was used for semi-quantitative RT-PCR analysis based on BUTX Lqq1a, Cyt1Aa and tCry1Ac/GNA specific primers (**Table 5.3**)

5.2.7 Western blot analysis

Western blot analysis of BUTX Lqq1a was performed according to the protocol followed in the **Chapter 3, section 3.2.8.**

5.2.8 Insect Bioassay

Insect bioassay was conducted to study the efficacy of recombinant *M. anisopliae* harboring BUTX-Lqq1a/Cyt1Aa and BUTX-Lqq1a/tCry1Ac-GNA constructs. Insect culture *S. litura* (National Accession No: NBAII-MP-NOC-02) eggs were procured from NBAIR, Bangalore, India and maintained on natural castor leaves diet with 16:8 hr light and dark condition at 25-28ºC with 60-70% relative humidity level. *P. smithi* adults were collected locally from Indian Institute of Technology Guwahati, Guwahati, Assam, India and maintained on 10% sucrose solution. Dipping or topical application procedure was performed with recombinant and wild type control strains at 2×10^{7}spores ml^{-1} to test the fungal virulence. The excess liquid on each insect was removed by placing them on dry sterile tissue paper and placed on natural castor leaves diet with 16:8 hr light and dark condition at 25-28ºC with 60-70% relative humidity. Insect mortality was record at every 24 hr interval.

5.2.9 Statistical analysis

Data analysis were conducted using GraphPad Prism software (version 6.0). Mean with standard deviation were used to express the values. The p-value < .05 was considered statistically significant data and the Kaplan-Meier survival plots were constructed using GraphPad Prism software (version 6.0), and comparison of survival curve was made using Log-rank (Mantel-Cox) test, and LT_{50} value was calculated based on Probit analysis (Finney 1952).

5.3 Results

5.3.1 pBUTX Lqq1a/Cyt1Aa vector construction

In the present study, initially codon optimized 5'UTR, Mcl1 signal peptide sequence and BUTX Lqq1a was successfully placed downstream of Mcl1 promoter (P*Mcl1*) using Gibson assembly method which resulted in P*Mcl1*-5'UTR-BUTX Lqq1a construct. This resultant construct was further cloned successfully in *Agrobacterium* binary vector pCAMBIA3300 which lead to pMcl1-BUTX Lqq1a vector development carrying scorpion toxic gene under the control of haemolyph specific promoter.

The Cytolytic toxin Cyt1Aa was cloned under the control of Glyceraldehyde 3-phosphate dehydrogenase promoter which allows the constitutive expression of Cyt1Aa. Initially, Cyt1Aa gene sequence was analysed and retrieved from NCBI: LC128536.1 and successfully amplified from the total genomic DNA isolated from *B. thuringiensis* subsp. *israelensis* using Cyt1Aa specific primers (**Fig. 5.1**). Similarly, GPDH promoter (P*gpdh*) and Mcl1 signal peptide sequence was also successfully amplified from *M. anisopliae* genomic DNA (**Fig. 5.1**). To further fuse all three fragments together, initially signal sequence was fused with Cyt1Aa successfully and this fragment was later placed successfully downstream of GPDH promoter (**Fig. 5.1**). The whole construct was successfully cloned in pCAMBIA binary vector which resulted in pBUTX-Lqq1a/Cyt1Aa expression vector which was further successfully confirmed by colony PCR (**Fig. 5.2**). **Fig. 5.3** depicts the arrangement of BUTX Lqq1a and Cyt1Aa in the *Agrobacterium* binary vector. Additionally, plasmids were isolated from the selected clones and successfully confirmed for the presence of scorpion and *B. thuringiensis* toxic genes (**Fig. 5.4**).

5.3.2 pBUTX Lqq1a/tCry1Ac-GNA vector construction

For the construction of gene pyramided vector, initial truncation studies were done in *B. thuringiensis* Cry1Ac gene sequence. Based on the Cry1Ac sequence analysis, it was successfully truncated to 1239 bp length from the full length construct amplified from genomic DNA of *B. thuringiensis* subsp. *kurstaki* (HD73) and GNA was also successfully amplified from plasmid pUC57 harboring Linker GNA (**Fig. 5.5**). Both the truncated Cry1Ac and GNA was effectively fused together using Gibson assembly which further resulted in fusion product tCry1Ac-GNA with the 1566 bp length (**Fig. 5.5**). The truncation and fusion strategies are clearly depicted in the **Fig. 5.6**.

The GAPDH promoter along with Mcl1 signal sequence was also amplified from the pBUTX Lqq1a/Cyt1Aa vector and successfully placed upstream of tCry1Ac-GNA fusion product which resulted in P*gpdh*-tCry1Ac-GNA fragment (**Fig. 5.7**). The final construct was successfully cloned in the pMcl1-BUTX Lqq1a binary vector which was confirmed by colony PCR with tCry1Ac-GNA specific primers (**Fig. 5.8**) and also by restriction enzyme digestion of isolated plasmid DNA (**Fig. 5.9**). The effective placement of fusion construct downstream of BUTX Lqq1a gene in the pMcl1-BUTX Lqq1a binary vector resulted in the development of expression vector containing scorpion toxin under the control of haemolymph specific Mcl1 promoter and fused truncated Cry1Ac and GNA under the control of constitutive GAPDH promoter. The arrangement of scorpion BUTX Lqq1a and truncated Cry1Ac-GNA in the recombinant *Agrobacterium* binary vector is depicted in the **Fig. 5.10**.

5.3.3 Genome integration analysis of BUTX Lqq1a and Cyt1Aa in *M. anisopliae*

Chromosomal integration is necessary for the proper expression of heterologous genes in the fungal system particularly *M. anisopliae.* In order to integrate scorpion and

Cyt1Aa, binary vector harbouring BUTX Lqq1a and Cyt1Aa was efficiently transferred into *M. anisopliae* using the optimized *Agrobacterium* mediated transformation and selected on glufosinate ammonium containing M-100 screening medium. To confirm the genomic integration of heterologous genes in *M. anisopliae* clones, genomic DNA was successfully isolated from the selected clones (**Fig. 5.11**) and PCR confirmation revealed that BUTX Lqq1a (**Fig. 5.12**) and Cyt1Aa (**Fig. 5.13**) was successfully integrated in the *M. anisopliae.*

5.3.4 Genome integration analysis of BUTX Lqq1a and tCry1Ac-GNA

Similar to Cyt1Aa and BUTX lqq1a clone confirmation, genomic integration of Scorpion and truncated Bt genes in the *M. anisopliae* was also confirmed by successfully isolating the genomic DNA (**Fig. 5.14**) from the selected *M. anisopliae* clones which have been consecutively grown without any selection pressure. **Fig. 5.15** represents the Scorpion BUTX Lqq1a gene amplified from the *M. anisopliae* clones indicating the successful integration. Additionally, truncated Cry1Ac/GNA (**Fig. 5.16**) as well as the BUTX Lqq1a along with Mcl1 promoter (**Fig. 5.17**) amplification clearly indicated the effective integration of both scorpion and Bt Cry genes.

5.3.5 Cyt1Aa and BUTX Lqq1a transcript analysis

The expression of Cyt1Aa and BUTX Lqq1a in both the modified transgenic and unmodified *M. anisopliae* clones was analysed by semi-quantitative RT-PCR. The modified clones showed varied accumulation of Cyt1Aa (**Fig. 5.18**) and BUTX Lqq1a (**Fig. 5.19**) whereas unmodified counterpart i.e. wildtype did not exhibited transcripts amplification thus clearly indicating the integration and expression of transgene from the modified *M. anisopliae.*

5.3.6 BUTX Lqq1a and tCry1Ac/GNA transcript analysis

The relative expression of BUTX Lqq1a and tCry1Ac-GNA in both the modified and unmodified *M. anisopliae* clones was analysed by semi-quantitative RT-PCR. The results exhibited substantial presence of transcripts such as BUTX Lqq1a (**Fig. 5.19**) and tCry1Ac-GNA (**Fig. 5.18**) in *M. anisopliae* clones carrying BUTX Lqq1a and tCry1Ac-GNA transgenes. However, no expression was observed in the unmodified wildtype *M. anisopliae*. **Fig. 5.20** represents the GNA transcripts amplified from tCry1Ac-GNA synthesized cDNA and **Fig. 5.21** represents the *gpdh* gene internal control.

5.3.7 Western blot analysis of BUTX Lqq1a

The expression of BUTX Lqq1a protein in both the transgenic *M. anisopliae* harbouring Cyt1Aa and tCry1Ac-GNA was evaluated using western blot analysis. The western blot analysis revealed that anti-BUTX Lqq1a antibody specifically reacted with BUTX Lqq1a expressed in the transgenic *M. ansiopliae* harbouring BUTX Lqq1a along with Cyt1Aa and tCry1Ac-GNA pyramided genes. **Fig. 5.22** represents the results of western blot hybridization experiment conducted with PCR-positive entomopathogenic fungi. The results clearly indicated that the BUTX Lqq1a gene had been integrated into the genome of the fungi as well as it was also able to translated into active BUTX Lqq1a protein.

5.3.8 Insect Bioassay

The entomopathogenecity of *M. anisopliae* expressing BUTX Lqq1a/Cyt1Aa and tCry1Aa-GNAwas performed on *P. smithi* based on topical application of spores. Kaplan-Meier survival plot of *P. smithi* (n=15, Log-rank (Mantel-Cox) test p=0.0082) bioassay conducted using *M. anisopliae* wildtype and *M. anisopliae* β-BUTX-Lqq1a/Cyt1Aa resulted in significant reduction in the survival where modified fungi exhibited LT_{50} of

3.7 days (R^2 = 96.53) post inoculation, however wild type fungus exhibited LT_{50} of 4.5 days (R^2 = 97.38) to kill the insect (**Fig. 5.23**). In addition, no difference in the mycelial growth of both wild type and modified fungal growth was observed (**Fig. 5.24**). In both, fungal infection lead to the severe mealanization of insect body within 48 hr post inoculation. Mycelial outgrowth was observed after 3 days of inoculation.

M. anisopliae expressing BUTX Lqq1a/tCry1Ac-GNA also acted on *P. smithi*, however, complete mortality of insects was observed after 8th day post application when compared to control (**Fig. 5. 25**). This mortality is not significant when compared to *M. anisopliae* expressing BUTX Lqq1a alone or in combination with Cyt1Aa. Predominant melanisation was observed in the infected insects of wild type as well as transgenic fungi. *S. litura* (4th instar) larvae injected with the modified fungi exhibited severe mortality when compared to control (**Fig. 5.26**). Fungal outgrowth was observed on 2nd day post injection, and complete sporulation was evident after 4th day post injection.

5.4 Discussion

The present study was experimented to determine the potency of combinatorial effect of scorpion, bacterial and plant insecticidal toxins on agricultural insect pests when delivered using entomopathogenic fungus *M. anisopliae*. Scorpion toxin such as AaIT1, LqhIT2, BmKIT and BjαIT were expressed in the entomopathogenic fungal system to control agricultural pests as well as vectors of disease causing agents (Chen et al. 2015, Deng et al. 2017, Peng and Xia 2014, Xie et al. 2015). *Bacillus thuringiensis* toxin, Cry1Ac is one of the important insecticidal toxic protein, being expressed in major agricultural crops such as cotton and maize to control variety of insect pests, particularly, *H. armigera, H. zea* and *Pectinopora gossypiella* (Li et al. 2019, Wang et al. 2019, Zhang et al. 2019). The Cytolytic toxin Cyt1Aa from *B. thuringiensis* subsp. *israelensis* has proven toxic to insect pest as well as synergistically acts to improve the toxicity of other Cry toxins when co-expressed (Zribi Zghal et al. 2019). Similarly, plant defense protein *Galanthus nivalis* agglutinin (GNA) from Snowdrop plant has also been expressed in many plant systems such as potato, wheat, and rice against aphids, green leafhopper and brown planthopper (Foissac et al. 2000, Mi et al. 2017, Stoger et al. 1999).

Despite the widespread usage and expression of the Cry toxins in the plant systems, fewer reports were available on expression of insecticidal toxins from *B. thuringiensis* in fungal system particularly entomopathogenic fungi. Zhang et al. (2014) expressed the Vegetative insecticidal protein (Vip3A1), an insect midgut specific toxin from *B. thuringiensis* in *M. anisopliae* for the management of *S. litura*. Similarly Vip3A1 was also expressed in *Beauveria bassiana* to protect the crop plants against *S. litura* (Qin et al. 2010).

The present study reported the use of heterologous *Aspergillus nidulens* glyceraldehyde 3-phosphate dehydrogenase promoter to express the heterologous toxic proteins. The Cyt1Aa a cytolytic toxic gene (NCBI:LC128536.1:99192-99941) from *B. thuringiensis* subsp. *israelensis* was successfully fused with the constitutive GPDH promoter from *M. anisopliae*. Use of endogenous promoter improved the typical expression of transgene than non-native promoters (Cao et al. 2012). In the present study, *M. anisopliae* GPDH promoter located 1773 bp upstream of GPDH gene (AZNF01000010.1 (region: 1053433-1055206)) was chosen based on the comparative studies with the *M. acridum* GPDH promoter (Cao et al. 2012, Hu et al. 2014). The comparative sequence analysis with the *M. acridum* GPDH promoter sequence (EFY84384.1) clearly indicated the presence of CT-rich region (166 bp) upstream of transcription start site (TSS) (**Fig. 5.27**).

For the Cry1Ac truncation, initial studies performed on full length Cry1Ac amino acid sequence (NCBI: AGE81486.1) which contains 1178 amino acids. However, upon maturation and proteolytic processing, 47 amino acids from N-terminal and 565 amino acids from C-terminal region were found to be absent which further resulted in 566 amino acid containing active mature Cry1Ac protein. This 566 amino acids code for three domains with distinct functional property. C-terminal domain of the mature protein code for carbohydrate and receptor binding property. Recent studies suggested that the frequent mutation in the insect midgut receptors cadherin, ABC transporters for these C-terminal domain lead to the development of resistance (Guo et al. 2019, Walsh et al. 2018). To avoid the resistance development, GNA (109 amino acids) from the Snowdrop was successfully fused by replacing the C-terminal domain from the mature Cry1Ac which resulted in 523 amino acid containing truncated Cry1Ac with GNA toxic protein in the

present study. The successfully fused DNA sequence was driven by *M. anisopliae* GPDH promoter. Additionally, the scorpion toxin BUTX Lqq1a was also driven by the native haemolymph specific promoter of *Metarhizium* collagen like protein (MCL1). Secretion of these two toxic proteins Cyt1Aa and tCry1Ac-GNA were controlled by Mcl1 signal peptide sequence.

These two toxin genes were successfully placed in the binary vector expression system to transfer into *M. anisopliae* using *Agrobacterium tumifaciens* EHA105 strain. Genome integration is an inevitable mechanism for the transgene expression, present study using the property of *Agrobacterium*. The BUTX Lqq1a/Cyt1Aa containing T-DNA was successfully integrated into the genome of *M. anisopliae* as confirmed by PCR. Similarly, BUTX Lqq1a/tCry1Ac-GNA successful PCR amplification confirmed the efficiency of T-DNA integration.

The presence of BUTX Lqq1a transcripts in the haemolymph induced fractions in both the clone was observed. Additionally, semi-quantitative RT-PCR analysis also suggested the presence of Cyt1Aa and tCry1Ac transcripts. However, the absence of transcripts in the wild type depicts the functional part of inducibility of *Metarhizum* collagen like promoter. The *Metarhizium* carrying the BUTX Lqq1a/Cyt1Aa and BUTX Lqq1a/tCry1Ac-GNA when analysed for the presence of scorpion toxin in the inducible fraction using western blot analysis, also suggested the presence of 8.3 kDa protein, while it is absent in wildtype.

Cyt1Aa is one of the promising insecticidal toxin which is being explored as an redressel to terminate the resistance development in insects. Cyt1Aa-hybrid toxins led to the development of lepidopteran specific Cyt1Aa toxin with reduced dipteran specificity (Torres-Quintero et al. 2018). Similarly, a mutated Cyt1Aa in the alpha-helical region

reduced the haemolytic activity, however 11-fold increase in insecticidal activity was observed against western corn rootworm (Bravo et al. 2018). In the present study, *M. anisopliae* expressing BUTX Lqqa and Cyt1Aa effectively acted on *P. smithi* which is one of the invasive pest of sugarcane. When compared to wildtype, significant 17% reduction was observed in half maximal lethal time. However, the percentage reduction was less compared to the *M. anisopliae* expressing only the scorpion toxin. Post topical application, infected insects movement was drasticically reduced and vigourous mycelial growth was observed in both the wild type and transgenic fungi after 3 days. Nearly 20% mortality was observed in transgenic fungal infected *P. smithi* when compared to wildtype. Complete mortality was observed on 6th day in both wildtype and transgenic fungi, post inoculation.

Similar to the Cyt1Aa, action of *M. anisopliae* carrying truncated Cry1Ac-GNA along with BUTX Lqq1a was also evaluated on *P. smithi* based on topical application method. Transgenic rice expressing full length Cry1Ac and GNA conferred broad level resistance against rice leaf folder, yellow stem borer and brown plant hopper (Loc et al. 2002, Maqbool et al. 2001). Similarly, when Cry1Ac along with *Pinellia ternata* agglutinin (PTA) expressed together in *Isatis indigotica* significantly inhibited the growth of diamondback moths and peach potato aphids (Xiao et al. 2012). Additionally Knight et al. (2004) identified the putative carbohydrate moieties as fucosylated mannose residues which could be a putative carbohydrate binding site of one of the domain of Cry toxins. In the present study, based on the semi quantitative RT-PCR analysis, presence of transcript confirms the constitutive expression of tCry1Ac-GNA, however, since Cry1Ac and GNA act on insect midgut receptors, these fungi need to be ingested to act on insect pests.

5.5 Conclusion

In the present study scorpion toxin along with Cytolytic toxin Cyt1Aa from *B. thuringiensis* subsp. *israelensis*, midgut acting crystal toxin Cry1Ac from *B. thuringiensis* subsp. *kurstaki* and plant defense protein GNA was successfully fused together using overlap extension PCR and Gibson assembly. Their integration into the genome and expression of the pyramided genes in the fungus was also successfully confirmed by transcript analysis and western blot. Potential of these transgene expressing fungal evaluation also suggested that it could be a prospective candidate fungus for biocontrol.

These studies clearly suggest the potential development of a biological insecticide based on *M. anisopliae* with heterologous genes, that would pave the way to reduce the impact of synthetic chemical pesticides on environment thus increasing the agricultural productivity.

Table 5.1 List of primers used for P*gpdh* and Cyt1Aa cloning

Primers	5'----------3'
LqqIT1 OH BamHI GPDH FP	GCGACTTTGTCACCATCAACTAATAAGGATCCGGCGTGGCAGGATGCCGGATATTT
GPDH RP Mcl1sp OH	CGAAGAAAGTTCACGCATTTTGCGTGTGTGTATATGGAGAGAGCTGGAG
GPDH OH Mcl1Sp FP	CTCCAGCTCTCTCCATATACACACACGCAAA ATG CGT GAA CTT TCT TCG GTT
Mcl1sp RP Cyt1Aa OH	TTCTAATGGACAATGATTTAAATTTTCCATTGCCGACGCCAGGGCCAG
Mcl1sp OH Cyt1Aa FP	TTGCTGGCCCTGGCGTCGGCAATGGAAAATTTAAATCATTGTCCATTAGAA
pCAM Hind III OH Cyt1Aa RP	TTGTAAAACGACGGCCAGTGCCAAGCTTTTATTAGAGGGTTCCATTAATAGCG

Table 5.2 List of primers used for P*gpdh* and tCry1Ac-GNA cloning

Primers	5'----------3'
pCAM OH HindIII-GNA RP	CACGACGTTGTAAAACGACGGCCAGTGCCAAGCTTTTATTAGCCGGTAGCCCAGCGGTC
Mcl1 RP-Cry1Ac OH	TCCAGCACCGGGAACAAATTCACTTGCCGACGCCAGGGCCAG
Cry1Ac FP-Mcl1sp OH	TTGCTGGCCCTGGCGTCGGCAAGTGAATTTGTTCCCGGTGCTGGA

Table 5.3 List of primers used for semi-quantitative RT-PCR analysis

Primers	5'----------3'
RT-Lqq FP	AAGAAGAACGGCTACGCTG
RT-Lqq RP	GTTGATGGTGACAAAGTCG
RT-Cry1Ac FP	GAATTTGTTCCCGGTGCTGGA
RT-Cry1Ac RP	AGGATCTGCTTCCCACTCTCT
RT-GNA FP	TGCCTGAGCGATAACATCCTG
RT-GNA RP	TAGTTACCGTTCTGACCGCC
RT-Cyt1Aa FP	CCATGGAAAACCCCTCAATCA
RT-Cyt1Aa RP	CATAACTCACTACAGCACCCA
RT-GPDH FP	TGAAGCTCCGGGAAAGATG
RT-GPDH RP	GACTTGCTGCTGACTCACG

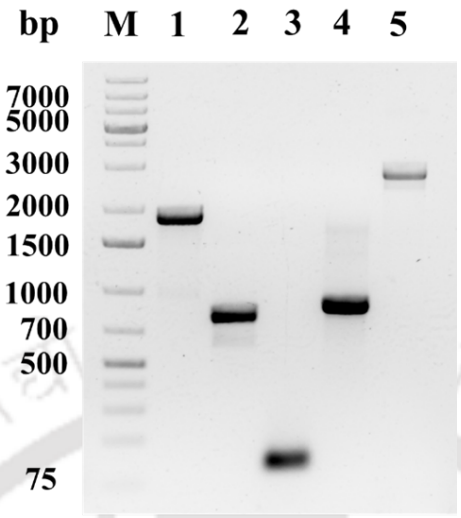

Fig. 5.1 Agarose gel electrophoresis analysis of PCR amplified and gel purified products for GPDH promoter, Mcl1sp and Cyt1Aa fusion. Lane 1: GPDH promoter amplified from *M. anisopliae* genomic DNA (1833 bp), Lane 2: Bt Cyt1Aa gene product (810 bp) from *Bacillus thuringiensis* HD-522, Lane 3: Mcl1 signal peptide (117 bp) from *M. anisopliae*, Lane 4: Mcl1 signal sequence and Bt Cyt1Aa fused product (867 bp), Lane 5: GPDH promoter, Mcl1 sp and Bt Cyt1Aa fused product (2,640 bp), and Lane M: O' GeneRuler 1 Kb Plus DNA Ladder.

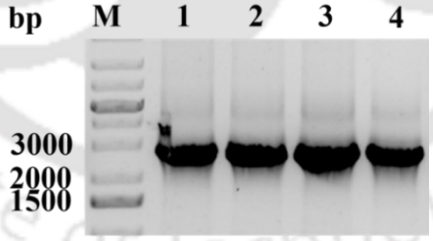

Fig. 5.2 Agarose gel electrophoresis analysis of Colony PCR clone confirmation for the pBUTX Lqq1a/Cyt1Aa clones. GPDH Cyt1Aa specific primers was employed to confirm the clones. Lane 1to 4: GPDH Cyt1Aa sequence amplified from Clones (size 2.580 Kbp), Lane M: O'GeneRuler 1 Kb Plus DNA Ladder.

Fig. 5.3 Schematic representation of arrangement of BUTX Lqq1a and Cyt1Aa constructs in the binary vector.

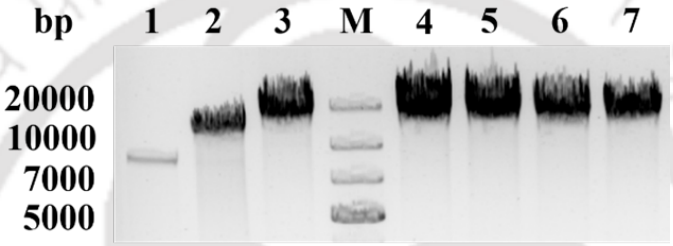

Fig. 5.4 Agarose gel electrophoresis analysis of plasmids isolated from pBUTX Lqq1a/Cyt1Aa clones. Lane 1: pCAMBIA 3300 binary vector alone (~8.3 Kbp), Lane 2: pMcl1-BUTX Lqq1a vector (~11.5 Kbp), Lane 3: pBUTX Lqq1a/Cyt1Aa (~15 Kbp), Lane 4 to 7: pBUTX Lqq1a/Cyt1Aa plasmids linearized with HindIII (~15 Kbp) and Lane M: O'GeneRuler 1 Kb Plus gene ruler.

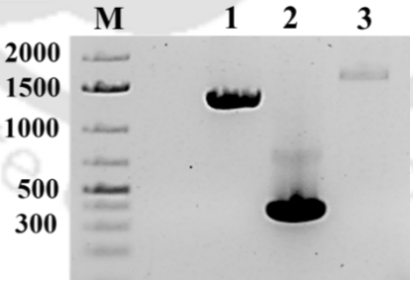

Fig. 5.5 Agarose gel electrophoresis image analysis of PCR amplified and gel purified fragments. Lane 1: Bt truncated Cry1Ac gene product (1239 bp), Lane 2: GNA product (327 bp), Lane 3: Bt truncated Cry1Ac/GNA product (1566 bp) and Lane M: O' GeneRuler 1 Kb Plus DNA Ladder.

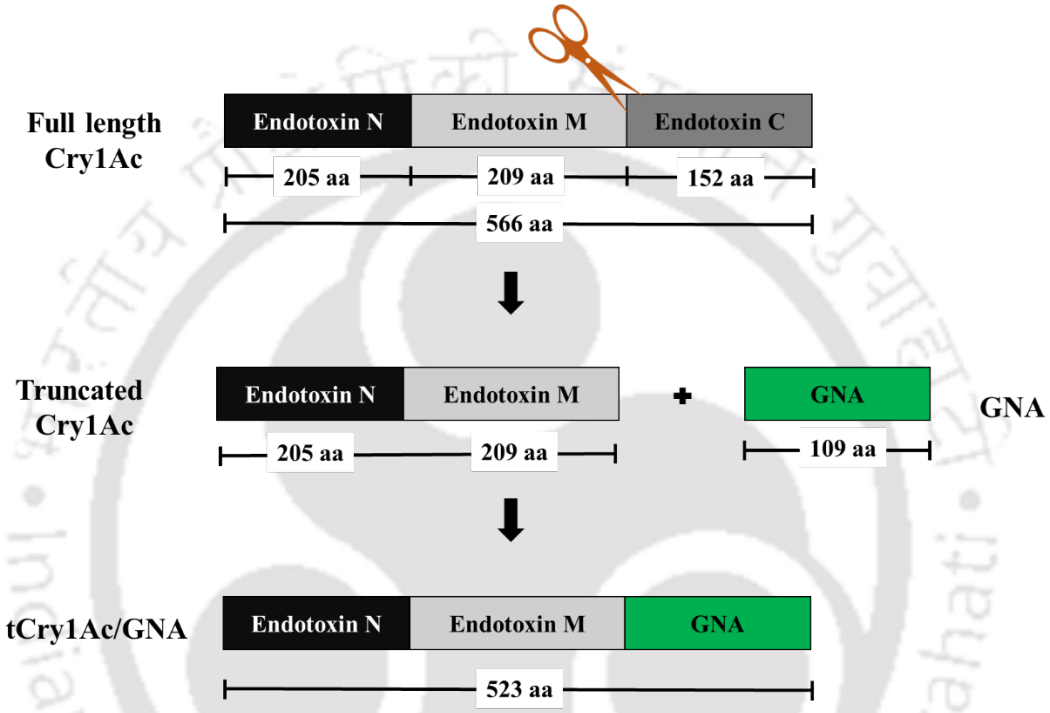

Fig. 5.6 Schematic representation of Cry1Ac truncation and fusion with GNA.

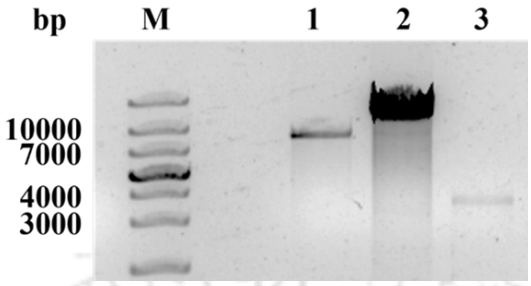

Fig. 5.7 Agarose gel electrophoresis analysis of restriction enzyme digested plasmids and PCR purified fusion fragments. Lane 1: Empty pCAMBIA vector (~8.34 Kbp), Lane 2: pMcl1-BUTX Lqq1a (~11.4 Kbp), Lane 3: P*gpdh*-Mcl1sp-tCry1Ac/GNA pcr product (~3.4 Kbp), and Lane M: O' GeneRuler 1 Kb Plus DNA Ladder.

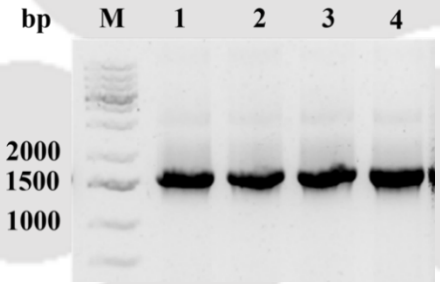

Fig. 5.8 Agarose gel electrophoresis analysis of colony PCR clone confirmation. Lane 1 to 4 tCry1Ac-GNA sequence amplified from slected pBUTX Lqq1a/tCry1Ac-GNA Clones (size 1.572 Kbp), and Lane M: O' GeneRuler 1 Kb Plus DNA Ladder.

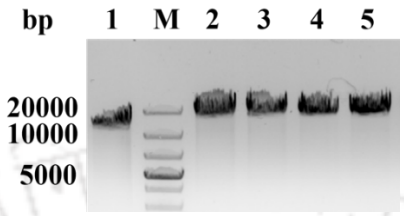

Fig. 5.9 Agarose gel electrophoresis analysis of pBUTX Lqq1a/tCry1Ac-GNA clone confirmation by restriction enzyme digestion. Lane 1: pMcl1-BUTXLqq1a vector (~11.5 Kbp), Lane 2 to 5: pBUTX Lqq1a/tCry1Ac-GNA clonal plasmids linearized with Hind III restriction enzyme (~15 Kbp), and Lane M: O' GeneRuler 1 Kb Plus DNA Ladder.

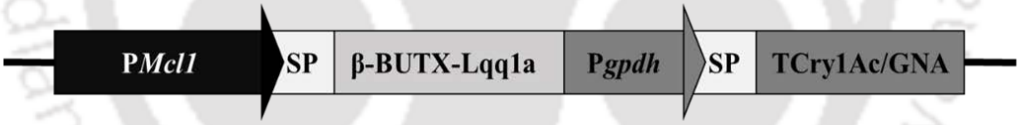

Fig. 5.10 Graphical representation of arrangement of pyramided genes in the binary vector pBUTX Lqq1a/tCry1Ac-GNA.

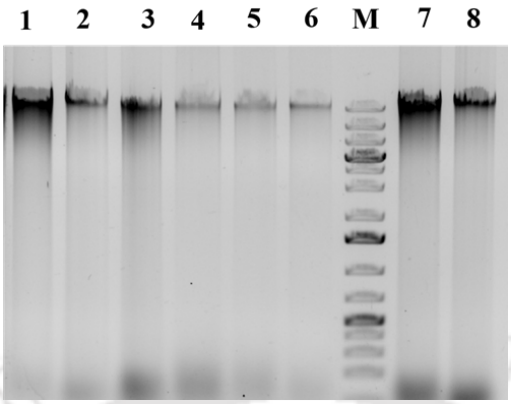

Fig. 5.11 Agarose gel electrophoresis analysis of genomic DNA isolated from Ma-BUTX Lqq1a/Cyt1Aa clones. Lane 1 to 8 Ma-BUTX Lqq1a/Cyt1Aa genomic DNA and Lane M: O' GeneRuler 1 Kb Plus DNA Ladder.

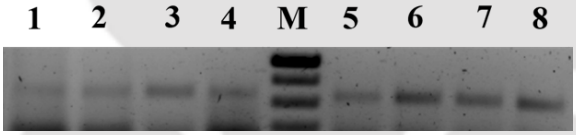

Fig. 5.12 Agarose gel electrophoresis analysis pBUTX Lqq1a/Cyt1Aa PCR clone confirmation. Lane 1 to 8: BUTX Lqq1a gene amplified from Ma-BUTX Lqq1a/Cyt1Aa clones (size 327 bp), Lane M: O' GeneRuler 1 Kb Plus DNA Ladder and M-represents 500, 400, 300, 200 bp bands from top to bottom order.

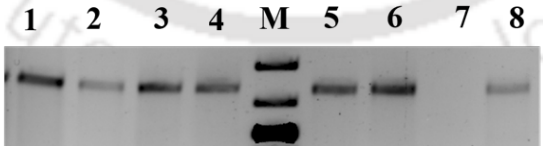

Fig. 5. 13 Agarose gel electrophoresis analysis pBUTX Lqq1a/Cyt1Aa PCR clone confirmation. Lane 1,2,3,4,5,6, and 8: Cyt1Aa gene amplified from Ma-BUTX Lqq1a/Cyt1Aa clones (size 810 bp), Lane M: O' GeneRuler 1 Kb Plus DNA Ladder, and M-represents 1000, 700, 500 bp bands from top to bottom order.

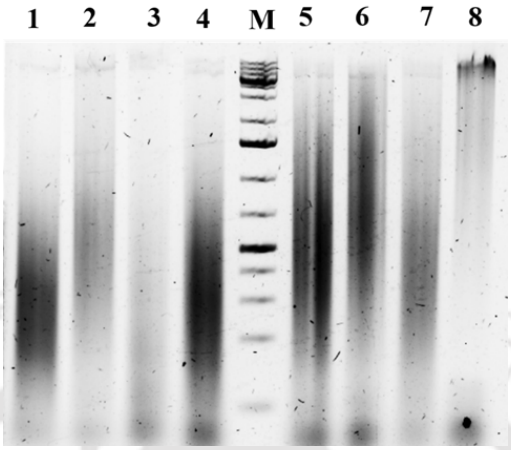

Fig. 5.14 Agarose gel electrophoresis analysis of genomic DNA isolated from selected clones. Lane 1 to 8: genomic DNA isolated from *M. anisopliae* BUTX Lqq1a/tCry1Ac-GNA clones and Lane M: O' GeneRuler 1 Kb Plus DNA Ladder.

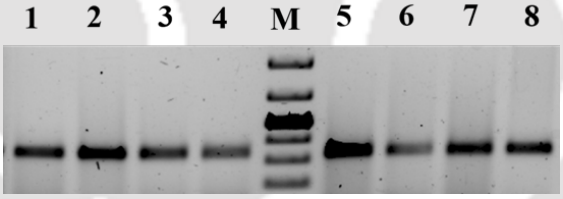

Fig. 5.15 Agarose gel electrophoresis analysis of PCR clone confirmation. Lane 1 to 8 BUTX Lqq1a gene amplified from Ma-BUTX Lqq1a/tCry1Ac GNA clones genomic DNA (size 327 bp), Lane M: O' GeneRuler 1 Kb Plus DNA Ladder, and M- represents 1000, 750, 500, 400, 300, 200 bp bands from top to bottom order.

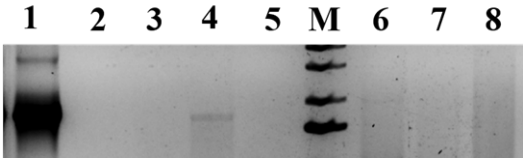

Fig. 5.16 Agarose gel electrophoresis analysis of PCR clone confirmation. Lane 1 and 4: tCry1Ac-GNA gene amplified from Ma-BUTX Lqq1a/tCry1Ac GNA clones genomic DNA (size 1567 bp), Lane M: O' GeneRuler 1 Kb Plus DNA Ladder, and M- represents 4000, 3000, 2000, 1500 bp bands from top to bottom order.

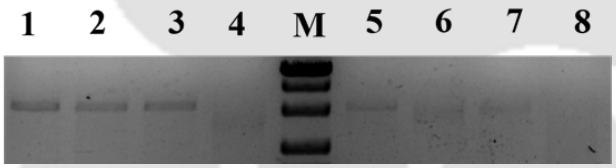

Fig. 5.17 Agarose gel electrophoresis analysis of PCR clone confirmation. Lane 1, 2, 3, 5, 6, and 7: P*Mcl1*-BUTX Lqq1a gene amplified from Ma-BUTX Lqq1a/tCry1Ac GNA clones genomic DNA (size 3.21 kbp), Lane M: O' GeneRuler 1 Kb Plus DNA Ladder, and M- represents 5000, 4000, 3000, 2000 bp bands from top to bottom order.

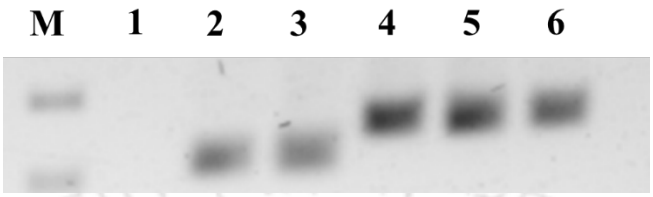

Fig. 5.18 Semi-quantitative RT-PCR analysis. Lane 1: *M. anisopliae* wild type control, Lane 2 and 3: tCry1Ac transcripts from Ma-BUTX Lqq1a/tCry1Ac-GNA clones, Lane 4, 5, and 6: Cyt1Aa transcripts amplified from Ma-BUTX Lqq1a/Cyt1Aa clones, Lane M: O' GeneRuler 1 Kb Plus DNA Ladder, and M- represents 200, 75 bp bands from top to bottom order.

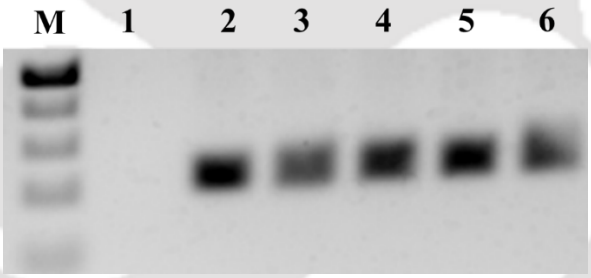

Fig. 5.19 Semi-quantitative RT-PCR analysis. Lane 1: *M. anisopliae* wild type control, Lane 2 and 3: BUTX Lqq1a transcript from Ma-BUTX Lqq1a/tCry1Ac-GNA clones, Lane 4, 5, and 6: BUTX Lqq1a transcript amplified from Ma-BUTX Lqq1a/Cyt1Aa clones, Lane M: O' GeneRuler 1 Kb Plus DNA Ladder, and M- represents 500, 400, 300, 200, 75 bp bands from top to bottom order.

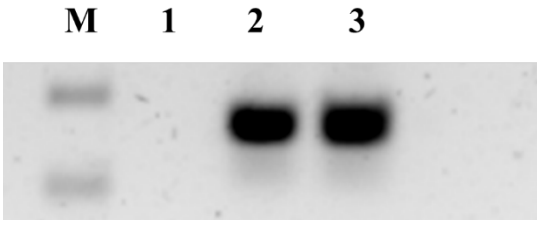

Fig. 5.20 Semi-quantitative RT-PCR analysis. Lane 1: *M. anisopliae* wild type control, Lane 2 and 3: GNA transcript from Ma-BUTX Lqq1a/tCry1Ac-GNA clones, Lane M: O' GeneRuler 1 Kb Plus DNA Ladder, and M- represents 300, 200 bp bands from top to bottom order.

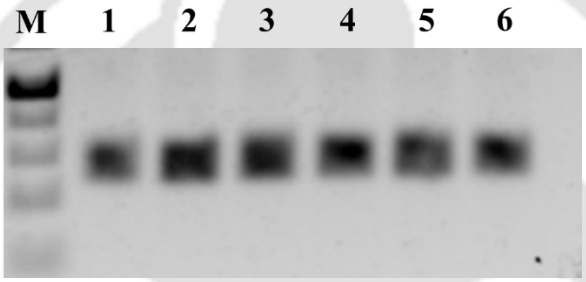

Fig. 5.21 Semi-quantitative RT-PCR analysis *gpdh* internal control. Lane 1: *M. anisopliae* wild type control, Lane 2 and 3: *gpdh* transcript from Ma-BUTX Lqq1a/tCry1Ac-GNA clones, Lane 4, 5, and 6: *gpdh* transcript amplified from Ma-BUTX Lqq1a/Cyt1Aa clones, Lane M: O' GeneRuler 1 Kb Plus DNA Ladder, and M- represents 300, 200 bp bands from top to bottom order.

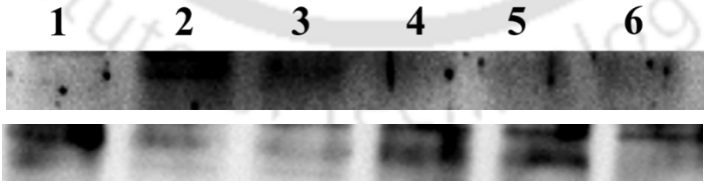

Fig. 5.22 Western blotting analysis of hemolymph induced Ma-wild type and Ma-BUTX Lqq1a/Cyt1Aa and tCry1Ac-GNA strain and Loading control (β-tubulin). Lane 1 represents the unmodified wild type *M. anisopliae*, Lane 2, and 3 indicates the BUTX Lqq1a from Ma-BUTX Lqq1a/tCry1Ac-GNA strain and Lane 4, 5, and 6 indicates Ma-BUTX Lqq1a/Cyt1Aa strain.

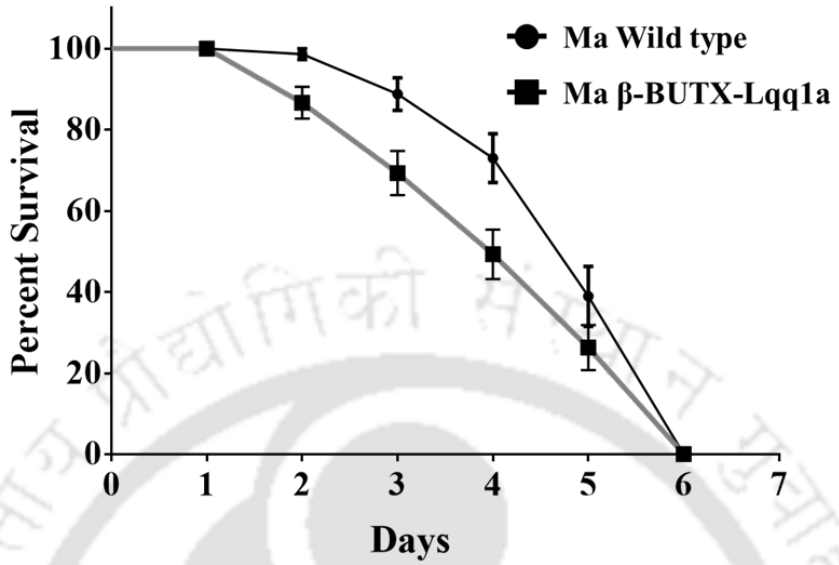

Fig. 5.23 Insect bioassay performed with wild type *M. anisopliae* and Ma-BUTX Lqq1a/Cyt1Aa clones. Kaplan-Meier survival plot of *Phyllophaga smithi* (n=15, Log-rank (Mantel-Cox) test p=0.0082) bioassay conducted with *M. anisopliae* wild type and *M. anisopliae* β-BUTX-Lqq1a/Cyt1Aa.

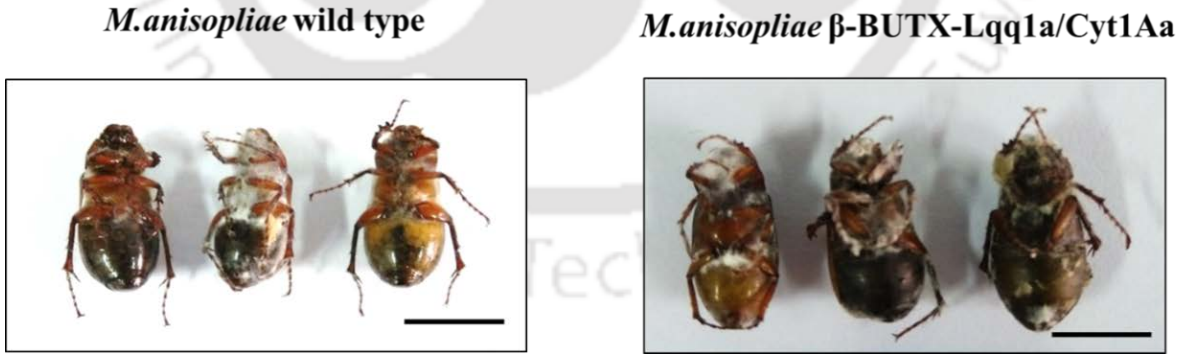

Fig. 5.24 *Phyllophaga* insect bioassay. A) *M. anisopliae* wild type infected *Phyllophaga* and B) *M. anisopliae* expressing BUTX-Lqq1a/Cyt1Aa infected *Phyllophaga* insects. Scale bar represents 1 cm.

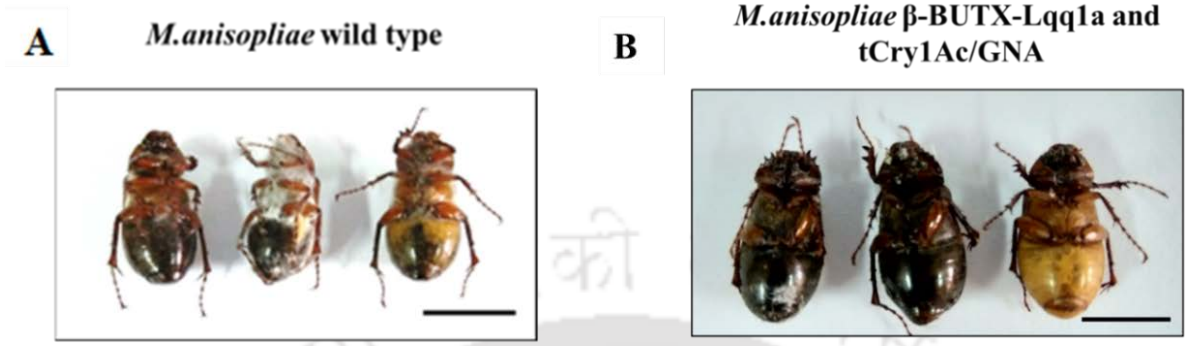

Fig. 5.25 *Phyllophaga* insect bioassay with *M. anisopliae* expressing BUTX Lqq1a/tCry1Ac-GNA A) *M. anisopliae* wild type infected *Phyllophaga* and B) *M. anisopliae* expressing β-BUTX Lqq1a/Cyt1Aa infected *Phyllophaga* insects. Scale bar represents 1 cm.

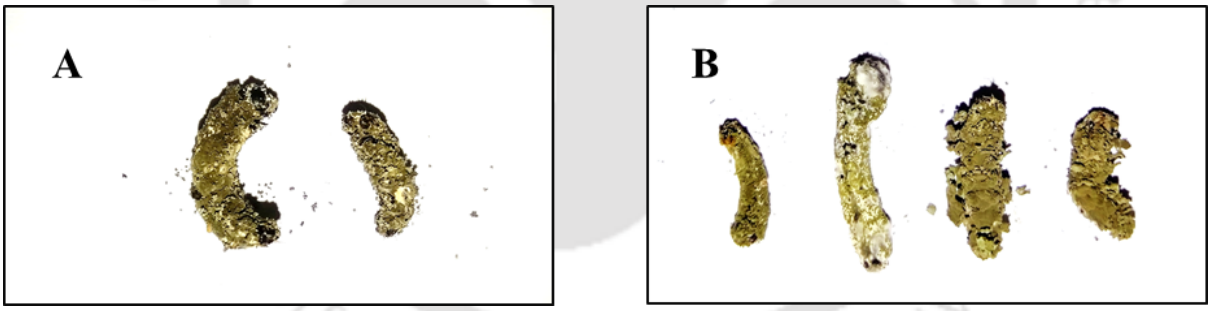

Fig. 5.26 Injection bioassay conducted with *M. anisopliae* spores on *S. litura.* A) *M. anisopliae* wild type and B) *M. anisopliae* expressing BUTX Lqq1a/tCry1Ac-GNA infection on *S. litura.*

GGCGTGGCAGGATGCCGGATATTTCGCACAGGGCATCGAATTCCGGAGCGCTGGCAG
CGGTGATGAGGCGGTTGGACAGCGACGGCCACCTTTGCGTCCTGATTATTCCATGCG
CGGCGAAGCGTGCGTCATCCGCCATTTGCTGGCGTCTCAAAGCGCAGGATTTTGCTG
ATGCTTGAATGAGGCATGAGCCAATTTTGGGACTGTCTACACCACAATAGAATGGAT
GAACCGGCGATTGTCTCGCAAATTATCTGCCGTGTAGGATGGAAACATTAAACATGG
CACACTGGTGGAGACGATTTCATGGATGGCAAGACTAAGCATTGGGCCCAGACACGG
GGGTTGACACACGGGCAGGTTGCCCCGGTCCAGGTGGAAGTTTACGATTGAAAACTT
CCGAAGAGCTTGTATTCCCTGTGGGCAAAGTTCGGGACGACGAGAACTGTTCCTGGT
GTTCCCGACGACTGTCCCCGGGCGGACGCGGCTGCAAAGGCCAGAGCCGCCCGCAGC
CGTGAAGCTCCGGGAAAGATGGGCAAAACGGGCGAATGGATGGCCAATACAGATGA
ACCATTTCCCGCCATGCATCCGAGCCGCCCACACGACCAGAGGGGCCCCGGAATTAA
TTAGATTGAGGTCATCGTGAAGGCATTCCGCTGCTGAGAGTGCGACAGAGCTGGCGT
CGGTACATTTTGGACATGTCTGGGCCGTCTGATTTTTTTTTCCGTCTCCTCTCACACCT
GACCCTGCGTGAGTCAGCAGCAAGTCGTCACCGCGACCGGAGACACGTTTTGAGTGA
TTTATCATGGCTATTACTCGCGGTCTTGCTGCCAGCAGGCATATCTACAACACGATAA
GGCCAGCAGGGCCTACCACGGGGGTACATGGACGCCAGGCTGCGACAACCATGGAA
CAGCGGGTACCCCTCATGTCCATGTTTTTTTTCTCTCTCAAGGTGGTGCTCATGTGCTC
GTCGGTGTGGTTGAGAGAGCGTTTCTATTAACGAATTGTGTCCCCGCCGGATCCGTAA
AAAGACGCATCGGCTGGGTGGAGCAAGGCGAGGCCCGTCAAAGCATCATCAATGGC
TGAGCTCATTCGATTCCTCATCAAATTACATGGCGCAGGGAAGCATCGTTGGCGAATT
TTGCCTTTGCGGTGCATGCAAGTGGCGGCTGGCTGGGATATTGGATGGCCACTTGCAC
GACCACGGCGAGGATGGACATGAAGCCCGCGGCGTCTGGCATGGCAAGGCAATTGA
AATATCGTCTCGTTGAATAGCGTGAATAGTAGTACCGCTCGTGTATCAGAACCGGGC
TCCGTCTCACGGTGCAAGTGTGAATGATGCATGCACCCGCTTGGCTAGGTTTGCGTGC
ACCAGTTGTTGGCCGCTGACGTCTGCTGGTCTCAACAGTCCCGACGCCGTGGCCAGCC
AAGACGCAGCCAGTTGCGCGCCCAGCAACACACCAGACACCCCAAGCACCAGACCC
AAGCTCCCAAGCTCCAGGGACATGGACTGACCACTATTTTGTCCCGCCTTCCCTCCGT
CCCCTCCGACTCCATCCTCTTCCCTCTTCCTCTTCCTTTTTCTTCTTTTCTTCCCGCTCTT
CATACAACTTCACCATTCTTTCCACCAGGCACTTTGTCCGGTATGTATCCCATCCTGC
ATTGGCTGAGCAGAGCTTGACCACAGCTCGACACCAGCTCCGTCTCTAGCTTCCCAG
ACTCCCGTGCTGACGTCCAAGCTCCAGCTCTCTCCATATACACACACGCAAA

Fig. 5.27 *M. anisopliae* GPDH promoter sequence retrieved from NCBI *M. anisopliae* ARSEF 549 scaffold_10, whole genome shotgun sequence (Genbank: AZNF01000010.1, region 1053433-1055206). Highlighted region represents CT-rich region of the promoter.

CHAPTER 6

Time expression analysis of β-BUTX Lqq1a/sGFP in

M. anisopliae

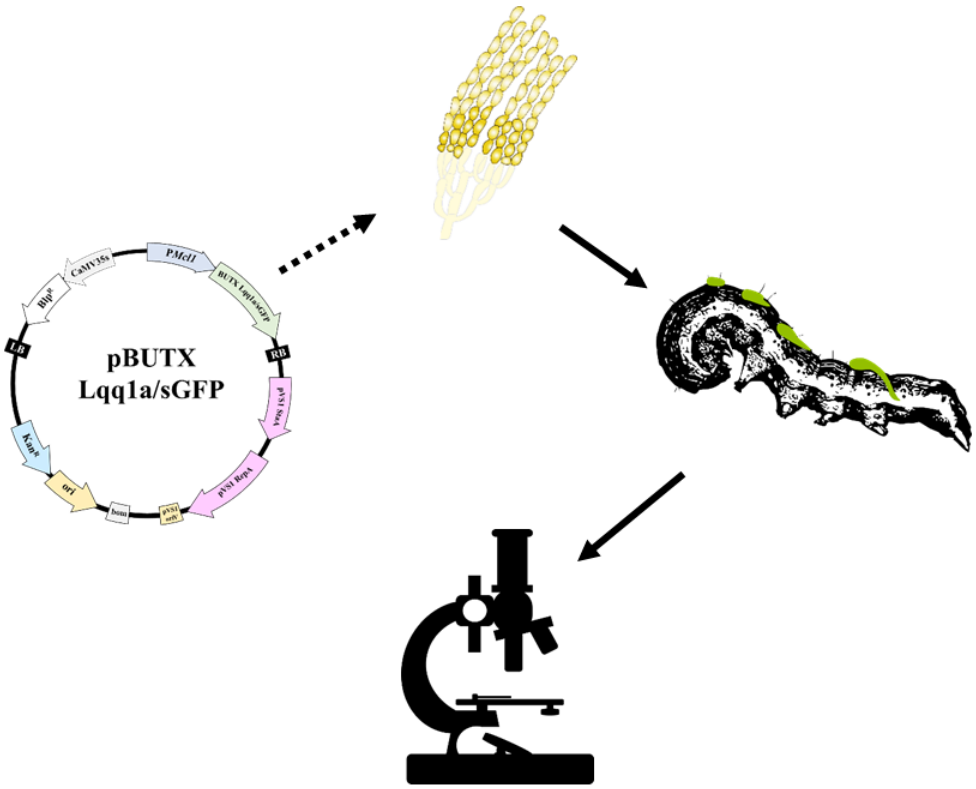

6.1 Introduction

The green fluorescent protein (GFP) has unprecedentedly become an inevitable tool in studying gene expression as well as real time localization of biological macromolecule in biological sciences since its discovery in 1960s (Chalfie et al. 1994). It has been widely used in the protein-protein interaction studies such as fluorescence resonance energy transfer (FRET) and bioluminescence resonance energy transfer (BRET) (Felce et al. 2019, Okamoto et al. 2019, Sun et al. 2019, Tóth et al. 2019). This 28 kDa, β-barrel fluorescent protein was first discovered and extracted from *Aequorea victoria* by Shimomura et al. (1962) and structurally elucidated further by many researchers globally (Ormö et al. 1996, Prasher et al. 1992, Yang et al. 1996). Since then many variants of GFP have evolved due to the structural modification with enhanced spectral as well as fluorescent properties to be utilized in the bacterial, fungal, plant and animal models (Andersen et al. 1998, Davis and Vierstra 1998, Heim and Tsien 1996, Lozoya-Pérez et al. 2018, Pédelacq et al. 2006).

M. anisopliae is a filamentous, entomopathogenic fungus extensively studied and applied as biological control agent that is being regarded as environmental friendly (Roberts and St Leger 2004). This biocontrol agent is reported to be pathogenic against diversified agricultural insect pests since it possess the ability to penetrate insect cuticle based on contact infestation (Thomas and Read 2007). This entomopathogen secrete various pathogenicity related proteins during the infection process such as cuticle degrading chitinase and protease (Fang et al. 2005). In addition to that, several regulatory proteins also play role in spore attachment, appressorium formation and insect immune evasion (Wang and Leger 2006, Wang and Leger 2007, Wang and St Leger 2007a).

Fluorescent labelling studies in the biological organisms help in augmenting the relationship between host-pathogen interaction such as *Metarhizum* interaction with maize roots and bean plants (Barelli et al. 2018, Cai et al. 2019). The importance of Laccase in determining the virulence, conidiation, pigmentation and abiotic stress related factors was studied by fluorescently labelling the laccase gene from *Metarhizum* (Fang et al. 2010). Another protein Perilipin homolog MPL1 from *M. anisopliae* was also studied for their regulatory role in lipid metabolism, virulence and appressorium turgor pressure during the pathogenesis by tagging the perilipin with the GFP (Wang and Leger 2007). Infectivity in the non-target organism could be easily monitored by fluorescent labelling of the transgene of interest (Hu and Leger 2002).

In the present study, fluorescently tagging the scorpion neurotoxin BUTX Lqq1a from *Leiurus quinquestriatus quinquestriatus* which is driven by hemolymph specific promoter Mcl1 from *M. anisopliae* localized as well as the real time expression of BUTX Lqq1a during the insect pathogenesis was carried out.

6.2 Materials and Methods

6.2.1 Microbial strains and culture conditions

Metarhizum anisopliae (MTCC 892) cultures procured from Microbial Type Culture Collection and Gene Bank (MTCC, India) and further maintained in PDA (Potato Dextrose Agar) medium at 25±2ºC. *Escherichia coli* DH5-α was used for bacterial cloning and maintenance of plasmids, and culture was maintained in Luria Bertani (LB) medium at 37ºC. *Agrobacterium tumifaciens* EHA 105 strain grown in LB medium supplemented with Rifampicin (10 µg ml^{-1}) was used for transferring the binary vector and *M. anisopliae* transformation

6.2.2 Vector construction

6.2.2.1 BUTX Lqq1a gene synthesis

Entomopathogenic fungi codon optimized BUTX Lqq1a gene was synthesized as mentioned in the **section 3.2.2 of Chapter 3.** BUTX Lqq1a with 5'-untranslated region and Mcl1 signal sequence was cloned into pUC57 vector (**Fig. 6.1**) and maintained in *E.coli* DH5-α with ampicillin supplemented LB medium.

6.2.2.2 Synthetic Green Fluorescent Protein (sGFP) coding gene amplification

The sGFP harboring vector pAL1 was procured from Fungal Genetic Stock Center, USA (**Fig. 6.2**). The pAL1 was maintained in *E. coli* DH5-α with ampicillin supplemented LB medium. Primers specific for sGFP were designed with BUTX Lqq1a and binary vector overhangs and synthesized (**Table 6.1**) (IDT, Malaysia). The sGFP gene sequence was amplified using pAL1 as a template DNA. The PCR reaction components were 1x HF buffer, 1 µl of 10 mM dNTPs (200 µM), 2.5 µl of 10 µM Forward primer (500 nM), 2.5 µl of 10 µM Reverse primer (500 nM), 1.5 µl of DMSO (3%), 1 µl of plasmid DNA (20 ng), and 1 unit of Phusion DNA Polymerase

(ThermoScientific, USA). The amplification conditions are initial denaturation at 98ºC for 3 min, denaturation at 98ºC for 20 sec, annealing at 62ºC for 45 sec and extension for 45 sec at 72ºC and cycles were repeated for 25-30 times. The final extension was performed at 72ºC for 10 min. Similarly, Promoter Mcl1 along with BUTX Lqq1a was amplified from pMcl1 BUTX Lqq1a using the primers designed to contain the overhangs of binary vector and sGFP gene sequence with annealing temperature of 59ºC. The sGFP and P*Mcl1*-BUTX Lqq1a PCR amplified fragments were gel purified and analyzed using 1% agarose gel electrophoresis.

6.2.2.3 Overlap extension PCR

The P*Mcl1*-BUTX Lqq1a and sGFP fragments were fused using overlap extension PCR. The PCR reaction mixture used were 1x HF buffer, 1 µl of 10 mM dNTPs (200 µM), 2.5 µl of 10 µM Forward primer (500 nM), 1.5 µl of PCR purified sGFP fragment containing BUTX Lqq1a and pCAMBIA overhangs, 1.5 µl of DMSO (3%), 1 µl of plasmid DNA (20 ng), and 1 unit of Phusion DNA Polymerase (ThermoScientific, USA). The amplification conditions used initial denaturation at 98ºC for 3 min, denaturation at 98ºC for 20 sec, annealing at 59ºC for 90 sec and extension for 45 sec at 72ºC and cycles were repeated for 30-35 times. The final extension was performed at 72ºC for 10 min. The final PCR products were gel purified and analyzed using 1% agarose gel electrophoresis.

6.2.2.4 Gibson assembly reaction

The *Agrobacterium* binary vector pCAMBIA3300 (5 µg) was double digested with EcoRI and HindIII restriction enzymes in NEB cutsmart buffer at 37ºC for 3-4 hr and gel extracted using TAKARA Gel extraction kit. The purified plasmid was analyzed in 1% agarose gel electrophoresis and visualized using a ChemiDoc XRS™ gel

documentation system (Bio-rad, USA). The double digested binary vector and the PCR fragments were taken in different ratios (1:1, 3:1 and 1:3) and ligated using Gibson assembly reaction at 50ºC for 45-60 min. The ligated product (5 µl) was transferred into DH5-α chemical competent cell prepared using the protocol followed in the **section3.2.3.1.2** of **Chapter 3** and screening was performed in the kanamycin antibiotic (50 µg ml^{-1}) containing LB medium.

6.2.2.5 Colony PCR clone confirmation

Colony PCR was performed on the colonies growing on the antibiotic selection medium. A loop full of cultures were transferred into 5 µl nuclease free water and PCR reaction components containing BUTX Lqq1a specific primers were added and reaction was performed with normal PCR conditions using Taq DNA polymerase (NEB, USA) and the annealing temperature 57ºC was followed for the amplification. The amplified PCR products were analyzed using 1% agarose gel electrophoresis and visualized using ChemiDoc XRS™ gel documentation system (Bio-rad, USA).

6.2.2.6 Plasmid isolation

Plasmid DNA was isolated according to Bimboim and Doly (1979) modified alkaline lysis method with modifications. Plasmid DNA isolation was performed according to the modified protocol mentioned in the **section 3.2.3.1.4 of Chapter 3.**

6.2.2.7 Clone confirmation by Double digestion

The plasmid (2 µg) isolated was double digested in NEB cutsmart buffer with XbaI and HindIII restriction enzymes at 37ºC for 1 hr and the digested fragments were analyzed in 1% Agarose gel electrophoresis, and imaging was performed in ChemiDoc XRS™ gel documentation system (Bio-rad, USA).

6.2.3 *Agrobacterium* mediated transformation

6.2.3.1 *Agrobacterium* electro-competent cell preparation

Electro-competent *Agrobacterium* cells were prepared according to the protocol followed in the **Chapter 3 of section 3.2.5.1.**

6.2.3.2 Electroporation

PCR positive clones were used for the electroporation. The plasmids suspended in nuclease free water were used to avoid the arching during the electroporation**.** Plasmid (5 µg) was mixed with 100 µl electro-competent *Agrobacterium* cells and transferred into 0.2 cm electroporation cuvette and incubated for 20-30 min on ice. Further electroporation was performed at following conditions 1000-1200 V, 25 µF, 600 Ω using Biorad Gene PulserXcell™ electroporation apparatus. LB medium was immediately added to the electroporated cultures aseptically and incubated for 2 hr at 28ºC in 200 rpm. Post-incubation *Agrobacterium* cells were plated on LB Agar containing rifampicin (20 µg ml^{-1}) and kanamycin (50 µg ml^{-1}) and then incubated for two days at 28ºC in static condition. The plasmid was isolated from the randomly selected clones and gene-specific PCR confirmation was carried out on (1%) agarose gel electrophoresis system.

6.2.3.3 Co-cultivation with *M. anisopliae*

Agrobacterium harboring plasmids were used for the co-cultivation with *M. anisopliae.* Co-cultivation was performed according to the protocol Sevim et al. (2012) with little modifications that is mentioned in the **section 3.2.5.3 of Chapter 3.** Transformants selection was carried out in the glufosinate ammonium containing M-100 minimal medium.

6.2.4 *M. anisopliae* clonal confirmation

Clonal confirmation was performed by isolation of genomic DNA from the *M. anisopliae* clones consecutively grown for 3-4 generations without any selection pressure. Genomic DNA isolation was performed according to the protocol followed in **Chapter 3: Section 3.2.6** and PCR was performed with gene specific primers and analyzed using 1% agarose gel electrophoresis.

6.2.5 Haemolymph induction and Reverse transcription-PCR analysis

6.2.5.1 Haemolymph induction

All clones and control were evaluated for the hemolymph inducing ability of the promoter, using the hemolymph extracted from *Samia Cynthia* silk worm. Initially, inoculum culture was grown in Potato Dextrose Broth (PDB) for two days at 28ºC in orbital incubator shaker. Post-growth, wet culture (1 g) was transferred onto 10 ml of silkworm hemolymph. After culturing at 28ºC for 12 hr, mycelium was collected by centrifugation for RNA extraction, and the filtrate was stored in -20ºC for further western blot analysis.

6.2.5.2 RNA extraction and transcript analysis

Total RNA was extracted using RNAiso Plus kit (Takara, Japan) and genomic DNA contamination was removed by using DNAse I treatment (Promega). One microgram of total RNA was used for cDNA synthesis (SuperScript™ III first-strand synthesis system, Invitrogen, USA). Synthesized cDNA was used for semi-quantitative RT-PCR analysis based on BUTX Lqq1a gene specific primers and GPDH used as internal control (**Table 6.2**).

6.2.6 Western blot analysis

The relative expression of fusion protein was evaluated based on the hemolymph induction and specific binding affinity to the antibody. The western blotting analysis was performed according to the protocol followed in the **Chapter 3 of Section 3.2.8.**

6.2.7 Fluorescence microscopy analysis

Expressional pattern of scorpion toxin fused with sGFP was evaluated using fluorescent microscopy analysis. Initially, *M. anisopliae* initial inoculum was prepared by growing the culture for 36-48 hr in the potato dextrose broth. Harvested mycelial culture was inoculated in the hemolymph added medium and observed under Nikon Eclipse Ti2 inverted fluorescence microscope using excitation filter 490 nm at 0, 1, 3 and 6 hr interval to assess the time of expression of sGFP. Image processing was performed with NIS elements (V4.5) analysis software.

6.3 Results

6.3.1 pBUTX Lqq1a/sGFP vector construction

In the present study to express the fusion protein containing scorpion toxin and fluorescent probe sGFP protein, initially scorpion toxin was codon optimized successfully to express in the entomopathogenic fungus *M. anisopliae.* This codon optimized gene along with Mcl1 promoter (P*Mcl1*), 5'-untransllated region and Mcl1 signal peptide sequence were successfully amplified form the plasmid pMcl1-BUTX Lqq1a (**Fig. 6.3**). Subsequently, sGFP amplified from pAL1 vector was efficiently fused downstream of BUTX Lqq1a using Gibson assembly reaction which further resulted in the fusion fragment containing P*Mcl1*-BUTX Lqq1a/sGFP (**Fig. 6.3**). Following the successful fusion, fragment was ligated with vector pCAMBIA 3300, which led to the development of *Agrobacterium* binary vector pBUTX Lqq1a/sGFP. The confirmation of P*Mcl1*-BUTX Lqq1a/sGFP ligation in the binary vector was successfully done by PCR amplification (**Fig. 6.4**) followed by plasmid isolation (**Fig. 6.5**) and restriction enzyme digestion (**Fig. 6.6**). **Fig. 6.7** represents the schematic arrangement of fused fragments in the binary vector.

6.3.2 Genomic integration analysis

Genomic integration is an essential requisite step in the stable expression of the transgene in *M. anisopliae. Agrobacterium* carrying the BUTX Lqq1a/sGFP in the binary vector was successfully used to transfer the transgene into *M. anisopliae* and the clones were further screened on glufosinate-ammonium containing selection medium. Subsequently, mitotically stable clones were selected by growing in the PDA without any selection pressure. Genomic DNA was isolated successfully from the randomly selected positive clones (**Fig. 6.8**). Having isolated genomic DNA, clonal confirmation was

successfully done by PCR with initially bar gene specific primers (**Fig. 6.9**), BUTX Lqq1a/sGFP specific primers (**Fig. 6.10**) and finally with P*Mcl1*-BUTX Lqq1a/sGFP specific primers (**Fig. 6.11**).

6.3.3 Semi-quantitative RT-PCR analysis

Semi-quantitative RT-PCR analysis was performed to assess the relative expression of transcripts at the mRNA level. Total RNA was successfully isolated from the hemolymph induced clones and the wild type and converted into cDNA. The use of cDNA as template for the amplification of BUTX Lqq1a clearly indicated the presence of transcripts at relatively greater density and absence of the same transcript in the wild type suggested that not only the genomic integration but also the expression of BUTX Lqq1a/sGFP (**Fig. 6.12**)

6.3.4 Western blot analysis

Western blott analysis was carried out to analyze the ability of the Mcl1 promoter to induce the expression of scorpion toxic gene fused with the fluorescent probe sGFP. Hemolymph induced fractions when analyzed by western blot specified the inducing ability of Promoter Mcl1, which could be observed through the ability of BUTX Lqq1a antibody binding (**Fig. 6.13**).

6.3.5 Fluorescence microscopy analysis

The relative time of BUTX Lqq1a expressional analysis was assessed based on the sGFP expression when induced with hemolymph for various time interval. Initial assessment of sGFP expression at 0 hr resulted in almost negligible intensity of fluorescence signal as observed in the induced as well as the wild type control (**Fig. 6.14**). However, the fluorescence intensity of sGFP at 1 hr (**Fig. 6.15**) and 3 hr (**Fig. 6.16**)

interval have increased exponentially when compared to the wild type control Subsequent analysis resulted in the relatively reduced expression when compared to 1 and 3 hr expression.

6.4 Discussion

The present study was experimented to ascertain the relative expressional time of scorpion toxic protein during the insect pathogenesis process that has been driven by hemolymph specific inducible promoter Mcl1 by coupling with fluorescent molecule. Fluorescent markers played a major role in the development of effective eukaryotic promoter with reduced size and magnified transgene expression. GFP which is driven by *Metarhizium* collagen like promoter truncation studies have led to the development of efficiently reduced size promoter with enhanced GFP expression (Kanjo et al. 2019). The expression of class 1 laccase (MLac1) by GFP fusion led to understanding ultimate changes attributed to the laccase expression during pathogenesis (Fang et al. 2010). Similarly, F-actin dynamic studies were also conducted in *Neurospora crassa* by co-expressing the fluorescent protein with the actin binding proteins (Berepiki et al. 2010).

In the present study, in order to monitor expression in real-time, synthetic green fluorescent protein was fused C-terminally to the scorpion toxic gene BUTX Lqq1a successfully. The most widely studied toxin AaIT was also fused N-terminally to the green fluorescent protein and its relative expression was studied by RT-PCR as well as microscopic analysis. A fluorescently labelled AaIT, which is a neurotoxic insecticidal protein from *Androctonus australis* when expressed under the control of P*Mcl1*, led to the understanding of AaIT relative expression during pathogenesis of *Manduca sexta* and *Aedes aegypti*. Real time analysis of AaIT expression in the hemolymph by using RT-PCR analysis revealed the abundance of AaIT transcripts within 30 minutes of induction (Wang and St Leger 2007b). Similarly, BUTX Lqq1a coupled with sGFP also revealed the inducability of P*Mcl1* promoter. Initially negligible GFP expression was observed however, enhanced GFP fluorescence intensity was observed after 1 hr of hemolymph

induction. *M. anisopliae* transformed to express GFP constitutively, was able to track the expression in the thorax of *A. aegypti* mosquito (Wang and St Leger 2007b).

These experiments suggested that, functionally tagging the fluorescent molecule with the protein of interest or particular microorganism, could pave the way to understand the host-pathogen interactions dynamically in real time as well as the expression of gene of interest in real time in localized position within the host or pathogen when driven by specific promoter.

6.5 Conclusion

In the present study, BUTX Lqq1a was fused with synthetic green fluorescent protein and cloned in pCAMBIA binary vector which resulted in the development of hemolymph specific expression vector pBUTX Lqq1a/sGFP which was further used to transform *M. anisopliae*. Semi-quantitative RT-PCR and western blot analysis indicated the genomic integration and functional expression of the fusion protein. Fluorescent microscopy analysis also led to the understanding of the sGFP expression during the hemolymph induction. This suggests that, functionally fusing the sGFP with virulence factors, their expression could be monitored in real time, and also could help us to understand the host range of fluorescently tagged entomopathogenic fungi.

Table 6.1 List of primers used for BUTX Lqq1a and sGFP fusion

Primers	5’----------3’
LqqIT1 RP-GFP OH	CAGCTCCTCGCCCTTGCTCACCATGGCGGCGGCCTCGGCGTTGATGGTGACAAAGTCGC
LqqIT1-Linker-GFP-FP	GCGACTTTGTCACCATCAACGCCGAGGCCGCCGCCATGGTGAGCAAGGGCGAG
pCAM OH-EcoRI-MCL1 PRO-FP	GGAAACAGCTATGACCATGATTACGAATTCAATCATGCAGCGCTATGAGAGC
sGFP-RP-HindIII- pCAM OH	CGTTGTAAAACGACGGCCAGTGCCAAGCTTTTACTTGTACAGCTCGTCCATGCC

Table 6.2 List of primers used for semi-quantitative RT-PCR analysis

Primers	5’----------3’
RT-Lqq FP	AAGAAGAACGGCTACGCTG
RT-Lqq RP	GTTGATGGTGACAAAGTCG
RT-GPDH FP	TGAAGCTCCGGGAAAGATG
RT-GPDH RP	GACTTGCTGCTGACTCACG

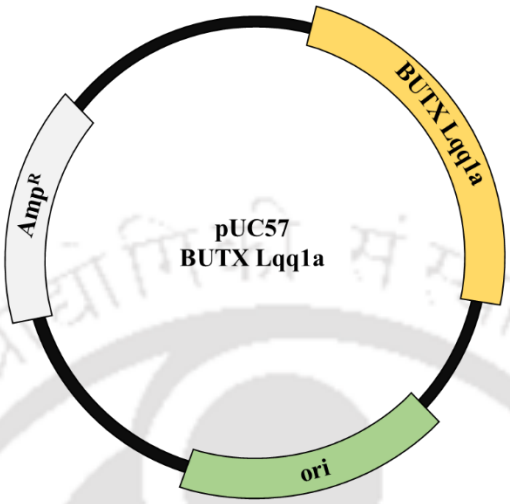

Fig. 6.1 Plasmid map of pUC57 harboring BUTX Lqq1a

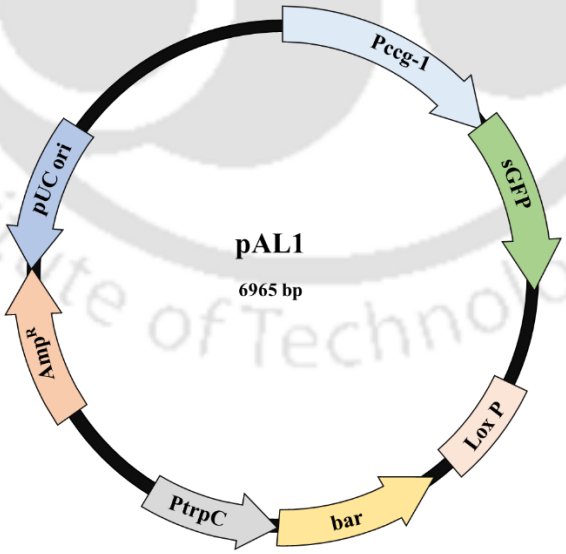

Fig. 6.2 Plasmid map of pAL1 harboring sGFP

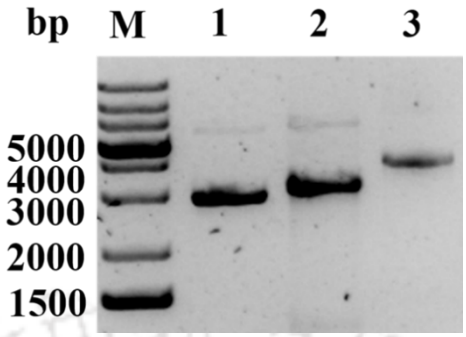

Fig. 6.3 PCR fragments amplified for BUTX Lqq1a/sGFP cloning into pCAMBIA3300 vector. Lane 1: Mcl1 Promoter (calculated size ~2.9 kb), Lane 2: P*Mcl1* BUTX Lqq1a (calculated size ~3.1 Kbp), Lane 3: P*Mcl1*-BUTX Lqq1a/sGFP (Size ~3.8 Kbp) and Lane M: O' GeneRuler 1 Kb Plus DNA Ladder.

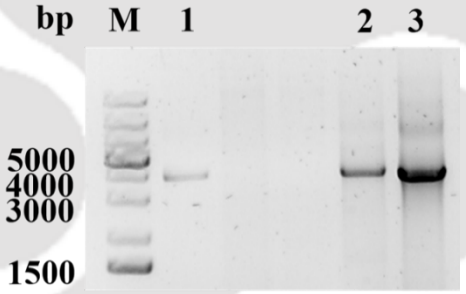

Fig. 6.4 Colony PCR confirmation for BUTX Lqq1a/sGFP cloning into pCAMBIA vector. Lane 1: Positive control (calculated size ~3.8 Kbp), Lane 2 and 3: P*Mcl1*-BUTX-Lqq1a/sGFP (calculated size ~3.8 Kbp), and Lane M: O' GeneRuler 1 Kb Plus DNA Ladder.

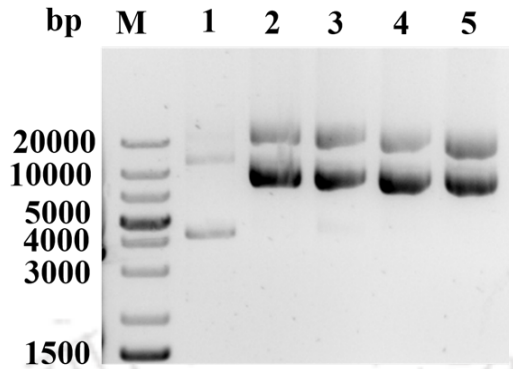

Fig. 6.5 Plasmids isolated from the pBUTX Lqq1a/sGFP clones. Lane 1: pCAMBIA 3300 alone, Lane 2-5: pBUTX Lqq1a/sGFP (calculated size ~12 Kbp), and Lane M: O' GeneRuler 1 Kb Plus DNA Ladder.

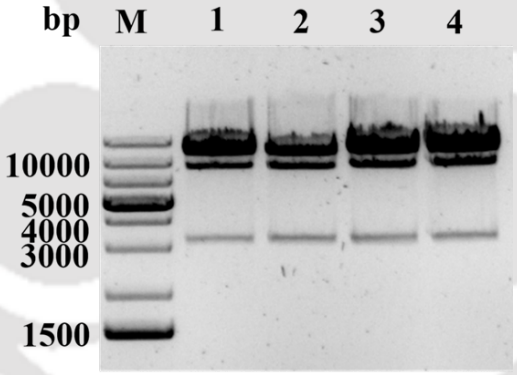

Fig. 6.6 Clone confirmation by restriction enzyme digestion of pBUTX Lqq1a/sGFP clonal plasmids. Lane 1-4: pBUTX Lqq1a/sGFP digested with XbaI and HindIII (calculated size ~3.150 Kbp), and Lane M: O' GeneRuler 1 Kb Plus DNA Ladder.

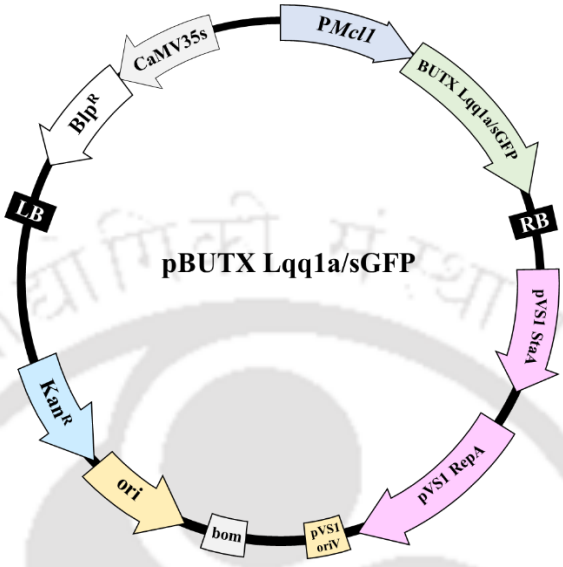

Fig. 6.7 Schematic representation of pBUTX Lqq1a/sGFP binary vector

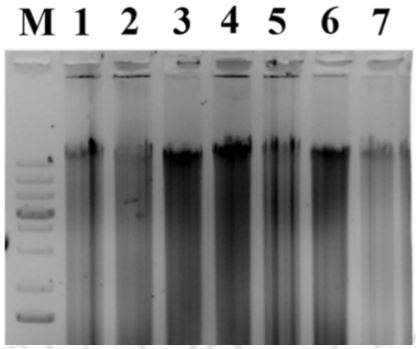

Fig. 6.8 Genomic DNA isolated from *M. anisopliae* carrying BUTX Lqq1a/sGFP. Lane 1 to 7: Genomic DNA isolated from clones Ma-BUTX Lqq1a/sGFP, and Lane M: O' GeneRuler 1 Kb Plus DNA Ladder.

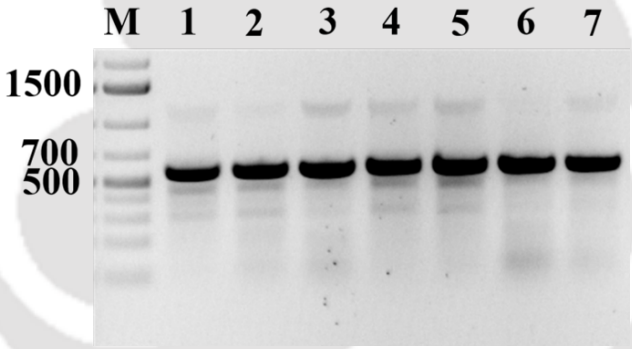

Fig.6.9 Clonal confirmation by *bar* gene amplification for *M. anisopliae* carrying BUTX Lqq1a/sGFP. Lane 1 to 7: *bar* gene amplified from clones Ma-BUTX-Lqq1a/sGFP (size~552 bp), and Lane M: O' GeneRuler 1 Kb Plus DNA Ladder.

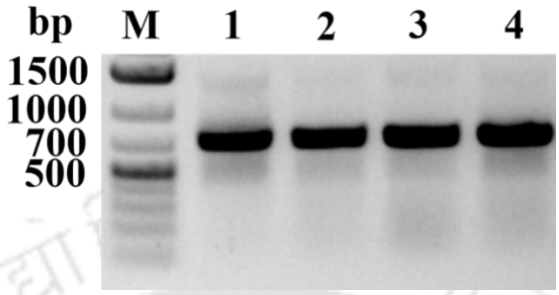

Fig. 6.10 PCR clonal confirmation by BUTX Lqq1a/sGFP gene amplification from Ma-BUTX Lqq1a/sGFP. Lane 1 to 4: BUTX Lqq1a/sGFP gene amplification from clones Ma-BUTX Lqq1a/sGFP (size~930 bp), and Lane M: O' GeneRuler 1 Kb Plus DNA Ladder.

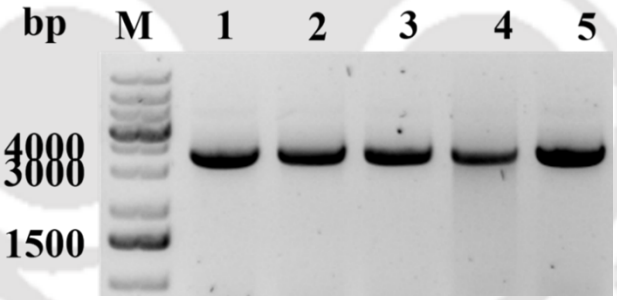

Fig. 6.11 PCR clonal confirmation for the P*Mcl1*-BUTX Lqq1a/sGFP gene amplified from Ma-BUTX Lqq1a/sGFP. Lane 1 to 5: P*Mcl1*-BUTX Lqq1a/sGFP gene amplified from clones Ma-BUTX-Lqq1a/sGFP (size~3815 bp), and Lane M: O' GeneRuler 1 Kb Plus DNA Ladder.

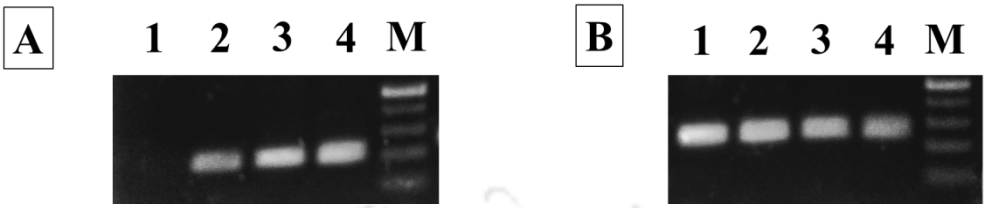

Fig. 6.12 Semi-quantitative RT-PCR analysis of BUTX Lqq1a transcripts amplification from Ma-BUTX Lqq1a/sGFP clones. A) Lane 1: Ma-wild type, Lane 2-4: BUTX Lqq1a amplified from Ma-BUTX Lqq1a/sGFP clones. B) GPDH internal control amplified from wild type (Lane 1) and clones (Lane 2-4), and Lane M: O' GeneRuler 1 Kb Plus DNA Ladder. Bands represent 500, 400, 300, 200 and 75 bp from top to bottom order.

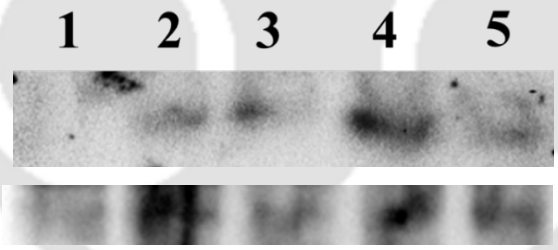

Fig. 6.13 Western blot analysis of fusion protein BUTX Lqq1a/sGFP expression from Ma-BUTX Lqq1a/sGFP clones and Loading control (β-tubulin). Lane 1: Wild type *M. anisopliae* induced with hemolymph and Lane 2 to 5: BUTX Lqq1a/sGFP detected using BUTX Lqq1a primary antibody.

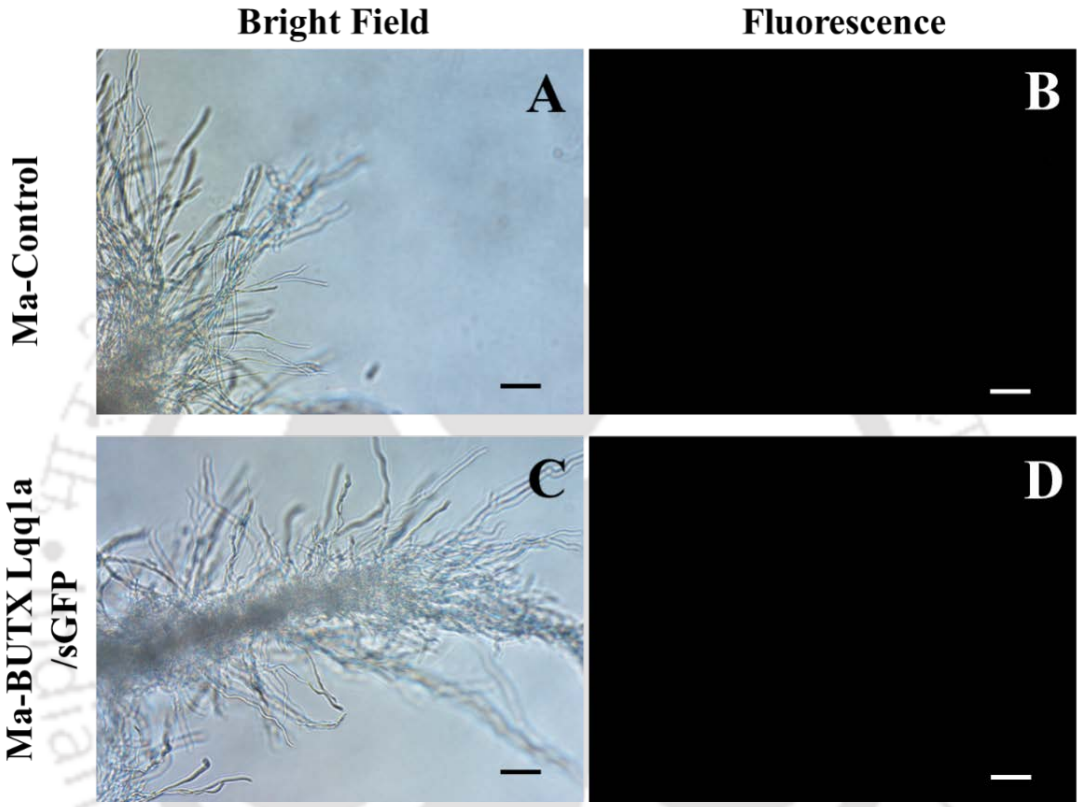

Fig. 6.14 Time of expressional analysis of BUTX Lqq1a/sGFP from Ma-BUTX Lqq1a/sGFP clones using Fluorescence microscopy. A and B indicates the wild type *M. anisopliae* induced with hemolymph at 0 hr in bright field as well as fluorescence field. C and D represents the Ma-BUTX Lqq1a/sGFP induced at 0 hr in bright field as well as fluorescence field. Scale bar represents 20 µM.

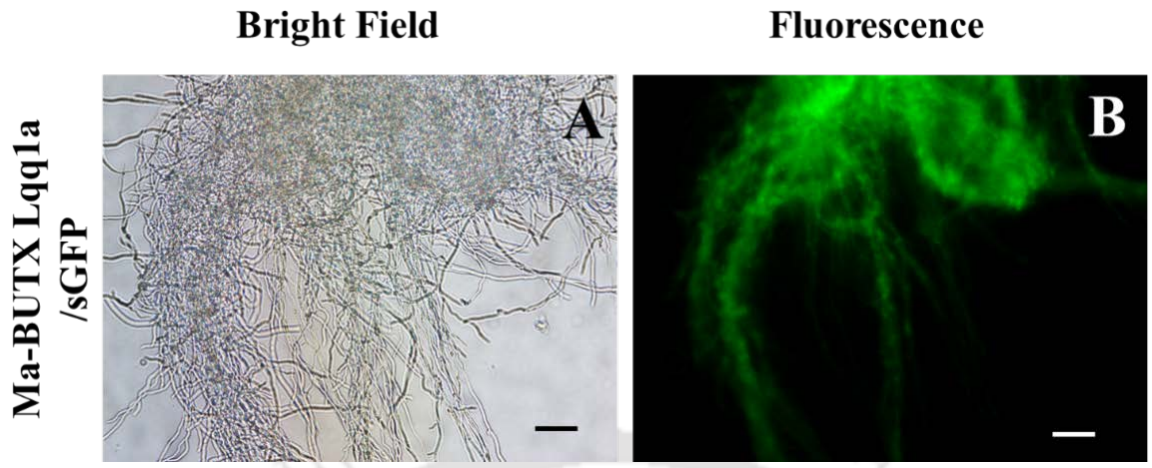

Fig. 6.15 Time of expressional analysis of BUTX Lqq1a/sGFP from Ma-BUTX Lqq1a/sGFP clones using Fluorescence microscopy at 1 hr interval. A and B represents the Ma-BUTX Lqq1a/sGFP induced at 1 hr interval in bright field as well as fluorescence field. Scale bar represents 20 µM.

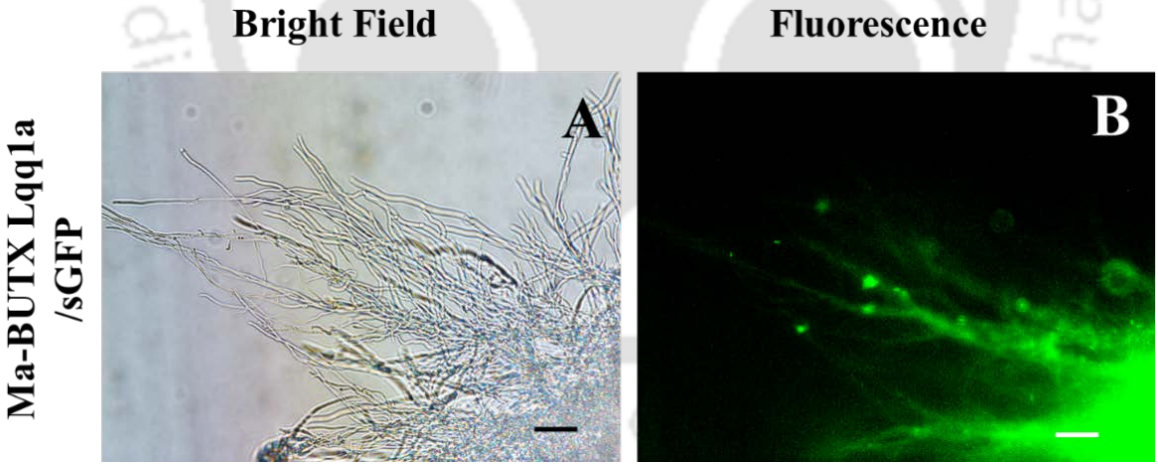

Fig. 6.16 Time of expressional analysis of BUTX Lqq1a/sGFP from Ma-BUTX Lqq1a/sGFP clones using Fluorescence microscopy at 3 hr interval. A and B represents the Ma-BUTX Lqq1a/sGFP induced at 3 hr interval in bright field as well as fluorescence field. Scale bar represents 20 µM.

REFERENCES

Abbas, N., Shad, S. A., Razaq, M., Waheed, A. and Aslam, M. (2014) Resistance of *Spodoptera litura* (Lepidoptera: Noctuidae) to profenofos: Relative fitness and cross resistance. *Crop Protection, 58*, pp. 49-54.

Agra-Neto, A. C., Napoleao, T. H., Pontual, E. V., Santos, N. D. D., Luz, L. D., de Oliveira, C. M. F., de Melo-Santos, M. A. V., Coelho, L. C. B. B., Navarro, D. M. D. F. and Paiva, P. M. G. (2014) Effect of *Moringa oleifera* lectins on survival and enzyme activities of A*edes aegypti* larvae susceptible and resistant to organophosphate. *Parasitology Research, 113*(1), pp. 175-184.

Ali, G., van der Werf, W. and Vlak, J. M. (2018) Biological and genetic characterization of a Pakistani isolate of *Spodoptera litura* nucleopolyhedrovirus. *Biocontrol Science and Technology, 28*(1), pp. 20-33.

Ali, M. P., Kato, T. and Park, E. Y. (2015) Improved insecticidal activity of a recombinant baculovirus expressing spider venom cyto-insectotoxin. *Applied Microbiology and Biotechnology, 99*(23), pp. 10261-10269.

Alikhani, M., Safavi, S. A. and Iranipour, S. (2019) Effect of the entomopathogenic fungus, *Metarhizium anisopliae* (Metschnikoff) Sorokin, on demographic fitness of the tomato leaf miner, *Tuta absoluta* (Meyrick)(Lepidoptera: Gelechiidae). *Egyptian Journal of Biological Pest Control, 29*(1), pp. 23.

Almaaytah, A., Zhou, M., Wang, L., Chen, T. B., Walker, B. and Shaw, C. (2012) Antimicrobial/cytolytic peptides from the venom of the North African scorpion, *Androctonus amoreuxi:* Biochemical and functional characterization of natural peptides and a single site-substituted analog. *Peptides, 35*(2), pp. 291-299.

Andersen, J. B., Sternberg, C., Poulsen, L. K., Bjørn, S. P., Givskov, M. and Molin, S. (1998) New unstable variants of green fluorescent protein for studies of transient gene expression in bacteria. *Applied Environmental Microbiology, 64*(6), pp. 2240-2246.

Ansari, M. S., Moraiet, M. A. and Ahmad, S. (2014) Insecticides: impact on the environment and human health. in *Environmental deterioration and human health*: Springer. pp. 99-123.

AshaRani, P. V., Mun, G. L. K., Hande, M. P. and Valiyaveettil, S. (2009) Cytotoxicity and Genotoxicity of Silver Nanoparticles in Human Cells. *ACS Nano, 3*(2), pp. 279-290.

Au, S., Wu, W., Zhou, L. X., Theilmann, D. A. and Pante, N. (2016) A new mechanism for nuclear import by actin-based propulsion used by a baculovirus nucleocapsid. *Journal of Cell Science, 129*(15), pp. 2905-2911.

Ba, M. N., Huesing, J. E., Tamo, M., Higgins, T. J. V., Pittendrigh, B. R. and Murdock, L. L. (2018) An assessment of the risk of Bt-cowpea to non-target organisms in West Africa. *Journal of Pest Science, 91*(4), pp. 1165-1179.

Bagga, S., Hu, G., Screen, S. E. and Leger, R. J. S. (2004) Reconstructing the diversification of subtilisins in the pathogenic fungus *Metarhizium anisopliae*. *Gene, 324*, pp. 159-169.

Banerjee, S., Vishwanath, P., Cui, J., Kelleher, D. J., Gilmore, R., Robbins, P. W. and Samuelson, J. (2007) The evolution of N-glycan-dependent endoplasmic reticulum quality control factors for glycoprotein folding and degradation. *Proceedings of National Academy of Science of United States of America, 104*(28), pp. 11676-11681.

Barelli, L., Moreira, C. C. and Bidochka, M. J. (2018) Initial stages of endophytic colonization by *Metarhizium* involves rhizoplane colonization. *Microbiology, 164*(12), pp. 1531-1540.

Batcho, A., Ali, M., Samuel, A. O., Shehzad, K. and Rashid, B. (2018) Comparative study of the effects of five *Beauveria bassiana* (Balsamo) Vuillemin (Ascomycota: Hypocreales) strains on

cabbage moth *Plutella xylostella* (L.)(Lepidoptera: Plutellidae). *Cogent Environmental Science, 4*(1), pp. 1477542.

Bayramoglu, Z., Gencer, D., Muratoglu, H., Efe, D., Nalcacioglu, R., Demirbag, Z. and Demir, I. (2018) Characterization of a nucleopolyhedrovirus variant of the gypsy moth, *Lymantria dispar* (Lepidoptera: Lymantriidae) in Turkey. *International Journal of Pest Management, 64*(2), pp. 119-127.

Bebber, D. P., Holmes, T., Smith, D. and Gurr, S. J. (2014) Economic and physical determinants of the global distributions of crop pests and pathogens. *New Phytologist, 202*(3), pp. 901-910.

Beketov, M. A., Kefford, B. J., Schäfer, R. B. and Liess, M. (2013) Pesticides reduce regional biodiversity of stream invertebrates. *Proceedings of the National Academy of Sciences, 110*(27), pp. 11039-11043.

Bell, H. A., Fitches, E. C., Down, R. E., Marris, G. C., Edwards, J. P., Gatehouse, J. A. and Gatehouse, A. M. R. (1999) The effect of snowdrop lectin (GNA) delivered via artificial diet and transgenic plants on *Eulophus pennicornis* (Hymenoptera : Eulophidae), a parasitoid of the tomato moth *Lacanobia oleracea* (Lepidoptera : Noctuidae). *Journal of Insect Physiology, 45*(11), pp. 983-991.

Beneteau, J., Renard, D., Marche, L., Douville, E., Lavenant, L., Rahbe, Y., Dupont, D., Vilaine, F. and Dinant, S. (2010) Binding properties of the N-Acetylglucosamine and high-mannose N-glycan Pp2-A1 phloem lectin in *Arabidopsis*. *Plant Physiology, 153*(3), pp. 1345-1361.

Berepiki, A., Lichius, A., Shoji, J. Y., Tilsner, J. and Read, N. D. (2010) F-Actin Dynamics in *Neurospora crassa*. *Eukaryotic Cell, 9*(4), pp. 547-557.

Bernardi, O., Sorgatto, R. J., Barbosa, A. D., Domingues, F. A., Dourado, P. M., Carvalho, R. A., Martinelli, S., Head, G. P. and Omoto, C. (2014) Low susceptibility of S*podoptera cosmioides, Spodoptera eridania* and *Spodoptera frugiperda* (Lepidoptera: Noctuidae) to genetically-modified soybean expressing Cry1Ac protein. *Crop Protection, 58*, pp. 33-40.

Berry, C. (2012) The bacterium, *Lysinibacillus sphaericus*, as an insect pathogen. *Journal of Invertebrate Pathology, 109*(1), pp. 1-10.

Bharathi, Y., Kumar, S. V., Pasalu, I. C., Balachandran, S. M., Reddy, V. D. and Rao, K. V. (2011) Pyramided rice lines harbouring *Allium sativum* (asal) and *Galanthus nivalis* (gna) lectin genes impart enhanced resistance against major sap-sucking pests. *Journal of Biotechnology, 152*(3), pp. 63-71.

Bidari, F., Shams-Bakhsh, M. and Mehrabadi, M. (2018) Isolation and characterization of a Serratia marcescens with insecticidal activity from *Polyphylla olivieri* (Col.: Scarabaeidae). *Journal of Applied Entomology, 142*(1-2), pp. 162-172.

Bideshi, D. K., Waldrop, G., Fernandez-Luna, M. T., Diaz-Mendoza, M., Wirth, M. C., Johnson, J. J., Park, H. W. and Federici, B. A. (2013) Intermolecular interaction between Cry2Aa and Cyt1Aa and its effect on larvicidal activity against *Culex quinquefasciatus*. *Journal of Microbiology and Biotechnology, 23*(8), pp. 1107-1115.

Bilgo, E., Lovett, B., Fang, W. G., Bende, N., King, G. F., Diabate, A. and St Leger, R. J. (2017) Improved efficacy of an arthropod toxin expressing fungus against insecticide-resistant malaria-vector mosquitoes. *Scientific Reports, 7*.

Bimboim, H. and Doly, J. (1979) A rapid alkaline extraction procedure for screening recombinant plasmid DNA. *Nucleic Acids Research, 7*(6), pp. 1513-1523.

Birch, A. N. E., Geoghegan, I. E., Majerus, M. E. N., McNicol, J. W., Hackett, C. A., Gatehouse, A. M. R. and Gatehouse, J. A. (1999) Tri-trophic interactions involving pest aphids, predatory

2-spot ladybirds and transgenic potatoes expressing snowdrop lectin for aphid resistance. *Molecular Breeding, 5*(1), pp. 75-83.

Bird, L. J. (2018) Pyrethroid and carbamate resistance in Australian *Helicoverpa armigera* (Lepidoptera: Noctuidae) from 2008 to 2015: what has changed since the introduction of Bt cotton? *Bulletin of Entomological Research, 108*(6), pp. 781-791.

Boddupally, D., Tamirisa, S., Gundra, S. R., Vudem, D. R. and Khareedu, V. R. (2018) Expression of hybrid fusion protein (Cry1Ac::ASAL) in transgenic rice plants imparts resistance against multiple insect pests. *Scientific reports, 8*.

Bogo, M. R., Vainstein, M. H., Aragao, F. J. L., Rech, E. and Schrank, A. (1996) High frequency gene conversion among benomyl resistant transformants in the entomopathogenic fungus *Metarhizium anisopliae*. *FEMS Microbiology Letters, 142*(1), pp. 123-127.

Boone, M. D., Hammond, S. A., Veldhoen, N., Youngquist, M. and Helbing, C. C. (2013) Specific time of exposure during tadpole development influences biological effects of the insecticide carbaryl in green frogs (*Lithobates clamitans*). *Aquatic toxicology, 130*, pp. 139-148.

Bosch, D., Schipper, B., Vanderkleij, H., Demaagd, R. A. and Stiekema, W. J. (1994) Recombinant *Bacillus thuringiensis* crystal proteins with new properties - possibilities for resistance management. *Bio-Technology, 12*(9), pp. 915-918.

Bosmans, F. and Tytgat, J. (2007) Voltage-gated sodium channel modulation by scorpion α-toxins. *Toxicon, 49*(2), pp. 142-158.

Boyer, S., Zhang, H. and Lempérière, G. (2012) A review of control methods and resistance mechanisms in stored-product insects. *Bulletin in Entomological Research, 102*(2), pp. 213-229.

Bravo, A., Likitvivatanavong, S., Gill, S. S. and Soberón, M. (2011) *Bacillus thuringiensis*: a story of a successful bioinsecticide. *Insect Biochemistry and Molecular Biology, 41*(7), pp. 423-431.

Bravo, A., Lopez-Diaz, J. A., Yamamoto, T., Harding, K., Zhao, J. Z., Mendoza, G., Onofre, J., Torres-Quintero, M. C., Nelson, M. E., Wu, G. S., Sethi, A. and Soberon, M. (2018) Susceptible and mCry3A resistant corn rootworm larvae killed by a non-hemolytic *Bacillus thuringiensis* Cyt1Aa mutant. *Scientific Reports, 8*.

Briefs, I. (2017) Global Status of Commercialized Biotech/GM Crops in 2017: Biotech crop adoption surges as economic benefits accumulate in 22 years.

Bruce, T. J. A. (2012) GM as a route for delivery of sustainable crop protection. *Journal of Experimental Botany, 63*(2), pp. 537-541.

Cai, N., Wang, F., Nong, X., Wang, G., McNeill, M., Cao, G., Hao, K., Liu, S. and Zhang, Z. (2019) Visualising confirmation of the endophytic relationship of *Metarhizium anisopliae* with maize roots using molecular tools and fluorescent labelling. *Biocontrol Science and Technology*, pp. 1-14.

Calderaro, A., Gorrini, C., Piccolo, G., Montecchini, S., Buttrini, M., Rossi, S., Piergianni, M., Arcangeletti, M. C., De Conto, F. and Chezzi, C. (2014) Identification of *Borrelia* species after creation of an in-house MALDI-TOF MS database. *Plos One, 9*(2), pp. e88895.

Cao, Y. Q., Jiao, R. and Xia, Y. X. (2012) A strong promoter, PMagpd, provides a tool for high gene expression in entomopathogenic fungus, *Metarhizium acridum*. *Biotechnology Letters, 34*(3), pp. 557-562.

Carriere, Y., Degain, B. A., Unnithan, G. C., Harpold, V. S., Heuberger, S., Li, X. C. and Tabashnik, B. E. (2018) Effects of seasonal changes in cotton plants on the evolution of resistance to

pyramided cotton producing the Bt toxins Cry1Ac and Cry1F in *Helicoverpa zea*. *Pest Management Science, 74*(3), pp. 627-637.

Catterall, W. A., Cestèle, S., Yarov-Yarovoy, V., Frank, H. Y., Konoki, K. and Scheuer, T. (2007) Voltage-gated ion channels and gating modifier toxins. *Toxicon, 49*(2), pp. 124-141.

Cestèle, S. and Catterall, W. A. (2000) Molecular mechanisms of neurotoxin action on voltage-gated sodium channels. *Biochimie, 82*(9-10), pp. 883-892.

Chakraborty, J., Sen, S., Ghosh, P., Sengupta, A., Basu, D. and Das, S. (2016) Homologous promoter derived constitutive and chloroplast targeted expression of synthetic cry1Ac in transgenic chickpea confers resistance against *Helicoverpa armigera*. *Plant Cell Tissue and Organ Culture, 125*(3), pp. 521-535.

Chalfie, M., Tu, Y., Euskirchen, G., Ward, W. W. and Prasher, D. C. (1994) Green fluorescent protein as a marker for gene expression. *Science, 263*(5148), pp. 802-805.

Chang, J. H., Choi, J. Y., Jin, B. R., Roh, J. Y., Olszewski, J. A., Seo, S. J., O'Reilly, D. R. and Je, Y. H. (2003) An improved baculovirus insecticide producing occlusion bodies that contain *Bacillus thuringiensis* insect toxin. *Journal of Invertebrate Pathology, 84*(1), pp. 30-37.

Chen, C. Y., Han, P., Yan, W. Y., Wang, S. Y., Shi, X. Y., Zhou, X. G., Desneux, N. and Gao, X. W. (2018) Uptake of quercetin reduces larval sensitivity to lambda-cyhalothrin in *Helicoverpa armigera*. *Journal of Pest Science, 91*(2), pp. 919-926.

Chen, J. J., Lai, Y. L., Wang, L. L., Zhai, S. Z., Zou, G., Zhou, Z. H., Cui, C. L. and Wang, S. B. (2017) CRISPR/Cas9-mediated efficient genome editing via blastospore-based transformation in entomopathogenic fungus *Beauveria bassiana*. *Scientific Reports, 7*.

Chen, X. Y., Zaro, J. L. and Shen, W. C. (2013) Fusion protein linkers: Property, design and functionality. *Advanced Drug Delivery Reviews, 65*(10), pp. 1357-1369.

Chen, Y., Qi, B., Zheng, G., Zhang, Y., Deng, F., Wan, F. and Li, C. (2019) Identification and genomic sequence analysis of a new *Spodoptera exigua* multiple nucleopolyhedrovirus, SeMNPV-QD, isolated from Qingdao, China. *Journal of Invertebrate Pathology, 160*, pp. 8-17.

Chen, Z. W., He, F., Xiao, Y. T., Liu, C. X., Li, J. H., Yang, Y. B., Ai, H., Peng, J. X., Hong, H. Z. and Liu, K. Y. (2015) Endogenous expression of a Bt toxin receptor in the Cry1Ac-susceptible insect cell line and its synergistic effect with cadherin on cytotoxicity of activated Cry1Ac. *Insect Biochemistry and Molecular Biology, 59*, pp. 1-17.

Cho, E.-M., Liu, L., Farmerie, W. and Keyhani, N. O. (2006) EST analysis of cDNA libraries from the entomopathogenic fungus *Beauveria (Cordyceps) bassiana*. I. Evidence for stage-specific gene expression in aerial conidia, in vitro blastospores and submerged conidia. *Microbiology, 152*(9), pp. 2843-2854.

Chong, Y., Hayes, J. L., Sollod, B., Wen, S. P., Wilson, D. T., Hains, P. G., Hodgson, W. C., Broady, K. W., King, G. F. and Nicholson, G. M. (2007) The omega-atracotoxins: Selective blockers of insect M-LVA and HVA calcium channels. *Biochemical Pharmacology, 74*(4), pp. 623-638.

Cohen, S., Albeck, S., Ben-Dov, E., Cahan, R., Firer, M., Zaritsky, A. and Dym, O. (2011) Cyt1Aa Toxin: crystal structure reveals implications for its membrane-perforating function. *Journal of Molecular Biology, 413*(4), pp. 804-814.

Cohen, S. N., Chang, A. C. and Hsu, L. (1972) Nonchromosomal antibiotic resistance in bacteria: genetic transformation of *Escherichia coli* by R-factor DNA. *Proceedings of the National Academy of Sciences, 69*(8), pp. 2110-2114.

Cornut, J., De Respinis, S., Tonolla, M., Petrini, O., Bärlocher, F., Chauvet, E. and Bruder, A. (2019) Rapid characterization of aquatic hyphomycetes by matrix-assisted laser desorption/ionization time-of-flight mass spectrometry. *Mycologia, 111*(1), pp. 177-189.

Correa-Cuadros, J. P., Saenz-Aponte, A. and Rodriguez-Bocanegra, M. X. (2016) In vitro interaction of *Metarhizium anisopliae* Ma9236 and *Beauveria bassiana* Bb9205 with *Heterorhabditis bacteriophora* HNI0100 for the control of *Plutella xylostella*. *Springerplus, 5*.

Corzo, G., Escoubas, P., Stankiewicz, M., Pelhate, M., Kristensen, C. P. and Nakajima, T. (2000) Isolation, synthesis and pharmacological characterization of delta-palutoxins IT, novel insecticidal toxins from the spider *Paracoelotes luctuosus* (Amaurobiidae). *European Journal of Biochemistry, 267*(18), pp. 5783-5795.

Crava, C., Bel, Y., Ferré, J. and Escriche, B. (2014) Susceptibility to C ry proteins of a S panish O strinia nubilalis glasshouse population repeatedly sprayed with *Bacillus thuringiensis* formulations. *Journal of Applied Entomology, 138*(1-2), pp. 78-86.

Cuartas, P. E., Barrera, G. P., Belaich, M. N., Barreto, E., Ghiringhelli, P. D. and Villamizar, L. F. (2015) The Complete Sequence of the First *Spodoptera frugiperda* Betabaculovirus Genome: A Natural Multiple Recombinant Virus. *Viruses-Basel, 7*(1), pp. 394-421.

Dai, H., Yin, S., Li, T., Cao, Z., Ji, Y., Wu, Y. and Li, W. (2012) Recombinant expression, purification, and characterization of scorpion toxin BmαTX14. *Protein expression and purification, 82*(2), pp. 325-331.

Damalas, C. and Koutroubas, S. (2018) Current status and recent developments in biopesticide use. in: Multidisciplinary Digital Publishing Institute.

Davis, S. J. and Vierstra, R. D. (1998) Soluble, highly fluorescent variants of green fluorescent protein (GFP) for use in higher plants. *Plant molecular biology, 36*(4), pp. 521-528.

Davis, T. S., Mann, A. J., Malesky, D., Jankowski, E. and Bradley, C. (2018) Laboratory and Field Evaluation of the Entomopathogenic Fungus *Beauveria bassiana* (Deuteromycotina: Hyphomycetes) for Population Management of Spruce Beetle, *Dendroctonus rufipennis* (Coleoptera: Scolytinae), in Felled Trees and Factors Limiting Pathogen Success. *Environmental Entomology, 47*(3), pp. 594-602.

de Andrade Luz, L., Rossato, F. A., e Costa, R. A. P., Napoleão, T. H., Paiva, P. M. G. and Coelho, L. C. B. B. (2017) Cytotoxicity of the coagulant *Moringa oleifera* lectin (cMoL) to B16-F10 melanoma cells. *Toxicology in Vitro, 44*, pp. 94-99.

de Faria, M. R. and Wraight, S. P. (2007) Mycoinsecticides and mycoacaricides: a comprehensive list with worldwide coverage and international classification of formulation types. *Biological Control, 43*(3), pp. 237-256.

de Maagd, R. A., Weemen-Hendriks, M., Stiekema, W. and Bosch, D. (2000) *Bacillus thuringiensis* Delta-Endotoxin Cry1C Domain III Can Function as a Specificity Determinant for *Spodoptera exigua* in Different, but Not All, Cry1-Cry1C Hybrids. *Applied Environmental Microbiology, 66*(4), pp. 1559-1563.

de Oliveira, C. F. R., Luz, L. A., Paiva, P. M. G., Coelho, L. C. B. B., Marangoni, S. and Macedo, M. L. R. (2011) Evaluation of seed coagulant *Moringa oleifera* lectin (cMoL) as a bioinsecticidal tool with potential for the control of insects. *Process Biochemistry, 46*(2), pp. 498-504.

Deknock, A., De Troyer, N., Houbraken, M., Dominguez-Granda, L., Nolivos, I., Van Echelpoel, W., Forio, M. A. E., Spanoghe, P. and Goethals, P. (2019) Distribution of agricultural pesticides in the freshwater environment of the Guayas river basin (Ecuador). *Science of the Total Environment, 646*, pp. 996-1008.

References

Deng, S. Q., Cai, Q. D., Deng, M. Z., Huang, Q. and Peng, H. J. (2017) Scorpion neurotoxin AaIT-expressing *Beauveria bassiana* enhances the virulence against *Aedes albopictus* mosquitoes. *AMB Express, 7*.

Deng, S. Q., Huang, Q., Wei, H. X., Zhou, L. J., Yao, L. J., Li, D. L., Wu, S. Z., Chen, J. T. and Peng, H. J. (2019) *Beauveria bassiana* infection reduces the vectorial capacity of Aedes albopictus for the Zika virus. *Journal of Pest Science, 92*(2), pp. 781-789.

Dengler, W. A., Schulte, J., Berger, D. P., Mertelsmann, R. and Fiebig, H. H. (1995) Development of a propidium iodide fluorescence assay for proliferation and cytotoxicity assays. *Anti-Cancer Drugs, 6*(4), pp. 522-532.

Derbyshire, D. J., Ellar, D. J. and Li, J. (2001) Crystallization of the *Bacillus thuringiensis* toxin Cry1Ac and its complex with the receptor ligand N-acetyl-D-galactosamine. *Acta Crystallographica Section D-Structural Biology, 57*, pp. 1938-1944.

Dhar, S., Jindal, V., Jariyal, M. and Gupta, V. (2019) Molecular characterization of new isolates of the entomopathogenic fungus *Beauveria bassiana* and their efficacy against the tobacco caterpillar, *Spodoptera litura* (Fabricius)(Lepidoptera: Noctuidae). *Egyptian Journal of Biological Pest Control, 29*(1), pp. 8.

Does, M. P., Ng, D. K., Dekker, H. L., Peumans, W. J., Houterman, P. M., Van Damme, E. J. M. and Cornelissen, B. J. C. (1999) Characterization of *Urtica dioica* agglutinin isolectins and the encoding gene family. *Plant Molecular Biology, 39*(2), pp. 335-347.

dos Reis, M. C., Fungaro, M. H. P., Duarte, R. T. D., Furlaneto, L. and Furlaneto, M. C. (2004) *Agrobacterium tumefaciens*-mediated genetic transformation of the entomopathogenic fungus *Beauveria bassiana*. *Journal of Microbiological Methods, 58*(2), pp. 197-202.

Dourado, P. M., Bacalhau, F. B., Amado, D., Carvalho, R. A., Martinelli, S. and Head, G. P. (2016) High susceptibility to cry1ac and low resistance allele frequency reduce the risk of resistance of *Helicoverpa armigera* to Bt soybean in brazil (vol 11, e0161388, 2016). *Plos One, 11*(10).

Dowd, P. F., Zuo, W. N., Gillikin, J. W., Johnson, E. T. and Boston, R. S. (2003) Enhanced resistance to *Helicoverpa zea* in tobacco expressing an activated form of maize ribosome-inactivating protein. *Journal of Agricultural and Food Chemistry, 51*(12), pp. 3568-3574.

Down, R. E., Fitches, E. C., Wiles, D. P., Corti, P., Bell, H. A., Gatehouse, J. A. and Edwards, J. P. (2006) Insecticidal spider venom toxin fused to snowdrop lectin is toxic to the peach-potato aphid, *Myzus persicae* (Hemiptera : Aphididae) and the rice brown planthopper, *Nilaparvata lugens* (Hemiptera : Delphacidae). *Pest Management Science, 62*(1), pp. 77-85.

Duarte, R. T. D., Staats, C. C., Fungaro, M. H. P., Schrank, A., Vainsten, M. H., Furlaneto-Maia, L., Nakamura, C. V., de Souza, W. and Furlaneto, M. C. (2007) Development of a simple and rapid *Agrobacterium tumefaciens*-mediated transformation system for the entomopathogenic fungus *Metarhizium anisopliae* var. *acridum*. *Letters in Applied Microbiology, 44*(3), pp. 248-254.

Dutra, A. A., Sousa, L. O., Resende, R. R., Brandao, R. L., Kalapothakis, E. and Castro, I. M. (2008) Expression and characterization of LTx2, a neurotoxin from *Lasiodora sp* effecting on calcium channels. *Peptides, 29*(9), pp. 1505-1513.

Eley, K. L., Halo, L. M., Song, Z. S., Powles, H., Cox, R. J., Bailey, A. M., Lazarus, C. M. and Simpson, T. J. (2007) Biosynthesis of the 2-pyridone tenellin in the insect pathogenic fungus *Beauveria bassiana*. *Chembiochem, 8*(3), pp. 289-297.

Elleuch, J., Jacca, S., Darriet, F., Chandre, F., Tounsi, S. and Zghal, R. Z. (2015) Cry4Ba and Cyt1Aa proteins from *Bacillus thuringiensis israelensis:* Interactions and toxicity mechanism against *Aedes aegypti*. *Toxicon, 104*, pp. 83-90.

Elleuch, J., Zghal, R. Z., Jemaà, M., Azzouz, H., Tounsi, S. and Jaoua, S. (2014) New *Bacillus thuringiensis* toxin combinations for biological control of lepidopteran larvae. *International Journal of Biological Macromolecules, 65*, pp. 148-154.

Enserink, M., Hines, P. J., Vignieri, S. N., Wigginton, N. S. and Yeston, J. S. (2013) The pesticide paradox. in: American Association for the Advancement of Science.

Esen, H., Alpdağtaş, S., Mervan Çakar, M. and Binay, B. (2019) Tailoring of recombinant FDH: effect of histidine tag location on solubility and catalytic properties of *Chaetomium thermophilum* formate dehydrogenase (CtFDH). *Preparative Biochemistry and Biotechnology, 49*(5), pp. 529-534.

Fabrick, J., Oppert, C., Lorenzen, M. D., Morris, K., Oppert, B. and Jurat-Fuentes, J. L. (2009) A Novel *Tenebrio molitor* cadherin is a functional receptor for *Bacillus thuringiensis* Cry3Aa Toxin. *Journal of Biological Chemistry, 284*(27), pp. 18401-18410.

Fabrick, J. A., Mathew, L. G., LeRoy, D. M., Hull, J. J., Unnithan, G. C., Yelich, A. J., Carriere, Y., Li, X. and Tabashnik, B. E. (2019) Reduced cadherin expression associated with resistance to Bt toxin Cry1Ac in pink bollworm. *Pest Management Science*

Fan, Y., Fang, W., Guo, S., Pei, X., Zhang, Y., Xiao, Y., Li, D., Jin, K., Bidochka, M. J. and Pei, Y. (2007) Increased insect virulence in *Beauveria bassiana* strains overexpressing an engineered chitinase. *Applied Environmental Microbiology, 73*(1), pp. 295-302.

Fan, Y., Guo, S., Pei, X., Zhang, Y., Luo, Z. and Pei, Y. (2011) Effects of chitin binding domain on enzymatic properties and insecticidal activity of *Bombyx mori* chitinase. *World Journal of Microbiology and Biotechnology, 27*(7), pp. 1551-1558.

Fan, Y., Pei, X., Guo, S., Zhang, Y., Luo, Z., Liao, X. and Pei, Y. (2010) Increased virulence using engineered protease-chitin binding domain hybrid expressed in the entomopathogenic fungus *Beauveria bassiana*. *Microbial pathogenesis, 49*(6), pp. 376-380.

Fang, W., Feng, J., Fan, Y., Zhang, Y., Bidochka, M. J., Leger, R. J. S. and Pei, Y. (2009) Expressing a fusion protein with protease and chitinase activities increases the virulence of the insect pathogen *Beauveria bassiana*. *Journal of Invertebrate Pathology, 102*(2), pp. 155-159.

Fang, W., Leng, B., Xiao, Y., Jin, K., Ma, J., Fan, Y., Feng, J., Yang, X., Zhang, Y. and Pei, Y. (2005) Cloning of *Beauveria bassiana* chitinase gene Bbchit1 and its application to improve fungal strain virulence. *Applied Environemental Microbiology, 71*(1), pp. 363-370.

Fang, W. G., Fernandes, E. K. K., Roberts, D. W., Bidochka, M. J. and Leger, R. J. S. (2010) A laccase exclusively expressed by *Metarhizium anisopliae* during isotropic growth is involved in pigmentation, tolerance to abiotic stresses and virulence. *Fungal Genetics and Biology, 47*(7), pp. 602-607.

Fang, W. G., Pei, Y. and Bidochka, M. J. (2006) Transformation of *Metarhizium anisopliae* mediated by *Agrobacterium tumefaciens*. *Canadian Journal of Microbiology, 52*(7), pp. 623-626.

Fang, W. G., Zhang, Y. J., Yang, X. Y., Zheng, X. L., Duan, H., Li, Y. and Pei, Y. (2004) *Agrobacterium tumefaciens*-mediated transformation of *Beauveria bassiana* using an herbicide resistance gene as a selection marker. *Journal of Invertebrate Pathology, 85*(1), pp. 18-24.

Federici, B. A. and Bauer, L. S. (1998) Cyt1Aa Protein of *Bacillus thuringiensis* is toxic to the Cottonwood Leaf Beetle, *Chrysomela scripta*, and suppresses high levels of resistance to Cry3Aa. *Applied Environemental Microbiology, 64*(11), pp. 4368-4371.

References

Felce, J. H., MacRae, A. and Davis, S. J. (2019) Constraints on GPCR heterodimerization revealed by the type-4 induced-association BRET assay. *Biophysical journal, 116*(1), pp. 31-41.

Fernandes, É. K., Angelo, I. C., Rangel, D. E., Bahiense, T. C., Moraes, Á. M., Roberts, D. W. and Bittencourt, V. R. (2011) An intensive search for promising fungal biological control agents of ticks, particularly *Rhipicephalus microplus*. *Veterinary parasitology, 182*(2-4), pp. 307-318.

Finney, D. J. (1952a) Probit analysis: a statistical treatment of the sigmoid response curve, Cambridge university press, Cambridge.

Fitches, E., Audsley, N., Gatehouse, J. A. and Edwards, J. P. (2002) Fusion proteins containing neuropeptides as novel insect contol agents: snowdrop lectin delivers fused allatostatin to insect haemolymph following oral ingestion. *Insect Biochemistry and Molecular Biology, 32*(12), pp. 1653-1661.

Fitches, E., Edwards, M. G., Mee, C., Grishin, E., Gatehouse, A. M. R., Edwards, J. P. and Gatehouse, J. A. (2004) Fusion proteins containing insect-specific toxins as pest control agents: snowdrop lectin delivers fused insecticidal spider venom toxin to insect haemolymph following oral ingestion. *Journal of Insectect Physiology, 50*(1), pp. 61-71.

Fitches, E., Gatehouse, A. M. R. and Gatehouse, J. A. (1997) Effects of snowdrop lectin (GNA) delivered via artificial diet and transgenic plants on the development of tomato moth (*Lacanobia oleracea*) larvae in laboratory and glasshouse trials. *Journal of Insect Physiology, 43*(8), pp. 727-739.

Fitches, E., Woodhouse, S. D., Edwards, J. P. and Gatehouse, J. A. (2001) In vitro and in vivo binding of snowdrop (*Galanthus nivalis* agglutinin; GNA) and jackbean (*Canavalia ensiformis;* Con A) lectins within tomato moth (*Lacanobia oleracea*) larvae; mechanisms of insecticidal action. *Journal of Insect Physiology,47*(7), pp. 777-787.

Fitches, E. C., Bell, H. A., Powell, M. E., Back, E., Sargiotti, C., Weaver, R. J. and Gatehouse, J. A. (2010) Insecticidal activity of scorpion toxin (ButaIT) and snowdrop lectin (GNA) containing fusion proteins towards pest species of different orders. *Pest Management Science, 66*(1), pp. 74-83.

Fitches, E. C., Pyati, P., King, G. F. and Gatehouse, J. A. (2012) Fusion to snowdrop lectin magnifies the oral activity of insecticidal ω-hexatoxin-Hv1a peptide by enabling its delivery to the central nervous system. *Plos One, 7*(6), pp. e39389.

Foissac, X., Thi Loc, N., Christou, P., Gatehouse, A. M. and Gatehouse, J. A. (2000) Resistance to green leafhopper (*Nephotettix virescens*) and brown planthopper (*Nilaparvata lugens*) in transgenic rice expressing snowdrop lectin (*Galanthus nivalis* agglutinin; GNA). *Journal of Insect Physiology,46*(4), pp. 573-583.

Gao, P. P., Li, M. C., Jin, K. and Xia, Y. X. (2019) The homeobox gene MaH1 governs microcycle conidiation for increased conidial yield by mediating transcription of conidiation pattern shift-related genes in *Metarhizium acridum*. *Applied Microbiology and Biotechnology, 103*(5), pp. 2251-2262.

Gao, T. N., Wang, Z. L., Huang, Y., Keyhani, N. O. and Huang, Z. (2017) Lack of resistance development in *Bemisia tabaci* to *Isaria fumosorosea* after multiple generations of selection. *Scientific Reports, 7*.

García-Gómez, B. I., Sánchez, J., de Castro, D. L. M., Ibarra, J. E., Bravo, A. and Soberón, M. (2013) Efficient production of *Bacillus thuringiensis* Cry1AMod toxins under regulation of cry3Aa promoter and single cysteine mutations in the protoxin region. *Applied Environmental Microbiology, 79*(22), pp. 6969-6973.

Garg, H., Suri, P., Gupta, J. C., Talwar, G. P. and Dubey, S. (2016) Survivin: a unique target for tumor therapy. *Cancer Cell International, 16*.

Gasteiger, E., Hoogland, C., Gattiker, A., Wilkins, M. R., Appel, R. D. and Bairoch, A. (2005) Protein identification and analysis tools on the ExPASy server. in *The proteomics protocols handbook*: Springer. pp. 571-607.

Gauthier, N., Clouet, C., Perrakis, A., Kapantaidaki, D., Peterschmitt, M. and Tsagkarakou, A. (2014) Genetic structure of *Bemisia tabaci* Med populations from home-range countries, inferred by nuclear and cytoplasmic markers: impact on the distribution of the insecticide resistance genes. *Pest Manag Sci, 70*(10), pp. 1477-1491.

Gershburg, E., Stockholm, D., Froy, O., Rashi, S., Gurevitz, M. and Chejanovsky, N. (1998) Baculovirus-mediated expression of a scorpion depressant toxin improves the insecticidal efficacy achieved with excitatory toxins. *FEBS Letters, 422*(2), pp. 132-136.

Ghosh, G., Ganguly, S., Purohit, A., Chaudhuri, R. K., Das, S. and Chakraborti, D. (2017) Transgenic pigeonpea events expressing Cry1Ac and Cry2Aa exhibit resistance to *Helicoverpa armigera. Plant Cell Reports, 36*(7), pp. 1037-1051.

Gidrol, X., Chrestin, H., Tan, H. L. and Kush, A. (1994) Hevein, a Lectin-Like Protein from Hevea-Brasiliensis (Rubber Tree) Is Involved in the Coagulation of Latex. *Journal of Biological Chemistry, 269*(12), pp. 9278-9283.

Gindin, G., Levski, S., Glazer, I. and Soroker, V. (2006) Evaluation of the entomopathogenic fungi *Metarhizium anisopliae* and *Beauveria bassiana* against the red palm weevil *Rhynchophorus ferrugineus*. *Phytoparasitica, 34*(4), pp. 370-379.

Ginting, S., Santoso, T., Munara, Y. K., Anwar, R. and Sudirman, L. I. (2018) Pathogenicity of *Helicoverpa armigera* Nucleopolyhedro virus (HearNPV) and *Lecanicillium sp.* against *Helicoverpa armigera*. *Journal of Biopesticides, 11*(2), pp. 128-135.

Godfray, H. C. J., Beddington, J. R., Crute, I. R., Haddad, L., Lawrence, D., Muir, J. F., Pretty, J., Robinson, S., Thomas, S. M. and Toulmin, C. (2010) Food Security: The Challenge of Feeding 9 Billion People. *Science, 327*(5967), pp. 812-818.

Goettel, M. S., Leger, R. J. S., Bhairi, S., Jung, M. K., Oakley, B. R., Roberts, D. W. and Staples, R. C. (1990) Pathogenicity and growth of *Metarhizium anisopliae* stably transformed to benomyl resistance. *Current Genetics, 17*(2), pp. 129-132.

Gómez, I., Flores, B., Bravo, A. and Soberón, M. (2015) *Bacillus thuringiensis* Cry1AbMod toxin counters tolerance associated with low cadherin expression but not that associated with low alkaline phosphatase expression in *Manduca sexta*. *Peptides, 68*, pp. 130-133.

Gondim, A. C. S., Romero-Canelon, I., Sousa, E. H. S., Blindauer, C. A., Butler, J. S., Romero, M. J., Sanchez-Cano, C., Sousa, B. L., Chaves, R. P., Nagano, C. S., Cavada, B. S. and Sadler, P. J. (2017) The potent anti-cancer activity of *Dioclea lasiocarpa* lectin. *Journal of Inorganic Biochemistry, 175*, pp. 179-189.

Gressel, J. (2001) Potential failsafe mechanisms against the spread and introgression of transgenic hypervirulent biocontrol fungi. *Trends Biotechnol, 19*(4), pp. 149-54.

Gross, C. H., Russell, R. L. Q. and Rohrmann, G. F. (1994) *Orgyia pseudotsugata* Baculovirus p10 and polyhedron envelope protein genes - analysis of their relative expression levels and role in polyhedron structure. *Journal of General Virology, 75*, pp. 1115-1123.

Guo, W., Kain, W. and Wang, P. (2019) Effects of disruption of the peritrophic membrane on larval susceptibility to Bt toxin Cry1Ac in cabbage loopers. *Journal of Insect Physiology 117*, pp. 103897.

References

Guo, Z. J., Kang, S., Chen, D. F., Wu, Q. J., Wang, S. L., Xie, W., Zhu, X., Baxter, S. W., Zhou, X. G., Jurat-Fuentes, J. L. and Zhang, Y. J. (2015) MAPK signaling pathway alters expression of midgut alp and abcc genes and causes resistance to *Bacillus thuringiensis* cry1ac toxin in diamondback moth. *Plos Genetics, 11*(4).

Guo, Z. J., Sun, D., Kang, S., Zhou, J. L., Gong, L. J., Qin, J. Y., Guo, L., Zhu, L. H., Bai, Y., Luo, L. and Zhang, Y. J. (2019) CRISPR/Cas9-mediated knockout of both the PxABCC2 and PxABCC3 genes confers high-level resistance to *Bacillus thuringiensis* Cry1Ac toxin in the diamondback moth, *Plutella xylostella* (L.). *Insect Biochemistry and Molecular Biology, 107*, pp. 31-38.

Gurevitz, M. (2012) Mapping of scorpion toxin receptor sites at voltage-gated sodium channels. *Toxicon, 60*(4), pp. 502-511.

Hardy, M. (2014) Resistance is not futile: It shapes insecticide discovery. *Insects, 5*(1), pp. 227-242.

Hegedus, D., Erlandson, M., Gillott, C. and Toprak, U. (2009) New insights into peritrophic matrix synthesis, architecture, and function. *Annual review of entomology, 54*, pp. 285-302.

Heim, R. and Tsien, R. Y. (1996) Engineering green fluorescent protein for improved brightness, longer wavelengths and fluorescence resonance energy transfer. *Current biology, 6*(2), pp. 178-182.

Helou, K., Harmouche-Karaki, M., Karake, S. and Narbonne, J.-F. (2019) A review of organochlorine pesticides and polychlorinated biphenyls in Lebanon: Environmental and human contaminants. *Chemosphere*.

Henry, M., Beguin, M., Requier, F., Rollin, O., Odoux, J.-F., Aupinel, P., Aptel, J., Tchamitchian, S. and Decourtye, A. (2012) A common pesticide decreases foraging success and survival in honey bees. *Science, 336*(6079), pp. 348-350.

Hernandez, C. S. and Ferre, J. (2005) Common receptor for *Bacillus thuringiensis* toxins Cry1Ac, Cry1Fa, and Cry1Ja in *Helicoverpa armigera, Helicoverpa zea,* and *Spodoptera exigua*. *Applied Environmental Microbiology, 71*(9), pp. 5627-9.

Hester, G., Kaku, H., Goldstein, I. J. and Wright, C. S. (1995) Structure of Mannose-Specific Snowdrop (*Galanthus nivalis*) lectin is representative of a new plant lectin family. *Nature Structural Biology, 2*(6), pp. 472-479.

Hibbard, B. E., Frank, D. L., Kurtz, R., Boudreau, E., Ellersieck, M. R. and Odhiambo, J. F. (2011) Mortality impact of bt transgenic maize roots expressing eCry3.1Ab, mCry3A, and eCry3.1Ab Plus mCry3A on western corn rootworm larvae in the field. *Journal of Economic Entomology, 104*(5), pp. 1584-1591.

Hinse, D., Vollmer, T., Erhard, M., Welker, M., Moore, E., Kleesiek, K. and Dreier, J. (2011) Differentiation of species of the S*treptococcus bovis/equinus*-complex by MALDI-TOF mass spectrometry in comparison to sodA sequence analyses. *Systematic and Applied Microbiology, 34*(1), pp. 52-57.

Hodgson, J. J., Buchon, N. and Blissard, G. W. (2019) Identification of insect genes involved in baculovirus AcMNPV entry into insect cells. *Virology, 527*, pp. 1-11.

Hu, G. and Leger, R. J. S. (2002) Field studies using a recombinant mycoinsecticide (*Metarhizium anisopliae*) reveal that it is rhizosphere competent. *Applied Environmental Microbiology, 68*(12), pp. 6383-6387.

Hu, J. and Xia, Y. X. (2019) Increased virulence in the locust-specific fungal pathogen *Metarhizium acridum* expressing dsRNAs targeting the host F1F0-ATPase subunit genes. *Pest Management Science, 75*(1), pp. 180-186.

Hu, X., Xiao, G. H., Zheng, P., Shang, Y. F., Su, Y., Zhang, X. Y., Liu, X. Z., Zhan, S., St Leger, R. J. and Wang, C. S. (2014) Trajectory and genomic determinants of fungal-pathogen speciation and host adaptation. *Proceedings of the National Academy of Sciences of the United States of America, 111*(47), pp. 16796-16801.

Huang, H. W., Liu, B. S., Chien, K. Y., Chiang, L. C., Huang, S. Y., Sung, W. C. and Wu, W. G. (2015) Cobra venom proteome and glycome determined from individual snakes of *Naja atra* reveal medically important dynamic range and systematic geographic variation. *Journal of Proteomics, 128*, pp. 92-104.

Huang, W., Shang, Y., Chen, P., Gao, Q. and Wang, C. (2015) MrpacC regulates sporulation, insect cuticle penetration and immune evasion in *Metarhizium robertsii*. *Environmental Microbiology, 17*(4), pp. 994-1008.

Hurst, M. R., Beattie, A., Jones, S. A., Laugraud, A., van Koten, C. and Harper, L. (2018) Characterization of Serratia proteamaculans strain AGR96X encoding an anti-feeding prophage (tailocin) with activity against grass grub (*Costelytra giveni*) and manuka beetle (*Pyronota spp*.) larvae. *Applied Environmental Microbiology*, pp. AEM. 02739-17.

Ilinsky, Y., Lunev, E., Toshchakov, S., Podgwaite, J. and Martemyanov, V. (2018) Comparative genome analysis of related *Lymantria dispar* nucleopolyhedrovirus isolates differing in virulence. *Biodiversity: Genomics and Evolution (BioGenEvo-2018)*, pp. 21.

Jaber, L. R. and Araj, S. E. (2018) Interactions among endophytic fungal entomopathogens (Ascomycota: Hypocreales), the green peach aphid *Myzus persicae* Sulzer (Homoptera: Aphididae), and the aphid endoparasitoid *Aphidius colemani* Viereck (Hymenoptera: Braconidae). *Biological Control, 116*, pp. 53-61.

Jaber, L. R., Araj, S. E. and Qasem, J. R. (2018) Compatibility of endophytic fungal entomopathogens with plant extracts for the management of sweetpotato whitefly *Bemesia tabaci* Gennadius (Homoptera: Aleyrodidae). *Biological Control, 117*, pp. 164-171.

Jackson, T., Glare, T. and O'Callaghan, M. (1991) Pathotypic boundaries for *Serratia ssp*. causing amber disease in the New Zealand grass grub, *Costelytra zealandica*. *Bulletin OILB SROP (France)*.

Jakka, S. R., Gong, L., Hasler, J., Banerjee, R., Sheets, J. J., Narva, K., Blanco, C. A. and Jurat-Fuentes, J. L. (2015) Field-evolved Mode 1 fall armyworm resistance to Bt corn associated with reduced Cry1Fa toxin binding and midgut alkaline phosphatase expression. *Applied Environmental Microbiology*, pp. AEM. 02871-15.

Jamil, R. Z. R., Vandervoort, C. and Wise, J. C. (2019) Residual toxicity of insecticides to *Neoseiulus fallacis* (Acari: Phytoseiidae) in Apples. *Journal of Economic Entomology*

Ji, S. J., Feng, L., Li, E. Q. and Zhu, Y. X. (2002) Recombinant scorpion insectotoxin AaIT kills specifically insect cells but not human cells. *Cell research, 12*(2), pp. 143.

Jiang, A., Yuan, Y., Yang, R., Zhang, N., Xie, Y., Lai, W. M., Peng, X. R., Yang, G. Y. and Gu, X. B. (2019) *Beauveria bassiana* is a potential effective biological agent against *Psoroptes ovis* var. *cuniculi* mites. *Biological Control, 131*, pp. 43-48.

Jiang, G. Y., Xu, Y. J., Zhu, X. S., Su, Y. H. and Zhu, Y. X. (2001) Prokaryotically expressed *Buthus martensii* Karsch insect depressant toxin has insecticidal effects. *Toxicon, 39*(4), pp. 469-476.

Jiang, Q., Ying, S. H. and Feng, M. G. (2007) Enhanced frequency of *Beauveria bassiana* blastospore transformation by restriction enzyme-mediated integration and electroporation. *Journal of Microbiological Methods, 69*(3), pp. 512-517.

References

Jones, K. H. and Senft, J. A. (1985) An improved method to determine cell viability by simultaneous staining with fluorescein diacetate propidium iodide. *Journal of Histochemistry & Cytochemistry, 33*(1), pp. 77-79.

Kang, S., Odom, O., Malone, C., Thangamani, S. and Herrin, D. (2018) Expression of a synthetic gene for the major cytotoxin (Cyt1Aa) of *Bacillus thuringiensis* subsp. *israelensis* in the chloroplast of wild-type *Chlamydomonas*. *Biology, 7*(2), pp. 29.

Kanjo, K., Surin, S. I., Gupta, T., Dhanasingh, M., Singh, B. and Saini, G. K. (2019) Truncated, strong inducible promoter Pmcl1 from *Metarhizium anisopliae*. *3 Biotech, 9*(3), pp. 75.

Kao, M. C., Rao, Y. K., Hsieh, Y. W., Weng, S. H., Lu, T. L., Tzeng, D. T. W., Liu, J. J., Lin, C. J., Lai, C. H. and Tzeng, Y. M. (2015) A cyclohexadepsipeptide from entomogenous fungi *Metarhizium anisopliae* inhibits the *Helicobacter pylori* induced pathogenesis through attenuation of vacuolating cytotoxin-A activity. *Process Biochemistry, 50*(1), pp. 134-139.

Karasaki, Y., Tsukamoto, S., Mizusaki, K., Sugiura, T. and Gotoh, S. (2001) A garlic lectin exerted an antitumor activity and induced apoptosis in human tumor cells. *Food Research International, 34*(1), pp. 7-13.

Kellen, W. R., Clark, T. B., Lindegren, J. E., Ho, B. C., Rogoff, M. H. and Singer, S. (1965) *Bacillus sphaericus* Neide as a pathogen of mosquitoes. *Journal of Invertebrate Pathology, 7*(4), pp. 442-+.

Kelly, D. C., Brown, D. A., Ayres, M. D., Allen, C. J. and Walker, I. O. (1983) Properties of the major nucleocapsid protein of *Heliothis zea* singly enveloped nuclear polyhedrosis-virus. *Journal of General Virology, 64*(Feb), pp. 399-408.

Khamessi, O., Ben Mabrouk, H., ElFessi-Magouri, R. and Kharrat, R. (2018) RK1, the first very short peptide from *Buthus occitanus tunetanus* inhibits tumor cell migration, proliferation and angiogenesis. *Biochemical and Biophysical Research Communications, 499*(1), pp. 1-7.

Khan, S. A., Zafar, Y., Briddon, R. W., Malik, K. A. and Mukhtar, Z. (2006) Spider venom toxin protects plants from insect attack. *Transgenic Research, 15*(3), pp. 349-357.

Kim, C.-S., Lee, J.-B., Kim, B.-S., Nam, Y.-H., Shin, K.-S., Kim, J.-W., Kim, J.-E. and Kwon, G.-S. (2014) A technique for the prevention of greenhouse whitefly (*Trialeurodes vaporariorum*) using the entomopathogenic fungus *Beauveria bassiana* M130. *J. Microbiol. Biotechn, 24*, pp. 1-7.

Kim, J. S., Choi, J. Y., Lee, J. H., Park, J. B., Fu, Z., Liu, Q., Tao, X., Jin, B. R., Skinner, M. and Parker, B. L. (2013) Bumblebee venom serine protease increases fungal insecticidal virulence by inducing insect melanization. *Plos One, 8*(4), pp. e62555.

Kim, M., Rao, M. V., Tweardy, D. J., Prakash, M., Galili, U. and Gorelik, E. (1993) Lectin-induced apoptosis of tumor-cells. *Glycobiology, 3*(5), pp. 447-453.

Knight, K., Head, G. and Rogers, J. (2015) Relationships between Cry1Ac and Cry2Ab protein expression in field-grown Bollgard II (R) cotton and efficacy against *Helicoverpa armigera* and *Helicoverpa punctigera* (Lepidoptera: Noctuidae). *Crop Protection, 79*, pp. 150-158.

Knight, P. J., Carroll, J. and Ellar, D. J. (2004) Analysis of glycan structures on the 120 kDa aminopeptidase N of *Manduca sexta* and their interactions with *Bacillus thuringiensis* Cry1Ac toxin. *Insect Biochemistry and Molecular Biology, 34*(1), pp. 101-112.

Kopeyan, C., Mansuelle, P., Sampieri, F., Brando, T., Bahraoui, E. M., Rochat, H. and Granier, C. (1990) Primary structure of scorpion anti-insect toxins isolated from the venom of *Leiurus quinquestriatus quinquestriatu*s. *FEBS letters, 261*(2), pp. 423-426.

Kopeyan, C., Martinez, G., Lissitzky, S., Miranda, F. and Rochat, H. (1974) Disulfide bonds of toxin II of the scorpion *Androctonus australis* Hector. *European Journal of Biochemistry, 47*(3), pp. 483-9.

Kosir, J. M., Macpherson, J. M. and Khachatourians, G. G. (1991) Genomic analysis of a virulent and a less virulent-strain of the entomopathogenic fungus *Beauveria bassiana*, using restriction-fragment-length-polymorphisms. *Canadian Journal of Microbiology, 37*(7), pp. 534-541.

Krassilstschik, I. (1888) La production industrielle des parasites végétaux pour la destruction des insectes nuisibles. *Bulletin Biologique de la France et de la Belgique, 19*, pp. 461-472.

Kukanur, V. S., Singh, T., Kranthi, K. R. and Andow, D. A. (2018) Cry1Ac resistance allele frequency in field populations of *Helicoverpa armigera* (Hübner) collected in Telangana and Andhra Pradesh, India. *Crop protection, 107*, pp. 34-40.

Kumar, K. K., Sridhar, J., Murali-Baskaran, R. K., Senthil-Nathan, S., Kaushal, P., Dara, S. K. and Arthurs, S. (2019) Microbial biopesticides for insect pest management in India: Current status and future prospects. *Journal of Invertebrate Pathology, 165*, pp. 74-81.

Kuzmenkov, A. I., Nekrasova, O. V., Kudryashova, K. S., Peigneur, S., Tytgat, J., Stepanov, A. V., Kirpichnikov, M. P., Grishin, E. V., Feofanov, A. V. and Vassilevski, A. A. (2016) Fluorescent protein-scorpion toxin chimera is a convenient molecular tool for studies of potassium channels. *Scientific reports, 6*, pp. 33314.

Lacey, L., Liu, T.-X., Buchman, J., Munyaneza, J., Goolsby, J. and Horton, D. (2011) Entomopathogenic fungi (Hypocreales) for control of potato psyllid, *Bactericera cockerelli* (Šulc)(Hemiptera: Triozidae) in an area endemic for zebra chip disease of potato. *Biological Control, 56*(3), pp. 271-278.

Lannoo, N. and Van Damme, E. J. M. (2010) Nucleocytoplasmic plant lectins. *Biochimica Et Biophysica Acta-General Subjects, 1800*(2), pp. 190-201.

Leclerque, A., Wan, H., Abschutz, A., Chen, S., Mitina, G. V., Zimmermann, G. and Schairer, H. U. (2004) *Agrobacterium*-mediated insertional mutagenesis (AIM) of the entomopathogenic fungus *Beauveria bassiana*. *Current Genetics, 45*(2), pp. 111-119.

Lee, M. K., Miles, P. and Chen, J. S. (2006) Brush border membrane binding properties of *Bacillus thuringiensis* Vip3A toxin to *Heliothis virescens* and *Helicoverpa zea* midguts. *Biochemical and Biophysical Research Communications, 339*(4), pp. 1043-1047.

Lee, S. J., Yu, J. S., Parker, B. L., Skinner, M., Je, Y. H. and Kim, J. S. (2015) Production of antibacterial *Bombyx mori* cecropin A in mealworm-pathogenic *Beauveria bassiana* ERL1170. *Journal of Industrial Microbiology & Biotechnology, 42*(1), pp. 151-156.

Lee, S. R., Kufner, M., Park, M., Jung, W. H., Choi, S. U., Beemelmanns, C. and Kim, K. H. (2019) Beauvetetraones A-C, phomaligadione-derived polyketide dimers from the entomopathogenic fungus, *Beauveria bassiana*. *Organic Chemistry Frontiers, 6*(2), pp. 162-166.

Lee, S. R., Lee, S., Eom, H. J., Kang, H. R., Yu, J. S., Lee, T. K., Baek, J., Lee, D., Suh, W. S. and Kim, K. H. (2016) (-)-Bassianolide, a cyclodepsipeptide from *Bombycis Corpus*: Total synthesis and evaluation of its antitumor activity. *Planta Medica, 82*.

Leger, R. J. S. and Wang, C. (2010) Genetic engineering of fungal biocontrol agents to achieve greater efficacy against insect pests. *Applied Microbiology and Biotechnology, 85*(4), pp. 901-907.

Leipold, E., Borges, A. and Heinemann, S. H. (2012) Scorpion β-toxin interference with NaV channel voltage sensor gives rise to excitatory and depressant modes. *The Journal of general physiology, 139*(4), pp. 305-319.

References

Li, J., Koni, P. A. and Ellar, D. J. (1996) Structure of the mosquitocidal δ-Endotoxin CytB from *Bacillus thuringiensis sp. kyushuensis* and implications for membrane pore formation. *Journal of Molecular Biology, 257*(1), pp. 129-152.

Li, S., Hussain, F., Unnithan, G. C., Dong, S., UlAbdin, Z., Gu, S., Mathew, L. G., Fabrick, J. A., Ni, X., Carriere, Y., Tabashnik, B. E. and Li, X. (2019) A long non-coding RNA regulates cadherin transcription and susceptibility to Bt toxin Cry1Ac in pink bollworm, *Pectinophora gossypiella. Pesticide Biochemistry and Physiology, 158*, pp. 54-60.

Li, Y. and Romeis, J. (2009) Impact of snowdrop lectin (*Galanthus nivalis* agglutinin; GNA) on adults of the green lacewing, *Chrysoperla carnea*. *Journal of Insect Physiology, 55*(2), pp. 135-42.

Liang, H., Zhu, Y.-F., Zhu, Z., Sun, D.-F. and Jia, X. (2004) Obtainment of transgenic wheat with the insecticidal lectin from snowdrop (*Galanthus nivalis* agglutinin; GNA) gene and analysis of resistance to aphid. *Yi chuan xue bao= Acta genetica Sinica, 31*(2), pp. 189-194.

Lichtenstein, R. G. and Rabinovich, G. A. (2013) Glycobiology of cell death: when glycans and lectins govern cell fate. *Cell Death and Differentiation, 20*(8), pp. 976-986.

Lin, L. C., Wang, F. Q. and Wei, D. Z. (2011) Chlorimuron ethyl as a new selectable marker for disrupting genes in the insect-pathogenic fungus *Metarhizium robertsii*. *Journal of Microbiological Methods, 87*(2), pp. 241-243.

Liu, B., Li, C. Y., Bian, H. J., Min, M. W., Chen, L. F. and Bao, J. K. (2009) Antiproliferative activity and apoptosis-inducing mechanism of Concanavalin A on human melanoma A375 cells. *Archives of Biochemistry and Biophysics, 482*(1-2), pp. 1-6.

Liu, S. M., Li, J., Zhu, J. Q., Wang, X. W., Wang, C. S., Liu, S. S., Chen, X. X. and Li, S. (2016) Transgenic plants expressing the AaIT/GNA fusion protein show increased resistance and toxicity to both chewing and sucking pests. *Insect Science, 23*(2), pp. 265-276.

Liu, Y.-J., Liu, J., Ying, S.-H., Liu, S.-S. and Feng, M.-G. (2013) A fungal insecticide engineered for fast per os killing of caterpillars has high field efficacy and safety in full-season control of cabbage insect pests. *Applied Environmental Microbiology, 79*(20), pp. 6452-6458.

Liu, Z., Liu, B., Zhang, Z. T., Zhou, T. T., Bian, H. J., Min, M. W., Liu, Y. H., Chen, J. and Bao, J. K. (2008) A mannose-binding lectin from *Sophora flavescens* induces apoptosis in HeLa cells. *Phytomedicine, 15*(10), pp. 867-875.

Liu, Z., Zhu, Z. and Zhang, T. (2019) Development of transgenic CryIA (c)+ GNA cotton plants via pollen-tube pathway method confers resistance to *Helicoverpa armigera* and *Aphis gossypii* Glover. in *Transgenic Cotton*: Springer. pp. 233-244.

Livak, K. J. and Schmittgen, T. D. (2001) Analysis of relative gene expression data using real-time quantitative PCR and the 2(T)(-Delta Delta C) method. *Methods, 25*(4), pp. 402-408.

Lo Verde, G., Torta, L., Mondello, V., Caldarella, C. G., Burruano, S. and Caleca, V. (2015) Pathogenicity bioassays of isolates of *Beauveria bassiana* on *Rhynchophorus ferrugineus*. *Pest Management Science, 71*(2), pp. 323-328.

Loc, N. T., Tinjuangjun, P., Gatehouse, A. M., Christou, P. and Gatehouse, J. A. (2002) Linear transgene constructs lacking vector backbone sequences generate transgenic rice plants which accumulate higher levels of proteins conferring insect resistance. *Molecular Breeding, 9*(4), pp. 231-244.

Longstaff, M., Powell, K. S., Gatehouse, J. A., Raemaekers, R., Nevell, C. A. and Hamilton, W. D. O. (1998) Production and purification of active snowdrop lectin in *Escherichia coli*. *European Journal of Biochemistry, 252*(1), pp. 59-65.

Lopez-Cruzan, M., Sharma, R., Tiwari, M., Karbach, S., Holstein, D., Martin, C. R., Lechleitert, J. D. and Herman, B. (2016) Caspase-2 resides in the mitochondria and mediates apoptosis directly from the mitochondrial compartment. *Cell Death Discovery, 2*.

Loret, E. P., Mansuelle, P., Rochat, H. and Granier, C. (1990) Neurotoxins active on insects - amino-acid-sequences, chemical modifications, and secondary structure estimation by circular-dichroism of toxins from the scorpion *Androctonus australis* Hector. *Biochemistry, 29*(6), pp. 1492-1501.

Lozano-Tovar, M. D., Garrido-Jurado, I., Lafont, F. and Quesada-Moraga, E. (2015) Insecticidal activity of a destruxin- containing extract of *Metarhizium brunneum* Against *Ceratitis capitata* (Diptera: Tephritidae). *Journal of Economic Entomology, 108*(2), pp. 462-472.

Lozano-Tovar, M. D., Garrido-Jurado, I., Quesada-Moraga, E., Raya-Ortega, M. C. and Trapero-Casas, A. (2017) *Metarhizium brunneum* and *Beauveria bassiana* release secondary metabolites with antagonistic activity against *Verticillium dahliae* and *Phytophthora megasperma* olive pathogens. *Crop Protection, 100*, pp. 186-195.

Lozoya-Pérez, N. E., Casas-Flores, S., Martínez-Álvarez, J. A., López-Ramírez, L. A., Lopes-Bezerra, L. M., Franco, B. and Mora-Montes, H. M. (2018) Generation of *Sporothrix schenckii* mutants expressing the green fluorescent protein suitable for the study of host-fungus interactions. *Fungal biology, 122*(10), pp. 1023-1030.

Lu, D., Pava-Ripoll, M., Li, Z. and Wang, C. (2008) Insecticidal evaluation of *Beauveria bassiana* engineered to express a scorpion neurotoxin and a cuticle degrading protease. *Applied Microbiology and Biotechnology, 81*(3), pp. 515-522.

Luo, S. L., Zhangsun, D. T. and Tang, K. X. (2005) Functional GNA expressed in *Escherichia coli* with high efficiency and its effect on *Ceratovacuna lanigera* Zehntner. *Applied Microbiology and Biotechnology, 69*(2), pp. 184-191.

Madej, T., Lanczycki, C. J., Zhang, D. C., Thiessen, P. A., Geer, R. C., Marchler-Bauer, A. and Bryant, S. H. (2014) MMDB and VAST+: tracking structural similarities between macromolecular complexes. *Nucleic Acids Research, 42*(D1), pp. D297-D303.

Mahot, H. C., Membang, G., Hanna, R., Begoude, B., Beilhe, L. B. and Bilong, B. (2019) Laboratory assessment of virulence of Cameroonian isolates of *Beauveria bassiana* and *Metarhizium anisopliae* against mirid bugs *Sahlbergella singularis* Haglund (Hemiptera: Miridae). *African Entomology, 27*(1), pp. 86-96.

Maqbool, S. B., Riazuddin, S., Loc, N. T., Gatehouse, A. M., Gatehouse, J. A. and Christou, P. (2001) Expression of multiple insecticidal genes confers broad resistance against a range of different rice pests. *Molecular Breeding, 7*(1), pp. 85-93.

Marques, L. H., Santos, A. C., Castro, B. A., Storer, N. P., Babcock, J. M., Lepping, M. D., Sa, V., Moscardini, V. F., Rule, D. M. and Fernandes, O. A. (2018) Impact of transgenic soybean expressing Cry1Ac and Cry1F proteins on the non-target arthropod community associated with soybean in Brazil. *Plos One, 13*(2).

McCafferty, H. R. K., Moore, P. H. and Zhu, Y. J. (2008) Papaya transformed with the *Galanthus nivalis* GNA gene produces a biologically active lectin with spider mite control activity. *Plant Science, 175*(3), pp. 385-393.

Melander, M., Ahman, I., Kamnert, E. and Stromdahl, A. C. (2003) Pea lectin expressed transgenically in oilseed rape reduces growth rate of pollen beetle larvae. *Transgenic Research, 12*(5), pp. 555-567.

References

Metschnikoff, E. (1879) Maladies des hannetons ble. *Zapiski imperatorskogo obshchestua sel'ska Khozyaistra yuzhnoi rossii*, pp. 17-50.

Mi, X. X., Liu, X., Yan, H. L., Liang, L. N., Zhou, X. Y., Yang, J. W., Si, H. J. and Zhang, N. (2017) Expression of the *Galanthus nivalis* agglutinin (GNA) gene in transgenic potato plants confers resistance to aphids. *Comptes Rendus Biologies, 340*(1), pp. 7-12.

Miao, J., Wu, Y. Q., Xu, W. G., Hu, L., Yu, Z. X. and Xu, Q. F. (2011) The Impact of Transgenic Wheat Expressing GNA (snowdrop lectin) on the *Aphids Sitobion* avenae, *Schizaphis graminum,* and *Rhopalosiphum padi. Environmental Entomology, 40*(3), pp. 743-748.

Michielse, C. B., Hooykaas, P. J. J., van den Hondel, C. A. M. J. J. and Ram, A. F. J. (2005) *Agrobacterium*-mediated transformation as a tool for functional genomics in fungi. *Current Genetics, 48*(1), pp. 1-17.

Mnyone, L. L., Ng'habi, K. R., Mazigo, H. D., Katakweba, A. A. and Lyimo, I. N. (2012) Entomopathogenic fungi, *Metarhizium anisopliae* and *Beauveria bassiana* reduce the survival of *Xenopsylla brasiliensis* larvae (Siphonaptera: Pulicidae). *Parasites & Vectors, 5*(1), pp. 204.

Molnar, I., Gibson, D. M. and Krasnoff, S. B. (2010) Secondary metabolites from entomopathogenic Hypocrealean fungi. *Natural Product Reports, 27*(9), pp. 1241-1275.

Mukhopadhyay, S., Panda, P. K., Behera, B., Das, C. K., Hassan, M. K., Das, D. N., Sinha, N., Bissoyi, A., Pramanik, K. and Maiti, T. K. (2014) In vitro and in vivo antitumor effects of Peanut agglutinin through induction of apoptotic and autophagic cell death. *Food and chemical toxicology, 64*, pp. 369-377.

Mulé, R., Sabella, G., Robba, L. and Manachini, B. (2017) Systematic review of the effects of chemical insecticides on four common butterfly families. *Frontiers in Environmental Science, 5*, pp. 32.

Muñóz-Garay, C., Portugal, L., Pardo-López, L., Jiménez-Juárez, N., Arenas, I., Gómez, I., Sánchez-López, R., Arroyo, R., Holzenburg, A. and Savva, C. G. (2009) Characterization of the mechanism of action of the genetically modified Cry1AbMod toxin that is active against Cry1Ab-resistant insects. *Biochimica et Biophysica Acta (BBA)-Biomembranes, 1788*(10), pp. 2229-2237.

Munoz-Garay, C., Soberon, M. and Bravo, A. (2010) Mode of Action of *Bacillus thuringiensis*-Genetically Modified Cry1AbMod and Cry1AcMod Toxins Role of Alkaline pH in Toxin Oligomerization. *Southwestern Entomologist, 35*(3), pp. 383-386.

Murdock, L. L., Huesing, J. E., Nielsen, S. S., Pratt, R. C. and Shade, R. E. (1990) Biological Effects of Plant-Lectins on the Cowpea Weevil. *Phytochemistry, 29*(1), pp. 85-89.

Murugan, D. and Saini, G. K. (2019) Cytotoxic and lethal effects of recombinant beta-BUTX-Lqq1a peptide against Lepidopteran insects and cell lines. *Toxicology in Vitro, 60*, pp. 44-50.

Mweke, A., Ulrichs, C., Nana, P., Akutse, K. S., Fiaboe, K. K. M., Maniania, N. K. and Ekesi, S. (2018) Evaluation of the entomopathogenic fungi *Metarhizium anisopliae, Beauveria bassiana* and *Isaria sp* for the Management of *Aphis craccivora* (Hemiptera: Aphididdae). *Journal of Economic Entomology, 111*(4), pp. 1587-1594.

Nagadhara, D., Ramesh, S., Pasalu, I. C., Rao, Y. K., Sarma, N. P., Reddy, V. D. and Rao, K. V. (2004) Transgenic rice plants expressing the snowdrop lectin gene (gna) exhibit high-level resistance to the whitebacked planthopper (*Sogatella furcifera*). *Theoretical and Applied Genetics, 109*(7), pp. 1399-1405.

Naimov, S., Nedyalkova, R., Staykov, N., Weemen-Hendriks, M., Minkov, I. and de Maagd, R. A. (2014) A novel Cry9Aa with increased toxicity for *Spodoptera exigua* (Hübner). *Journal of Invertebrate Pathology, 115*, pp. 99-101.

Naimov, S., Weemen-Hendriks, M., Dukiandjiev, S. and de Maagd, R. A. (2001) *Bacillus thuringiensis* delta-endotoxin Cry1 hybrid proteins with increased activity against the Colorado potato beetle. *Appl Environ Microbiol, 67*(11), pp. 5328-5330.

Nakaishi, Y., Sato, M., Bando, H. and Asano, S.-i. (2018) A mutation in *Plutella xylostella* ABCC2 causes resistance to *Bacillus thuringiensis* Cry1Ac by interfering with its receptor function. *Journal of Insect Biotechnology and Sericology, 87*(2), pp. 2_045-2_051.

Nakasu, E. Y., Edwards, M. G., Fitches, E., Gatehouse, J. A. and Gatehouse, A. M. (2014) Transgenic plants expressing ω-ACTX-Hv1a and snowdrop lectin (GNA) fusion protein show enhanced resistance to aphids. *Frontiers in plant science, 5*, pp. 673.

Napoleão, T. H., Albuquerque, L. P., Santos, N. D., Nova, I. C., Lima, T. A., Paiva, P. M. and Pontual, E. V. (2019) Insect midgut structures and molecules as targets of plant-derived protease inhibitors and lectins. *Pest Management Science, 75*(5), pp. 1212-1222.

Nkya, T. E., Akhouayri, I., Poupardin, R., Batengana, B., Mosha, F., Magesa, S., Kisinza, W. and David, J.-P. (2014) Insecticide resistance mechanisms associated with different environments in the malaria vector *Anopheles gambiae*: a case study in Tanzania. *Malaria Journal, 13*(1), pp. 28.

Ocelotl, J., Sanchez, J., Gomez, I., Tabashnik, B. E., Bravo, A. and Soberon, M. (2017) ABCC2 is associated with *Bacillus thuringiensis* Cry1Ac toxin oligomerization and membrane insertion in diamondback moth. *Scientific reports, 7*.

Okamoto, K., Hibino, K. and Sako, Y. (2019) In-cell single-molecule FRET measurements reveal three conformational state changes in RAF protein. *Biochimica et Biophysica Acta (BBA)-General Subjects*.

Oliveira, I., Pereira, J. A., Lino-Neto, T., Bento, A. and Baptista, P. (2012) Fungal diversity associated to the olive moth, *Prays oleae* Bernard: a survey for potential entomopathogenic fungi. *Microbial ecology, 63*(4), pp. 964-974.

Ormö, M., Cubitt, A. B., Kallio, K., Gross, L. A., Tsien, R. Y. and Remington, S. J. (1996) Crystal structure of the *Aequorea victoria* green fluorescent protein. *Science, 273*(5280), pp. 1392-1395.

Oukkache, N., El Jaoudi, R., Chgoury, F., Rochat, M. and Sabatier, J.-M. (2015) Characterization of Am IT, an anti-insect β-toxin isolated from the venom of scorpion *Androctonus mauretanicus*. *Acta physiologica Sonica, 25*, pp. 295-304.

Pal, N., Yamamoto, T., King, G. F., Waine, C. and Bonning, B. (2013) Aphicidal efficacy of scorpion- and spider-derived neurotoxins. *Toxicon, 70*, pp. 114-122.

Palmer, M. J., Moffat, C., Saranzewa, N., Harvey, J., Wright, G. A. and Connolly, C. N. (2013) Cholinergic pesticides cause mushroom body neuronal inactivation in honeybees. *Nature Communications, 4*, pp. 1634.

Pardo-Lopez, L., Soberon, M. and Bravo, A. (2013) *Bacillus thuringiensis* insecticidal three-domain Cry toxins: mode of action, insect resistance and consequences for crop protection. *FEMS microbiology reviews,* 37(1), pp. 3-22.

Pattapu, S., Mathew, T. B., Josephrajkumar, A. and Paul, A. (2018) Synergist induced susceptibility of tobacco caterpillar, *Spodoptera litura* (Fabricius) from Kerala, India exposed to conventional insecticides. *Phytoparasitica, 46*(1), pp. 97-104.

Paul Vuillemin, M. (1912) *Beauveria*, nouveau genre de Verticilliacées. Bulletin de la Société botanique de France, 59(1), pp. 34-40.

References

Pédelacq, J.-D., Cabantous, S., Tran, T., Terwilliger, T. C. and Waldo, G. S. (2006) Engineering and characterization of a superfolder green fluorescent protein. *Nature biotechnology, 24*(1), pp. 79.

Pedrini, N., Ortiz-Urquiza, A., Zhang, S. and Keyhani, N. O. (2013) Targeting of insect epicuticular lipids by the entomopathogenic fungus *Beauveria bassiana:* hydrocarbon oxidation within the context of a host-pathogen interaction. *Frontiers in Microbiology, 4*, pp. 24.

Peng, G. and Xia, Y. (2015) Integration of an insecticidal scorpion toxin (Bjα IT) gene into *Metarhizium acridum e*nhances fungal virulence towards *Locusta migratoria manilensis*. *Pest Management Science, 71*(1), pp. 58-64.

Peng, G. X. and Xia, Y. X. (2014) Expression of scorpion toxin LqhIT2 increases the virulence of *Metarhizium acridum* towards *Locusta migratoria manilensis*. *Journal of Industrial Microbiology & Biotechnology, 41*(11), pp. 1659-1666.

Peng, K., van Oers, M. M., Hu, Z. H., van Lent, J. W. M. and Vlak, J. M. (2010) Baculovirus *per os* infectivity factors form a complex on the surface of occlusion-derived virus. *Journal of Virology, 84*(18), pp. 9497-9504.

Perez, C., Fernandez, L. E., Sun, J. G., Folch, J. L., Gill, S. S., Soberon, M. and Bravo, A. (2005) *Bacillus thuringiensis* subsp *israelensis* Cyt1Aa synergizes Cry11Aa toxin by functioning as a membrane-bound receptor. *Proceedings of National Academy of Science of United States of America, 102*(51), pp. 18303-18308.

Pérez, C., Muñoz-Garay, C., Portugal, L. C., Sánchez, J., Gill, S. S., Soberón, M. and Bravo, A. (2007) *Bacillus thuringiensis* ssp. *israelensis* Cyt1Aa enhances activity of Cry11Aa toxin by facilitating the formation of a pre-pore oligomeric structure. *Cellular microbiology, 9*(12), pp. 2931-2937.

Pfeifer, T. A. and Khachatourians, G. G. (1987) The Formation of Protoplasts from *Beauveria bassiana*. *Applied Microbiology and Biotechnology, 26*(3), pp. 248-253.

Pfeifer, T. A. and Khachatourians, G. G. (1992) *Beauveria bassiana* protoplast regeneration and transformation using electroporation. *Applied Microbiology and Biotechnology, 38*(3), pp. 376-381.

Potts, S. G., Biesmeijer, J. C., Kremen, C., Neumann, P., Schweiger, O. and Kunin, W. E. (2010) Global pollinator declines: trends, impacts and drivers. *Trends in ecology & evolution, 25*(6), pp. 345-353.

Powell, K. S., Gatehouse, A. M. R., Hilder, V. A. and Gatehouse, J. A. (1995) Antifeedant effects of plant-lectins and an enzyme on the adult stage of the rice brown planthopper, *Nilaparvata lugens*. *Entomologia Experimentalis Et Applicata, 75*(1), pp. 51-59.

Powell, K. S., Spence, J., Bharathi, M., Gatehouse, J. A. and Gatehouse, A. M. R. (1998) Immunohistochemical and developmental studies to elucidate the mechanism of action of the snowdrop lectin on the rice brown planthopper, *Nilaparvata lugens* (Stal). *Journal of Insect Physiology, 44*(7-8), pp. 529-539.

Prasher, D. C., Eckenrode, V. K., Ward, W. W., Prendergast, F. G. and Cormier, M. J. (1992) Primary structure of the *Aequorea victoria* green-fluorescent protein. *Gene, 111*(2), pp. 229-233.

Promdonkoy, B. and Ellar, D. J. (2003) Investigation of the pore-forming mechanism of a cytolytic delta-endotoxin from *Bacillus thuringiensis. Biochemical Journal, 374*(Pt 1), pp. 255-9.

Qin, F. J., Xu, C. R., Lei, C. F., Hu, J. and Sun, X. L. (2018) *Autographa californica* multiple nucleopolyhedrovirus enters host cells via clathrin-mediated endocytosis and direct fusion with the plasma membrane. *Viruses-Basel, 10*(11).

Qin, Y., Ying, S.-H., Chen, Y., Shen, Z.-C. and Feng, M.-G. (2010) Integration of insecticidal protein Vip3Aa1 into *Beauveria bassiana* enhances fungal virulence to *Spodoptera litura* larvae by cuticle and per os infection.*Applied Environmental Microbiology, 76*(14), pp. 4611-4618.

Qiu, L., Cui, S. H., Liu, L., Zhang, B. Y., Ma, W. H., Wang, X. P., Lei, C. L. and Chen, L. Z. (2017) Aminopeptidase N1 is involved in *Bacillus thuringiensis* Cry1Ac toxicity in the beet armyworm, *Spodoptera exigua. Scientific reports, 7*.

Qiu, L., Hou, L. L., Zhang, B. Y., Liu, L., Li, B., Deng, P., Ma, W. H., Wang, X. P., Fabrick, J. A., Chen, L. Z. and Lei, C. L. (2015) Cadherin is involved in the action of *Bacillus thuringiensis* toxins Cry1Ac and Cry2Aa in the beet armyworm, *Spodoptera exigua. Journal of Invertebrate Pathology, 127*, pp. 47-53.

Ramanujam, B., Japur, K. and Poornesha, B. (2018) Field Efficacy of Entomopathogenic Fungi against Brinjal and Chilli Aphid (*Aphis gossypii* Glover)(Homoptera: Aphididae). *Pesticide Research Journal, 30*(2), pp. 159-162.

Rameshgar, F., Khajehali, J., Nauen, R., Bajda, S., Jonckheere, W., Dermauw, W. and Van Leeuwen, T. (2019) Point mutations in the voltage-gated sodium channel gene associated with pyrethroid resistance in Iranian populations of the European red mite *Panonychus ulmi*. *Pesticide Biochemistry and Physiology, 157*, pp. 80-87.

Ramzi, S. and Zibaee, A. (2014) Biochemical properties of different entomopathogenic fungi and their virulence against *Chilo suppressalis* (Lepidoptera: Crambidae) larvae. *Biocontrol Science and Technology, 24*(5), pp. 597-610.

Rao, G. R., Kumar, C. S., Sireesha, K. and Kumar, P. L. (2015) Role of nucleopolyhedroviruses (NPVs) in the management of lepidopteran pests in Asia. in *Biocontrol of lepidopteran pests*: Springer. pp. 11-52.

Rao, K., Rathore, K. S., Hodges, T. K., Fu, X., Stoger, E., Sudhakar, D., Williams, S., Christou, P., Bharathi, M. and Bown, D. P. (1998) Expression of snowdrop lectin (GNA) in transgenic rice plants confers resistance to rice brown planthopper. *The Plant Journal, 15*(4), pp. 469-477.

Ren, Q., Sun, M., Guan, G., Li, Y., Liu, Z., Liu, A., Ma, M., Niu, Q., Liu, J. and Yin, H. (2011) Biological control of engorged female *Haemaphysalis qinghaiensis* (Acari: Ixodidae) ticks with different Chinese isolates of *Beauveria bassiana*. *Parasitology Research, 109*(4), pp. 1059-1064.

Ren, X. L., Jiang, W. L., Ma, Y. J., Hu, H. Y., Ma, X. Y., Ma, Y. and Li, G. Q. (2016) The *Spodoptera exigua* (Lepidoptera: Noctuidae) ABCC2 mediates Cry1Ac cytotoxicity and, in conjunction with cadherin, contributes to enhance Cry1Ca toxicity in Sf9 Cells. *Journal of Economic Entomology, 109*(6), pp. 2281-2289.

Rhodes, E. M., Avery, P. B. and Liburd, O. E. (2018) Efficacy of entomopathogenic fungal products for biological control of spotted wing *Drosophila* (Diptera: Drosophilidae) under laboratory conditions. *Florida Entomologist, 101*(3), pp. 526-528.

Rice, P., Longden, I. and Bleasby, A. (2000) EMBOSS: The European molecular biology open software suite. *Trends in Genetics, 16*(6), pp. 276-277.

Rios-Moreno, A., Garrido-Jurado, I., Resquin-Romero, G., Arroyo-Manzanares, N., Arce, L. and Quesada-Moraga, E. (2016) Destruxin A production by *Metarhizium brunneum* strains during transient endophytic colonisation of *Solanum tuberosum*. *Biocontrol Science and Technology, 26*(11), pp. 1574-1585.

References

Ripoll, C., Favery, B., Lecomte, P., Van Damme, E., Peumans, W., Abad, P. and Jouanin, L. (2003) Evaluation of the ability of lectin from snowdrop (*Galanthus nivalis*) to protect plants against root-knot nematodes. *Plant Science, 164*(4), pp. 517-523.

Rivero-Borja, M., Guzman-Franco, A. W., Rodriguez-Leyva, E., Santillan-Ortega, C. and Perez-Panduro, A. (2018) Interaction of *Beauveria bassiana* and *Metarhizium anisopliae* with chlorpyrifos ethyl and spinosad in *Spodoptera frugiperda* larvae. *Pest Management Science, 74*(9), pp. 2047-2052.

Rivers, D. B., Rocco, M. M. and Frayha, A. R. (2002) Venom from the ectoparasitic wasp *Nasonia vitripennis* increases Na+ influx and activates phospholipase C and phospholipase A2 dependent signal transduction pathways in cultured insect cells. *Toxicon, 40*(1), pp. 9-21.

Roberts, D. W. and St Leger, R. J. (2004) *Metarhizium spp.*, cosmopolitan insect-pathogenic fungi: mycological aspects. *Advances in Applied Microbiology, 54*(1), pp. 1-70.

Rodriguez-Almazan, C., de Escudero, I. R., Canton, P. E., Munoz-Garay, C., Perez, C., Gill, S. S., Soberon, M. and Bravo, A. (2011) The amino- and carboxyl-terminal fragments of the *Bacillus thuringensis* Cyt1Aa toxin have differential roles in toxin oligomerization and pore formation. *Biochemistry, 50*(3), pp. 388-396.

Rojas-Azofeifa, D., Sasa, M., Lomonte, B., Diego-García, E., Ortiz, N., Bonilla, F., Murillo, R., Tytgat, J. and Díaz, C. (2019) Biochemical characterization of the venom of Central American scorpion *Didymocentrus krausi* Francke, 1978 (Diplocentridae) and its toxic effects in vivo and in vitro. *Comparative Biochemistry and Physiology Part C: Toxicology & Pharmacology, 217*, pp. 54-67.

Ruiu, L. (2018) Microbial Biopesticides in Agroecosystems. *Agronomy-Basel, 8*(11).

Rukarwa, R. J., Mukasa, S. B., Odongo, B., Ssemakula, G. and Ghislain, M. (2014) Identification of relevant non-target organisms exposed to weevil-resistant Bt sweetpotato in Uganda. *3 Biotech, 4*(3), pp. 217-226.

Sadeghi, A., Smagghe, G., Jurado-Jacome, E., Peumans, W. J. and Van Damme, E. J. M. (2009) Laboratory study of the effects of leek lectin (APA) in transgenic tobacco plants on the development of cotton leafworm *Spodoptera littoralis* (Lepidoptera: Noctuidae). *European Journal of Entomology, 106*(1), pp. 21-28.

Saeed, Q., Ahmad, F., Iqbal, N. and Zaka, S. M. (2019) Chemical control of polyphagous pests on their auxiliary hosts can minimize insecticide resistance: A case study of *Spodoptera exigua* Hubner (Lepidoptera: Noctuidae) in cotton agroecosystem. *Ecotoxicology and Environmental Safety, 171*, pp. 721-727.

Sahayaraj, K., Subash, N., Allingham, R., Kumar, V., Avery, P., Mehra, L., McKenzie, C. and Osborne, L. (2018) Lethal and sublethal effects of three microbial biocontrol agents on *Spodoptera litura* and its natural predator *Rhynocoris kumarii*. *Insects, 9*(3), pp. 101.

Şahin, B., Aygün, A., Gündüz, H., Şahin, K., Demir, E., Akocak, S. and Şen, F. (2018) Cytotoxic effects of platinum nanoparticles obtained from pomegranate extract by the green synthesis method on the MCF-7 cell line. *Colloids and Surfaces B: Biointerfaces, 163*, pp. 119-124.

Saleem, M., Hussain, D., Ghouse, G., Abbas, M. and Fisher, S. W. (2015) Monitoring of insecticide resistance in *Spodoptera litura* (Lepidoptera: Noctuidae) from four districts of Punjab, Pakistan to conventional and new chemistry insecticides. *Crop protection, 79*, pp. 177-184.

Sangbaramou, R., Camara, I., Huang, X. Z., Shen, J., Tan, S. Q. and Shi, W. P. (2018) Behavioral thermoregulation in *Locusta migratoria manilensis* (Orthoptera: Acrididae) in response to the entomopathogenic fungus, *Beauveria bassiana. Plos One, 13*(11).

Santana-Martinez, J. C., Silva, J. J. and Dussan, J. (2019) Efficacy of *Lysinibacillus sphaericus* against mixed-cultures of field-collected and laboratory larvae of *Aedes aegypti* and *Culex quinquefasciatus. Bulletin in Entomological Research, 109*(1), pp. 111-118.

Sato, Y., Hirayama, M., Morimoto, K., Yamamoto, N., Okuyama, S. and Hori, K. (2011) High mannose-binding lectin with preference for the cluster of alpha 1-2-mannose from the green alga *Boodlea coacta* is a potent entry inhibitor of HIV-1 and influenza viruses. *Journal of Biological Chemistry, 286*(22), pp. 19446-19458.

Sauvion, N., Charles, H., Febvay, G. and Rahbe, Y. (2004) Effects of jackbean lectin (ConA) on the feeding behaviour and kinetics of intoxication of the pea aphid, *Acyrthosiphon pisum. Entomologia Experimentalis Et Applicata, 110*(1), pp. 31-44.

Sayyed, A. H., Crickmore, N. and Wright, D. J. (2001) Cyt1Aa from *Bacillus thuringiensis subsp israelensis* is toxic to the diamondback moth, *Plutella xylostella,* and synergizes the activity of Cry1Ac towards a resistant strain. *Applied and Environmental Microbiology, 67*(12), pp. 5859-5861.

Sayyed, A. H., Crickmore, N. and Wright, D. J. (2001) Cyt1Aa from *Bacillus thuringiensis* subsp. *israelensis* is toxic to the diamondback moth, *Plutella xylostella,* and synergizes the activity of cry1ac towards a resistant strain. *Applied and Environmental Microbiology, 67*(12), pp. 5859-5861.

Sbaraini, N., Guedes, R. L. M., Andreis, F. C., Junges, A., de Morais, G. L., Vainstein, M. H., de Vasconcelos, A. T. R. and Schrank, A. (2016) Secondary metabolite gene clusters in the entomopathogen fungus *Metarhizium anisopliae:* genome identification and patterns of expression in a cuticle infection model. *BMC Genomics, 17*.

Selvi, C., Krishnamoorthy, S. and Sivasubramanian, P. (2012) Bioefficacy of Bt cotton hybrids containing the fusion gene Cry1Ac-1Ab against *Spodoptera litura. Indian Journal of Plant Protection, 40*(1), pp. 22-25.

Sevim, A., Donzelli, B. G., Wu, D., Demirbag, Z., Gibson, D. M. and Turgeon, B. G. (2012) Hydrophobin genes of the entomopathogenic fungus, *Metarhizium brunneum,* are differentially expressed and corresponding mutants are decreased in virulence. *Current genetics, 58*(2), pp. 79-92.

Shah, F. M., Razaq, M., Ali, Q., Shad, S. A., Aslarn, M. and Hardy, I. C. W. (2019) Field evaluation of synthetic and neem-derived alternative insecticides in developing action thresholds against cauliflower pests. *Scientific Reports, 9*.

Shah, P. A., Gatehouse, A. M. R., Clark, S. J. and Pell, J. K. (2005) Wheat containing snowdrop lectin (GNA) does not affect infection of the cereal aphid *Metopolophium dirhodum* by the fungal natural enemy *Pandora neoaphidis. Transgenic Research, 14*(4), pp. 473-476.

Shaw, C. H. (1995) Introduction of cloning plasmids into *Agrobacterium tumefaciens.* in *Plant Gene Transfer and Expression Protocols*: Springer. pp. 33-37.

Shim, H. J., Choi, J. Y., Li, M. S., Wang, Y., Roh, J. Y., Woo, S.-D., Jin, B. R. and Je, Y. H. (2009) A novel recombinant baculovirus expressing insect neurotoxin and producing occlusion bodies that contain *Bacillus thuringiensis* Cry toxin. *Journal of Asia-Pacific Entomology, 12*(4), pp. 217-220.

References

Shimomura, O., Johnson, F. H. and Saiga, Y. (1962) Extraction, purification and properties of aequorin, a bioluminescent protein from the luminous hydromedusan, *Aequorea*. *Journal of Cellular and Comparative Physiology, 59*, pp. 223-39.

Shrestha, A., Bao, K., Chen, Y. R., Chen, W. B., Wang, P., Fei, Z. J. and Blissard, G. W. (2018) global analysis of baculovirus *Autographa californica* multiple nucleopolyhedrovirus gene expression in the midgut of the lepidopteran host *Trichoplusia ni*. *Journal of Virology, 92*(23).

Silva, A., Beserra, E. B. and Dantas, J. P. (2008) Utilização de *Metarhizium anisopliae* e extratos vegetais para o controle de *Spodoptera frugiperda* e *Helicoverpa zea* (Lepdoptera: Noctuidae) em milho. *Engenharia Ambiental, 5*(1).

Singh, D. and Kaur, G. (2014a) The antileukaemic cell cycle regulatory activities of swainsonine purified from *Metarhizium anisopliae* fermentation broth. *Natural Product Research, 28*(22), pp. 2044-2047.

Singh, D. and Kaur, G. (2014b) Swainsonine, a novel fungal metabolite: optimization of fermentative production and bioreactor operations using evolutionary programming. *Bioprocess and Biosystems Engineering, 37*(8), pp. 1599-1607.

Soberon, M., Pardo-Lopez, L., Lopez, I., Gomez, I., Tabashnik, B. E. and Bravo, A. (2007) Engineering modified Bt toxins to counter insect resistance. *Science, 318*(5856), pp. 1640-1642.

Song, M. H., Yu, J. S., Kim, S., Lee, S. J., Kim, J. C., Nai, Y. S., Shin, T. Y. and Kim, J. S. (2019) Downstream processing of *Beauveria bassiana* and *Metarhizium anisopliae*-based fungal biopesticides against *Riptortus pedestris:* solid culture and delivery of conidia. *Biocontrol Science and Technology, 29*(6), pp. 514-532.

Song, W. Z., Du, Y. Z., Liu, Z. Q., Luo, N. G., Turkov, M., Gordon, D., Gurevitz, M., Goldin, A. L. and Dong, K. (2011) Substitutions in the Domain III Voltage-sensing Module Enhance the Sensitivity of an Insect Sodium Channel to a Scorpion beta-Toxin. *Journal of Biological Chemistry, 286*(18).

Sonthayanon, P., Jaresitthikunchai, J., Mangmee, S., Thiangtrongjit, T., Wuthiekanun, V., Amornchai, P., Newton, P., Phetsouvanh, R., Day, N. P. and Roytrakul, S. (2019) Whole cell matrix assisted laser desorption/ionization time-of-flight mass spectrometry (MALDI-TOF MS) for identification of *Leptospira spp*. in Thailand and Lao PDR. *PLoS neglected tropical diseases, 13*(4), pp. e0007232.

Sparks, T. C. and Nauen, R. (2015) IRAC: Mode of action classification and insecticide resistance management. *Pesticide Biochemistry and Physiology, 121*, pp. 122-128.

St Leger, R., Cooper, R. M. and Charnley, A. K. (1987) Production of cuticle-degrading enzymes by the entomopathogen *Metarhizium anisopliae* during infection of cuticles from *Calliphora vomitoria* and *Manduca sexta*. *Microbiology, 133*(5), pp. 1371-1382.

St. Leger, R. J. (1995) The role of cuticle-degrading proteases in fungal pathogenesis of insects. *Canadian Journal of Botany, 73*(S1), pp. 1119-1125.

Staats, C. C., Junges, A., Fitarelli, M., Furlaneto, M. C., Vainstein, M. H. and Schrank, A. (2007) Gene inactivation mediated by *Agrobacterium tumefaciens* in the filamentous fungi *Metarhizium anisopliae*. *Applied Microbiology and Biotechnology, 76*(4), pp. 945-950.

Stevens, R. B. (1974) Mycology guidebook.

Stewart, L. M., Hirst, M., Ferber, M. L., Merryweather, A. T., Cayley, P. J. and Possee, R. D. (1991) Construction of an improved baculovirus insecticide containing an insect-specific toxin gene. *Nature, 352*(6330), pp. 85.

StLeger, R. J., Joshi, L., Bidochka, M. J. and Roberts, D. W. (1996) Construction of an improved mycoinsecticide overexpressing a toxic protease. *Proceedings of the National Academy of Science of United States of America, 93*(13), pp. 6349-6354.

Stoger, E., Williams, S., Christou, P., Down, R. E. and Gatehouse, J. A. (1999) Expression of the insecticidal lectin from snowdrop (*Galanthus nivalis* agglutinin; GNA) in transgenic wheat plants: effects on predation by the grain aphid *Sitobion avenae*. *Molecular Breeding, 5*(1), pp. 65-73.

Storkey, J., Bruce, T. J., McMillan, V. E. and Neve, P. (2019) The future of sustainable crop protection relies on increased diversity of cropping systems and landscapes. in *Agroecosystem Diversity*: Elsevier. pp. 199-209.

Su, J., Zhang, Z., Wu, M. and Gao, C. (2014) Changes in insecticide resistance of the rice striped stem borer (Lepidoptera: Crambidae). *Journal of Economic Entomology, 107*(1), pp. 333-341.

Sufyan, M., Abbasi, A., Wakil, W., Gogi, M. D., Arshad, M., Nawaz, A. and Shabbir, Z. (2019) Efficacy of *Beauveria bassiana and Bacillus thuringiensis* against maize stem borer *Chilo partellus* (Swinhoe)(Lepidoptera: Pyralidae). *Gesunde Pflanzen*, pp. 1-8.

Sun, S., Liu, Y., Xia, J., Wang, M., Tang, R., Lei, C., Huang, Y., Nie, Z. and Yao, S. (2019) A semisynthetic fluorescent protein assembly-based FRET probe for real-time profiling of cell membrane protease functions in situ. *Chemical communications, 55*(15), pp. 2218-2221.

Sundstrom, J., Albihn, A., Boqvist, S., Ljungvall, K., Marstorp, H., Martiin, C., Nyberg, K., Vagsholm, I., Yuen, J. and Magnusson, U. (2014) Future threats to agricultural food production posed by environmental degradation, climate change, and animal and plant diseases - a risk analysis in three economic and climate settings. *Food Security, 6*(2), pp. 201-215.

Tahir, M., Wakil, W., Ali, A. and Sahi, S. T. (2019) Pathogenicity of *Beauveria bassiana* and *Metarhizium anisopliae* isolates against larvae of the polyphagous pest *Helicoverpa armigera*. *Entomologia Generalis, 38*(3), pp. 225-242.

Tajne, S., Boddupally, D., Sadumpati, V., Vudem, D. R. and Khareedu, V. R. (2014) Synthetic fusion-protein containing domains of Bt Cry1Ac and *Allium sativum* lectin (ASAL) conferred enhanced insecticidal activity against major lepidopteran pests. *Journal of biotechnology, 171*, pp. 71-75.

Takamatsu, N., Watanabe, Y., Yanagi, H., Meshi, T., Shiba, T. and Okada, Y. (1990) Production of enkephalin in tobacco protoplasts using tobacco mosaic-virus rna vector. *FEBS letters, 269*(1), pp. 73-76.

Tang, J. F., Liu, X. Y., Ding, Y. C., Jiang, W. J. and Xie, J. Q. (2019) Evaluation of *Metarhizium anisopliae* for rice planthopper control and its synergy with selected insecticides. *Crop Protection, 121*, pp. 132-138.

Thomas, M. B. and Read, A. F. (2007a) Can fungal biopesticides control malaria? *Nature Reviews Microbiology, 5*(5), pp. 377.

Thomas, M. B. and Read, A. F. (2007b) Fungal bioinsecticide with a sting. *Nature biotechnology, 25*(12), pp. 1367.

Tian, J.-C., Wang, X.-P., Chen, Y., Romeis, J., Naranjo, S. E., Hellmich, R. L., Wang, P. and Shelton, A. M. (2018) Bt cotton producing Cry1Ac and Cry2Ab does not harm two parasitoids, *Cotesia marginiventris* and *Copidosoma floridanum*. *Scientific reports, 8*(1), pp. 307.

References

Tian, J. F., Li, P. J., Li, X. X., Sun, P. H., Gao, H., Liu, X. Z., Huang, P., Tang, J. S. and Yao, X. S. (2016) New antibacterial isocoumarin glycosides from a wetland soil derived fungal strain *Metarhizium anisopliae*. *Bioorganic & Medicinal Chemistry Letters, 26*(5), pp. 1391-1396.

Tianpei, X. Z., Zhu, Y. G. and Li, S. Q. (2014) Optimized scorpion polypeptide LMX: a pest control protein effective against rice leaf folder. *Plos One, 9*(6).

Tinel, A. and Tschopp, J. (2004) The PIDDosome, a protein complex implicated in activation of caspase-2 in response to genotoxic stress. *Science, 304*(5672), pp. 843-846.

Torres-Quintero, M. C., Gomez, I., Pacheco, S., Sanchez, J., Flores, H., Osuna, J., Mendoza, G., Soberon, M. and Bravo, A. (2018) Engineering *Bacillus thuringiensis* Cyt1Aa toxin specificity from dipteran to lepidopteran toxicity. *Scientific Reports, 8*.

Tóth, J. T., Gulyás, G., Hunyady, L. and Várnai, P. (2019) Development of nonspecific BRET-based biosensors to monitor plasma membrane inositol lipids in living cells. in *Intracellular Lipid Transport*: Springer. pp. 23-34.

Trung, N. P., Fitches, E. and Gatehouse, J. A. (2006) A fusion protein containing a lepidopteran-specific toxin from the South Indian red scorpion (*Mesobuthus tamulus*) and snowdrop lectin shows oral toxicity to target insects. *BMC Biotechnology, 6*.

Tuncer, C., Kushiyev, R., Erper, I., Ozdemir, I. O. and Saruhan, I. (2019) Efficacy of native isolates of *Metarhizium anisopliae* and *Beauveria bassiana* against the invasive ambrosia beetle, *Xylosandrus germanus* Blandford (Coleoptera: Curculionidae: Scolytinae). *Egyptian Journal of Biological Pest Control, 29*(1), pp. 28.

United Nations, 2015, https://population.un.org/wpp/Publications/Files/WPP2019_Highlights.pdf

United Nations Food and Agricultural Organization,2009, How to feed the world in 2050?. http://www.fao.org/fileadmin/templates/wsfs/docs/expert_paper/How_to_Feed_the_World_in_2050.pdf

United Nations Food and Agricultural Organization, 2008 http://www.fao.org/fileadmin/templates/agphome/documents/Biodiversity pollination/SURVEY_DEC_08_Small.pdf

Van Damme, E. J., Lannoo, N. and Peumans, W. J. (2008) Plant lectins. in *Advances in botanical research*: Elsevier. pp. 107-209.

Van der Sluijs, J. P., Amaral-Rogers, V., Belzunces, L., Van Lexmond, M. B., Bonmatin, J.-M., Chagnon, M., Downs, C., Furlan, L., Gibbons, D. and Giorio, C. (2015) Conclusions of the Worldwide Integrated Assessment on the risks of neonicotinoids and fipronil to biodiversity and ecosystem functioning. in: Springer.

van Oers, M. M. and Vlak, J. M. (2007) Baculovirus genomics. *Current drug targets, 8*(10), pp. 1051-1068.

Vandamme, E. J. M., Allen, A. K. and Peumans, W. J. (1987) Isolation and characterization of a lectin with exclusive specificity towards mannose from snowdrop (*Galanthus nivalis*) Bulbs. *FEBS Letters, 215*(1), pp. 140-144.

Vandamme, E. J. M., Kaku, H., Perini, F., Goldstein, I. J., Peeters, B., Yagi, F., Decock, B. and Peumans, W. J. (1991) Biosynthesis, Primary Structure and Molecular-Cloning of Snowdrop (*Galanthus nivalis* L) Lectin. *European Journal of Biochemistry, 202*(1), pp. 23-30.

Vandenborre, G., Smagghe, G. and Van Damme, E. J. (2011) Plant lectins as defense proteins against phytophagous insects. *Phytochemistry, 72*(13), pp. 1538-1550.

Vontas, J., Hernandez-Crespo, P., Margaritopoulos, J. T., Ortego, F., Feng, H. T., Mathiopoulos, K. D. and Hsu, J. C. (2011) Insecticide resistance in Tephritid flies. *Pesticide Biochemistry and Physiology, 100*(3), pp. 199-205.

Walsh, T., James, B., Chakroun, M., Ferre, J. and Downes, S. (2018) Isolating, characterising and identifying a Cry1Ac resistance mutation in field populations of *Helicoverpa punctigera*. *Scientific reports, 8*.

Walters, F. S., deFontes, C. M., Hart, H., Warren, G. W. and Chen, J. S. (2010) Lepidopteran-active variable-region sequence imparts coleopteran activity in eCry3.1Ab, an engineered *Bacillus thuringiensis* hybrid insecticidal protein. *Applied Environmental Microbiology, 76*(10), pp. 3082-3088.

Wang, C. and Feng, M.-G. (2014) Advances in fundamental and applied studies in China of fungal biocontrol agents for use against arthropod pests. *Biological Control, 68*, pp. 129-135.

Wang, C. and Leger, R. J. S. (2006) A collagenous protective coat enables *Metarhizium anisopliae* to evade insect immune responses. *Proceedings of the National Academy of Sciences, 103*(17), pp. 6647-6652.

Wang, C. and Leger, R. J. S. (2007) The *Metarhizium anisopliae* perilipin homolog MPL1 regulates lipid metabolism, appressorial turgor pressure, and virulence. *Journal of Biological Chemistry, 282*(29), pp. 21110-21115.

Wang, C. and St Leger, R. J. (2007a) The MAD1 adhesin of *Metarhizium anisopliae* links adhesion with blastospore production and virulence to insects, and the MAD2 adhesin enables attachment to plants. *Eukaryotic cell, 6*(5), pp. 808-816.

Wang, C. and St Leger, R. J. (2007b) A scorpion neurotoxin increases the potency of a fungal insecticide. *Nature biotechnology, 25*(12), pp. 1455.

Wang, H., Lei, Z., Reitz, S., Li, Y. and Xu, X. (2013) Production of microsclerotia of the fungal entomopathogen *Lecanicillium lecanii* (Hypocreales: Cordycipitaceae) as a biological control agent against soil-dwelling stages of *Frankliniella occidentalis* (Thysanoptera: Thripidae). *Biocontrol Science and Technology, 23*(2), pp. 234-238.

Wang, J., Zhang, H., Wang, H. D., Zhao, S., Zuo, Y., Yang, Y. H. and Wu, Y. D. (2016) Functional validation of cadherin as a receptor of Bt toxin Cry1Ac in *Helicoverpa armigera* utilizing the CRISPR/Cas9 system. *Insect Biochemistry and Molecular Biology, 76*, pp. 11-17.

Wang, P. P., Ma, J. H., Head, G. P., Xia, D. P., Li, J., Wang, H. Q., Yang, M. L., Xie, Z. M., Zalucki, M. P. and Lu, Z. Z. (2019) Susceptibility of *Helicoverpa armigera* to two Bt toxins, Cry1Ac and Cry2Ab, in northwestern China: toward developing an IRM strategy. *Journal of Pest Science, 92*(2), pp. 923-931.

Wang, X. Y., Shao, Z. M., Chen, Q. Y., Xu, J. P., Sun, X., Xu, Z. P., Li, M. W. and Wu, Y. C. (2019) Knockdown of BmTCP-1beta Delays BmNPV Infection in vitro. *Fronters in Microbiology, 10*, pp. 578.

Wang, Z. K., Yang, J., Xin, C. Y., Xing, X. R., Yin, Y. P., Chen, L. and Song, Z. Y. (2019) Regulation of conidiation, dimorphic transition, and microsclerotia formation by MrSwi6 transcription factor in dimorphic fungus *Metarhizium rileyi*. *World Journal of Microbiology & Biotechnology, 35*(3).

Wang, Z. X., Jiang, Y. Y., Li, Y. D., Feng, J. Y. and Huang, B. (2019) MrArk1, an actin-regulating kinase gene, is required for endocytosis and involved in sustaining conidiation capacity

and virulence in *Metarhizium robertsii*. *Applied Microbiology and Biotechnology, 103*(12), pp. 4859-4868.

Wang, Z. Y., Sun, X. F., Wang, F., Tang, K. X. and Zhang, J. R. (2005) Enhanced resistance of snowdrop lectin (*Galanthus nivalis* L. agglutinin)-expressing maize to Asian corn borer (*Ostrinia furnacalis* Guenee). *Journal of Integrative Plant Biology, 47*(7), pp. 873-880.

Wei, J., Zhang, M., Liang, G., Wu, K., Guo, Y., Ni, X. and Li, X. (2016) APN1 is a functional receptor of Cry1Ac but not Cry2Ab in *Helicoverpa zea*. *Scientific reports, 6*, pp. 19179.

Whitehorn, P. R., O'connor, S., Wackers, F. L. and Goulson, D. (2012) Neonicotinoid pesticide reduces bumble bee colony growth and queen production. *Science, 336*(6079), pp. 351-352.

Wieser, A., Schneider, L., Jung, J. and Schubert, S. (2012) MALDI-TOF MS in microbiological diagnostics—identification of microorganisms and beyond (mini review). *Applied Microbiology and Biotechnology, 93*(3), pp. 965-974.

Williams, C. D., Dillon, A. B., Harvey, C. D., Hennessy, R., Mc Namara, L. and Griffin, C. T. (2013) Control of a major pest of forestry, *Hylobius abietis*, with entomopathogenic nematodes and fungi using eradicant and prophylactic strategies. *Forest Ecology and Management, 305*, pp. 212-222.

Wirth, M. C., Park, H. W., Walton, W. E. and Federici, B. A. (2005) Cyt1A of *Bacillus thuringiensis* delays evolution of resistance to Cry11A in the mosquito *Culex quinquefasciatus*. *Applied Environmental Microbiology, 71*(1), pp. 185-189.

Wright, C. S. and Hester, G. (1996) The 2.0 angstrom structure of a cross-linked complex between snowdrop lectin and a branched mannopentaose: Evidence for two unique binding modes. *Structure, 4*(11), pp. 1339-1352.

Wrobel, K., Claudio, E., Segade, F., Ramos, S. and Lazo, P. S. (1996) Measurement of cytotoxicity by propidium iodide staining of target cell DNA - Application to the quantification of murine TNF-alpha. *Journal of Immunological Methods, 189*(2), pp. 243-249.

Wu, J., Ridgway, H., Carpenter, M. and Glare, T. (2008) Efficient transformation of *Beauveria bassiana* by *Agrobacterium tumefaciens*-mediated insertional mutagenesis. *Australasian Plant Pathology, 37*(6), pp. 537-542.

Wu, S.-Y., Huang, Y.-J., Tzeng, Y.-M., Huang, C.-Y., Hsiao, M., Wu, A. and Huang, T.-H. (2018) Destruxin B suppresses drug-resistant colon tumorigenesis and stemness is associated with the upregulation of miR-214 and downregulation of mTOR/β-catenin pathway. *Cancers, 10*(10), pp. 353.

Wu, S., Gao, Y., Xu, X., Zhang, Y., Wang, J., Lei, Z. and Smagghe, G. (2013) Laboratory and greenhouse evaluation of a new entomopathogenic strain of *Beauveria bassiana* for control of the onion thrips Thrips tabaci. *Biocontrol Science and Technology, 23*(7), pp. 794-802.

Xiao, Y., Wang, K., Ding, R., Zhang, H., Di, P., Chen, J., Zhang, L. and Chen, W. (2012) Transgenic tetraploid *Isatis indigotica* expressing Bt Cry1Ac and *Pinellia ternata* agglutinin showed enhanced resistance to moths and aphids. *Molecular biology reports, 39*(1), pp. 485-491.

Xie, M., Zhang, Y. J., Zhai, X. M., Zhao, J. J., Peng, D. L. and Wu, G. (2015) Expression of a scorpion toxin gene BmKit enhances the virulence of *Lecanicillium lecanii* against aphids. *Journal of Pest Science, 88*(3), pp. 637-644.

Xie, M. S., Zhou, X., Xia, Y. X. and Cao, Y. Q. (2019) Mid1 affects ion transport, cell wall integrity, and host penetration of the entomopathogenic fungus *Metarhizium acridum*. *Applied Microbiology and Biotechnology, 103*(4), pp. 1801-1810.

Xing, Y. J., Qin, Z. F., Feng, M. Y., Li, A. M., Zhang, L., Wang, Y., Dong, X. H., Zhang, Y. X., Tan, S. Q. and Shi, W. P. (2019) The impact of Bt maize expressing the Cry1Ac protein on non-target arthropods. *Environmental Science and Pollution Research, 26*(6), pp. 5814-5819.

Xu, C., Zhang, X., Qian, Y., Chen, X. X., Liu, R., Zeng, G. H., Zhao, H. and Fang, W. G. (2014) A High-Throughput Gene Disruption Methodology for the Entomopathogenic Fungus *Metarhizium robertsii. Plos One, 9*(9).

Xu, D. and Zhang, Y. (2012) Ab initio protein structure assembly using continuous structure fragments and optimized knowledge-based force field. *Proteins: Structure, Function, and Bioinformatics, 80*(7), pp. 1715-1735.

Xu, D. and Zhang, Y. (2013) Toward optimal fragment generations for ab initio protein structure assembly. *Proteins: Structure, Function, and Bioinformatics, 81*(2), pp. 229-239.

Yang, F., Gonzalez, J. C. S., Williams, J., Cook, D. C., Gilreath, R. T. and Kerns, D. L. (2019) Occurrence and ear damage of *Helicoverpa zea* on Transgenic *Bacillus thuringiensis* maize in the field in texas, US and its susceptibility to Vip3A Protein. *Toxins, 11*(2).

Yang, F., Liu, S., Zhang, Y. Y., Qin, C. H., Xu, L. N., Li, W. H., Cao, Z. J., Li, W. X. and Wu, Y. L. (2018) Expression of recombinant alpha-toxin BmKM9 from scorpion *Buthus martensii* Karsch and its functional characterization on sodium channels. *Peptides, 99*, pp. 153-160.

Yang, F., Moss, L. G. and Phillips, G. N. (1996) The molecular structure of green fluorescent protein. *Nature biotechnology, 14*(10), pp. 1246.

Yang, S., Fitches, E., Pyati, P. and Gatehouse, J. A. (2015) Effect of insecticidal fusion proteins containing spider toxins targeting sodium and calcium ion channels on pyrethroid-resistant strains of peach-potato aphid (*Myzus persicae*). *Pest Management Science, 71*(7), pp. 951-956.

Yang, S., Pyati, P., Fitches, E. and Gatehouse, J. A. (2014) A recombinant fusion protein containing a spider toxin specific for the insect voltage-gated sodium ion channel shows oral toxicity towards insects of different orders. *Insect Biochemistry and Molecular Biology, 47*, pp. 1-11.

Ye, X. Y., Ng, T. B., Tsang, P. W. K. and Wang, J. (2001) Isolation of a homodimeric lectin with antifungal and antiviral activities from red kidney bean (*Phaseolus vulgaris*) seeds. *Journal of Protein Chemistry, 20*(5), pp. 367-375.

Ying, S. H. and Feng, M. G. (2006) Novel blastospore-based transformation system for integration of phosphinothricin resistance and green fluorescence protein genes into *Beauveria bassiana*. *Applied Microbiology and Biotechnology, 72*(1), pp. 206-210.

Yu, H. L., Romeis, J., Li, Y. H., Li, X. J. and Wu, K. M. (2014) Acquisition of Cry1Ac Protein by Non-Target Arthropods in Bt Soybean Fields. *Plos One, 9*(8).

Zhang, J., Wang, Z. L., Keyhani, N. O., Peng, G. X., Jin, K. and Xia, Y. X. (2019) The protein phosphatase gene MaPpt1 acts as a programmer of microcycle conidiation and a negative regulator of UV-B tolerance in *Metarhizium acridum. Applied Microbiology and Biotechnology, 103*(3), pp. 1351-1362.

Zhang, L., Ying, H. S. and Feng, M. G. (2014) Assessment of oral virulence against Spodoptera litura, acquired by a previously non-pathogenic *Metarhizium anisopliae* isolate, following integration of a midgut-specific insecticidal toxin. *Biological Control, 79*, pp. 8-15.

References

Zhang, L. W., Liu, Y. J., Yao, J., Wang, B., Huang, B., Li, Z. Z., Fan, M. Z. and Sun, J. H. (2011) Evaluation of *Beauveria bassiana* (Hyphomycetes) isolates as potential agents for control of *Dendroctonus valens*. *Insect Science, 18*(2), pp. 209-216.

Zhang, M., Wei, J. Z., Ni, X. Z., Zhang, J., Jurat-Fuentes, J. L., Fabrick, J. A., Carriere, Y., Tabashnik, B. E. and Li, X. C. (2019) Decreased Cry1Ac activation by midgut proteases associated with Cry1Ac resistance in *Helicoverpa zea*. *Pest Management Science, 75*(4), pp. 1099-1106.

Zhang, S., Xia, Y. X., Kim, B. and Keyhani, N. O. (2011) Two hydrophobins are involved in fungal spore coat rodlet layer assembly and each play distinct roles in surface interactions, development and pathogenesis in the entomopathogenic fungus, *Beauveria bassiana*. *Molecular Microbiology, 80*(3), pp. 811-826.

Zhang, X. R., Lei, Z. R., Reitz, S. R., Wu, S. Y. and Gao, Y. L. (2019) Laboratory and Greenhouse Evaluation of a Granular Formulation of *Beauveria bassiana* for Control of Western Flower Thrips, *Frankliniella occidentalis*. *Insects, 10*(2).

Zhang, Y., Zhang, J., Jiang, X., Wang, G., Luo, Z., Fan, Y., Wu, Z. and Pei, Y. (2010) Requirement of a mitogen-activated protein kinase for appressorium formation and penetration of insect cuticle by the entomopathogenic fungus *Beauveria bassiana*. *Applied Environmental Microbiology, 76*(7), pp. 2262-2270.

Zhao, M., Yuan, X. D., Wei, J. Z., Zhang, W. N., Wang, B. J., Khaing, M. M. and Liang, G. M. (2017) Functional roles of cadherin, aminopeptidase-N and alkaline phosphatase from *Helicoverpa armigera* (Hubner) in the action mechanism of *Bacillus thuringiensis* Cry2Aa. *Scientific Reports, 7*.

Zhou, X., Li, X. D., Yuan, J. Z., Tang, Z. H. and Liu, W. Y. (2000) Toxicity of cinnamomin - a new type II ribosome-inactivating protein to bollworm and mosquito. *Insect Biochemistry and Molecular Biology, 30*(3), pp. 259-264.

Zimmer, C. T., Muller, A., Heimbach, U. and Nauen, R. (2014) Target-site resistance to pyrethroid insecticides in German populations of the cabbage stem flea beetle, *Psylliodes chrysocephala* L. (Coleoptera: Chrysomelidae). *Pesticide Biochemistry and Physiology, 108*, pp. 1-7.

Zlotkin, E., Fishman, Y. and Elazar, M. (2000) AaIT: From neurotoxin to insecticide. *Biochimie, 82*(9-10), pp. 869-881.

Zlotkin, E., Kadouri, D., Gordon, D., Pelhate, M., Martin, M. and Rochat, H. (1985) An excitatory and a depressant insect toxin from scorpion venom both affect sodium conductance and possess a common binding site. *Archives of Biochemistry and Biophysics, 240*(2), pp. 877-887.

Zou, X. H., He, Y. W., Qiao, J. P., Zhang, C. L. and Cao, Z. Y. (2016) The natural scorpion peptide, BmK NT1 activates voltage-gated sodium channels and produces neurotoxicity in primary cultured cerebellar granule cells. *Toxicon, 109*, pp. 33-41.

Zribi Zghal, R., Frikha, F., Elleuch, J., Darriet, F., Chandre, F., Jaoua, S. and Tounsi, S. (2019) The combinatory effect of Cyt1Aa flexibility and specificity against dipteran larvae improves the toxicity of *Bacillus thuringensis kurstaki* toxins. *International Journal of Biological Macromolecule, 123*, pp. 42-49.

Manuscript published:

Murugan, D. and Saini, G.K., 2019. Cytotoxic and lethal effects of recombinant β-BUTX-Lqq1a peptide against Lepidopteran insects and cell lines. *Toxicology in Vitro, 60,* pp.44-50.

Manuscript under Preparation:

Dhanasingh M and Gurvinder Kaur Saini, Fusion protein containing scorpion neurotoxin β-BUTX-Lqq1a and Snowdrop lectin mediates G2/M phase cell cycle arrest and caspase dependent cell death in *Spodoptera frugiperda* cell line

Dhanasingh M and Gurvinder Kaur Saini, Effect of *M. anisopliae* expressing scorpion neurotoxin neurotoxin β-BUTX Lqq1a on *Phyllophaga smithi*

Other publications:

Kanjo, K., Surin, S.I., Gupta, T., **Dhanasingh, M.,** Singh, B. and Saini, G.K., 2019. Truncated, strong inducible promoter Pmcl1 from *Metarhizium anisopliae.* 3 Biotech, 9(3), p.75.

Manuscript under preparation

Biswaranjan Jena, **Dhanasingh M**, Gurvinder Kaur Saini, Cell cycle arrest and Apoptosis mediated death caused by Entomopathogenic fungi based Silver Nano-particles (Under preparation)

Dhanasingh M, Jyothirmay singh, Gurvinder Kaur Saini, Cytotoxicity studies of silver nanoparticles synthesized from various *Bacillus thuringiensis* strains on insect cell lines (under preparation)

International Conference Proceedings:

1. **Dhanasingh, M** and Gurvinder Kaur, 2016. Engineering enmopathogenic fungus, *Beauveria bassiana* to express heterologous insect specific scorpion neurotoxin. 57th Annual Conference of AMI & International Symposium on "Microbes and Biosphere: What's new what's next, November, 24-27, Gauhati University, Guwahati, Assam. Pp. 313

2. **Dhanasingh, M** and Gurvinder Kaur, 2017. Novel insect-specific neurotoxin, LqqIT1 as a potential candidature for biopesticide 'International Symposium on Plant Biotechnology for Crop Improvement (ISPBCI 2017), IIT Guwahati, India during January 20-22, 2017.Poster A52- Page No:70

VITAE

The author was born on June 3, 1989 in Tirunelveli District of Tamil Nadu state, India. He passed the Higher and senior Secondary examinations conducted by the State Board of Secondary Education, from St. Xaviers. Higher Secondary School, Palayamkottai, Tirunelveli in the year 2004-2006. He completed B.Tech Biotechnology from Tamil Nadu Agricultural University, Coimbatore in 2010 and M.Tech in Biotechnology and Biochemical engineering from Indian Institute of Technology, Kharagpur in the year 2013.

Mr. Dhanasingh M joined the Ph.D programme at the Department of Biosciences and Bioengineering, Indian Institute of Technology Guwahati, Guwahati, Assam, India, in the year 2013. He gave the open seminar (PhD Synopsis) on April 2019 and presented his thesis work satisfactorily before the Doctoral Committee. He Submitted the PhD thesis in August 2019.